



Thèse

2015

Open Access

This version of the publication is provided by the author(s) and made available in accordance with the copyright holder(s).

The role of JAM-C in innate leukocyte migration and the immune response
to *Leishmania major* infection

Ballet, Romain Roger

How to cite

BALLET, Romain Roger. The role of JAM-C in innate leukocyte migration and the immune response to *Leishmania major* infection. 2015. doi: 10.13097/archive-ouverte/unige:55650

This publication URL: <https://archive-ouverte.unige.ch/unige:55650>

Publication DOI: [10.13097/archive-ouverte/unige:55650](https://doi.org/10.13097/archive-ouverte/unige:55650)

UNIVERSITÉ DE GENÈVE

Département de biologie cellulaire

FACULTE DES SCIENCES
Professeur J.-C. Martinou

Département de pathologie et immunologie

FACULTE DE MEDECINE
Professeur B. A. Imhof

**The role of JAM-C in innate leukocyte migration and
the immune response to *Leishmania major* infection**

THÈSE

Présentée à la faculté des sciences de l'Université de Genève
pour obtenir le grade de Docteur ès sciences, mention biologie

par

Romain BALLET

de
FRANCE

Thèse n°4772

Genève

Atelier d'impression Repromail
2015



**UNIVERSITÉ
DE GENÈVE**

FACULTÉ DES SCIENCES

**Doctorat ès sciences
Mention biologie**

Thèse de **Monsieur Romain Roger BALLET**

intitulée :

**"The Role of JAM-C in Innate Leukocyte Migration and the
Immune Response to *Leishmania Major* Infection"**

La Faculté des sciences, sur le préavis de Monsieur B. A. IMHOF, professeur ordinaire et directeur de thèse (Faculté de médecine, Département de pathologie et immunologie), Monsieur J.-C. MARTINO, professeur ordinaire et codirecteur de thèse (Département de biologie cellulaire), Madame F. TACCHINI-COTTIER, professeure (Université de Lausanne, Département de biochimie, Lausanne, Suisse) et Madame B. ENGELHARDT, professeure (Universität Bern, Theodor Kocher Institute, Berne, Suisse), autorise l'impression de la présente thèse, sans exprimer d'opinion sur les propositions qui y sont énoncées.

Genève, le 11 mars 2015

Thèse - 4772 -

Le Doyen

N.B. - La thèse doit porter la déclaration précédente et remplir les conditions énumérées dans les "Informations relatives aux thèses de doctorat à l'Université de Genève".

Table of content

1. Summary	5
1.1. Résumé	7
1.2. Summary	8
2. Introduction	9
2.1. The inflammatory response: from pathogen sensing to leukocyte trafficking	11
2.1.1 Functions of the immune system	11
2.1.2 Introducing inflammation	11
2.1.3 Pathogen sensing	12
2.1.4 The leukocyte adhesion cascade	13
2.1.5 The interstitial migration toward the pathogen	31
2.1.6 The migration of leukocytes to lymph nodes	33
2.2. JAM-C in inflammation and disease	37
2.2.1 The JAM family, an overview	37
2.2.2 JAM-C expression profile	39
2.2.3 JAM-C ligands	40
2.2.4 JAM-C and leukocyte migration	42
2.2.5 JAM-C and vascular permeability	44
2.2.6 JAM-C and cell polarity	45
2.2.7 Role and function of other JAM members	45
2.3. The <i>Leishmania major</i> model of cutaneous leishmaniasis	50
2.3.1 Leishmaniasis, an overview	50
2.3.2 Immunobiology of <i>L. major</i> infection: resistance versus susceptibility ?	54
2.3.3 The role of neutrophils in the mouse model of cutaneous leishmaniasis	56
2.3.4 The role of monocytes and DCs in the mouse model of cutaneous leishmaniasis	58
2.3.5 Role of adhesion molecules in cutaneous leishmaniasis	62
3. Aim of the thesis	63
4. Materials and methods	67
4.1. Ethic statement	69
4.2. Mice and parasites	69
4.3. Flow cytometry analysis of ear endothelial cells	69
4.4. Leukocyte emigration for ear skin explants and FACS analysis	69
4.5. Flow cytometry analysis of leukocyte populations in steady state	70
4.6. FITC painting experiments	71
4.7. Immunofluorescence microscopy	71
4.8. Vascular permeability assay	72
4.9. CCL3 level in ear following <i>L. major</i> infection	72
4.10. T cell response in the draining lymph node and cytokine detection	72
4.11. Lesion area measurement and parasite load	73
4.12. Statistical analysis	73
5. Results	75

5.1. The antibody H33 mimics JAM-C downregulation after <i>L. major</i> inoculation, and locally increases vascular permeability after infection.	77
5.2. Blocking JAM-C increases the number of circulating cells recruited in response to <i>L. major</i> infection	78
5.3. Blocking JAM-C increases the number of DCs migrating to the draining lymph node	79
5.4. Blocking JAM-C improves the Th1 cell response and favours healing in C57BL/6 mice	79
5.5. Blocking JAM-C boosts the Th2 cell response and worsens the disease in BALB/c mice	80
6. Figures.....	81
6.1. Figure 1.....	83
6.2. Figure 2.....	85
6.3. Figure 3.....	86
6.4. Figure 4.....	87
6.5. Figure 5.....	88
6.6. Figure S1.....	90
6.7. Figure S2.....	91
6.8. Figure S3.....	92
6.9. Figure S4.....	93
6.10. Figure S5.....	94
6.11. Figure S6.....	95
6.12. Figure S7.....	96
6.13. Figure S8.....	97
6.14. Figure S9.....	98
7. General discussion	99
7.1. Overview of the discussion	101
7.2. Role of JAM-C in vascular permeability: JAM-C as a gatekeeper?	101
7.3. Role of JAM-C in leukocyte migration: a role in adhesion or transmigration?	102
7.4. Similarities between JAM-C and other adhesion molecules	108
7.5. Migration of DCs through lymphatics: passive or active process?	109
7.6. The role of neutrophils in <i>L. major</i> infection: a need for specific neutrophil depletion.....	110
7.7. Importance of innate cell trafficking in <i>L. major</i> infection: lessons from JAM-C manipulation	112
8. Conclusion	113
9. Acknowledgements	117
9.1. Remerciements	119
9.2. Acknowledgements	120
10. Appendix	123
11. References	137

1. Summary

1.1. Résumé

Le recrutement des leucocytes, des vaisseaux sanguins vers le foyer infectieux, suivi de la migration des cellules dendritiques du foyer infectieux vers les ganglions drainants sont des étapes clefs dans l'initiation d'une réponse immunitaire spécifique et protectrice contre un pathogène.

Notre laboratoire a découvert au début des années 2000 une protéine aux multiples facettes, la Molécule d'Adhésion Jonctionnelle C (JAM-C). Parmi ces différentes fonctions, nous avons découvert que cette protéine, située entre autres au niveau des jonctions serrées des cellules endothéliales, jouait un rôle dans la transmigration des leucocytes vers le site inflammatoire. À ce jour, ces découvertes restent limitées à des modèles *in vitro* ou bien des modèles *in vivo* dans le cadre d'inflammation stériles. Ainsi, le rôle potentiel de cette protéine dans le recrutement des leucocytes *in vivo* suite à une infection réelle n'a pas encore été élucidé. Le but de ce projet de thèse était donc d'étudier, chez la souris, le rôle de JAM-C dans le recrutement des leucocytes consécutive à l'infection avec *Leishmania major*, un parasite responsable de la Leishmaniose cutanée.

Après avoir initialement vérifié que JAM-C était bien présente à la surface des cellules endothéliales des vaisseaux sanguins et lymphatiques de la peau, j'ai tout d'abord étudié son niveau d'expression en surface suite à l'infection avec *L. major*. J'ai observé que son niveau d'expression diminuait en réponse à l'infection, au moment même où la migration des leucocytes des vaisseaux sanguins vers le tissu infectés est très élevée. J'ai donc fait l'hypothèse que JAM-C contrôlait l'intégrité et l'étanchéité de nos vaisseaux sanguins en l'absence de signaux inflammatoires, tandis que sa diminution suite à l'infection favorisait la perméabilité et la migration des leucocytes vers le foyer infectieux.

Pour comprendre le rôle de JAM-C dans ce modèle, j'ai utilisé un anticorps monoclonal dirigé contre JAM-C, le clone H33. J'ai non seulement observé que l'injection de l'anticorps *in vivo* redistribuait JAM-C hors des jonctions endothéliales, mais aussi que l'anticorps augmentait localement la perméabilité vasculaire en réponse à l'infection. En d'autres termes, cet anticorps mime et amplifie la diminution de JAM-C que j'observe naturellement en réponse à *L. major*.

Les multiples effets de l'anticorps H33 sur la redistribution de JAM-C et l'augmentation de la perméabilité ont eu de multiples répercussions sur la

réponse immunitaire. Chez des souris résistantes comme susceptibles à l'infection, j'ai observé que le nombre de leucocytes de l'immunité innée recrutés sur le site d'infection était plus élevé après traitement avec H33. De plus, la migration des cellules dendritiques du site inflammatoire vers les ganglions drainants était elle aussi amplifiée. Cette augmentation de la migration des cellules dendritiques vers les ganglions, où les lymphocytes résident, s'est accompagnée d'une amplification de la réponse lymphocytaire spécifique au pathogène.

En effet, chez les souris résistantes C57BL/6, le traitement avec l'anticorps H33 a indirectement augmenté la réponse T auxiliaire de type 1, caractérisée par l'augmentation de la production d'interféron gamma. Ceci s'est accompagné d'une diminution notable de la charge parasitaire et des lésions cutanées associées. En revanche, chez les souris susceptibles BALB/c, le traitement avec l'anticorps H33 s'est accompagné d'une amplification de la réponse T auxiliaire de type 2, caractérisée par l'augmentation de la production d'interleukine 4, exacerbant ainsi la maladie.

En conclusion, ce travail montre que la réponse immunitaire dirigée contre un pathogène peut être finement modulée de manière indirecte en jouant sur les propriétés d'une seule et unique molécule d'adhésion jonctionnelle.

1.2. Summary

The recruitment of dendritic cells to sites of infections and their migration to lymph nodes is fundamental for antigen processing and presentation to T cells. I showed that antibody blockade of junctional adhesion molecule C (JAM-C) on endothelial cells removed JAM-C away from junctions and increased vascular permeability after *L. major* infection. This has multiple consequences on the output of the immune response. In resistant C57BL/6 and susceptible BALB/c mice, I found higher numbers of innate immune cells migrating from blood to the site of infection. The subsequent migration of dendritic cells (DCs) from the skin to the draining lymph node was also improved, thereby boosting the induction of the adaptive immune response. In C57BL/6 mice, JAM-C blockade after *L. major* injection led to an enhanced IFN- γ dominated T helper 1 (Th1) response with reduced skin lesions and parasite burden. Conversely, anti JAM-C treatment increased the IL-4-driven T helper 2 (Th2) response in BALB/c mice with disease exacerbation. Overall, my results show that JAM-C blockade can finely-tune the innate cell migration and accelerate the consequent immune response to *L. major* without changing the type of the T helper cell response.

2. Introduction

2.1. The inflammatory response: from pathogen sensing to leukocyte trafficking

2.1.1 Functions of the immune system

Our body has evolved a complex system made of cells and molecules known as the immune system. The main function of this system is to protect ourselves from pathogen-induced diseases. In this regard, the cells of our immune system, namely leukocytes, have been educated to discriminate between self and non-self signatures. Leukocytes learn to recognize our self molecules, and not to react against our own cells, a process referred to as immune tolerance. Conversely, any pathogens, including viruses, bacteria, prions, fungi, or protozoans are detected by leukocytes as foreign infectious agents that have to be eliminated. In this thesis, I will particularly focus on the case of the infection caused by the protozoan parasite *Leishmania major*, which will be the focus of the third chapter of this introduction.

2.1.2 Introducing inflammation

The first barrier that protects our body from external infectious agents is the epithelium lining our skin, and all the internal surfaces lining our respiratory, intestinal, or urogenital tracts. When such physical barriers are breached, the body is exposed to pathogens, which can potentially cause diseases. To eradicate invading pathogens, we inherit from our parents a complex system of defence made of cells and molecules known as the innate immunity. Its main feature is to recognise and clear pathogens very quickly. The first players of this sophisticated machinery are effector cells that constantly sense their local environment for non-self signatures coming from foreign organisms. Once they recognised a pathogen, they secrete cytokines that trigger vasodilatation of surrounding blood vessels to facilitate fluids leakage and extravasation of additional effector cells from the blood to the site of infection. Altogether, this innate immune reaction is called inflammation (**Figure 1**).

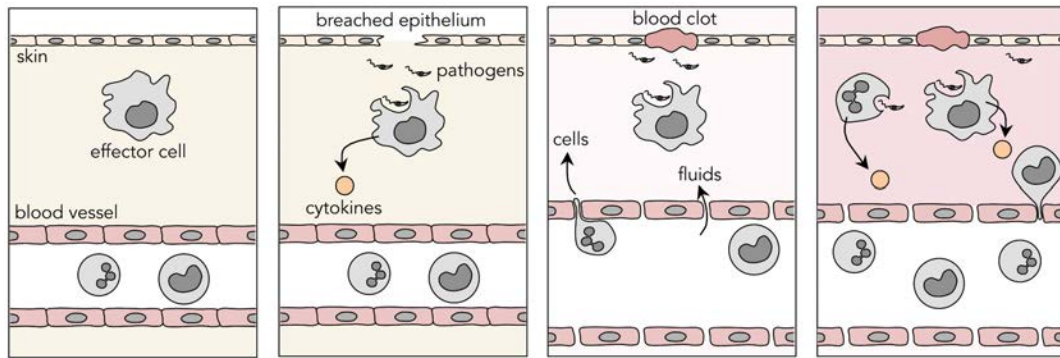


Figure 1. The inflammatory response to infection (Source : personal picture, adapted from Janeway's, Immunobiology)

In most of the cases, our innate immunity is sufficient to fight the infectious agents we face everyday. When the invading pathogen overtakes our innate immune defence, the innate immune cells alert lymphocytes, which adapt to and efficiently control the infection. This second line of defence is known as adaptive immunity, and will be discussed later through the fascinating example of *Leishmania major* model of cutaneous leishmaniasis.

2.1.3 Pathogen sensing

Contrary to what was originally thought, our innate immune system is not totally non-specific. It can make the difference between our self-signatures and many different Pathogen-Associated Molecular Patterns (**PAMPs**) using a broad set of Pathogen Recognition Receptors (PRRs). One important family of PRRs is the Toll-like Receptors family (**TLRs**), which includes 12 receptors in mammals [1]. TLRs are transmembrane proteins that are either expressed intracellularly (e.g. endosomes) or extracellularly at the cell surface. TLRs can be further subdivided depending on the PAMPs family they recognize: TLR1, TLR2, and TLR6 recognize lipids for instance, while TLR7, TLR8, and TLR9 recognize nucleic acids. Finally, some TLR can recognize different families of molecules, such as TLR4 that recognizes lipopolysacharride (LPS) from the membrane of gram-negative bacteria, and the respiratory syncytial virus (RSV) protein as well [1] (**Table 1**). TLRs are not restricted to innate immune cells such as neutrophils, macrophages or dendritic cells, they are also found on lymphocytes subsets. Interestingly, TLRs are also expressed by some stromal cells such as fibroblasts, pericytes, or endothelial cells, which are perfectly located within our tissue to sense pathogens and alert our immune system after pathogen invasion [1]. Engagement of any TLR with its specific ligand triggers the activation of complex signaling cascades, which ultimately leads to the production of pro-inflammatory cytokines. These cytokines activate the

surrounding innate immune effector cells for efficient pathogen killing, and more importantly triggers the recruitment of leukocytes to the site of infection [1].

Microbial Components	Species	TLR Usage
Bacteria		
LPS	Gram-negative bacteria	TLR4
Diacyl lipopeptides	<i>Mycoplasma</i>	TLR6/TLR2
Triacyl lipopeptides	Bacteria and mycobacteria	TLR1/TLR2
LTA	Group B <i>Streptococcus</i>	TLR6/TLR2
PG	Gram-positive bacteria	TLR2
Porins	<i>Neisseria</i>	TLR2
Lipoarabinomannan	Mycobacteria	TLR2
Flagellin	Flagellated bacteria	TLR5
CpG-DNA	Bacteria and mycobacteria	TLR9
ND	Uropathogenic bacteria	TLR11
Fungus		
Zyosan	<i>Saccharomyces cerevisiae</i>	TLR6/TLR2
Phospholipomannan	<i>Candida albicans</i>	TLR2
Mannan	<i>Candida albicans</i>	TLR4
Glucuronoxylomannan	<i>Cryptococcus neoformans</i>	TLR2 and TLR4
Parasites		
tGPI-mutin	<i>Trypanosoma</i>	TLR2
Glycoinositolphospholipids	<i>Trypanosoma</i>	TLR4
Hemozoin	<i>Plasmodium</i>	TLR9
Profilin-like molecule	<i>Toxoplasma gondii</i>	TLR11
Viruses		
DNA	Viruses	TLR9
dsRNA	Viruses	TLR3
ssRNA	RNA viruses	TLR7 and TLR8
Envelope proteins	RSV, MMTV	TLR4
Hemagglutinin protein	Measles virus	TLR2
ND	HCMV, HSV1	TLR2
Host		
Heat-shock protein 60, 70		TLR4
Fibrinogen		TLR4

ND = not determined. See text for references.

Table 1. TLR recognition of microbial components. Taken from [1].

2.1.4 The leukocyte adhesion cascade

The first evidence that blood cells could adhere to blood vessels and subsequently emigrate into tissues after inflammation was provided by intravital microscopy back in the nineteenth century [2]. In 1846, Augustus Waller stated: « Let us now examine the admirable manner in which nature has solved the apparent paradox, of eliminating, from a fluid circulating in closed tubes, certain particles floating in it, without causing any rupture or

perforation in the tubes » [3]. Strikingly, he set up an intravital microscopy setting to visualize cell movements in the frog tongue capillaries. He was likely the first to clearly observe leukocytes adhesion and transmigration (**Figure 2**).

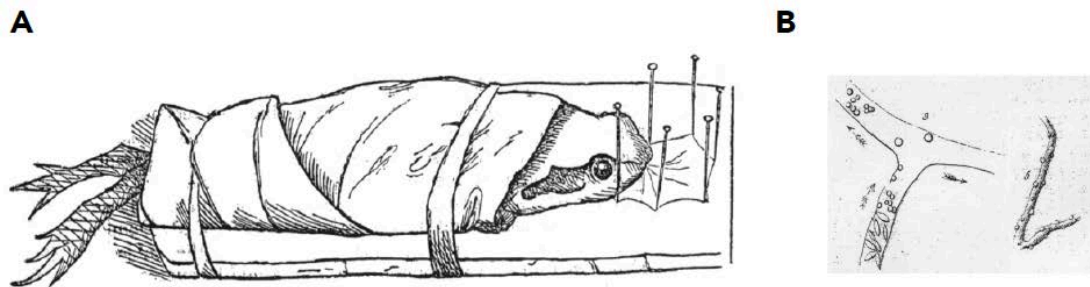


Figure 2. Waller's observations of frog capillaries in the 1840s. A) After unsuccessful attempts to observe the circulation in the prepuce of a human subject, Waller settled on the frog tongue as a window for observing the capillaries [3]. B) Leukocyte adhesion and transmigration as observed by Waller in the frog tongue. The legend reads as follows (referring first to the left, then the right image): "Blood-discs and corpuscles with a capillary; some of the latter near the sides were inspected for a long time, and remained fixed in the same situation, while a rapid current was traversing the vessel. ... Extra fibrination of a vessel. The smaller globules are probably globular particles of fibrine, the others are extravasated corpuscles". Text and figure adapted from [2].

A new step forward was made in the late eighties with the discovery of molecules acting in a sequential manner in the recruitment of leukocytes. The multi-step paradigm for leukocyte adhesion was born. The original model mentioned a three-steps cascade including rolling, activation, and firm adhesion [4,5]. Additional steps were described in the last two decades to complete our understanding of the leukocyte adhesion cascade [6].

In the updated adhesion cascade, leukocytes first tether and roll on the inflamed vasculature. Rolling then becomes slower and leukocytes subsequently activate to firmly adhere to the endothelium. Next, they start to crawl on the surface of the endothelium to either cross the endothelial barrier through junctions or directly through endothelial cells. In both cases, leukocytes still have to breach the basement membrane and finally swarm within the tissue (**Figure 3**). I will now describe each of these steps in details, whilst insisting on the case of neutrophils and monocytes, two key players of our innate immune responses against pathogens.

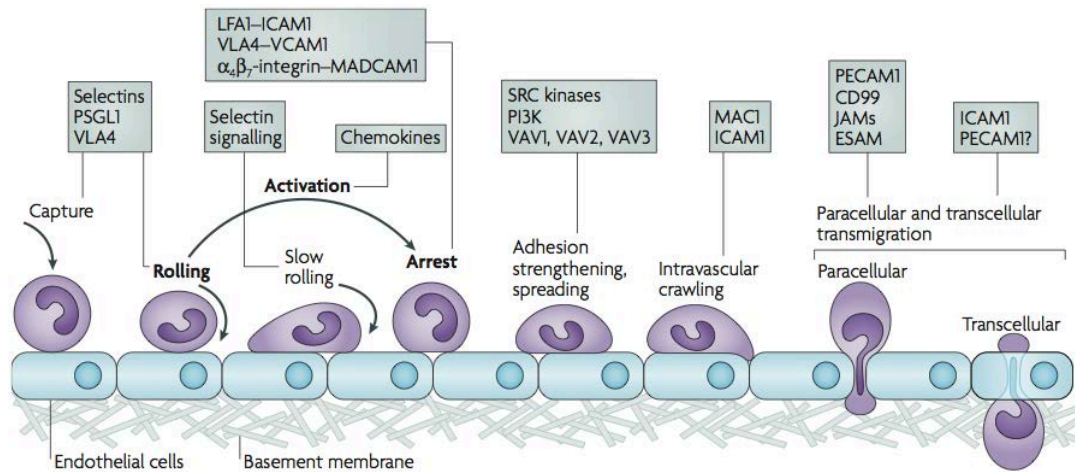


Figure 3. The updated leukocyte adhesion cascade. The original three steps are shown in bold: rolling, which is mediated by selectins, activation, which is mediated by chemokines, and arrest, which is mediated by integrins. Progress has been made in defining additional steps: capture (or tethering), slow rolling, adhesion strengthening and spreading, intravascular crawling, and paracellular and transcellular transmigration. Key molecules involved in each step are indicated in boxes. ESAM, endothelial cell-selective adhesion molecule; ICAM1, intercellular adhesion molecule 1; JAM, junctional adhesion molecule; LFA1, lymphocyte function-associated antigen 1 (also known as $\alpha_4\beta_2$ integrin); MAC1, macrophage antigen 1; MADCAM1, mucosal vascular addressin cell-adhesion molecule 1; PSGL1, P-selectin glycoprotein ligand 1; PECAM1, platelet/endothelial-cell adhesion molecule 1; PI3K, phosphoinositide 3-kinase; VCAM1, vascular cell-adhesion molecule 1; VLA4, very late antigen 4 (also known as $\alpha_4\beta_1$ -integrin). Text and figure taken from [6].

Tethering and rolling

The initial capture of circulating leukocytes to the lumen of the vasculature is mainly initiated by selectins (CD62) and their ligands. Selectins are named according to the cell type in which it was initially discovered: the first selectin discovered was **L-selectin** (CD62L) on Leukocytes [7], followed by **P-selectin** (CD62P), first observed on activated Platelets [8-10], and later found on endothelial cells [10,11]. The last one, **E-selectin** (CD62E), was exclusively observed on Endothelial cells [12-14].

Selectins are transmembrane molecules anchored to the cytoskeleton through their cytoplasmic domain [15-18] while their extracellular lectin domain mediates cell adhesion to fucosylated carbohydrate ligands similar to the sialyl Lewis^x determinant in a calcium dependent manner [19,20].

Although initially described as a P-selectin ligand, the P-Selectin Glycoprotein Ligand 1 (**PSGL1** or **CD162**) can bind all three selectins [21-26]. PSGL1 was originally found on leukocytes, but some later studies found the molecule on endothelial cells from lymph nodes, small intestine and atherosclerotic arteries where it mediates rolling of monocytes or T cells [27,28].

Leukocyte-expressed PSGL1 has two ways to induce rolling, either by interacting with endothelial P- or E-selectin, a process called primary rolling or tethering; or through leukocytes-expressed L-selectin to promote leukocyte-leukocyte interactions, a mechanism known as secondary rolling or tethering. The later amplifies the cascade of adhesion as adherent leukocytes can recruit further circulating leukocytes through the PSGL1/L-selectin interactions [29,30]. (**Figure 4**)

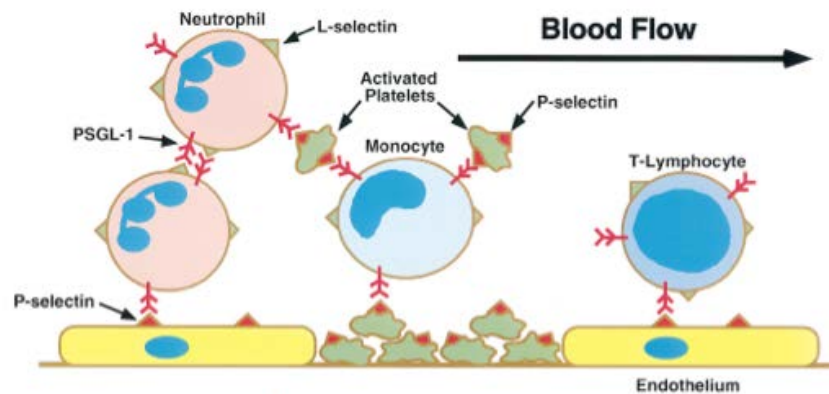


Figure 4. Multicellular interactions mediated by binding of PSGL-1 to P- and L-selectins under hydrodynamic flow. Binding of PSGL-1 to P-selectin promotes tethering and rolling of leukocytes on activated endothelial cells and platelets. Binding of PSGL-1 to L-selectin mediates tethering of leukocytes to other leukocytes, which may amplify recruitment of leukocytes to the vascular wall. Activated platelets, through P-selectin– PSGL-1 interactions, may connect additional leukocytes to sites of inflammation or tissue injury. Text and figure taken from [19].

In addition to PSGL1, L-selectin also binds a set of sialomucins molecules found in high endothelial venules (HEVs) of peripheral lymph nodes. For this reason, these molecules are known as Peripheral lymph Nodes Adressins (**PNAds**). It includes the Glycosylation-dependent Cell Adhesion Molecule (**GlyCAM1**) [31,32], **CD34** [32-34], and **podocalyxin** [35]. L-selectin also interacts with the mesenteric lymph nodes and Peyer’s patches expressed Mucosal Addressin Cell Adhesion Molecule (**MAdCAM1**) [36-38] (**Figure 5**).

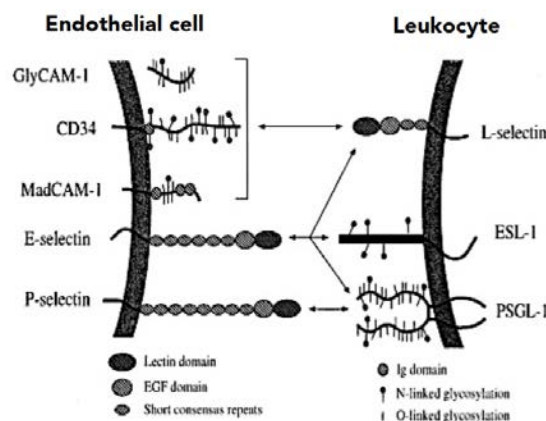


Figure 5. Selectin ligands that have been identified by affinity isolation with respective selectin as affinity probe. Except E-selectin ligand-1 (ESL-1), depicted ligands are sialomucins or contain at least a sialomucin domain.

L-selectin ligand mucosal addressin cell adhesion molecule- 1 (MAdCAM-1) was originally found as a ligand for integrin $\alpha_4\beta_7$. Sequencing revealed a sialomucin domain. A subpopulation of MAdCAM-1 molecules in high endothelial venule of mesenteric venules can indeed be expressed as an L-selectin binding glycoform, carrying posttranslational modifications that define peripheral node addressins. L-selectin is a major carbohydrate-presenting ligand for E-selectin on human neutrophils; however, L-selectin of human lymphocytes or mouse neutrophils is unable to bind E-selectin. P-selectin glycoprotein ligand-1 (PSGL-1) is the only selectin ligand so far that has been demonstrated to mediate leukocyte rolling on endothelium [39] and leukocyte recruitment into inflamed tissue in vivo [40,41]. Ig, immunoglobulin; GlyCAM-1, glycosylation-dependent cell adhesion molecule. Text and figure adapted from [42].

E-selectin also has a broad set of ligands, including L-selectin [43,44], the E-Selectin Ligand (**ESL1**) [45,46], and **CD44** [47,48]. In vivo, PSGL1, ESL1, and CD44 were shown to play distinct roles in the rolling of neutrophils to the inflamed endothelium [49] (**Figure 5**).

L-selectin is continuously expressed by leukocytes to facilitate leukocyte recirculation throughout the body [43,50,51]. Conversely, P-selectin is not expressed at the cell surface in absence of inflammatory stimuli. The molecule is stored in α -granules of platelets [8] or Weibel-Palade bodies of endothelial cells [11]. It is very rapidly expressed on cell surface upon stimulation where it plays a key role in rolling in the first hour of inflammation [8,11,52,53]. E-selectin is also induced after a stimuli challenge such as TNF- α or IL-1 β while its expression peaks a few hours after stimulation [12,13].

Strikingly, selectins and their ligands enable leukocyte rolling to the inflamed endothelium under conditions of high blood flow with strong shear stresses. This comes from the remarkable fast bond association/dissociation rates of selectins that allow the rapid and continuous formation of new bonds [54], and from the mechanical properties of the bonds to become stronger as the force applied augments (the so-called **catch bond**) [55].

The key role of selectins as the prerequisite step in the adhesion cascade was strengthened by the use of knock-out animals and blocking antibodies *in vivo*. Indeed, in mice deficient for P- and E-selectin, rolling, adhesion and emigration is totally impaired in models of sterile inflammations [56-58].

Finally, the binding of selectins to their ligands can, in addition to chemokines, trigger integrin activation on leukocytes. For instance, PSGL-1 engagement to P-selectin can induce the activation of the β_2 integrins $\alpha_L\beta_2$ (or Lymphocyte Function-associated Antigen 1, **LFA-1**, CD11a/CD18) and $\alpha_M\beta_2$ (or Macrophage antigen 1, **Mac-1**, CD11b/CD18) [59-62]. Similarly, neutrophil rolling on E-selectin was also reported to activate β_2 integrins for a firm cell adhesion [63-65].

Even though selectins are the most important rolling molecules, some members of the **integrin** family also participate in rolling or **slow rolling**. *In vitro*, the $\alpha_4\beta_7$ integrin induces rolling of T cells on recombinant MAdCAM1 [66], while chemokines potentiates the $\alpha_4\beta_1$ (or Very Late Antigen 4, **VLA4**) dependent rolling of T cells on endothelial Vascular Cell Adhesion Molecule 1 (**VCAM1**) [67,68]. The contribution of $\alpha_4\beta_1$ -dependent rolling was confirmed *in vivo* for CD8 T cells in inflamed venules [69]. In addition to α_4 integrins, the key role of the **β_2 integrins** in slow rolling is also well established. In particular, the intermediate affinity configuration of LFA-1 on leukocytes enables transient bindings to its vascular Intercellular Cell Adhesion Molecule 1 (**ICAM-1**) ligand on endothelial cells [70-72]. *In vivo*, the use of knock-out animals for LFA-1 and Mac-1 confirmed the role of both integrins to slow down the leukocyte rolling after a sterile inflammation [73].

Activation and firm adhesion

The firm attachment of circulating cells to the inflamed vasculature is mediated by the leukocytes-expressed **integrins** and their endothelial ligands. Integrins are cell surface-expressed heterodimers composed of one α and one β subunit. No less than 24 $\alpha\beta$ associations were identified to date in mammals [74,75]. Each leukocyte subset expresses at least one integrin from the β_2 family, even though each leukocyte has a specific sets of integrins. For instance, neutrophils mainly express β_2 integrins, but also β_1 and β_3 integrins at lower extents. Monocytes express β_1 and β_2 integrins. Conversely, lymphocytes can display β_1 , β_2 and β_7 depending on the subset [76].

In normal homeostasis, most leukocyte integrins are found in a non-activated, low affinity conformation [77], therefore preventing undesirable firm adhesion of leukocytes to the vasculature under steady state conditions. In order to display its pro-adhesive properties, integrins have to undergo conformational changes and/or accumulation into clusters at the cell surface, the combination of both being called **activation**. Indeed, activation enables integrins to switch from a **low affinity** bent conformation to extended conformations with intermediate or **high affinity** depending on whether the ligand-binding pocket is closed or open, respectively [78,79]. Conversely, the redistribution of integrins into clusters increases their **valency** [67,80-82]. Both mechanisms contribute to regulate the total **avidity** of integrins [67,74,83,84] (**Figure 6**).

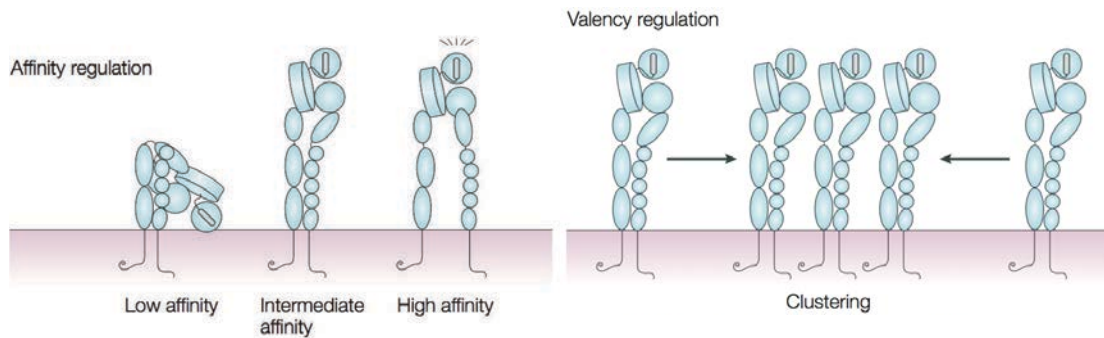


Figure 6. Integrin affinity and avidity. The left panel shows the different conformations of an integrin that are associated with distinct affinities: the bent head-piece conformation (low affinity), and the two extended head-piece conformations (intermediate affinity and high affinity). Intracellular activation signals induce a transition between these affinity states, which increases ligand binding. This process is known as affinity regulation of integrin avidity. The right panel shows clustering of integrins on the surface of a cell, which mediates multivalent interactions with ligands. This process is known as valency regulation of integrin avidity. (Although regulation of integrin avidity does not require changes in affinity, the schema depicts the extended conformation.). Text and figure adapted from [74].

As mentioned in the previous section, integrins activation can be mediated by selectins once they bound to their ligands. However, the most powerful activators of integrins are **chemokines**. They are relatively small molecules that can be secreted by cytokine-activated endothelial cells [85,86], stromal cells [87,88], platelets [89,90], or by leukocytes themselves [91]. In blood vessels, chemokines are sequestered by glycosaminoglycans (GAGs) on the luminal surface of endothelial cells to be ideally exposed to leukocytes [92-97]. Impairment of chemokine binding to GAGs disables leukocytes recruitment to sites of inflammation [97]. This shows the importance of chemokine sequestration by GAGs.

Chemokines activate integrins through their binding to G protein-coupled receptors (**GPCRs**) expressed by leukocytes. This binding induces an intracellular signalling pathway leading to integrin activation, a process referred as **inside-out** signalling. Strikingly, the structural rearrangement and redistribution of integrins occurs within milliseconds upon GPCRs ligation [67,84,98,99]. This inside-out signalling ultimately leads to the activation of small GTPase RAS-related Protein 1 (**RAP1**) [100]. Once activated, RAP1 associates with its effector protein RIAM to enable the actin binding protein **Talin-1** ligation to the cytoplasmic tail of the β chain [101]. This enables the unfolding of the α and β tails that finally shifts the integrin to its extended form [102,103] (**Figure 7**). Talin-1 knockdown studies further highlighted the role of Talin-1 as the common final step in integrin activation [104]. Growing evidences showed that kindlins, an additional family of actin binding

proteins, do also ligate the β subunit, and efficiently cooperate with talin-1 in the final step of integrin activation [105,106].

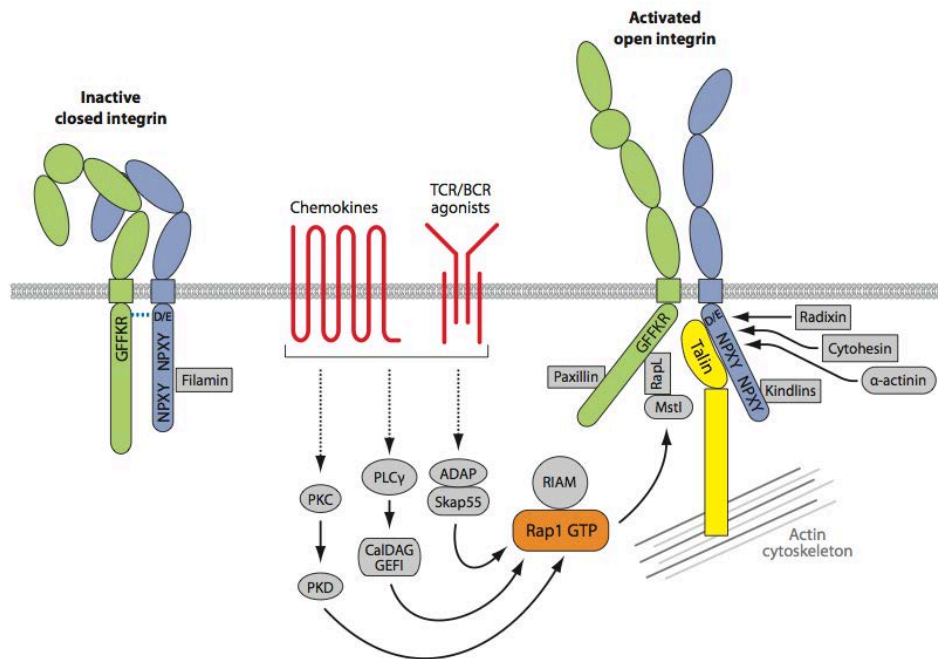


Figure 7. Integrin inside-out signaling. The figure outlines the key signaling events that occur downstream of chemokine and T and B cell receptors that lead to integrin activation. Inactive integrins exist in a bent conformation, and the α and β cytoplasmic tails are held in close proximity by a salt bridge between residues found in the membrane-proximal region of the tail. Activation of a variety of signaling pathways results in the recruitment of GTP-bound Rap1 and activated talin to the integrin, leading to tail separation. The conformational change in the cytoplasmic region is transmitted through the integrin transmembrane domain and results in structural changes in the extracellular region, leading to an open conformation that can bind ligand with high affinity. The C-terminal rod domain of talin interacts with the actin cytoskeleton to provide physical coupling of the integrin to the actin network of the cell. Many other molecules interact with integrin cytoplasmic tails, but exactly how these interactions are coordinated with integrin activation is unclear. Text and figure taken from [107].

Even though chemokines rapidly trigger the activation of integrins, this inside-out signalling is transient and not sufficient for prolonged adhesion of leukocytes to the inflamed endothelium. Fortunately, the binding of integrins to their endothelial ligand produces intracellular signals referred as **outside-in** signalling, leading to firm cell adhesion and cell spreading after cytoskeletal rearrangement [107]. It is widely believed that the clustering of integrins resulting from the multivalent ligand binding is required for efficient outside-in signalling [108-110]. Interestingly, ligand binding induces the separation of the α and β transmembrane and cytoplasmic domains, a step required for outside-in signalling [102,111]. In absence of this signal, neutrophils rapidly detach after initial arrest on endothelial cells under flow conditions [112]. The outside-in signalling is a complex cascade of biological events that ends with the modulation of the actin cytoskeleton (**Figure 8**).

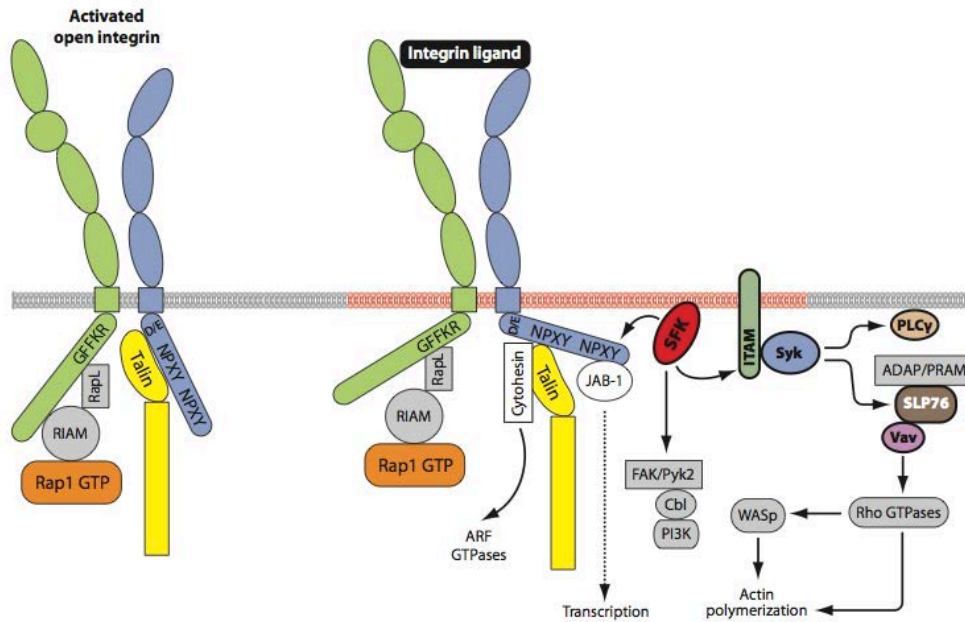


Figure 8. Integrin outside-in signaling. The figure details integrin-mediated signaling events that occur downstream of ligand binding. Zhu et al. [111] have shown that outside-in signaling requires structural changes with the cytoplasmic region of integrin tails. Activation of Src family kinases (SFKs) is a key step (although the exact mechanism by which this occurs is unclear) and results in phosphorylation of a variety of downstream molecules. These include ITAM-containing adapters that, when phosphorylated, lead to the recruitment and activation of Syk or ZAP-70 kinases. These kinases in turn phosphorylate various substrates, including SLP76 and Vav. This leads us to propose that integrin outside-in signaling is analogous to signaling downstream of immunoreceptors, as indicated by the molecules in bold [113,114]. Vav activates Rho GTPases, leading to actin cytoskeletal reorganization. SFKs can also activate FAK (focal adhesion kinase) and Pyk2 kinases, leading to Cbl phosphorylation and recruitment and activation of PI3K. Association of other molecules such as JAB (Jun-activating binding protein) and cytohesin with the integrin cytoplasmic tails activates other downstream signaling pathways. In this figure, signaling is depicted as happening in lipid rafts (indicated as red coloration in the membrane), although the role of rafts in integrin signaling differs in various cell types. Text and figure taken from [107].

Among the wide set of proteins activated in this pathway, the key role of the **Vav** family of Guanine Exchange Factor (GEF) has been well elucidated. Indeed, neutrophils lacking Vav1 and Vav3 have a similar tendency to detach from the endothelium *in vitro* and *in vivo* [115]. Altogether, these findings clearly illustrate the role of ligand-induced signalling in **adhesion strengthening**.

Within the very broad repertoire of integrins, four of them were shown *in vitro* or *in vivo* to be key mediators of the firm arrest of leukocytes: **LFA1** ($\alpha_L\beta_2$, CD11a/CD18), **Mac1** ($\alpha_M\beta_2$, CD11b:CD18), **VLA4** ($\alpha_4\beta_1$, CD49d/CD29) and **$\alpha_4\beta_7$** (Lymphocyte Peyer's patch Adhesion Molecule, LPAM1).

Indeed, **$\alpha_4\beta_7$** binding to MAdCAM1 is required for lymphocytes arrest on Peyer's patches high endothelial venules *in vivo* [116], in addition to mediate T cell rolling *in vitro* [66] as mentioned previously. The important role of **VLA4**, and its major endothelial counter-receptor **VCAM1**, on monocytes and lymphocytes arrest was well established *in vitro* under flow on Human

Umbilical Vein Endothelial Cells (HUVECs) [117-120]. These experiments used blocking antibodies to show that **VLA4**, together with β_2 integrins, controls monocytes arrest on inflamed endothelium. The contribution of the **β_2 integrins** on leukocyte arrest was further investigated using the β_2 deficient mice. The adhesion of leukocytes *in vivo* on inflamed venules was strikingly impaired in these animals [121], therefore reducing the migration of neutrophils to the inflamed skin for instance [122]. To better understand the distinct role of the two major β_2 integrins **LFA1** and **Mac1** in neutrophil adhesion, Mac1 and LFA1 knock-out mice were generated. This unravelled the predominant role of LFA1 over Mac1 in the firm adhesion of neutrophils to their main endothelial ligand ICAM1 [123]. It is worth noting that if the β_2 -dependent adhesion of leukocytes mainly requires **ICAM1** as the major endothelial counter-receptor, ICAM1 remains dispensable in some rare cases such as in lung homing [124].

Polarization and crawling

The bidirectional cues delivered by chemokines and integrin ligands induce the reorganization of the actin cytoskeleton and the redistribution of cell surface molecules. This enables cell **polarization**, which is the transformation of the cell from a round shape, to a polarized elongated “amoeboid” form with two distinct poles: the leading edge at the front, and the uropod at the back [125]. Polarization is a prerequisite for the cell to randomly slowly crawl on the endothelium and sense preferential sites for transmigration. This characteristic movement of polarized cells is called indifferently locomotion, **crawling**, or patrolling.

Even though leukocytes crawling was already described decades ago [126], its underlying mechanisms started to unravel within the last ten years [127]. In inflammatory monocytes (CD11b⁺ CD115⁺ Ly6c⁺), both **LFA1** and **Mac1**, together with their endothelial ligands ICAM1 and ICAM2, were shown to control the crawling to inter-endothelial junctions [128]. The picture is rather different in resident monocytes (CD11b⁺ CD115⁺ Ly6c⁻), an amazing subset of monocytes that constantly patrols along the resting vasculature [129]. Contrary to inflammatory monocytes, the patrolling of resident monocytes is **LFA1**-dependent. Moreover, mice lacking the chemokine receptor CX₃CR1 have reduced numbers of adhering and patrolling resident monocytes, which reinforces the role of GPCRs in the activation of integrins [129].

In neutrophils however, crawling was only **Mac1** and ICAM1 dependent, while the role of LFA1 in this process was only marginal [130]. Therefore, if

LFA1 overshadows Mac1 for neutrophil firm adhesion [123], then Mac1 has the best actor award for neutrophil subsequent crawling [130]. This is likely due to the cytoskeletal rearrangement and the Mac1 activation that follow LFA1-dependent outside-in signalling [131,132]. In line with this hypothesis, crawling was also impaired in neutrophils deficient for **Vav1** [133], a key molecule in LFA-1 induced cytoskeletal rearrangement [131].

Finally, the mechanisms of T cell crawling were also elucidated *in vitro*. It is mediated by LFA-1 on the cell surface, and requires the activation of RAP1 [134].

Transendothelial cell migration

After all these efforts to firmly adhere to the vessel wall, leukocytes have yet to face the challenge of going through the vessel wall, a process called **transendothelial cell migration** (TEM), transmigration or **diapedesis**. This final step is absolutely fascinating and intriguing. The first particularity of this process is that leukocytes can take two different routes to transmigrate, either through junctions between endothelial cells (paracellular pathway) or directly through the body of endothelial cells (transcellular pathway). In the first case scenario, leukocytes still have two choices: crossing through **bicellular**, or **multicellular** (3 or more) junctions [135].

All these pathways were observed *in vitro*, at different ratios depending on the model used [136]. This obviously resulted in intense debates regarding the preferential pathway followed by leukocytes [136]. Recently, the use of intravital microscopy provided clear answers, at least for myeloid cells. About 90% of neutrophils pass the endothelial barrier through junctions in a stimulus-independent manner [137]. This process takes approximately 5-8 minutes and is equally distributed between bicellular and multicellular junctions in terms of numbers of events analysed [137]. One should also take into account the surface of each structure. Indeed, the apical surface of endothelial cells being larger than bicellular junctions, itself being larger than multicellular junctions, these data highly suggest that the paracellular pathway between multicellular junctions is the preferential route for transmigration (**Figure 9**).

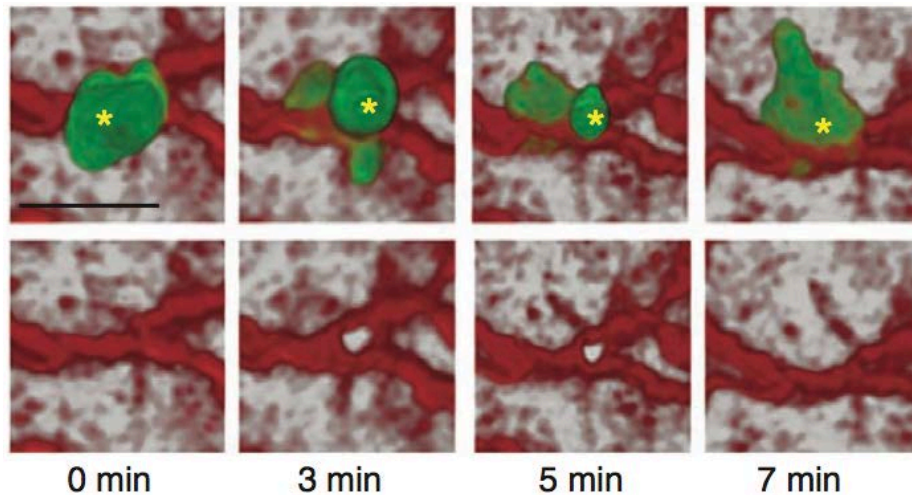


Figure 9. Neutrophil paracellular TEM in vivo. Paracellular TEM of a leukocyte (*; top row) and its associated transient junctional pore formation (bottom row) in IL-1 β -stimulated, PECAM-1-labeled tissues (red) of lys-EGFP-k mice (leukocytes, green; time (below images)). Text and legend adapted from [137].

Leukocyte **crawling** facilitates the paracellular pathway as random locomotion enables leukocytes to reach junctions [130]. Interestingly, when crawling is impaired, leukocytes cannot move efficiently to junctions and therefore preferentially use the transcellular pathway [130].

The **ICAM-1** dependent crawling is not only important to guide the leukocyte to the junction, but it also prepares the cell for its contraction and junctional opening. Indeed, ICAM-1 ligation induces a cascade of intracellular signals through its cytoplasmic domains, including the RHO GTPase activation and intracellular calcium flux [138,139]. This activates the myosin light-chain kinase (MLCK) that unfolds myosin 2 and leads to cell contraction [138,140]. Moreover, ICAM-1 is also involved in the formation of intriguing structures, the “**transmigratory cups**”. These structures look like endothelial domes rich in ICAM-1, VCAM-1, and cytoskeletal proteins used by leukocytes for docking [141,142]. In some situations, these cups can encapsulate the cell between two junctional seals, therefore decreasing vascular permeability [143] (**Figure 10**).

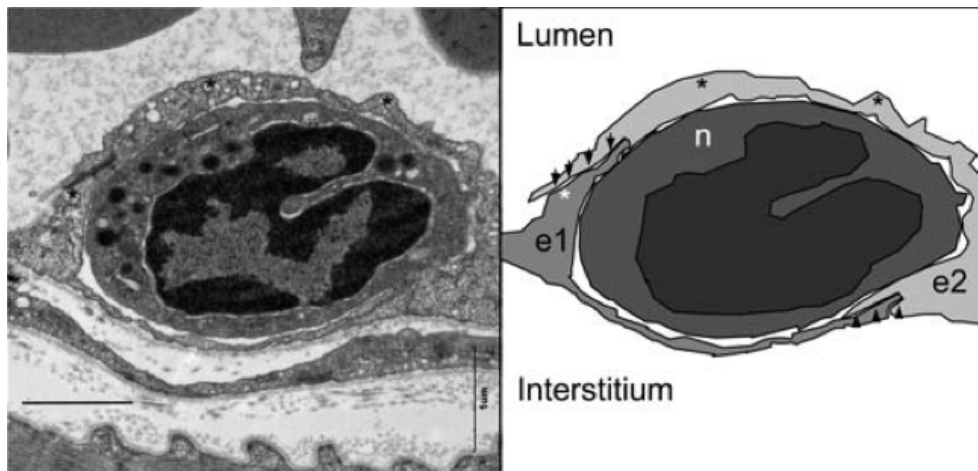


Figure 10. Endothelial encapsulation of transmigrating neutrophils. Electron micrograph and cartoon of transmigrating wild-type neutrophils. The arrowheads mark the junctions, the thin endothelial sheet that covers the transmigrating cells is marked with *, e1, e2 and n represent individual endothelial cells and neutrophils respectively. Scale bars correspond to 1 μ m. The images represent 1 out of 40 analyzed wild-type neutrophils. Text and figure adapted from [143].

With the exception of ICAM-1, uniformly expressed on the surface of endothelial cells, all the molecules that control the paracellular transmigration are located at junctions. In blood vessels, the endothelial cell junctional regions are composed of two types of junctions: the **adherens junctions** that maintain the cell integrity through its link to the cytoskeleton, and the **tight junctions** that constitute an impermeable cell barrier [144]. I will now describe all the players that mediate the **paracellular pathway** except the members of the Junctional Adhesion Molecules (JAMs) family, which will be fully reviewed in the next chapter.

The first molecule that was proposed to regulate transendothelial cell migration was the Platelet Endothelial Cell Adhesion Molecule 1 (PECAM-1, or CD31) [145,146]. **PECAM-1** belongs to the immunoglobulin superfamily and contains 6 immunoglobulin-like domains. In addition to be highly expressed at inter-endothelial cell junctions, PECAM-1 was also found on platelets, neutrophils, monocytes and subsets of lymphocytes [136,140]. PECAM-1 mainly engages homophilic interactions with leukocytes-expressed or endothelium-expressed PECAM-1, even though heterophilic interactions were also described [147]. The cytoplasmic tail of PECAM-1 contains an Immunoreceptor Tyrosine-based Inhibitory Motif (ITIM) that mediated most of its biological functions, among which the control of vascular permeability [148-152]. PECAM-1 acts at two different steps during diapedesis. The first step requires the amino terminal portion of PECAM-1 that plays the role of an adhesion molecule. The blockade of the amino terminal portion with antibodies or soluble forms of PECAM-1 almost completely abolish leukocytes diapedesis *in vitro* [153,154] or *in vivo* [155-157]. Interestingly, at

this first step, leukocytes still adhere but can not cross the endothelial barrier [153,154] (**Figure 11**).

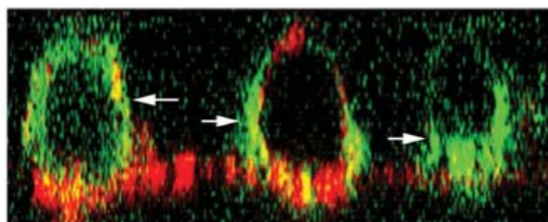


Figure 11. Monoclonal antibodies against PECAM-1 blocking leukocyte arrest at step 1. Transmigration assays were run for 1 h in the presence of antibodies to PECAM-1. The cells were then fixed, stained to visualize the endothelial monolayers (CD99, red) or monocytes (CD14, green) and examined by confocal microscopy. A series of images was recorded as a stack in the x-y plane parallel to the endothelial monolayer. z-series reconstructions of representative areas of the monolayers, which provide a cross-sectional view along a single x-z plane, are shown. The red signal was amplified to delineate the endothelial monolayer in nonjunctional areas. The apical surface of the monolayer is facing upwards. Arrows indicate monocytes arrested on the apical surface. Text and legend adapted from [158].

The second step that PECAM-1 controls is the migration of leukocytes through the subendothelial basal lamina. The homophilic ligation of PECAM-1 on neutrophils upregulates the $\alpha_6\beta_1$ integrin that is required for leukocyte migration through the basement membrane [159]. Antibodies against the $\alpha_6\beta_1$ integrin blocks leukocytes between endothelium and the perivascular basement membrane, a phenotype similarly observed in PECAM-1 knock-out animals [159-161] (**Figure 12**). This second step requires the membrane-proximal region of PECAM-1 as antibodies against this domain also results in leukocytes being stuck below the endothelium [154].

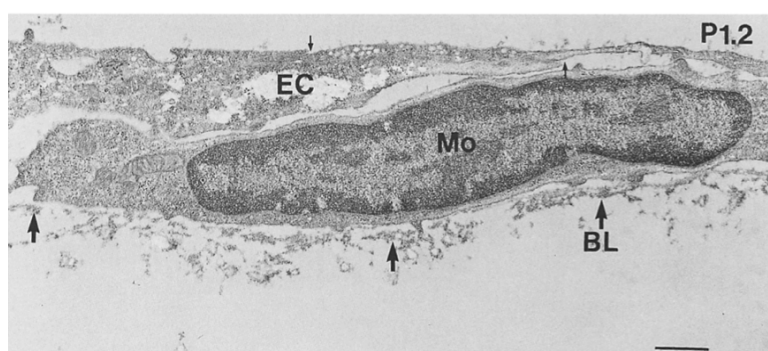


Figure 12. Monoclonal antibodies against PECAM-1 blocking leukocyte arrest at step 2. Monocytes were allowed to interact with HEC monolayers for two hours in the presence of anti-PECAM mAb P1.2 at 20 $\mu\text{g/ml}$ final concentration. Monolayers were then fixed and processed for electron microscopy. The picture shows the appearance of typical monocytes still in contact with the under surface of the EC in the presence of anti-domain 6 mAb P1.2. They have migrated through the interendothelial junction (small arrows) and lie between the basal surface of the EC and the endothelial basal lamina (BL, large arrows). Note filopodia probing through the BL into the underlying collagen gel, which extends well beyond the field of this photograph. Bar, 1 μm . Text and figure adapted from [154].

CD99 is a small transmembrane molecule, highly glycosylated, with a unique structure that does not belong to any family of proteins currently known [162]. CD99 was initially observed on most hematopoietic cells [136,140]. Strikingly enough, the expression of CD99 at the borders of endothelial cells, and its function in the transmigration of leukocytes was described for the first time more than ten years after its discovery in 1989 [158]. Yet, its role on the diapedesis of many leukocyte subsets is spectacular [158,163,164]. CD99 blockade on endothelial cells and/or leukocytes impairs 80% of human neutrophils or monocytes transmigration through HUVECs [158,164], and also prevents T cell migration to the skin *in vivo* [163]. CD99 functions in a homophilic manner similarly to PECAM-1. However, CD99 acts at a different level than PECAM-1 in the transmigration process [158]. Indeed, CD99 blockade leads to monocytes arrest part way through junctions, the leading edge being below the junctions while the trailing edge still within the lumen. In other words, CD99 acts just in between the two steps of PECAM-1 described earlier (**Figure 13**). Consequently, the effect of PECAM-1 and CD99 blockade is additive and almost completely abolishes transmigration [158]. One young relative of CD99 is the CD99 antigen-like 2 (**CD99L2**) [165]. CD99L2 is expressed by endothelial cells, circulating B and T cells, and neutrophils [166]. Some evidences suggest that CD99L2 acts during the same step as CD99 [167], and facilitates the extravasation of neutrophils *in vivo* [166]. However, the recent use of CD99L2 knock out chimeras suggested that the endothelial CD99L2, but not leukocytes CD99L2, controls the extravasation of leukocytes [168].

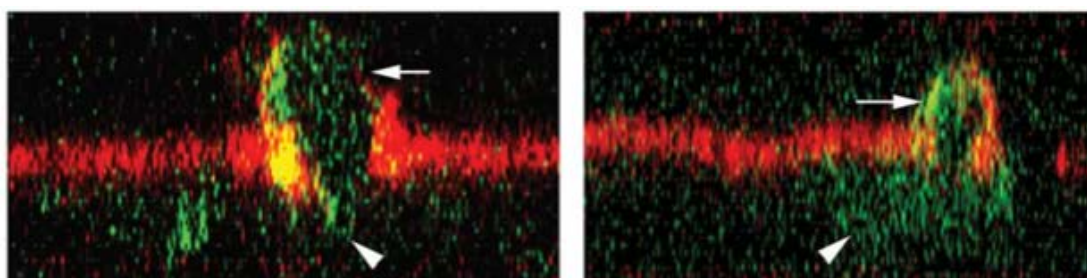


Figure 13. Blocking CD99 arrests monocytes part way through the endothelial cell junction. Transmigration assays were run for 1 h in the presence of antibodies to CD99. The cells were then fixed, stained to visualize the endothelial monolayers (CD99, red) or monocytes (CD14, green) and examined by confocal microscopy. A series of images was recorded as a stack in the x-y plane parallel to the endothelial monolayer. z-series reconstructions of representative areas of the monolayers, which provide a cross-sectional view along a single x-z plane, are shown. The red signal was amplified to delineate the endothelial monolayer in nonjunctional areas. The apical surface of the monolayer is facing upwards. Arrows indicate the portion of the monocytes above the monolayer. Arrowheads indicate a portion of monocytes below the HUVEC monolayer. Text and legend adapted from [158].

Vascular Endothelial cadherin (**VE-cadherin**) is the major component of the adherens junctions between endothelial cells. VE-cadherin forms a complex with catenins to link with the actin cytoskeleton [136,169]. By the time of the discovery, its key function in maintaining cell-cell contacts was already

observed as vascular permeability increases after antibody blockade [170]. Real time imaging of a fluorescent VE-cadherin construct in HUVECs clearly showed that VE-cadherin was transiently removed from the junctions at the time of leukocyte transmigration [171,172]. In line with these *in vitro* studies, the administration of blocking antibodies redistributes VE-cadherin out of cell-cell contacts [173], which destabilizes the junctions and leads to increased vascular permeability and leukocyte extravasation *in vivo* [173,174]. Conversely, stabilizing the adhesive properties of VE-cadherin in knock-in animals significantly reduces vascular permeability and leukocyte extravasation in response to inflammation [175,176]. Altogether, this suggests that VE-cadherin homophilic interactions act as a barrier that opens for diapedesis and closes subsequently to stabilize the junctions.

Since its cloning in 1989 [177], **ICAM-2** has often been overshadowed by his old brother ICAM-1 discovered three years before [178]. In addition to their homologies and shared β_2 integrin ligands, ICAM-2 was first believed to function in concert with ICAM-1 to promote transmigration [179-181]. Even though both molecules have overlapping functions, ICAM-2 displays specific functions as well. First, ICAM-2 is constitutively expressed by endothelial cells, and not inducible upon inflammation contrary to ICAM-1 [182]. Interestingly, while ICAM-1 is uniformly expressed at the surface of endothelial cells [183], ICAM-2 is mainly localized at junctions [184], which suggests a role for transmigration rather than adhesion. In line with this observation, neutrophil transmigration is impaired when ICAM-2 is blocked or genetically deleted, while adhesion is unchanged [184]. Recently, two studies showed that ICAM-2 also facilitates the intraluminal leukocyte crawling that precedes paracellular or transcellular diapedesis [185,186].

Some additional, but not less important players were described lately. For instance, monocytes use DNAM-1 to interact with the endothelial poliovirus receptor (**PVR**). Even though DNAM-1 or PVR blockade impair monocytes transmigration, this interaction seems to be involved in adhesion, which is a prerequisite for the subsequent transmigration [187]. Moreover, the endothelial but not neutrophil Leukocyte Specific Protein 1 (**LSP1**) is also believed to facilitate neutrophil extravasation *in vivo* [188], potentially through its role in the formation of the transmigratory cups [189]. Similarly, the endothelial integrin-associated protein **CD47**, but not leukocyte CD47, participates in T cell recruitment *in vivo*, either by regulating LFA1 and VLA4 adhesive properties [190], or by promoting the phosphorylation of a VE-cadherin residue that controls diapedesis [191].

In addition to the paracellular pathway, the first indisputable *in vivo* evidence of leukocyte **transcellular migration** was provided in 1998 [192]. Since then, many studies also reported migration through endothelial cells as a minor, but yet reliable pathway to extravasate [193]. This migration pathway is initiated by the striking palpation/probing of the endothelial cell surfaces by leukocyte extensions called **podosomes** [194]. At the same time, ICAM-1 clustering at the cell surface leads to its translocation into **caveolae**, which are small vesicles made by lipid rafts for intracellular molecule transport. These ICAM-1-rich caveolae associate with actin to surround and interact with the leukocyte podosomes through ICAM-1 binding. Finally, the translocation of the actin and ICAM-1-rich caveolae to the basal membrane creates a channel that guides the leukocyte through the body of the endothelial cell [194,195] (**Figure 14**). Recently, it was suggested that transcellular migration also requires additional vesicles rich in PECAM-1, CD99, and JAM-A, the so-called Lateral Border Recycling Compartments (**LBRCs**). Indeed, the blockade of PECAM-1 and CD99 blocks the transcellular pathway, so as the depolymerisation of microtubules [196]. The same investigators had also previously reported the role of LBRCs in the paracellular pathway [197,198], therefore proposing LBRCs a unifying model of transmigration [193].

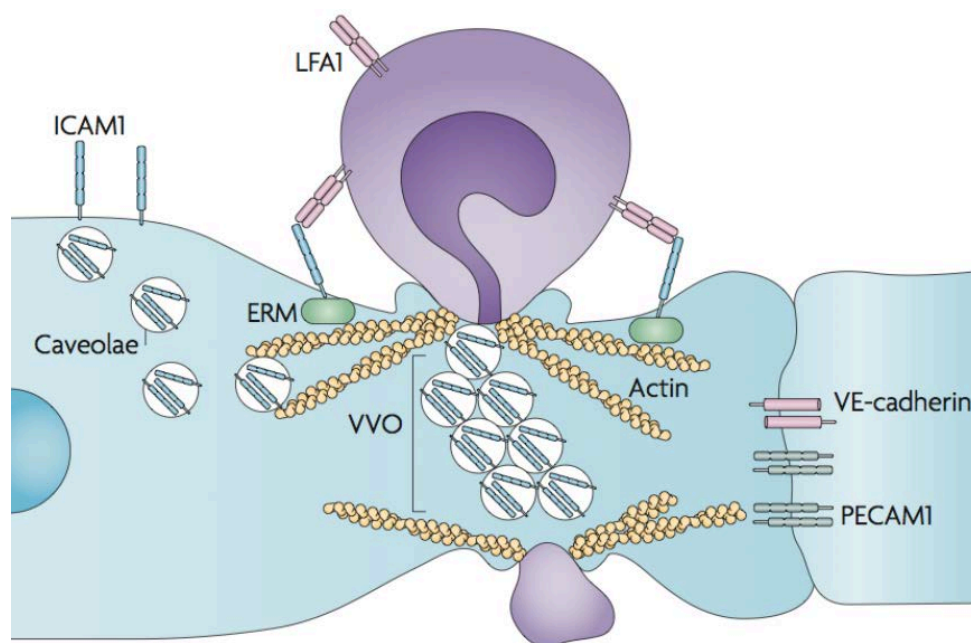


Figure 14. Transcellular migration of leukocyte. Transcellular migration occurs in 'thin' parts of the endothelium, and therefore there is less distance for a leukocyte to migrate. ICAM1 ligation leads to translocation of ICAM1 to actin- and caveolae-rich regions. ICAM1-containing caveolae link together forming vesiculo-vacuolar organelles (VVOs) that form an intracellular channel through which a leukocyte can migrate. Ezrin, radixin and moesin (ERM) proteins could act as linkers between ICAM1 and cytoskeletal proteins (such as actin and vimentin), causing their localization around the channel, thereby providing structural support for the cell under these conditions. Text and figure adapted from [6].

Migration through the pericyte layer and basement membrane

The endothelial barrier being crossed, leukocytes have to find their way through the pericyte sheath and the basement membrane that surrounds the vasculature. Pericytes are contractile cells that have many physiological functions such as the regulation of the blood flow or the formation of new blood vessels. Pericytes are embedded in the basement membrane, which consists of matrix and not a membrane, contrary to what its name suggests. Indeed, the basement membrane is made of two distinct networks, one of type IV collagen and one of laminins, bridged together with the glycoproteins nidogen-2 and perlecan [199] (**Figure 15**).

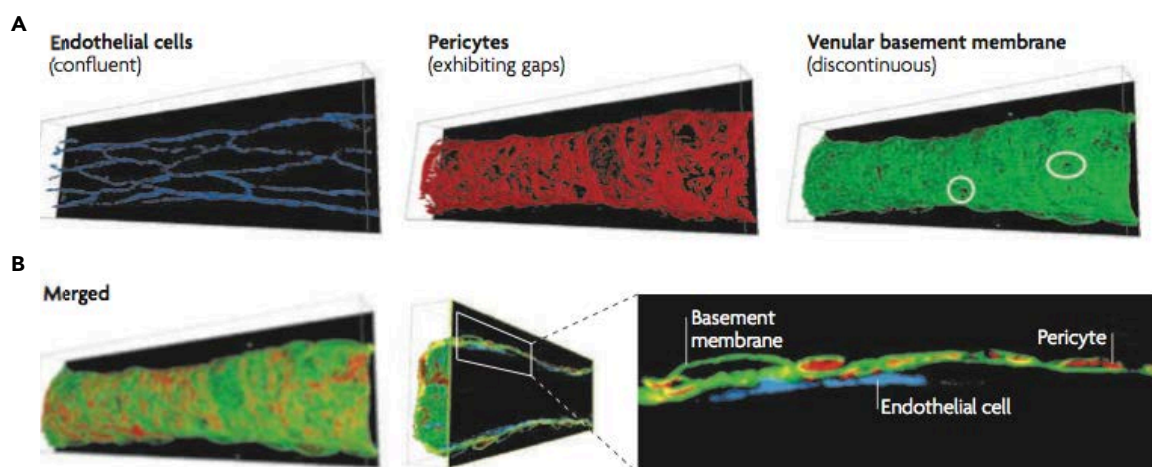


Figure 15. The pericyte layer and the basement membrane. A) Confocal microscopy images acquired from a cremasteric venule that is triple immunofluorescently stained for different components of the venular wall: endothelial cells (labelled for PECAM1), pericytes (labelled for α -SMA) and the venular basement membrane (labelled for laminin). The images show the different expression profiles of these structures: endothelial cells (which are confluent), pericytes (which exhibit gaps between adjacent cells) and a heterogeneous expression profile of basement membrane matrix protein (with low-expression regions; examples indicated with white circles). B) Analysis of the triple-stained venular wall cross-section illustrates the relative localization of the vessel wall components: endothelial cells line the lumen and pericytes are embedded in the venular basement membrane that is generated as a result of the combined deposition of matrix proteins by both endothelial cells and pericytes. Text and figure adapted from [200].

I have already mentioned that ligation of PECAM-1 at the time of the transmigration upregulates expression of integrin $\alpha_6\beta_1$ on neutrophils. Interestingly, $\alpha_6\beta_1$ is the main leukocyte receptor for laminin [159,201]. Therefore, the PECAM-1 dependent upregulation of $\alpha_6\beta_1$ is a first mechanism for neutrophils to interact with the basement membrane to ultimately reach the tissue. In a similar way, engagement of β_2 integrins on human neutrophils can induce the expression of β_1 integrins that are important for migration through the extracellular matrix [202].

A few years after these observations, the simple examination of basement membrane from unstimulated venules leads to a key finding: the existence of

Low Expression Regions (LERs) for collagen IV and laminin $\alpha_5\beta_1\gamma_1$ (old nomenclature was laminin 10), which coincide with gaps between pericytes [203,204]. As pericytes control the basement membrane assembly [205], they may also regulate its remodeling to facilitate neutrophil extravasation [206]. Indeed, neutrophils were shown to preferentially use these gaps to migrate through the basement membrane [203]. This finding was then extended to monocytes [207]. Contrary to the latter, neutrophils enlarged the preexisting gaps of α_5 but not α_4 laminin during their migration, a process that likely involves neutrophil proteases such as elastase [203]. In line with this hypothesis, neutrophil elastase efficiently cleaves laminins to generate membrane gaps and laminin fragments with chemotactic properties [208,209]. Therefore, neutrophil proteases may facilitate LER enlargement and produce chemotactic cues to guide neutrophils [200].

2.1.5 The interstitial migration toward the pathogen

The interstitial migration implies that leukocytes move in the three-dimensional (3D) surrounding tissue, which can be either the extracellular matrix, or the organs parenchymae. This completely differs from the two-dimensional (2D) migration of leukocytes on the luminal surface of blood vessels described before. Indeed, the locomotion of leukocytes on 2D surfaces requires adhesive forces, mainly driven by integrins. In contrast, 3D locomotion is rather low adhesive, fast, does not degrade tissue, and seems to follow paths of least resistance [200,210-212]. There is yet a common feature between 2D and 3D locomotion, the polarized amoeboid-like movement adopted by leukocytes to squeeze and move through the interstitial space. This requires extensive morphological changes and reorganization of the cytoskeleton, which are here again mediated by chemokines, or other chemoattracting molecules signaling through GPCRs [200,210-212].

Interestingly, such signals do not only trigger polarization but also serve as molecular cues to guide the cell until its final destination within the tissue (chemotaxis). Hence, the name chemokine stems from **chemotactic cytokine**. However, the question arises how can leukocytes be told to extravasate without receiving superior chemotactic cues from the tissue that would overshadow intraluminal chemotactic signals [213]? Strikingly, this is exactly what happens, at least for neutrophils [213]. Indeed, it is well accepted that neutrophils establish an intracellular hierarchy of signals, preferentially choosing one direction when facing two opposite chemotactic gradients *in*

vitro [214-216]. These superior chemotactic cues are referred as **end-target signals**, and include the complement component C5a or formyl peptides (fMLP) produced by bacteria or mitochondria from dead cells. These findings were recently confirmed *in vivo* in a mouse model of focal hepatic necrosis [213]. In this model, neutrophils use an intraluminal gradient of CXCL2 to migrate through blood vessel as close as two hundreds microns apart from the site of injury. From here, neutrophils extravasate and follow a gradient of formyl peptides released by the necrotic cells to reach the site of injury [213]. In addition to the end-target signals released at the site of inflammation that control the recruitment of an initial wave of neutrophils, neutrophils themselves can produce leukotriene B4 (LTB4), a potent chemoattractant that amplifies neutrophil swarming to the site of injury [217].

Two main intracellular forces govern the deformability of leukocytes essential for squeezing, namely the actin polymerization and the myosin-II-dependent contraction. The **actin polymerization** is a force that deforms the plasma membrane at the leading edge to create protrusions on leukocytes such as the dendrites of dendritic cells to sense the local environment. On the other hand, the **myosin-II dependent contraction** at the trailing edge detaches the back from any adhesive support and propels the cytoplasmic content to the front of the cell [200,210,211]. These two forces are well coordinated to control cell motility (**Figure 16**). Impairment of key molecules that regulate both intracellular pathways result in significantly reduced cell movement [200,210,211,218]. However, myosin contraction may not be always required for efficient cell motility contrary to actin polymerization, especially in loose interstitial spaces [219].

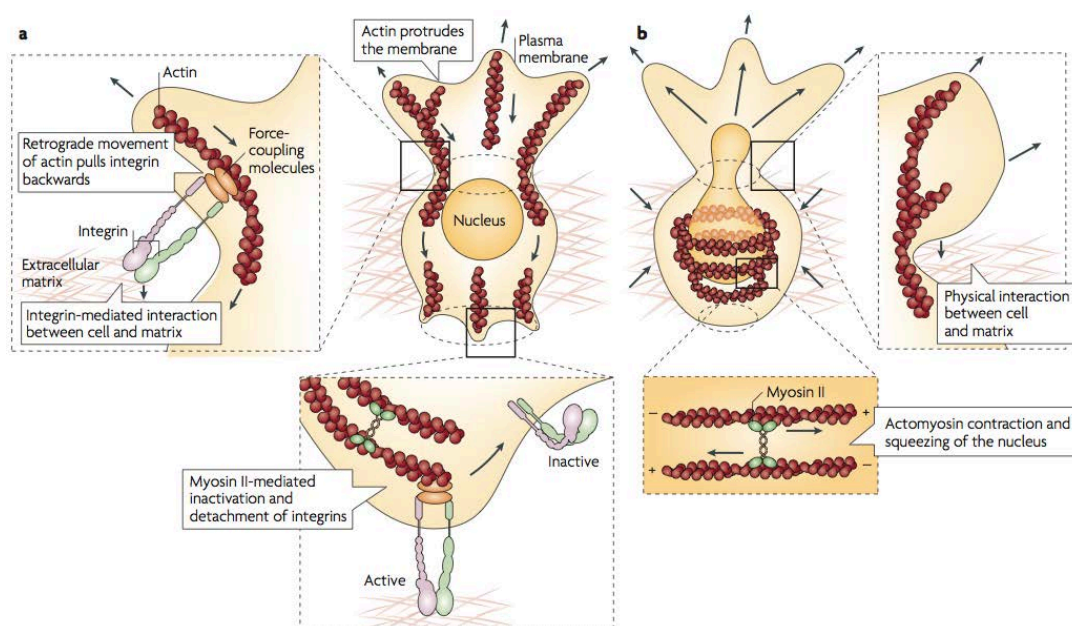


Figure 16. Protrusive and hydrostatic principles cooperate to propel leukocytes through a porous interstitium. a) Cell protrusion through a pore in the interstitium, using the force of actin polymerization to bulge out the leading membrane. Pushing against the leading membrane drives the membrane forwards while actin filaments slide towards the trailing edge. If integrins successfully interact at the contact site between cell and substrate, the retrograde sliding of actin is turned into a force that pulls the substrate backwards and thereby the cell body forwards. At the trailing edge, myosin II slides antiparallel actin filaments against each other, leading to the contraction of the actin cortex and subsequent retraction of the tail. Simultaneously, active myosin II causes physical and biochemical inactivation and thus detachment of the integrins. b) Cell protrusion through a pore in the interstitium that is too narrow to allow passage of the rigid nucleus. In this case, actomyosin contraction at the trailing edge leads to shrinkage of the actin cortex and thereby squeezes and deforms the nucleus and propels it through the pore. Actomyosin contraction also creates hydrostatic pressure that aids in protruding the membrane or might even protrude the membrane by itself by inducing the formation of actin-free membrane blebs (not shown). If integrin receptors are absent or unable to bind to the substrate, the cell can physically interact with the substrate as the actin cortex braces the membrane and thereby pushes against the substrate, providing the counter-force that is required to advance the cell body. Text and figure taken from [200]

In addition to actin polymerization and myosin contraction, the requirement of adhesive support is still a matter of debate. Some reports claim for integrin-dependent interstitial migration, while others state the opposite. This may come from limitations of experimental design or leukocyte subset specific functions [210]. For neutrophils, two initial *in vivo* studies identified a key role for β_1 integrins [220,221] using blocking antibodies. Conversely, a recent report used Talin-1 deficient neutrophils, in which integrin activation is impaired, to conclude for a dispensable role of integrins in this process [217]. For dendritic cells (DCs), the use of pan-integrin deficient or Talin-1 deficient DCs confirmed an integrin-independent model of interstitial migration *in vivo* [219]. Finally, a recent report highlights the key role of the α_v integrin in the interstitial migration of effector CD4⁺ T cells [222]. In conclusion, additional studies are needed to elucidate the role of integrins, in addition to the indisputable role of actomyosin forces.

2.1.6 The migration of leukocytes to lymph nodes

Among all the different types of leukocytes that extravasate from blood vessels to the inflamed tissue, and/or migrate within the tissue towards the pathogen or the injury, one type is particularly well suited to migrate to the draining lymph nodes via lymphatic vessels. These are dendritic cells (DCs). DCs are the major link between the innate and the adaptive immune responses. After launching an inflammation, DCs can either stem from emigrating inflammatory monocytes that differentiates locally into DCs (so-called monocyte-derived DCs, mo-DCs) [223], or consist of “resident” differentiated cells located within tissues where they constantly sense their environment for pathogens [224]. In both scenarios, DCs are able to acquire, process and present antigen signatures better than any other antigen-presenting cell. Moreover, they display amazing properties to migrate to, and enter afferent lymphatic vessels to educate specific T cells located in the

draining lymph nodes. For all these reasons, DCs migration to lymph nodes was studied more extensively than any other leukocytes. Given the personal results I will present in this manuscript, I will now particularly focus on the migration of DCs to the lymph node.

DCs en route to lymph nodes use the lymphatic vessels as roads to their final destination. The organization and the structure of the lymphatic vasculature differs from the blood vasculature in many aspects. As one of the main function of the lymphatic system is to pump the interstitial fluid (i.e. the lymph) from the tissue to the lymph nodes, the lymphatic system begins with blind-ended capillaries. In line with its function, these initial lymphatic capillaries display a fascinating oak leaf shape with overlapping flaps between neighbouring cells [225]. Moreover, the flap borders exhibit discontinuous button-like junctions rich in VE-cadherin and tight junctions molecules [225] (**Figure 17**). This specialized structure seems perfectly designed for the interstitial fluid to enter via openings between the button-like junctions. Lymphatic capillaries then converge into larger collecting vessels with zipper-like junctions that resemble those of blood vessels (**Figure 17**), therefore less absorptive than initial capillaries. Finally, collecting lymphatics extend to the lymph node as afferent lymphatics.

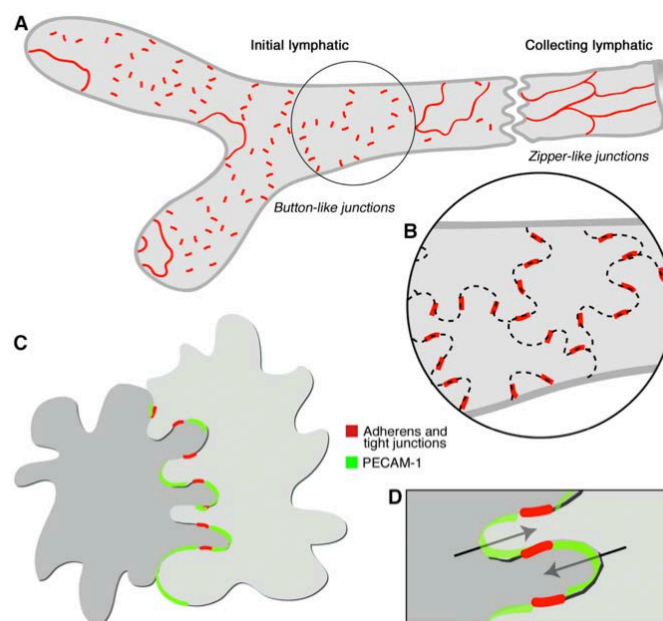


Figure 17. Buttons in initial lymphatics border sites of fluid entry. (A) Schematic diagram showing distinctive, discontinuous buttons in endo- thelium of initial lymphatics and continuous zippers in collecting lymphatics. Both types of junction consist of proteins typical of adherens junctions and tight junctions. (B) More detailed view showing the oak leaf shape of endothelial cells (dashed lines) of initial lymphatics. Buttons (red) appear to be oriented perpendicular to the cell border but are in fact parallel to the sides of flaps. In contrast, most PECAM-1 expression is at the tips of flaps. (C and D) Enlarged views of buttons show that flaps of adjacent oak leaf-shaped endothelial cells have complementary shapes with overlapping edges. Adherens junctions and tight junctions at the sides of flaps direct fluid entry (arrows) to the junction-free region at the tip without repetitive disruption and reformation of junctions. Text and figure taken from [225].

Even though DCs constantly use this route to reach lymph nodes in absence of inflammatory signals, their migration to lymph nodes is dramatically enhanced under inflammatory conditions. The pro-inflammatory cytokines and Pathogen-Associated Molecular Patterns (PAMPs) released at the inflammatory locus shaped immature DCs to a mature phenotype expressing high levels of the chemokine receptor CCR7 [226-229]. This chemokine receptor is absolutely required for efficient DC migration to lymph nodes [230]. CCR7 deficient DCs fail to migrate to lymph node, hence resulting in poor T cell responses [231]. The two CCR7 ligands CCL19 and CCL21 are crucial for DC migration [232,233], yet CCL21 efficiently mediates migration in absence of CCL19 [234]. CCL19 is soluble [235] while CCL21 bound to glycosaminoglycans [236]. However, CCL21 can be cleaved by DCs to generate a soluble form of CCL21 that is functionally similar to CCL19 [237]. CCL21 is produced by Lymphatic Endothelial Cells (LECs), and is distributed either as puncta on initial lymphatic capillaries [238], or as an extracellular decaying gradient immobilized to heparin sulfates [236]. This gradient efficiently drives the interstitial migration of DCs towards initial lymphatic capillaries [237] in an integrin-independent manner [219]. Disruption of CCL21 binding to heparin sulfates impairs the migration of DCs in direction of lymphatic vessels [237]. It is worth noting that this haptotactic interstitial migration obviously requires the actomyosin locomotion machinery described previously. The deletion of key molecules that regulate the polarization of DCs or the cytoskeletal rearrangement significantly impairs the migration of DCs to lymph nodes [239-241].

Once DCs are in close proximity to the initial lymphatics, they face the basement membrane. In a similar manner as the leukocyte extravasation from blood vessels, DCs seek preexisting gaps to squeeze across the basement membrane [242]. Important to note that in contrast to blood vessels, lymphatic vessels have no pericyte coverage [243], which may facilitate DC passage. Under steady state conditions, DCs cross the oak leaf shape of the capillaries through “preformed portals” between button-like junctions in an integrin-independent manner [219,242] (**Figure 18**).

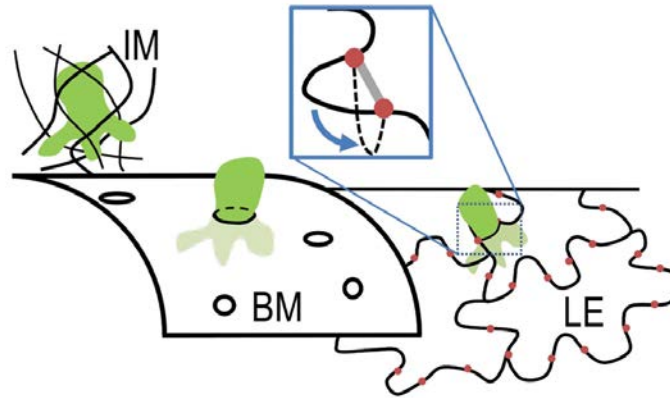


Figure 18. DCs enter vessel lumen via endothelial flap valves. DCs (green) arrive via the interstitial matrix (IM) and encounter the porous BM of the initial lymphatic vessel. They enter by squeezing through the pores and subsequently encounter the lymphatic endothelial layer (LE). The oak leaf-shaped lymphatic endothelial cells are interconnected by junctional complexes organized as buttons (red) at the base of flexible lobes. DCs enter the endothelial layer without opening the junctions by pushing the flap valves into the vessel lumen (inset). Text and figure adapted from [242].

This picture is rather different under inflammatory conditions as both ICAM-1 and VCAM-1 are upregulated by LECs, and are required for transmigration of DCs through lymphatics [244-246].

Finally, once DCs have entered the initial lymphatic vessel, they start to crawl on the luminal wall, while the higher flow rate of collecting vessels is likely to induce DC free flowing until the lymph nodes [238]. Within the lymph nodes, DCs cross the subcapsular sinus in a CCR7-dependent manner to finally reach the T cell zone in the center of the lymph node [247].

2.2. JAM-C in inflammation and disease

2.2.1 The JAM family, an overview

The Junctional Adhesion Molecules (JAMs) family is currently composed of 7 proteins that belong to the immunoglobulin superfamily (IgSf). As such, each JAM consists of two immunoglobulin-like extracellular domains, one single transmembrane domain, and a cytoplasmic tail with a PDZ domain [248-250]. The membrane proximal immunoglobulin domain of JAMs is similar to the one of the CTX (Cortical Thymocyte marker for *Xenopus*) family, which could potentially represent the ancestor of the T and B cell receptor [251]. According to the length of the cytoplasmic tails, the JAM family can be further divided into 2 branches: the **classical** members JAM-A, JAM-B, and JAM-C, and the **non-classical** members ESAM (Endothelial cell-Selective Adhesion Molecule), CAR (Coxsackie Adenovirus Receptor), JAM-4, and JAM-L (JAM-like) [248-250]. Indeed, the classical JAMs display a short cytoplasmic tail with class II PDZ domains, while non-classical JAMs exhibit longer cytoplasmic tails with class I PDZ domains with the exception of JAM-L [252] (**Figure 19**). Even though each JAM has distinct distribution and expression patterns, they are all expressed, with the unique exception of JAM-L, at tight junctions of epithelial and/or endothelial cells. Therefore, most of the JAMs have been implicated in the control of leukocyte transendothelial migration and/or vascular permeability [248-250].

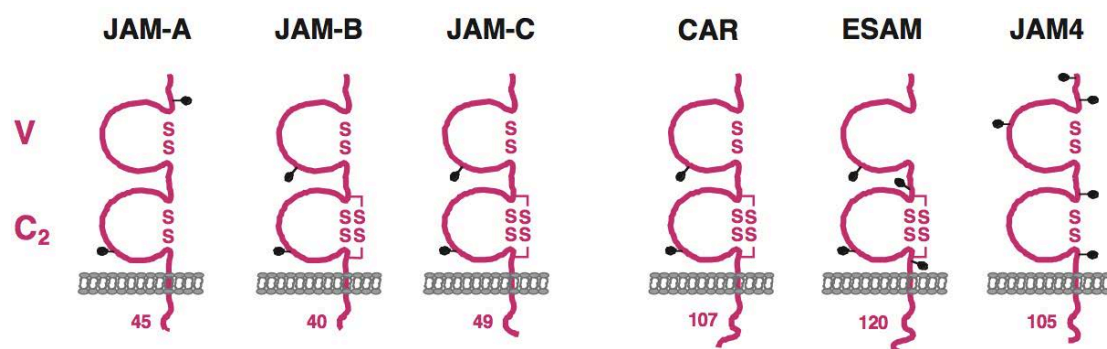


Figure 19. The JAM family. All IgSF proteins present at tight junctions belong to the CD2 subfamily with a membrane-distal V-type Ig-domain and a membrane-proximal C2-type Ig-domain. Putative N-linked glycosylation sites are illustrated by dots. Disulfide bridges and putative additional intramolecular disulfide bridges formed by conserved cysteine residues in the C2-type Ig-domain are indicated. The sizes of the cytoplasmic domains (mouse molecules) are indicated at the bottom of each molecule. Tight junction localization has so far been shown for JAM-A, JAM-C, CAR, ESAM and JAM4. Text and figure adapted from [252].

The classical JAMs have 51-54% homology and 32-36% similarity in the amino acid sequences [253-255]. To date, only the crystal structures of the extracellular domains of JAM-A have been resolved, both in mouse [256] and

human [257]. In these studies, recombinant JAM-A molecules form a U-shaped dimer interacting in cis with the membrane distal domain. Moreover, the model proposes that JAM-A dimers in cis interact with JAM-A dimers in trans on the opposing cell membranes [256]. The cis-dimerization motif being conserved between JAM-A, JAM-B, and JAM-C, it is assumed that JAM-B and JAM-C may dimerize in a similar manner [249] (**Figure 20**). Important to note that all three JAMs interact with ZO-1 and PAR-3 through their cytoplasmic domains [252,258-260]. An overview of the JAM family members is provided in **Table 2**, while the following sections will now focus on JAM-C in inflammation and disease.

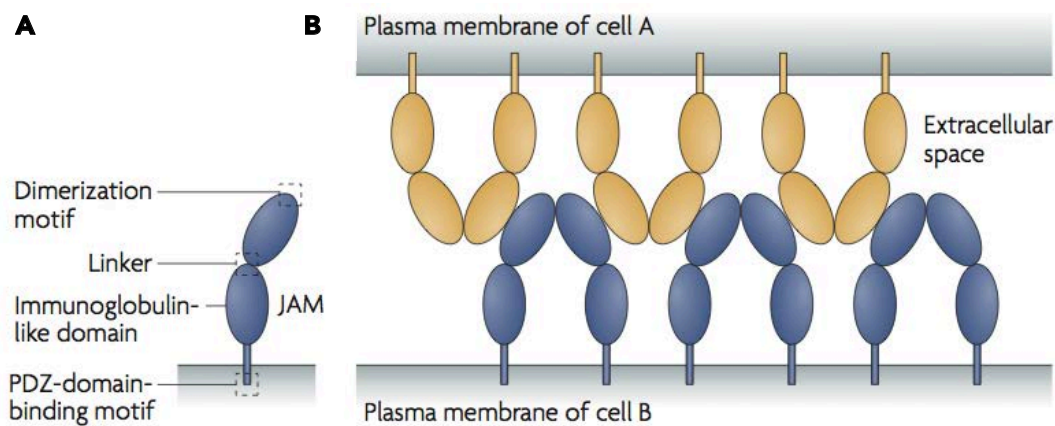


Figure 20. Structural features of the JAM-family members and a molecular model for JAM homophilic adhesion. A) The junctional adhesion molecule (JAM)-family members are characterized by two immunoglobulin-like domains in the extracellular portion, a single transmembrane segment and a short cytoplasmic tail with a PDZ-domain-binding motif (Phe-Leu-Val). A short linker sequence Val-Leu-Val connects the two immunoglobulin domains to impose a bent conformation. A dimerization motif Arg-(Val/Leu/Ile)-Glu in the membrane-distal domain is essential for homodimer formation. (B) A molecular model for homophilic interactions of JAMs has been proposed. In this model [256], JAM-A molecules form homodimers in cis (via the dimerization motif in the membrane-distal immunoglobulin domain) that emerge from the cell surface in the shape of an inverted 'U'. At intercellular junctions, these cis-homodimers bind in trans to JAM-A homodimers from an adjacent cell surface. Text and figure adapted from [249].

Class	Name	Expression	Function
I	CAR	Epithelial cells ⁵⁴ Cardiomyocytes ⁷⁸ Male germ cells ⁷⁹ Spermatozoa ⁷⁹	Transepithelial migration of neutrophils ⁵⁴ Survival signals during embryogenesis ⁷⁸ Spermatogenesis ⁷⁹
I	ESAM	Endothelial cells ⁷⁰	Transendothelial migration of neutrophils during inflammation ⁷² Angiogenesis during tumour growth ⁷⁴
I	JAM4	Epithelial cells ⁸¹ Male germ cell progenitors ⁸² Haemopoietic cell ⁸²	Regulation of permeability ⁸¹ Unknown
II	JAM-A	Endothelial cells ^{27,28} Epithelial cells ^{27,28} Neutrophils ²⁷ Platelets ^{25,27} Monocytes ²⁷ Lymphocyte subsets ²⁷	Maintenance of tight junctions ^{27,30} Leukocyte transmigration ^{27,28} Assembly and remodelling of tight junctions ³⁰ Regulation of polarised migration ³⁵ Unknown
II	JAM-B	Endothelial cells ^{98,99}	Maintenance of endothelial tight junctions mediated by interactions with JAM-C ^{41,99} (see below)
II	JAM-C	Endothelial cells ⁶² Fibroblasts ¹⁰⁰ Human epithelial cells ⁵² Human dendritic cells ⁴⁴ NK cells ⁴⁴ T cells ⁴⁴ B cells ^{43,69} Platelets ^{40,42}	Maintenance of endothelial tight junctions ⁶² Regulation of neutrophil, monocyte and lymphocyte accumulation at sites of inflammation ^{40,43} Maintenance of adherens-like junctions ¹⁰⁰ Neutrophil transepithelial migration ⁵² Unknown
-	JAML	Neutrophils ²¹	Transepithelial migration ⁵⁴

Table 2. Summary of JAM-Related Protein (Class I PDZ Binding Domain) and Classical JAM (Class II PDZ Binding Domain) Expression Profiles and Described Functions. Table taken from [248].

2.2.2 JAM-C expression profile

Mouse JAM-C (also known as JAM3, hJAM3 and mJAM-2) was first discovered in 2000 in a thymic endothelial cell line by RNA display [253,261], while human JAM-C was cloned shortly after [262]. In this first mouse study [253], it was already clear that the molecule was expressed at cell borders of endothelial cells. Later on, additional studies also identified JAM-C in desmosomes of human epithelial cells [263], in adherens-like junctions of fibroblasts [259], on primary smooth muscle cells [264,265], in peripheral nerves [266], and in spermatids [267]. On hematopoietic cells, JAM-C expression differs from rodent to human cells. To date, JAM-C was not found on any murine circulating cell [262,268], in contrast to human JAM-C that was observed on human dendritic cells and NK cells [269], activated T cells [262], naïve and memory B cells [270], and platelets [255]. The expression of JAM-C on endothelial cells was further documented in many different tissues, including aorta, kidney, lymph node, Peyer's patches, lung, cremaster muscle, skin, pancreas, and tonsils [253,254,264,265,271-273]. Under steady

state conditions, JAM-C mainly appears at interendothelial junctions in a zipper-like molecular pattern.

The differential expression of the molecule under inflammatory conditions tends to be stimuli-dependent [249]. *In vitro*, treatment of HUVECs with oxidized LDL (Low Density Lipoprotein) seems to redistribute JAM-C out of junctions although the data were not explicitly shown in [264]. Conversely, treatment of HUVECs with VEGF shortly increases the expression of JAM-C at junctions [274]. *In vivo*, JAM-C expression is upregulated in vessels and smooth muscle cells in chronic inflammation such as atherosclerosis [264]. In contrast, intracellular and junctional JAM-C is downregulated in response to ischemia reperfusion injury [137]. Finally, cell surface JAM-C is reduced in ear and lymph node endothelial cells after skin hypersensitivity (personal observation).

2.2.3 JAM-C ligands

To date, 4 ligands have been identified for JAM-C. Two of them support interendothelial interactions, namely **JAM-B** and **JAM-C** itself, while the two others, the integrins **Mac1** and $\alpha_X\beta_2$, allow leukocytes adhesion to the endothelium (**Figure 21**).

JAM-B was the first ligand identified by the time of JAM-C discovery [262]. The JAM-B binding to JAM-C was shown by ELISA, pull-down assay, and adhesion assay [262,269]. In the first paper cited, the protein-protein interaction assay already revealed that JAM-C could also bind to **JAM-C**, but to less extent than to JAM-B [262]. The formal demonstration that JAM-B/JAM-C interactions are stronger than JAM-C/JAM-C interactions came up three years after [275]. In this study, the authors show that JAM-B is able to recruit and stabilize JAM-C at cell-cell contacts in transfected cells [275]. This interaction requires the membrane distal immunoglobulin like domain of JAM-C. Strikingly, soluble JAM-B dissociates JAM-C/JAM-C homodimers to create JAM-B/JAM-C heterodimers with higher affinity [275]. Important to note that JAM-C/JAM-C homodimers or JAM-B/JAM-C heterodimers requires the Glutamate amino acid residue 66 (E66) [275].

The leukocyte integrin **Mac1** ($\alpha_M\beta_2$), described in many details in the previous chapter, was identified as one of JAM-C ligands soon after JAM-B. The interaction was originally shown between human platelets expressing JAM-C and a monocyte cell line expressing Mac1 [255]. These findings were confirmed with Mac1 expressing-human neutrophils that bind to JAM-C from

an epithelial cell line [263]. Finally, one report shows that JAM-C binds to the I domain of Mac-1, and that Mac1/JAM-C interaction would be of lower affinity than JAM-C/JAM-C [276].

Finally, the interaction between JAM-C and **CD11c/CD18** appeared to be marginal. CD11c/CD18 is an integrin mainly found on DCs, but also on macrophages, and some lymphocytes subsets [277-279]. Only two studies report the binding of CD11c/CD18 to JAM-C. First, transfection of CD11c/CD18 in K562 leukaemia cell line promotes its adhesion to immobilized JAM-C, although to lower extent than Mac1 [255]. In a second report that used Bone-Marrow-derived Dendritic Cells (BMDCs), the same conclusions were drawn [280].

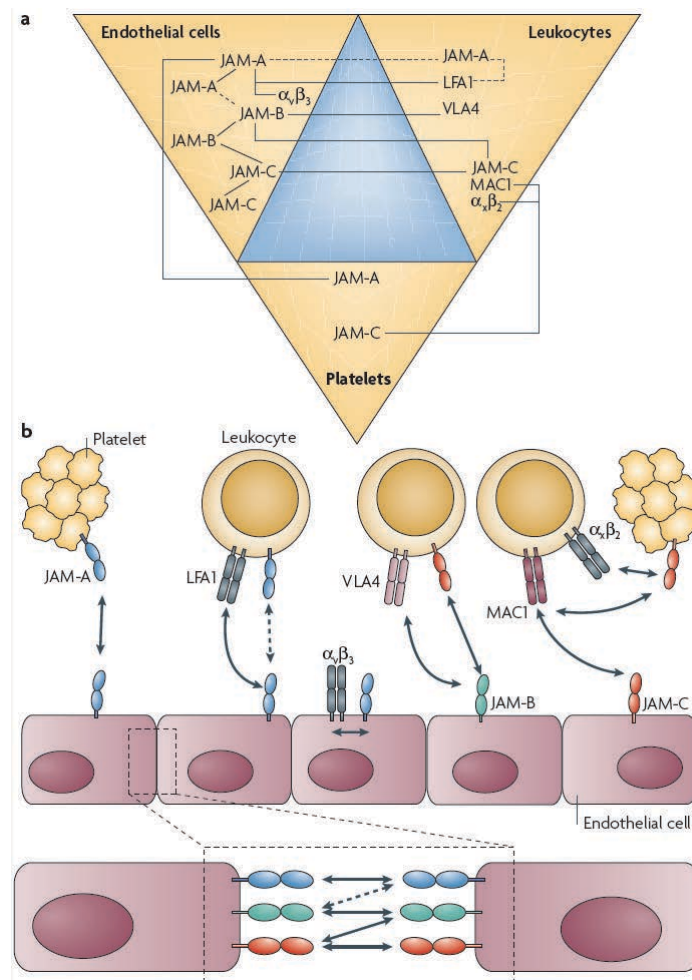


Figure 21. Cellular expression and extracellular ligands of JAMs. Junctional adhesion molecule A (JAM-A), JAM-B and JAM-C expressed by endothelial cells, leukocytes and platelets support various homophilic and heterophilic interactions. JAM interactions that have been reported in the published literature are indicated with solid lines and predicted interactions are indicated with dashed lines. a | At endothelial-cell junctions, JAMs support both homophilic and heterophilic interactions. JAMs on endothelial cells also bind integrins expressed on leukocytes. The integrin lymphocyte function-associated antigen 1 (LFA1) interacts with JAM-A, very late antigen 4 (VLA4) interacts with JAM-B, and MAC1 interacts with JAM-C. b | Binding of leukocytes to the endothelium is supported by interactions between integrins and JAMs. JAM-A homophilic interactions support platelet adhesion to the endothelium and JAM-C heterophilic interactions with integrins support platelet adhesion to leukocytes. Text and figure taken from [249].

2.2.4 JAM-C and leukocyte migration

The junctional localization of JAM-C in endothelial cells immediately suggested a potential role in leukocyte migration. The first evidence was provided *in vitro*, where JAM-C overexpression in a thymic endothelial cell line resulted in increased transmigration of lymphocytes across the endothelial monolayer [271]. In the same report, transmigration of human peripheral blood leukocytes through naïve HUVECs was blocked in presence of antibodies against JAM-C. As endothelial cells and leukocytes express JAM-C in the human system, it is complicated to decipher which of the two is responsible for the effect [271]. Also in neutrophils, the precise role of JAM-C in transmigration has been investigated in several studies *in vitro*. First, it was shown that transmigration, but not adhesion, of human neutrophils through naïve HUVECs was blocked in presence of soluble JAM-C [281]. This finding was reproduced in an independent experiment using the same settings [268]. Important to note, as mentioned in our previous section, that JAM-C not only binds JAM-C, but also JAM-B and Mac1. Therefore, it is difficult to conclude whether soluble JAM-C acts and blocks JAM-C or JAM-B on endothelial cells, Mac1 on human neutrophils, or it may block yet unknown JAM-C ligands. In reference [268], the authors also investigated the role of JAM-C on neutrophil migration through TNF- α -activated HUVECs, and observed no difference after treatment with soluble JAM-C in such conditions. To better mimic the shear stress naturally observed in blood vessels, investigators then study transmigration *in vitro* under physiological flow conditions. They found that blockade of human JAM-C with different monoclonal antibodies has no effect on transmigration [282]. With human monocytes however, the picture was different, as JAM-C blockade with soluble JAM-C or with the monoclonal antibody H33 increased reverse and repeated transmigration on activated HUVECs under flow conditions [283] (**Figure 22**).

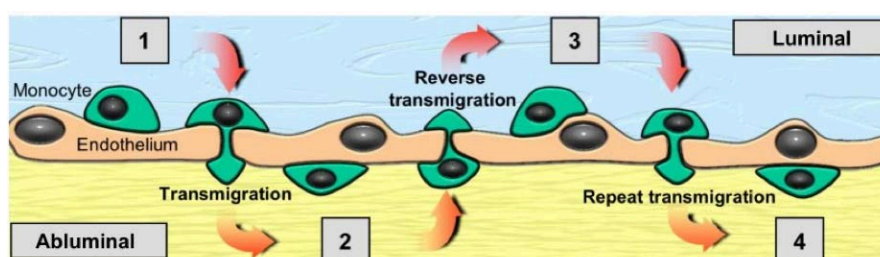


Figure 22. Increased multiple transmigration events of human monocytes with anti-JAM-C H33 antibody. Monocytes captured from free flow became activated and firmly adhered to HUVEC luminal surfaces (step 1). Monocytes migrating on luminal surfaces could move into the ablumen by migrating between junctions of adjacent endothelial cells (transmigration; step 2), which could be followed by transmigration in the abluminal-to-luminal direction (reverse transmigration) back onto luminal surfaces (step 3). A further transendothelial migration event (repeat transmigration) led to a return to the ablumen (step 4). Text and figure adapted from [283].

In vivo, however, JAM-C manipulation has always been associated with changes in leukocyte migration. The first evidence for a role of JAM-C *in vivo* was provided in 2004 using a mouse model of thioglycolate-induced peritonitis [281]. In this study, the investigators observed a decreased recruitment of neutrophils into the inflamed peritoneum after injection of soluble JAM-C [281]. Unfortunately, this study design does not tell whether the soluble JAM-C blocks endothelial JAM-C, endothelial JAM-B, or neutrophil Mac1, therefore making the interpretation of results difficult. New evidences came from the use of monoclonal antibodies to specifically target JAM-C. In 2005, Aurrand-Lions et al. used the rat anti-mouse JAM-C clone D33 in a model of LPS-induced lung inflammation [268]. They observed a temporary decrease in monocytes and granulocytes recruitment to the inflamed lung [268]. In the same study, the authors used a transgenic mouse overexpressing JAM-C under the control of the endothelial specific Tie2 promoter. In these mice, the transmigration of granulocytes and monocytes was increased in lungs after LPS instillation [268]. In a mouse model of ischemia reperfusion injury, mice overexpressing endothelial JAM-C displayed enhanced leukocytes adhesion and transmigration [284]. This was confirmed in a mouse model of IL-1 β -induced cremasteric venule inflammation [268]. Conversely, knock-out mice for JAM-C exhibited reduced adhesion and transmigration in the mouse model of ischemia reperfusion injury [284]. In a mouse model of contact hypersensitivity, the use of polyclonal antibodies against JAM-C reduced leukocytes infiltration into the inflamed skin [272]. Similarly, the use of antibodies against JAM-C reduced the infiltration of leukocytes into the inflamed pancreas [273]. Altogether, these results suggest that JAM-C plays a role in the adhesion of leukocytes, and therefore in the subsequent transmigration *in vivo*.

One antibody generated by our lab exhibits amazing properties *in vitro* and *in vivo*, namely the rat anti-mouse JAM-C clone **H33**. This antibody specifically blocks JAM-B/JAM-C interactions *in vitro* [275]. More importantly, H33 redistributes JAM-C out of interendothelial junctions *in vivo* [137,275]. As mentioned previously within this section, H33 enhances reverse and repeated transmigration of monocytes *in vitro* under flow [283]. This was indirectly confirmed *in vivo* for monocytes. Indeed, based on the postulate that L-selectin is shed from transmigrating monocytes, Bradfield et al. enumerated the numbers of L-selectin negative inflammatory monocytes in the blood after a thioglycolate-induced peritonitis [283]. They found increased numbers of L-selectin⁻ monocytes 30 minutes after inflammation, and reduced numbers of L-selectin⁻ monocytes in the blood one hour after inflammation. This suggested that H33 increases reverse, and repeated transmigration of monocytes *in vivo*. This indirect evidence was recently

confirmed by a direct proof with neutrophils in the mouse model of ischemia reperfusion injury [137]. In this model, the percentage of reverse and repeated transmigration of neutrophils was augmented after treatment with H33 [137]. Important to note that the antibody H33 was the antibody used in all my experiments. One part of the discussion will therefore be dedicated to the difference of biological effects observed between the different JAM-C manipulations (knock-out, overexpression, polyclonal antibodies, monoclonal antibodies, antibody H33), to better dissect the exact role of JAM-C in leukocyte migration.

2.2.5 JAM-C and vascular permeability

Previous findings reported that JAM-C stabilizes mainly cell junctions through trans-heterophilic, high affinity, low turnover interactions with its main partner JAM-B, while homophilic JAM-C-JAM-C interactions are weaker and occur with rapid dynamics [275]. The function of JAM-C in regulating endothelial permeability has been addressed by *in vivo* and *in vitro* studies using different approaches. *In vitro*, our laboratory has first reported that CHO cells transfected with JAM-C exhibit an increased barrier function [253]. Shortly afterwards, our laboratory observed the opposite phenotype in MDCK cells transfected with JAM-C [254]. When HUVEC cells were stimulated with the permeability factors VEGF or thrombin, JAM-C redistributed rapidly into cell-cell contacts and permeability was augmented [274,285]. Overexpression of JAM-C *in vitro* also renders endothelial cells more permeable, probably due to the association *in cis* with the integrin $\alpha\beta 3$ [285]. More recently, Chavakis and coworkers observed a reduced permeability *in vitro* in human dermal microvascular endothelial cells knockdown for JAM-C [286]. In this study, the authors showed that JAM-C was important for cell contractility, and that JAM-C knockdown increased the phosphorylation of the small GTPase Ras Associated Protein 1 (RAP1) that regulates VE-Cadherin function at cell-cell contacts. Lastly, the authors addressed the permeability question *in vivo* by using wild type mice treated with soluble recombinant JAM-C in a histamine-mediated vascular permeability model [286]. They reported that soluble JAM-C reduces vascular permeability in this particular model. Here again, it is worth noting that soluble JAM-C binds to JAM-C but can also engage strong interactions with JAM-B, or with other unknown ligands. Therefore, the effect of soluble JAM-C may be the sum of several interactions, making interpretation of these results difficult.

2.2.6 JAM-C and cell polarity

The tight junction localization of JAM-C, and the presence of an intracellular PDZ binding domain suggested a role for JAM-C in cell polarity. The first indication came from the analysis of the JAM-C DNA sequence where a putative Protein Kinase C phosphorylation site was found at serine residue 281 of the cytoplasmic tail [255]. The serine residue 281 was indeed phosphorylated in CHO cells transfected with murine JAM-C [260]. Interestingly, in the carcinoma cell line KLN205, the introduction of a mutation that impairs the phosphorylation of the residue 281 abolishes the cell polarity [287]. An additional indication for a role of JAM-C in cell polarity came from a study showing the direct interaction between JAM-C and the polarity protein PAR-3, and the indirect association with the polarity protein ZO-1 [260]. Finally, the generation of JAM-C knock-out animals provides a clear evidence for the key role of JAM-C in cell polarity. Indeed, JAM-C knock-out animals were strikingly infertile and fail to produce mature, polarized sperm cells [267]. JAM-C knockout spermatids display abnormal F-actin distribution and defects in cytoskeletal rearrangements [267]. This was explained by the capacity of JAM-C to recruit PAR-6, the small GTPase Cdc42 (Cell division cycle 42), PKC λ (protein kinase C λ), and PATJ (PALS1-associated Tight Junction protein) at the cell membrane [267]. This protein complex is well known for its function in cell polarity [267].

2.2.7 Role and function of other JAM members

JAM-A (also known as JAM, JAM-1, F11R, or 106 antigen) was the first Junctional Adhesion Molecule identified at tight junctions of epithelial and endothelial cells [288,289]. However, the expression of JAM-A is not restricted to stromal cells, as the molecule is also found on hematopoietic cells such as platelets, monocytes, lymphocytes, neutrophils, macrophages, and dendritic cells [289,290]. On endothelial cells, JAM-A is located apically within the tight junctions, and is associated with the cell polarity proteins ZO-1 and PAR3, similarly to JAM-C [258,291,292]. Stimulation of HUVECs with the pro-inflammatory cytokines TNF α and IFN- γ does not significantly change the level of cell surface JAM-A, but instead redistributes JAM-A away from junctions to the apical surface of the endothelial cells [293]. JAM-A has two ligands, namely JAM-A on the endothelial/epithelial cells, leukocytes, or platelets [249], and LFA-1 ($\alpha_L\beta_2$) on leukocytes [294]. On epithelial and endothelial cells, JAM-A engages homophilic interactions with JAM-A on the neighboring cells to stabilize the junction. Therefore, JAM-A acts as a gatekeeper that increases the tightness of endothelial and epithelial barriers

and decreases paracellular permeability under steady state conditions [290,295,296].

Under inflammatory conditions however, endothelium-expressed and leukocyte-expressed JAM-A has been shown to participate in the transmigration of leukocytes to the site of inflammation. At the time of JAM-A identification in 1998, the use of monoclonal antibodies already revealed a function for JAM-A *in vitro* and *in vivo* in the adhesion cascade [288]. *In vitro*, addition of anti-JAM-A antibodies reduced the transmigration of monocytes through endothelial cell monolayers [288]. *In vivo*, the same antibodies also reduced the recruitment of leukocytes in the air pouch model of sterile inflammation [288]. In both scenarios however, the study design does not allow to differentiate the contribution of leukocytes-expressed JAM-A as compared to endothelium-expressed JAM-A. In 2002, a new *in vitro* study separately treated T cells with anti-LFA-1 antibodies, and endothelial cells with anti-JAM-A antibodies, to better show the key role of endothelial JAM-A in the transmigration process as a ligand for leukocytes LFA-1 [294]. In line with the later study, it was clearly shown during transmigration of neutrophils through HUVECs that endothelium-expressed JAM-A redistributes to form a ring around the transmigrating neutrophils, which colocalizes with a similar ring-like structure of the neutrophil-expressed integrin LFA-1 [297].

It is worth noting that JAM-A tends to function in a stimulus-specific manner. Indeed, non-specific JAM-A blockade with antibodies *in vivo* has an effect in cytokine-induced experimental meningitis while no effect in viral or bacterial-induced meningitis [298,299]. Similarly, non-specific JAM-A blockade or the use of JAM-A knockout animals showed that JAM-A potentiates neutrophils transmigration in response to IL-1 β or ischemia reperfusion injury, but not LTB₄ (Leukotriene B₄) or PAF (Platelet Activation Factor)-induced inflammation [300].

Even though some discrepancies exist regarding the precise contribution of endothelium JAM-A versus leukocyte JAM-A in the adhesion cascade [300-302], the mechanism of action of JAM-A is partially unraveled. Indeed, endothelial-expressed JAM-A is believed to play a role at the initiation of leukocyte diapedesis [300]. Intravital microscopy in the JAM-A deficient vasculature revealed that neutrophils were blocked at the luminal surface in response to IL-1 β stimulation (**Figure 23**). Meanwhile, the implication of JAM-A in the adhesion step is not clear and might be context-dependent. Indeed, wild type monocytes adhere less efficiently to the JAM-A deficient vasculature in the ApoE deficient mouse suffering from atherosclerosis, whereas JAM-A deficiency does not modify significantly leukocyte adhesion

in response to IL-1 β or ischemia reperfusion injury [300]. On the other hand, leukocyte-expressed JAM-A mainly plays a role in leukocyte motility. For instance, neutrophils deficient for JAM-A display an impaired polarized movement and cell motility [301]. Conversely, JAM-A deficient DCs exhibit an increased migratory phenotype as compared to wildtype DCs [303]. In addition to its role in the leukocyte adhesion cascade, JAM-A has also been implicated in the control of vascular permeability, cell polarity, and angiogenesis [249].

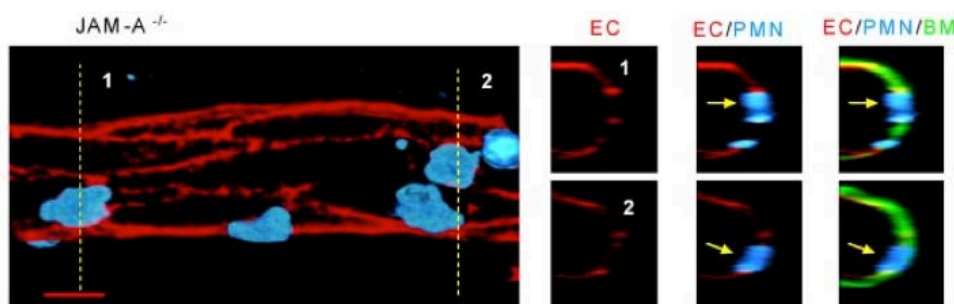


Figure 23. Leukocytes from JAM-A null mice arrest at the luminal surface after IL-1 β stimulation of cremasteric venules. Representative longitudinal (left panels) and cross-sectional (multiple small panels on the right) images of venules from JAM-A^{-/-}. The left panels show three-dimensional images of venules stained for endothelial cell junctions (red) and neutrophils (blue) only. The images on the right were obtained by cutting a cross-section (1 μ m thick) of the venules on the left along the indicated dotted lines. The cross sectional images corresponding to each of the numbered dotted lines are presented as a panel of 3 images in a row, showing the staining of endothelial-cell junctions (EC; red), neutrophils (PMN; blue), and the endothelial-cell basement membrane (BM; green). The arrows show the location of selected neutrophils, clearly indicating arrest of neutrophils at endothelial-cell junctions. Scale bar equals 10 μ m. Text and figure adapted from [300].

JAM-B (also known as JAM2, VE-JAM, hJAM2 and mJAM-3) was the second JAM member identified [304,305]. JAM-B expression is restricted to the junctional regions of endothelial cells [304-306]. JAM-B has been detected in various different tissues, including testes, heart, lymph nodes, Peyer's patches, and brain [267,272,304-307]. In humans, JAM-B binds to JAM-C from human T cells, NK cells, or DCs [307], while JAM-B/JAM-B homophilic interactions also occur but are less stable than JAM-B/JAM-C interactions [275]. T cells-expressed VLA-4 ($\alpha_4\beta_1$) is a ligand for human JAM-B, but JAM-C binding to JAM-B is a prerequisite for JAM-B to interact with VLA-4 [308]. JAM-B being a close homolog of JAM-A and JAM-C, experts in the field hypothesized a potential function of JAM-B in leukocyte trafficking. Yet, its role in the adhesion cascade remains elusive. One single study highlighted the contribution of JAM-B in the recruitment of leukocytes in a mouse model of contact dermatitis [272]. Important to note here again, that all the experiments mentioned earlier using soluble JAM-C to theoretically block JAM-C, might block JAM-B as well, as JAM-B/JAM-C interactions are stronger than JAM-C/JAM-C interactions [275]. Therefore, it is not excluded that the role of JAM-B in leukocyte trafficking and vascular permeability was

partially unravelled in such non-specific experiments. Lastly, JAM-B has also been recently implicated in melanoma cell metastasis [309].

To date, **ESAM** is the non-classical JAM member that plays the most prominent role in the leukocyte adhesion cascade, after the classical JAM-A and JAM-C molecules. ESAM is exclusively expressed by platelets and endothelial cells [310,311]. On endothelial cells, ESAM is located apically within tight junctions and colocalizes with ZO-1 [311]. ESAM also directly binds and recruits the MAGI-1 molecule (Membrane-Associated Guanylate kinase protein 1), which mediates intracellular signaling events [312]. No leukocyte ligand has been identified for ESAM to date, while homophilic ESAM/ESAM interactions on adjacent endothelial cells were described [310,311]. The use of ESAM knockout mice in different inflammatory models clearly demonstrated a role for ESAM in the control of vascular permeability and neutrophil extravasation [313]. Indeed, ESAM deficiency results in reduced permeability *in vivo* in the peritoneum after thioglycolate-induced inflammation, and in the skin after VEGF-induced stimulation [313]. This was explained by the diminution of the activated form of the Rho GTPase, a GTPase implicated in the tightness of junctions [313]. ESAM knockout have no effect on T cell migration, while the recruitment of neutrophils is only delayed in the inflamed peritoneum in mice deficient for ESAM [313]. Recently, platelet-expressed ESAM was associated with thrombus formation *in vivo* [314].

CAR was first identified as a receptor for Coxsackieviruses [315,316], and later for Adenoviruses [315,316]. For this reason, the receptor was named the Coxsackievirus Adenovirus Receptor (CAR). The crystal structure of CAR has also been resolved, and showed homodimers formation similar to JAM-A [317,318]. The localization of CAR within tight junctions of epithelial cells was elucidated in 2001 [319], that is sixteen years after its original identification. CAR is able to recruit ZO-1 at tight junctions and function as a physical barrier to strengthen the epithelial integrity [319]. However, Coxsackieviruses and Adenoviruses use CAR as a receptor to infect epithelial cells and break CAR/CAR interactions to breach the epithelial barrier [320]. Yet, the role of CAR in the leukocyte adhesion cascade remains poor. The unique report that described a role for epithelial CAR in leukocyte migration described the interaction between neutrophil JAM-L and epithelial CAR. Indeed, **JAM-L** is the only JAM member found exclusively on hematopoietic cells and not on non-hematopoietic cells. JAM-L is mainly expressed by granulocytes, but is also induced by myeloid leukemia cells [321]. *In vitro*, neutrophils use JAM-L to bind CAR, and the addition of fusion proteins or antibodies against these molecules reduces migration of neutrophils through transwells [322].

Finally, the seventh and last JAM member is **JAM-4**, expressed in epithelial tight junctions, mainly from the kidney and the intestine [323]. As such, JAM-4 might regulate the permeability of glomeruli and the intestine epithelial barrier, while its function in the adhesion cascade has not yet been established.

2.3. The *Leishmania major* model of cutaneous leishmaniasis

2.3.1 Leishmaniasis, an overview

Leishmaniasis is the name for a spectrum of diseases caused by the parasite of the genus *Leishmania*. The disease was already described on tablets from the 7th century before Christ, which are believed to derive from earlier texts [324]. The first to observe the pathogen was David Cunningham in 1885, but he did not know what it was at this time. In 1903, the Scottish pathologist William Leishman, and the Irish officer Charles Donovan, isolated independently the parasite from the spleen of patients with visceral leishmaniasis. For this reason, the genus was called *Leishmania*, the species observed *Leishmania donovani*, and the resulting disease Leishmaniasis [324]. *Leishmania* species are obligate intracellular protozoan parasites. As such, they need cells to replicate and survive, and a vector to propagate between hosts. The vector is a female blood-sucking sand fly of the genus *phlebotomus* or *lutzomya* (**Figure 24**). The host cells are professional phagocytic cells such as macrophages coming from a wide range of animals, including humans, dogs, and rodents.



Figure 24. Blood-fed *Lutzomyia longipalpis* sandfly. (2009) PLoS Pathogens Issue Image | Vol. 5(8) August 2009. PLoS Pathog 5(8): ev05.i08. doi:10.1371/image.ppat.v05.i08

Leishmania parasites exhibit two different lifecycle stages, the vector stage on one hand, and the host stage on the other hand. **The cycle of *Leishmania*** starts when the sand fly bites its target to suck fresh blood. Within the sand fly vector, the parasite adopts an elongated flagellated form, namely the promastigote (literally “with a flagellum”). The presence of the flagellum

allows the parasite to move from the midgut of the sand fly to its proboscis for efficient skin inoculation upon sand fly bites. The sand fly inoculates between 100-1000 metacyclic promastigotes [325], which are phagocytosed by macrophages, and will reside within phagolysosomes. In these organelles, promastigotes lose their flagellum and transform into a round-shape form, namely the amastigote (literally “without flagellum”). Amastigotes have the ability to efficiently replicate until the host cell dies and spreads amastigotes in the extracellular space. Free amastigotes then infect additional phagocytic cells afterwards. Alternatively, apoptotic infected cells can be cleared by professional phagocytic cells, leading to efficient parasite spreading into new host cells. Important to note that macrophages constitute the main host cells at later time points post infection. Once a new female sand fly bites the infected skin for a blood meal, it sucks free amastigotes or infected host cells. Within the midgut, amastigotes switch back into infective stage promastigotes, which completes the cycle of the parasite [325] (**Figure 25**).

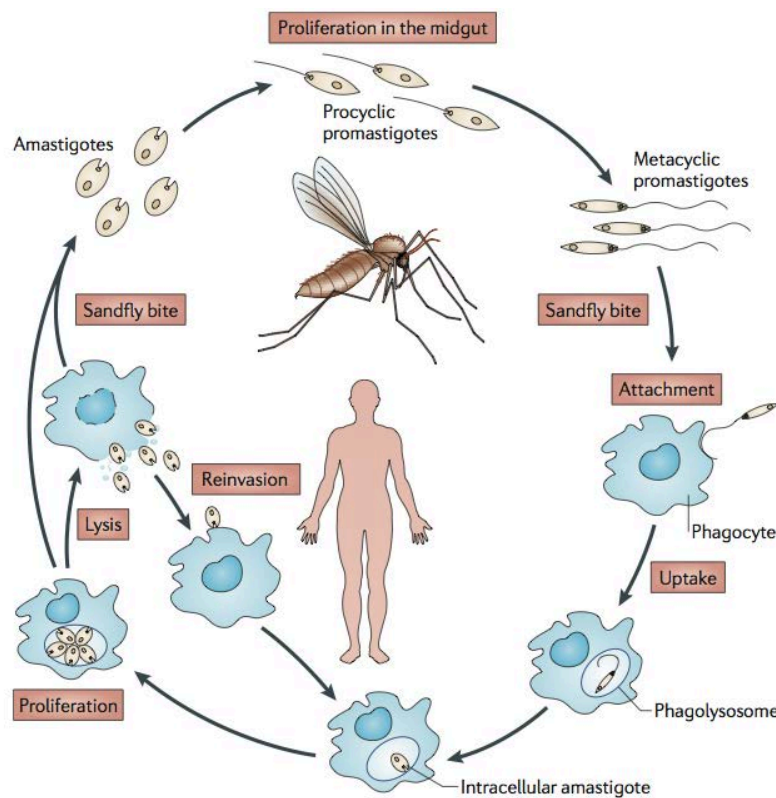


Figure 25. The life cycle of *Leishmania* parasites. Figure taken from [326].

The genus *Leishmania* comprises more than 20 species that cause three forms of leishmaniasis, depending on the species inoculated, and the genetic susceptibility of the host [327,328].

Cutaneous leishmaniasis (CL) is at the same time the most common, and the least severe form of the disease. The clinical symptoms are ulcerative skin lesions that heal with time. In the New World, the disease is caused by several species such as *Leishmania mexicana*, *amazonensis*, *pifanol*, *infantum*, or *braziliensis*. Conversely, *Leishmania major*, *tropica* or *aethiopica* are the main species causing CL in the Old World [326,328] (**Figure 26**).

Mucocutaneous leishmaniasis (MCL) is the most destructive form of the disease. Indeed, the parasites disseminate to mucosal regions such as the mouth, nose, and throat, and lead to extensive disfiguring. Therefore, MCL is a major cause of social exclusion. *Leishmania braziliensis* and *panamensis* are the main species responsible for MCL [326,328] (**Figure 26**).

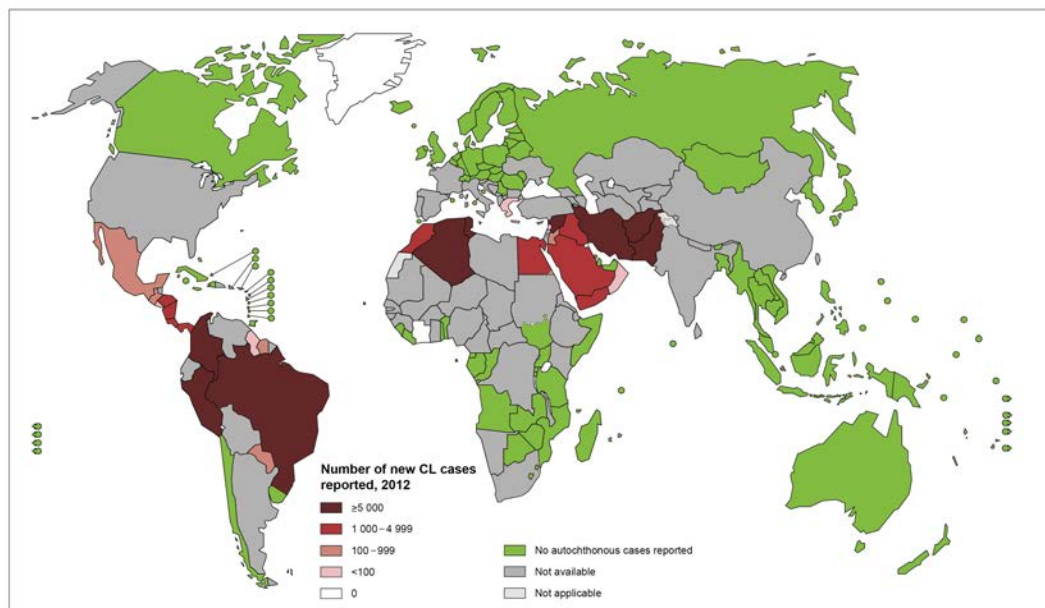
Visceral leishmaniasis (VL) is the most severe form of the disease and results to death if left untreated. In this case, the parasite disseminates to visceral organs such as spleen, but more importantly to the liver. The symptoms are fever, weight loss, splenomegaly, hepatomegaly, and anemia. VL species include *Leishmania donovani*, *Leishmania infantum* in the Old World, and *Leishmania infantum chagasi* in the New World [326,328] (**Figure 26**).



Figure 26. The clinical syndromes of leishmaniasis. (Source : left picture, <http://drugline.org/medic/term/visceral-leishmaniasis>; right picture, Wikipedia)

Leishmaniasis is found on five continents, and approximately 98 countries, the majority of which are developing countries (**Figure 27 and 28**). Indeed, leishmaniasis is a poor-related disease, which associates with malnutrition, poor housing, weak immune system, lack of resources, and also with population displacement. It mainly concerns tropical and subtropical regions of the world that are appropriate for the sand fly vector and the parasite development itself. Currently, 310 millions people are at risk, more than 12 million people are affected, and 1.3 millions new cases occur worldwide every year. Among these 1.3 millions cases, 1 million are cutaneous (or

muco-cutaneous) and 300.000 are visceral. About 20.000 to 40.000 people die from visceral leishmaniasis annually [329].

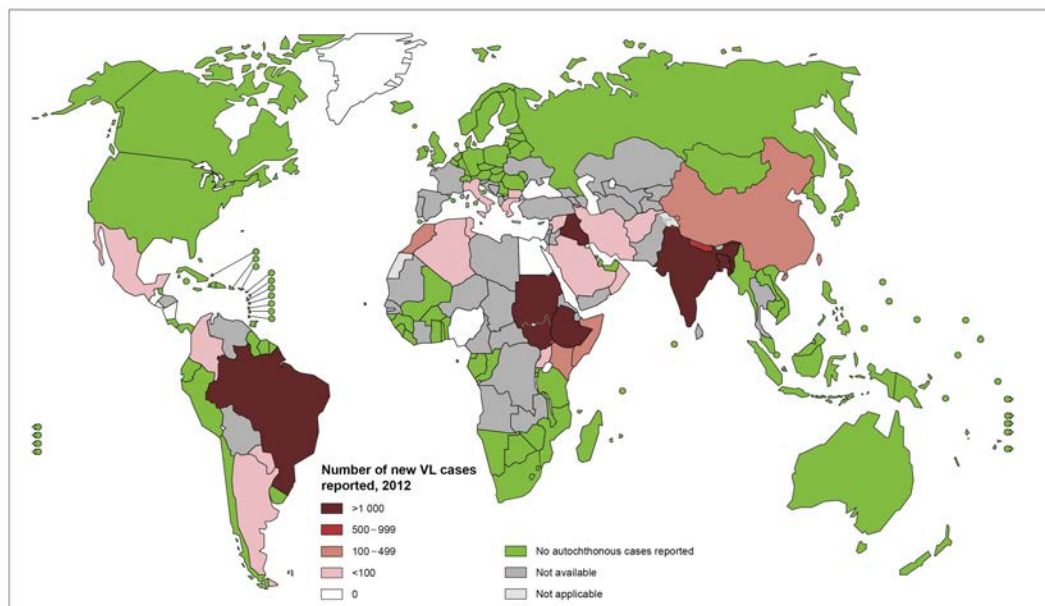


The boundaries and names shown and the designations used on this map do not imply the expression of any opinion whatsoever on the part of the World Health Organization concerning the legal status of any country, territory, city or area or of its authorities, or concerning the delimitation of its frontiers or boundaries. Dotted lines on maps represent approximate border lines for which there may not yet be full agreement. © WHO 2013. All rights reserved

Data Source: World Health Organization
Map Production: Control of Neglected Tropical Diseases (NTD)
World Health Organization



Figure 27. Status of endemicity of cutaneous leishmaniasis in 2012. (Source : WHO)



The boundaries and names shown and the designations used on this map do not imply the expression of any opinion whatsoever on the part of the World Health Organization concerning the legal status of any country, territory, city or area or of its authorities, or concerning the delimitation of its frontiers or boundaries. Dotted lines on maps represent approximate border lines for which there may not yet be full agreement. © WHO 2013. All rights reserved

Data Source: World Health Organization
Map Production: Control of Neglected Tropical Diseases (NTD)
World Health Organization



Figure 28. Status of endemicity of visceral leishmaniasis in 2012. (Source : WHO)

Treatments exist, but are not affordable for most of the population concerned. The use of therapeutic drugs (e.g. pentavalent antimonials) was the first treatment of choice [328]. Unfortunately, this does not always work, while it is often associated with strong side effects [328]. Alternatively, prevention is a good method to protect the population against leishmanial infections, but here again, the population concerned often lack resources to protect themselves efficiently. Finally, the development of a good vaccine appears as the best solution to protect people from infections [330]. Live vaccination with virulent parasites, also known as leishmanization, efficiently protected humans against cutaneous leishmaniasis. However, this was abandoned because of safety concerns, as it could result in immunosuppression or non-healing lesions [331]. Consequently, autoclaved-killed parasites were used in clinical trials as a replacement method against cutaneous leishmaniasis and visceral leishmaniasis. Unfortunately, the potency of the autoclaved parasites decreased with time [331]. Various attenuated parasites were also tested in animal models. Even though attenuated parasites could confer protection in mice and hamsters, the possibility that these parasites regain virulence is an important issue for human use [331]. Alternative approaches, including immunization with surface antigens, were tested in mouse models and canine visceral leishmaniasis. For instance, a formulation of the fucose mannose ligand expressed by the parasite has been licensed for use as a veterinary vaccine against canine visceral leishmaniasis. However, the production of these vaccines according to clinical manufacturing standards is a major hindrance for human applications [331]. Recombinant proteins have also been tested with success in preclinical models. One of these candidates, Leish-111F/MPL-SE, is currently being tested in human clinical trials. Nonetheless, the production and purification of recombinant protein is expensive [331]. However, DNA vaccines are currently being generated and these are much cheaper alternatives [331]. In conclusion, the road towards an ideal vaccine is yet tortuous, and still requires a better understanding of the biology of the different *Leishmania* species [330,331].

2.3.2 Immunobiology of *L. major* infection: resistance versus susceptibility ?

The fact that rodents are natural hosts for *Leishmania* species provides a unique biological model to better understand the biology of the different forms of leishmaniasis. In particular, studies with the *Leishmania major* mouse model of cutaneous leishmaniasis revealed to the scientific community the

fundamental role of the host genetic background in the resistance or susceptibility to infection [332].

Back in the early seventies, infectious studies with *Leishmania major* showed that some mouse strains, such as C57BL/6, were able to control the infection without parasite spreading to other organs than skin and draining lymph nodes. Such strains naturally heal, and are resistant to secondary challenge [333]. Conversely, some other strains, such as BALB/c, can not control the infection. In that case, the parasites multiply and ultimately spread to visceral organs, mimicking some of the symptoms of visceral leishmaniasis. This inexorably leads to death [333]. At the beginning of the eighties, new studies identified the key role of T cell populations to confer immunity or susceptibility to infection [334,335]. In 1989, resistance was linked to the production of IFN- γ (interferon gamma) by effector T cells, while susceptibility was associated with the production of IL-4 (interleukin 4) [336]. This was the first evidence that resistance and susceptibility were associated with T helper 1 and T helper 2 responses, respectively.

The mechanisms controlling the Th1/Th2 responses were extensively investigated. Surprisingly, both resistant and susceptible strains mount an IL-4 (i.e. Th2) response and fail to mount an IL-12 (i.e. Th1) response at very early time points [325]. However, resistant animals then start to produce IL-12 that redirects the Th2 response to a Th1 response. Therefore, resistant animals ultimately exhibit an IL-12-driven, IFN- γ -dominated Th1 response. The secretion of IFN- γ by Th1 cells activates infected macrophages, and leads to efficient killing of the parasites [326,337]. It is worth noting that both IL-12 and IFN- γ deficient mice default to the Th2 pathway, and display a phenotype similar to susceptible mice [338-340].

Conversely, BALB/c mice mount a non-protecting T helper 2 response characterized by production of anti-inflammatory cytokines [325,341]. Contrary to what was primarily thought, IL-4 is neither sufficient, nor always necessary for susceptibility [325]. Indeed, studies with knockout animals also highlight the key roles of IL-13, IL-10, and TGF- β as additional key factors controlling susceptibility [325].

The genetic basis of resistance versus susceptibility has also been investigated. Resistance has been genetically mapped to 6 chromosomal loci. Moreover, a multitude of combinations of these loci are capable to confer resistance [342]. Interestingly, when susceptible BALB/c are crossed with resistant C57BL/6 mice, the F1 generation developed a Th2 phenotype after intradermal infection in the dorsal skin, while a Th1 response after

subcutaneous footpad injections [343]. This clearly illustrates the complexity of this model. In line with the latter comment, it is important to note that various models of infection are currently in use, and result in some discrepancies depending on the vector used for injection (natural sand fly vector or needle inoculation), the *L. major* strain used (many strains exist), the route of injection (intra-dermal or subcutaneous), and the number of parasites inoculated (from 10^2 to 10^7). These indications have to be taken into account when reading the next sections.

Finally, T helper 17 and regulatory T cells have also been implicated in immune responses to *L. major* infection, but will not be detailed in this manuscript [344,345].

2.3.3 The role of neutrophils in the mouse model of cutaneous leishmaniasis

Neutrophils constitute as much as 40-70% of blood leukocytes found in mammals, therefore being the dominant leukocyte in the circulation. They are major players of innate immune responses following pathogen invasion of our body. Indeed, in response to many infectious diseases, neutrophils are massively recruited to the site of infection where they display a wide range of functions, from killing to orchestrating immune reactions. Indeed, their first role is to act as the front line killing cell. For this purpose, neutrophils display a wide toolbox to efficiently neutralize the pathogen, either through respiratory burst, or the production of nitric oxide, or even through the release of anti-microbial proteins [346,347]. In addition to these well-known anti-microbial strategies, it was recently described that neutrophils release extracellular traps of DNA content, the so-called NETs (Neutrophils Extracellular Traps), which neutralize pathogens in the extracellular space [348]. In addition to its killing function, neutrophils can secrete a wide set of cytokines and chemokines to modulate the immune response and contribute to the recruitment of additional leukocytes to the site of infection [349].

In the *Leishmania major* model of cutaneous leishmaniasis, neutrophils are the first cells to be recruited to the site of infections in both susceptible and resistant animals [350]. If neutrophils are massively recruited early after infection in both genetic backgrounds, at later time points however, the numbers of neutrophils decrease in C57BL/6 mice, contrary to BALB/c mice [351,352]. Regarding the strong chemotactic behaviour of neutrophils in the

direction of the parasite inoculum once they exit skin venules (**Figure 29**), it is likely that strong chemotactic gradients govern the massive recruitment of neutrophils to the site of infection. However, the exact contribution of the chemotactic cues that control this recruitment is still elusive [353]. It was reported that CXCL1 mRNA (also known as KC) is upregulated early after infection in C57BL/6 mice [354], but this report does not investigate the precise role of KC *in vivo*. *In vitro*, peritoneal macrophages from C57BL/6, stimulated with *L. major*, secrete high levels of CXCL1 and CXCL2 (also known as MIP-2 α) [355], while BALB/c-derived BMDMs (Bone Marrow Derived Macrophages) upregulate CXCL1 mRNA upon *L. major* stimulation [356]. Altogether, this only suggests a potential role for CXCL1 and CXCL2. In addition, a role for the chemotactic complement fragment C3 was also described *in vivo* [357]. Finally, a yet unidentified *Leishmania* chemotactic factor (LCF) secreted by *L. major* itself attracts human neutrophils *in vitro* [354,358].

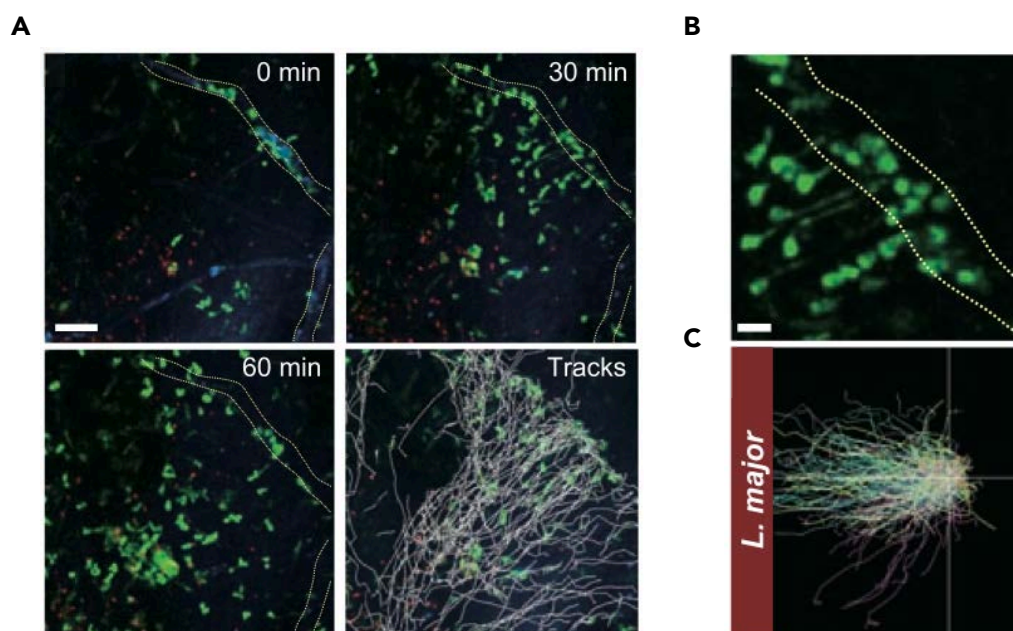


Figure 29. Rapid chemotactic attraction of neutrophils after intradermal inoculation of *L. major*. LYS-eGFP animals were subjected to 2 Photon intravital microscopy 30 min p.i. with 10^4 *L. major*-RFP. (A) Time-lapse images showing GFP⁺ (green) cells, *L. major*-RFP (red), and blood vessels (blue). Panel labeled “Tracks” shows the paths followed by cells from the vessel to site of inoculation of parasites over 60 min. (B) Magnified view from (A) showing neutrophil extravasation from vasculature. (C) Cell migration paths from three independent experiments (cyan, yellow, and purple tracks) were normalized for their origin and their position relative to the site of parasite deposition. Text and figure adapted from [350].

Once neutrophils have infiltrated the infected skin, they rapidly capture *L. major* [350]. However, *Leishmania* species have evolved a unique strategy to escape the oxidative burst in phagolysosomes of phagocytes [359,360]. As a consequence, infected neutrophils die by apoptosis. Apoptotic neutrophils either release free parasites before being cleared [350], or can also be phagocytosed before parasite release by macrophages or DCs [361,362]. The

latter mechanism was initially thought to be a Trojan horse strategy for *Leishmania* to infect macrophages or DCs. However, a recent report questioned this hypothesis as the efficient capture of infected neutrophils by DCs has immunosuppressive effects in C57BL/6 mice contrary to what was originally thought [361]. Yet, the same author has previously shown that infected macrophages were able to kill infected parasites coming from the neutrophils previously phagocytosed [362].

In addition to engulfment of *Leishmania* parasites, neutrophils also orchestrate the immune response by secreting cytokines. The best example came from a study in 2010, showing that neutrophils-derived CCL3 controls the recruitment of dendritic cells to the site of infection in resistant animals [91].

Finally, to understand the exact function of neutrophils in cutaneous leishmaniasis, neutrophils were depleted using different monoclonal antibodies. However, the site of infection, the quantity of parasites inoculated, the genetic background, and more importantly the lack of specificity of the depleting antibodies used, resulted in some discrepancies [350,351,361,363-365]. Therefore, these results will be detailed and discussed in the discussion part of this thesis.

2.3.4 The role of monocytes and DCs in the mouse model of cutaneous leishmaniasis

DCs are one of the most fascinating cell types of our immune system, as they constitute a bridge between innate and adaptive immunity. DCs are the most potent antigen presenting cells of our immune system [366]. They can either trigger immunity, or tolerance against the antigen they present on their Major Histocompatibility Complex (MHC), depending on their mature or immature status [366]. Indeed, DCs are particularly well suited to sense pathogen signatures through their pattern-recognition receptors (PRRs) such as Toll-like receptors (TLRs) [367]. Sensing of pathogen-associated molecular patterns (PAMPs) through PRRs activates DCs, which in turn upregulates costimulatory molecules such as CD40, CD80, CD86 at the cell surface [367]. Such mature DCs can present antigen to T cells and engage costimulatory molecules, altogether inducing immunogenic responses [366]. Alternatively, DCs also express a broad spectrum of cytokine receptors, and can therefore mature in response to inflammatory cytokines [368]. In absence of DC maturation, antigen presentation to T cells results in tolerance [366].

Even though all the above characteristics are shared by all DCs, many subsets have been described since their initial discovery in 1973 by Ralph Steinman [369], based on their location, phenotype, and their resulting function [370]. Two main functional groups exist, the plasmacytoid DCs (pDCs) and the conventional DCs (cDCs). The former sense viruses via their TLR 7 and 9 (**Table 1**, p.13), and subsequently produce high amounts of type I interferons upon maturation [371]. The latter can be further subdivided into migratory DCs and lymphoid-resident DCs. Migratory DCs are mainly found within the skin. This includes the Langerhans cells (LCs), which populate our first skin layer, the epidermis. LCs display amazing dendrites to sense their local environment (**Figure 30**), and are characterized by their high cell surface level of the transmembrane lectin Langerin [372]. In the underlying dermis (**Figure 30**), two types of dermal DCs (dDCs) are found, the Langerin⁺ CD103⁺ CD8 α ^{+/-} cross-presenting DCs, and the Langerin⁻ CD103⁻ DCs [370]. In secondary lymphoid organs, resident DCs include the CD11b⁺ CD4⁺ DCs and the cross-presenting CD11b⁻ CD8 α ⁺ DCs [370]. Finally, under inflammatory conditions, circulating monocytes that extravasate to the inflamed tissue can give rise to DCs. These are referred to as inflammatory DCs, TNF α /iNOS producing DCs (TIP DCs), or monocyte-derived DCs (mo-DCs) [373]. As mo-DCs derive from monocytes, they express the myeloid marker CD11b and the monocyte marker Ly6c [373]. Important to note, that all DCs share the integrin CD11c (also known as α_x) as ubiquitous DC marker [370]. All the above DCs subsets and phenotypes are listed in **Table 3**.

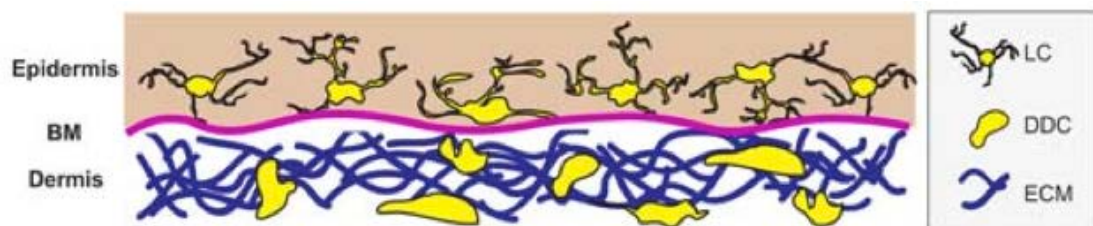


Figure 30. Schematic representation of DC localization in relation to different compartments in the skin.
Figure taken from [224].

	Skin derived DC			Lymphoid tissue resident DC		Inflammatory monocyte derived DC	pDCs
	Langerhans	Langerin ⁺	Langerin ⁻	CD11b ⁺	CD8 ⁺		
CD11c	+	+	+	+++	+++	int	int
CD11b	+	low	+	++	-	++	-
CD8 α	-/+	-/+	-	-	++	-	-
Langerin	+++	++	-	-	+	ND	-
DEC-205	++	+	-	-	+	ND	-
CD103	-	+	-	-	-	ND	-
Ly6C	-	-	-	-	-	++	++
B220	-	-	-	-	-	-	++
Clec9A	-	-	-	-	+	-	-
Sirp α	+	ND	+	+	-/low	ND	ND
CD24	ND	ND	ND	low	+	ND	ND
CD4	-	-	-	+/-	-	-	+/-
F4/80	+	+	-	-	-	ND	-
MHC-II	++	++	++	+++	+++	++	++
TLRs	TLR4	TLR 3		TLR9, TLR7	TLR3, TLR9	TLR7, 9	TLR7, TLR9
Half life	Slow	Fast	Fast	Fast	Fast	Fast	Fast
Location	Epidermis	Dermis	Dermis	LN, spleen, Peyer's patches, liver	LN, spleen, Peyer's patches, thymus, liver	Monocytes in the blood	Blood, LN, thymus, spleen, Peyer's patches
CCR7	-	*	*	+	+	*	+
Radiation	Resistant	Sensitive	Sensitive	Sensitive	Sensitive	Sensitive	Sensitive

Table 3. Surface markers of dendritic cell subsets in mice. Table taken from [370].

The ontogeny of DCs has been and is still a matter of intense debates. Initially, experts thought that DCs stem from a common DC progenitor. However, recent data suggest that cDCs, pDCs, and macrophages do not share a common progenitor contrary to what was originally thought [374,375].

All DCs subsets, without exception, have been shown to contribute to the immune response against *L. major* infection. However, they naturally play distinct immunomodulatory roles, and more importantly exhibit their APC function in sequential waves along the course of the disease [370] (**Figure 31**).

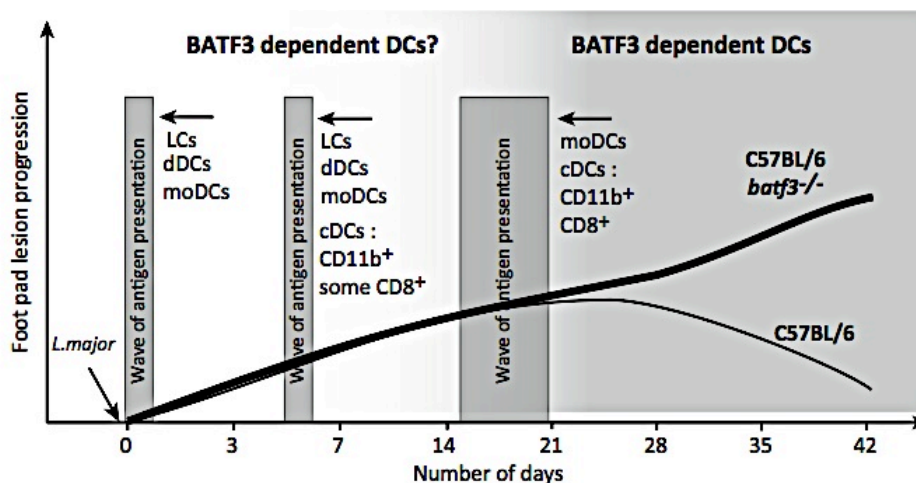


Figure 31. Schematic representation of infection progression in a mouse model of *Leishmania major* infection. Infection progression and healing in C57BL/6 wild type mice is shown over time by a thin black line. A thick black line represents infection progression without healing, as observed in *batf3*^{-/-} mice. Langerhans cells, dermal dendritic cells (dDCs), and mo-DCs form the first wave of antigen presentation following *L. major* infection. The second wave of antigen presentation involves mostly CD11b⁺, and CD8⁺ cDCs. The third wave of antigen presentation involves mo-DCs and CD8⁺ cDCs [45]. Background shading indicates the progression of infection. Text and figure are adapted from [370].

As early as 24h post infection, Langerhans cells, dermal DCs, and mo-DCs form the **first wave of antigen presentation**. **Langerhans cells** efficiently process and present *Leishmania* antigen and initiate a specific T cell response in draining lymph nodes [376]. Moreover, expression of the IL4 receptor was increased on infected LCs of susceptible mice, but not of resistant animals [377]. More recently, a study using high parasite doses (10^6) stated for a dispensable role for LCs in antigen presentation *in vivo* [378], while injection of 10^3 parasites revealed LCs as negative regulators of anti-*Leishmania* responses [379]. **Dermal DCs** can sense and incorporate parasites early after infection in the skin *in vivo* [224]. Moreover, dDCs were shown to transport *Leishmania* antigen to the lymph nodes as early as 16 hours post infection [380]. One study that focused on cross-presenting dermal DCs (Langerin⁺ CD103⁺) demonstrated their role in the early priming of CD8 T cells. However, this role was dispensable for the long-term protection observed in resistant mice [381]. The **CD8 α ⁻ lymph node resident DCs** also mediate antigen presentation to T cells 24 hours post infection [382]. In that case, resident-DCs acquire soluble *Leishmania* antigens likely through passive draining of antigens via afferent lymphatics [382]. Within 3 days post infection, **mo-DCs** are also found in increased numbers in the lymph nodes, while their prominent role in antigen presentation is well established at later time points post infection [223].

At one week post infection, the number of mo-DCs significantly decreases, meanwhile CD11b⁺ CD4⁺ lymph node resident DCs represent **the second wave of antigen presentation** to T cells at this later time point [380]. However, CD11b⁺ CD4⁺ resident DCs produce less IL-12 than CD11b⁻ CD8 α ⁺ DCs upon activation [383], while the latter are less permissive to infection with *L. major* *in vitro* [384].

Finally, a **third wave of antigen presentation** occurs from 2 to 4 weeks post infection [370]. The dominant DCs subset at that time point is constituted by mo-DCs that have migrated from the infected site to the draining lymph node. These mo-DCs are the most potent *leishmania*-derived antigen presenting cells at this time point [223]. In line with these results, an additional study showed that TIP DCs (phenotypically similar to mo-DCs) are the major infected cells during this chronic phase of the disease [385]. The fundamental role of monocytes and mo-DCs has been further highlighted with the use of the CCR2 knock-out mouse with C57BL/6 background. In these mice, the recruitment of mo-DC to the lymph nodes is severely reduced, diminishing the Th1 cells [385], and resulting in a non-healing phenotype similar to that observed in susceptible mice [386]. In addition to

mo-DCs, the role of the skin-derived and lymph node-resident cross-presenting DCs was recently unraveled using Batf3 (a transcription factor active in CD8 α ⁺ cDCs and CD103⁺ dDCs) knock-out animals [387]. Indeed, these animals exhibit an intermediate susceptibility phenotype [387]. However, resident CD8 α ⁺ cross presenting DCs being more potent antigen presenting cells at 3 weeks post infection than their skin-derived CD103⁺ counterparts, it is likely that the phenotype observed in Batf3 null mice is due to the absence of CD8 α ⁺ DCs rather than CD103⁺ dDCs [387].

2.3.5 Role of adhesion molecules in cutaneous leishmaniasis

The role of vascular adhesion molecules in the recruitment of leukocytes and the subsequent immune response to *L. major* infection was not investigated in much detail to date. The two reports that raised this question focused on the role of selectins [388,389]. The latest study used antibodies against all the selectins and some of their ligands to show that the recruitment of monocytes to the site of infection and to the draining lymph node was reduced upon antibody blockade. However, the authors did not investigate the consequences on the immune responses [389]. This was however done in the former study, which used simple P- or E-selectin knock out or double P- and E-selectin knock out mice, to assess the immunity of resistant animals lacking either one or both of these selectins on endothelial cells. Surprisingly, the lack of endothelial selectins had no significant effect on the clinical outcomes of the disease, showing that they were not required for protective immunity to infection [388]

3. Aim of the thesis

This thesis has two main objectives. On one hand, it aims to unravel the role of JAM-C in leukocyte trafficking in the context of an infectious disease, which has never been done before. For this purpose, we have decided to focus on the fascinating *L. major* model of cutaneous leishmaniasis. In this model, innate leukocytes are massively recruited in a chemotactic manner to the site of infection, therefore being the perfect model to elucidate the effect of JAM-C blockade on innate immune cells recruitment to the site of infection. Moreover, the migration of many DCs subsets from the infected site to the draining lymph nodes is reported to be fundamental in this model too. Many robust and easy-to-perform readouts exist to study both migration processes (from blood to tissue, and from tissue to lymph nodes). This makes this model ideally suited for our investigation.

On the other hand, the objective was also to explore the indirect consequences of JAM-C blockade on the immune responses. For this second purpose, the *L. major* model of cutaneous leishmaniasis was also well suited regarding the complex Th1/Th2 balance depending on the genetic background. As the recruitment of innate leukocytes differs from susceptible and resistant animals, the idea was to study whether JAM-C blockade would have an effect in both backgrounds, and allowing to observe the consequences on the type of the T cell response, and more importantly on the progression of the disease.

The combination of these two objectives not only provides evidence for the role of JAM-C in leukocyte trafficking during infection, but also highlights the manipulation of adhesion molecules as an efficient strategy to modulate the immune responses against infection.

4. Materials and methods

4.1. Ethic statement

All animal procedures were performed in accordance with the Institutional Ethical Committee of Animal Care in Geneva, Switzerland. The protocol has been approved by the Ethics and Federal Veterinary office regulations of the state of Geneva. Our laboratory has the authorization number 1005-3753.1.

4.2. Mice and parasites

Female C57BL/6J and BALB/c mice were purchased from Charles River (Lyon, France). Mice were bred in the P2 animal facility at the CMU, and used between 6-8 weeks of age. *Leishmania major* LV39 (MRHO/Sv/59/P Strain) were used. In all experiments, C57BL/6 mice were infected in the ear dermis with 2×10^6 stationary phase *L. major* promastigotes in a volume of 10 μ L. The disease outcome in BALB/c was followed after infection with 2×10^6 and 1×10^4 stationary phase *L. major* promastigotes in a volume of 10 μ L.

4.3. Flow cytometry analysis of ear endothelial cells

The ventral and dorsal sheets of mouse ears were split with forceps, and digested with 3mg/mL collagenase type IV (Invitrogen) and 1mg/mL DNase type I (Sigma Aldrich) for 45 minutes at 37°C, filtered through a 70 μ m gauge strainer (Becton Dickinson), and the cells labelled for FACS analysis. Fc receptors were blocked with the monoclonal antibody (mAb) 2.4G2 (Becton Dickinson). Cells were stained with the following reagents: Alexa Fluor 488-conjugated anti-mouse podoplanin (clone 8.1.1), PE-conjugated anti-mouse CD31 (clone 390), PE-Cy7-conjugated anti-mouse CD45 (clone 30-F11), all from affimetrix eBioscience. JAM-C was labelled with an affinity purified polyclonal anti-mouse JAM-C antibody raised in rabbit [274], while affinity purified rabbit IgG (Sigma) was used as a control. The secondary antibody used was an Alexa Fluor 647-conjugated anti-rabbit antibody (Jackson ImmunoResearch). Cells were analyzed with a Gallios FACS machine (Beckman Coulter) and the data were processed with Kaluza software (Beckman Coulters).

4.4. Leukocyte emigration for ear skin explants and FACS analysis

Mice were injected i.p. with the rat IgG2a anti-mouse JAM-C H33 or the rat IgG2a isotype control 2A3 (BioXCell), 200 μ g/mice, 2 hours before inoculation of *L. major* in the ear dermis. Twenty-four hours post infection, mice were sacrificed and ears explanted. The ventral and dorsal sheets of the ears were

separated with forceps, and transferred overnight in twelve well plates filled with RPMI-1640 medium supplemented with 10% fetal calf serum and antibiotics at 37°C. Over this period of time, the leukocytes that have been recruited to the infected ears spontaneously emigrated from the explants. Emigrated cells were then counted with a hemocytometer, and stained for FACS analysis. Fc receptors were blocked with the mAb 2.4G2. Cells were stained with the following reagents: Alexa Fluor 488-conjugated anti-mouse Ly6C (clone HK1.4, Biolegend), PercP-Cy5.5-conjugated anti-mouse Ly6G (clone 1A8, Biolegend), PE-Cy7-conjugated anti-mouse CD11b (clone M1/70, Biolegend), APC-Cy7-conjugated anti-mouse CD11c (clone N418, Biolegend), and efluor 450-conjugated anti-mouse IA/IE (clone M5/114.15.2, eBiosciences). Cells were analyzed with a Gallios FACS machine (Beckman Coulter) and data processed with Kaluza software (Beckman Coulters). The number of cells per population was calculated by multiplying the total number of emigrating cells with the percentage of cells of interest.

4.5. Flow cytometry analysis of leukocyte populations in steady state

Mice were injected i.p. with the mAb H33 or the control mAb 2A3 (200µg/mice). Mice were then sacrificed 24 hours after treatment to collect ears, blood and femurs. Ears were processed as described above. Femurs were flushed to extract bone marrow cells. Red blood cells from blood and bone marrow samples were lysed with Ammonium-Chloride-Potassium (ACK) lysis buffer. A fraction of each sample was used for FACS staining using BD Trucount tubes according to the manufacturer's instructions. Fc receptors were blocked with the mAb 2.4G2. Bone marrow cells were stained with the following reagents: Alexa Fluor 488-conjugated anti-mouse Ly6C (clone HK1.4, Biolegend), PE-conjugated anti-mouse CD115 (clone AFS98, eBiosciences), PercP-Cy5.5-conjugated anti-mouse Ly6G (clone 1A8, Biolegend), PE-Cy7-conjugated anti-mouse F4/80 (clone BM8, Biolegend), APC-conjugated anti-mouse CD11c (clone HL3, BD), APC-Cy7-conjugated anti-mouse TCR β (clone H57-597, Biolegend), efluor 450-conjugated anti-mouse CD11b (clone M1/70, eBiosciences), Brilliant Violet 785-conjugated anti-mouse CD8 α (clone 53-6.7, Biolegend). Blood cells were stained with the following reagents: Alexa Fluor 488-conjugated anti-mouse Ly6C (clone HK1.4, Biolegend), PE-conjugated anti-mouse CD115 (clone AFS98), PercP-Cy5.5-conjugated anti-mouse Ly6G (clone 1A8, Biolegend), PE-Cy7-conjugated anti-mouse CD4 (clone RM4-5, Biolegend), APC-conjugated anti-mouse NK1.1 (clone PK136, Biolegend), APC-Cy7-conjugated anti-mouse CD19 (clone 6D5, Biolegend), efluor 450-conjugated anti-mouse CD11b (clone M1/70, eBiosciences), Brilliant Violet 785-conjugated anti-mouse CD8 α

(clone 53-6.7, Biolegend). Cells were analyzed with a Gallios FACS machine (Beckman Coulter) and the data were processed with Kaluza software (Beckman Coulter). The number of cells per population was calculated by multiplying the total number of cells with the percentage of cells of interest. The total number of cells was calculated using the number of Trucount beads analyzed by the flow cytometer.

4.6. FITC painting experiments

Mice were injected i.p. with the mAb H33 or the control mAb 2A3 (200µg/mice) 2 hours before FITC painting of mice ears. FITC (Sigma) was used at 5mg/mL and dissolved in acetone: dibutyl phthalate (1:1, v:v). Twenty microliters were applied to each side of the ear. Eighteen hours after painting, the ear draining lymph node was harvested and digested with 3mg/mL collagenase type IV (Invitrogen) and 1mg/mL DNase type I (Sigma) for 45' at 37°C, and filtered through a 70µm gauge strainer (Becton Dickinson). The cells were counted with a hemocytometer, and labelled for FACS analysis. Fc receptors were blocked with the mAb 2.4G2. Cells were stained with the following reagents: APC-Cy7-conjugated anti-mouse CD11c, and efluor 450-conjugated anti-mouse IA/IE. Cells were analyzed with a Gallios FACS machine (Beckman Coulters) and data processed with Kaluza software (Beckman Coulters). The number of FITC⁺ migratory DCs was calculated by multiplying the total number of lymph node cells with the percentage of IA/IE^{high} CD11c⁺ FITC⁺ DCs.

4.7. Immunofluorescence microscopy

Mice were injected i.p. with the mAb H33 or the control mAb 2A3 (200µg/mice). Twenty-four hours after injection, ears were embedded in Tissue-Tek OCK compound, frozen at -80°C, then cut (5µm) with a cryostat. Fresh ear sections were fixed in cold acetone for 5 minutes, rehydrated in PBS for 10 minutes, and blocked with 10% normal donkey serum. CD31 was detected with an Alexa Fluor 647-conjugated rat anti mouse CD31 (clone GC51, home made), while JAM-C was detected with a polyclonal anti-mouse JAM-C antibody raised in rabbit [274] followed by an Alexa Fluor 488-conjugated donkey anti-rabbit antibody (Jackson ImmunoResearch). I used rabbit IgG as control for JAM-C staining. Cell nucleus was stained with DAPI and slides were mounted with mowiol mounting medium. Labelled ear sections were visualized with a Nikon A1R confocal microscope and the NIS Elements AR software. All images were acquired with a 100x objective. The maximal intensity projection image of the z-stack is shown. The images were analyzed with Image J. The distribution profile of JAM-C was plotted along the minor axis of the cells.

4.8. Vascular permeability assay

Mice were treated i.p. with the mAb H33 or the control mAb 2A3 (200µg/mice) 2 hours before 100µL of Evans blue (12mg/mL) was injected i.v. and *L. major* inoculated i.d. in the ear. Five hours after infection, mice were killed, and the permeability of Evans blue in the ear documented by picturing each ear. Ears were then cut, weighted, split into dorsal and ventral sheets, and finally transferred into formamide for 2 days at room temperature to extract the Evans blue dye. The absorbance of the samples was measured at 620 nm (Ledetect 96, Labexim) and normalized to the weight of tissue.

4.9. CCL3 level in ear following *L. major* infection

Mice were injected i.p. with H33 or the control mAb 2A3 (200µg/mice) 2 hours before *L. major* inoculation in the ear dermis. Eight or 24 hours after infection, ears were homogenized on ice in a protease inhibitor cocktail (Sigma Aldrich, P8340) using a polytron as tissue homogenizer. The expression of the chemokine CCL3 were measured in tissue homogenates with the BD CBA mouse Flex Set kit according to the manufacturer instructions. Beads were analyzed on a Cyan (Beckman Coulters) flow cytometer and data processed with the FCAP array software (Becton Dickinson).

4.10. T cell response in the draining lymph node and cytokine detection

The ear draining lymph nodes were digested with 3mg/mL collagenase type IV (Invitrogen) and 1mg/mL DNase type I (Sigma) for 45' at 37°C, and filtered through a 70µm gauge strainer (Becton Dickinson). The cells were counted with a hemacytometer and labelled for FACS analysis. Fc receptors were blocked with the mAb 2.4G2. Cells were stained for cell surface antigens with the following reagents: FITC-conjugated anti-mouse TCRβ (clone H57-597, eBioscience), Brilliant Violet 421-conjugated anti-mouse CD8α (clone 53-6.7, Biolegend), Brilliant Violet 785-conjugated anti-mouse CD4 (clone RM4-5, Biolegend). Cells were analyzed with a Gallios FACS machine (Beckman Coulters) and the data were processed with Kaluza software (Beckman Coulters). The number of cells per population was calculated by multiplying the total number of lymph nodes cells with the percentage of cells of interest. For T cell restimulation, draining lymph nodes cells were incubated at 37°C under 5% CO₂ for 72 hours in the presence of UV-irradiated *L. major* (ratio 5:1, cell:parasite). Supernatant were collected and the levels of IL-4 and

IFN- γ were measured by ELISA (eBioscience) or CBA (Becton Dickinson) according to the manufacturer instructions.

4.11. Lesion area measurement and parasite load

Mice were injected i.p. with the mAb H33 or the control mAb 2A3 (200 μ g/mice) 2 hours before inoculation of *L. major* in the ear dermis. Injections of mAbs (100 μ g/mice) were repeated twice a week for twenty-one days. The evolution of the lesion was documented weekly with a picture of each ear, as well as the picture of a 1 cm scale. The camera was fixed on a support for the scale to be unchanged from one picture to the other. The pictures were analyzed with ImageJ software. Briefly, the picture of the 1 cm scale provides the number of pixels per 1 cm unit. Each lesion was then defined manually with the software, and the precise lesion area calculated using the number of pixels in the selected area. For parasite burden, the infected ears were explanted, weighted, and separated into two halves. Ear leaflets were enzymatically digested before tissue dissociation with a gentleMACS Octo Dissociator (Miltenyi Biotech). Ears homogenates, lymph nodes or spleens cells were serially diluted, and the parasite load estimated by limiting dilution assay as described [390].

4.12. Statistical analysis

Data were analyzed with the GraphPad Prism statistics software. I used the Student's t-test for unpaired data for all experiments.

5. Results

5.1. The antibody H33 mimics JAM-C downregulation after *L. major* inoculation, and locally increases vascular permeability after infection.

Blood endothelial cells (BECs) and lymphatic endothelial cells (LECs) from the skin of mouse ears were analyzed by flow cytometry. In the steady state, BECs (CD45⁻ CD31⁺ gp38⁻) and LECs (CD45⁻ CD31⁺ gp38⁺) were JAM-C positive as previously described for other organs [284] (Figure 1A, p.83). Conversely, leukocytes recruited to the infected ear following *L. major* inoculation were all JAM-C negative (Figure S1, p.90). I observed a statistically significant decrease of JAM-C expression in BECs and LECs 24 hours after *L. major* infection (Figure 1A and B, p.83). This was not the consequence of tissue injury caused by the needle, as saline injection did not downregulate JAM-C (Figure S2, p.91). Interestingly, previous studies observed a peak of leukocytes migrating to the site of infection at the same time period [91,361]. Therefore, I postulated that JAM-C downregulation after infection could enhance vascular permeability and therefore promote inflammation and cell migration.

To study the effect of H33 on vascular permeability, I used a modified Miles assay in which mice were injected i.v. with Evan's blue [391]. Evan's blue is a small molecule that binds strongly to albumin. Consequently, this assay indirectly assesses the exudation of plasma into the tissue accounting for vascular permeability. Mice were treated with H33 or the isotype control antibody before injection of Evan's blue and *L. major* inoculation. Strikingly, treatment with H33 significantly increased the amount of Evan's blue that leaked into the inflamed tissue as compared to control. However, I did not observe any change in vascular permeability under steady state conditions (Figure 1C, p.83).

To understand the mechanism leading to the increased vascular permeability, I investigated by immunofluorescence in our system whether H33 redistributes JAM-C out of ear endothelial cell junctions as previously proposed for other organs [275]. In control mice, JAM-C was strongly expressed at the cell border of CD31 positive endothelial cells (Figure 1D, top panel, p.83), resulting in a U-shaped pattern of distribution of the molecule (Figure 1E, top panel, p.83). In H33-treated animals however, JAM-C was removed from endothelial cell junctions (Figure 1D, bottom panel, p.83), as confirmed by the smoothed pattern of distribution of JAM-C (Figure 1E, bottom panel, p.83). Control staining for JAM-C is provided in Figure S3 (p.92).

Altogether, we concluded that the blockade of JAM-C with H33 redistributes JAM-C out of junctions, and increases vascular permeability after *L. major* infection.

5.2. Blocking JAM-C increases the number of circulating cells recruited in response to *L. major* infection

To study whether the effect of H33 on vascular permeability potentiates leukocyte recruitment after *L. major* infection, I used wild type C57BL/6 mice treated with H33, and analyzed by FACS the number of emigrating leukocytes 24 hours after infection (Figure 2A, p.85). I observed a significant increase in the numbers of neutrophils, inflammatory monocytes, and mo-DCs in H33-treated animals as compared to control animals (Figure 2B-D, p.85). Meanwhile, the number of non-migrating dermal macrophages (dermal $\text{m}\phi$) was not modified (Figure 2E, p.85). Finally, the number of emigrating dermal DCs, a cell type that efficiently migrates to the draining lymph node once activated, was decreased in H33-treated animals (Figure 2F, p.85). In line with the absence of vascular permeability observed in the steady state (Figure 1F, p.83), JAM-C blockade did not increase leukocyte emigration in naïve mouse ears (Figure S4, p.93). Moreover, I found no difference in the number of leukocytes in the bone marrow and in the blood (Figure S5, p.94). This suggests that H33 does neither increase haematopoiesis nor leukocyte emigration from the bone marrow to the blood in normal homeostasis.

I also measured higher levels of the monocytes and mo-DCs attracting chemokine CCL3 in H33 treated animals early after infection (Figure 2G, p.85). This is in line with the increased number of neutrophils, a cell type known to produce CCL3 to attract mo-DCs in response to *L. major* [91]. Interestingly, the higher numbers of innate immune cells recruited with H33 did not impact on the parasite load early after infection (Figure 2H, p.85; and Figure S6, p.95). Moreover, the dissemination of the parasites to the draining lymph node was unchanged (Figure 2I, p.85; and Figure S6, p.95).

Overall, our data showed that JAM-C blockade with H33 increases leukocyte recruitment to the site of infection, and strongly suggest that H33 may influence DC migration to the draining lymph node.

5.3. Blocking JAM-C increases the number of DCs migrating to the draining lymph node

To investigate the effect of H33 on DC migration to the draining lymph node, I used the FITC painting assay. In this model, migration of dermal and epidermal DCs to lymph nodes is induced and peaks 18 hours after painting [392]. Based on MHC class II (IA) and CD11c, two populations of DCs can be distinguished by FACS in the lymph node: MHC-II^{high} CD11c⁺ migratory DCs, and MHC-II⁺ CD11c^{high} lymphoid resident DCs (Figure 3A, p.86). Strikingly, I found higher numbers of FITC⁺ IA^{high} CD11c⁺ migratory DCs in lymph nodes of H33-treated mice as compared to control animals (Figure 3A and B, p.86; and Figure S7, p.96). Therefore, H33 treatment not only increases leukocyte recruitment to the site of infection, but also increases the migration of DCs to the draining lymph node.

5.4. Blocking JAM-C improves the Th1 cell response and favours healing in C57BL/6 mice

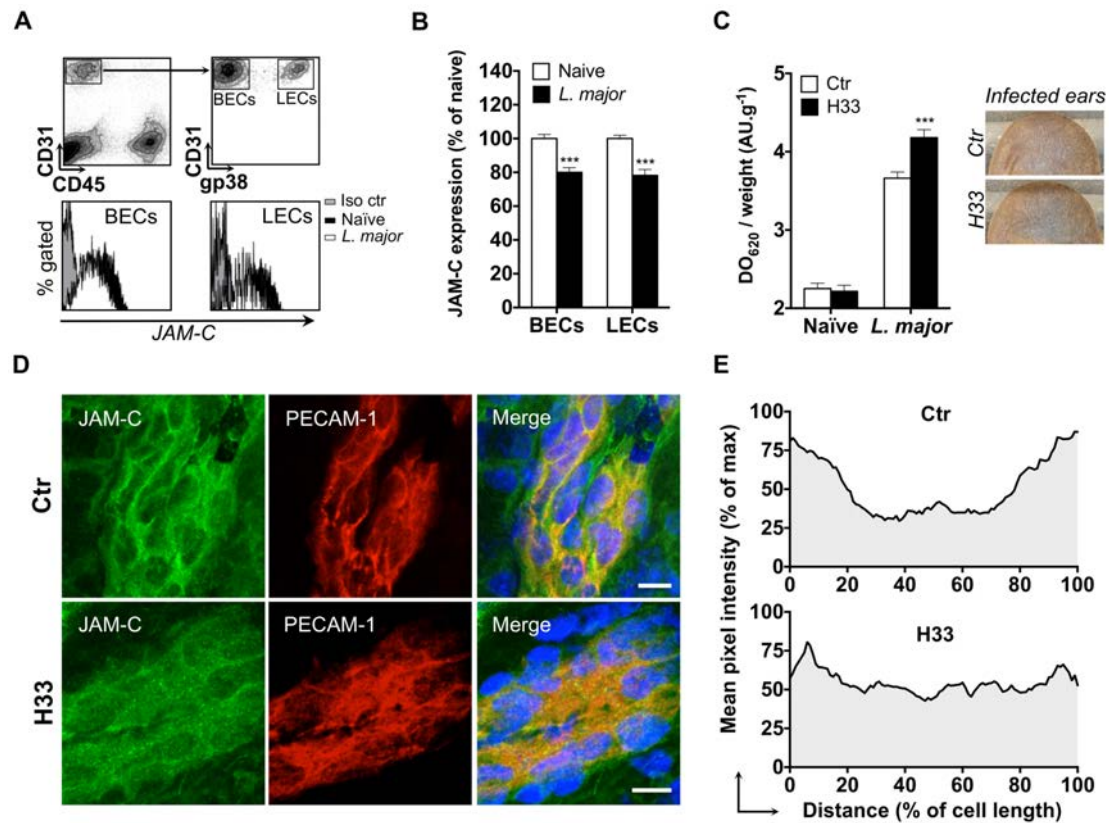
The increased DC migration to the draining lymph node in mice treated with H33 raised the question of an eventual effect on the subsequent T cell response and disease outcome. As previously reported, the induction of the T cell response starts between the second and third week after infection [223]. Therefore, mice were infected with *L. major* and treated with H33 for 3 weeks in order to boost DC migration and T cell activation. The disease was followed weekly by measuring the area of the lesions, and I assessed the *L. major* specific T cell response together with the parasite burden 4 weeks and 8 weeks post infection (p.i.). In C57BL/6 mice, I found smaller lesions in H33-treated compared to control animals at both time points (Figure 4A, p.87). Moreover, the reduction of the lesion area between the groups correlated with the decrease of the parasite load (Figure 4B, p.87; and Figure S8, p.97). These results were in line with the increased numbers of CD4⁺ and CD8⁺ T cells observed (Figure 4C and D, p.87). More importantly, draining lymph nodes T cells restimulated with UV-irradiated *L. major* produced significantly higher levels of IFN- γ at 8 weeks post infection, which accounts for the reduced lesion size and parasite load observed (Figure 4E, p.87; and Figure S8, p.97). Taken together, these data suggest that H33 increases DC migration and therefore indirectly boosts the *L. major* specific IFN- γ -dominated Th1 cell response, resulting in a reduced severity of the disease.

5.5. Blocking JAM-C boosts the Th2 cell response and worsens the disease in BALB/c mice

Contrary to the C57BL/6 background, BALB/c mice develop a Th2 response promoting susceptibility rather than resistance to *L. major* infection [325]. Therefore, I investigated the effect of JAM-C blockade on leukocyte migration and disease outcome in susceptible BALB/c animals. After 24 hours of infection, I found increased numbers of neutrophils, and mo-DCs recruited to the site of infection in H33-treated BALB/c mice as compared to isotype control-treated mice (Figure 5A and B, p.88). Moreover, I observed a decreased number of dermal DCs while unchanged numbers of dermal macrophages (Figure 5C and D, p.88). These results showed that H33 influences leukocyte migration in a similar manner in BALB/c than in C57BL/6 mice. I next wanted to assess whether this increased leukocyte migration could change the dominance of the Th2 response over the Th1 response along the course of the disease. To this end, BALB/c mice were injected with the same dose of *L. major* used with C57BL/6 mice. I did not find any change in the disease outcome with H33, most likely as a result of an exaggerated Th2 polarization with high parasite doses (Figure 5E, p.88). Therefore, we designed a new experiment with 200 fold less parasites inoculated. Strikingly, we now observed higher lesions in H33-treated animals (Figure 5F, p.88). This correlated with increased parasite loads in ears and draining lymph nodes (Figure 5G and H, p.88), while parasites were undetectable in spleens (Figure S9, p.98). The number of T cells was also augmented in draining lymph nodes (Figure 5I and J, p.88) and they secreted higher levels of IL-4 upon restimulation with UV-irradiated *L. major* (Figure 5K, p.88). The production of IFN- γ was however unchanged (Figure 5L, p.88). Altogether, these results show that the increased DC migration boosts the polarized Th2 immune response without changing the type of the T helper cell response.

6. Figures

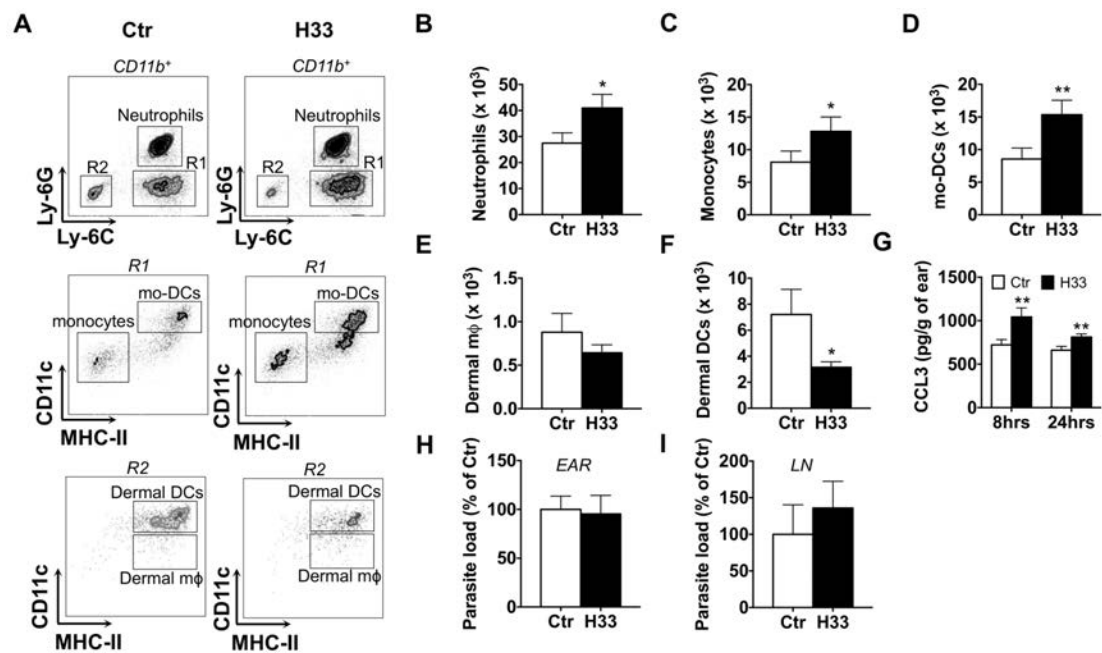
6.1. Figure 1



The antibody H33 mimics JAM-C downregulation after *L. major* inoculation, and locally increases vascular permeability after infection. (A) JAM-C levels in endothelial cells populations of mouse ear. Ears were enzymatically digested and stained for FACS analysis. CD45⁻CD31⁺gp38⁻ cells represent blood endothelial cells (BECs), whereas CD45⁻CD31⁺gp38⁺ cells are lymphatic endothelial cells (LECs). For each population, a representative histogram overlay is shown with JAM-C in endothelial cells from naïve ears (black filled), JAM-C in endothelial cells from *L. major* infected ears (blank filled), and the isotype control staining (grey filled). (B) The median fluorescence intensity (MFI) of JAM-C in naïve mouse ears (white bars) versus *L. major* infected mouse ears (black bars) was measured in BECs and LECs. The Y-axis scale represents MFI normalized to the mean MFI of naïve ears. Data represent the mean \pm SEM of ten individual mice pooled from two separate experiments, and were analyzed by the unpaired Student's t test with ***: $p < 0.001$. (C) Mice were treated with H33 or control antibody 2 hours before Evans blue was injected i.v. and *L. major* inoculated i.d. in the ear dermis. Skin permeability was assessed by the absorbance of Evans blue extracted from the sample normalized to the weight of ear. Results are shown for naïve versus *L. major* infected animals

treated with H33 (black bars) or control antibody (blank bars). Representative ear pictures are shown. Data represent the mean \pm SEM of seventeen mice per group pooled from two separate experiments, and were analyzed by the unpaired Student's t test with ***: $p < 0.001$. (D) Ear sections from control antibody-treated (top panel) or H33-treated mice (bottom panel) were stained for JAM-C (green) and CD31 (red). Nucleus was stained with DAPI (blue). Scale bars, 10 μm . Control staining for JAM-C is shown in Figure S3. (E) The pixel intensity across 10 representative cells of similar size taken from three mice per group was measured and expressed as a percentage of the maximal pixel intensity. Data represent the average profile plot for the 10 cells per group analyzed.

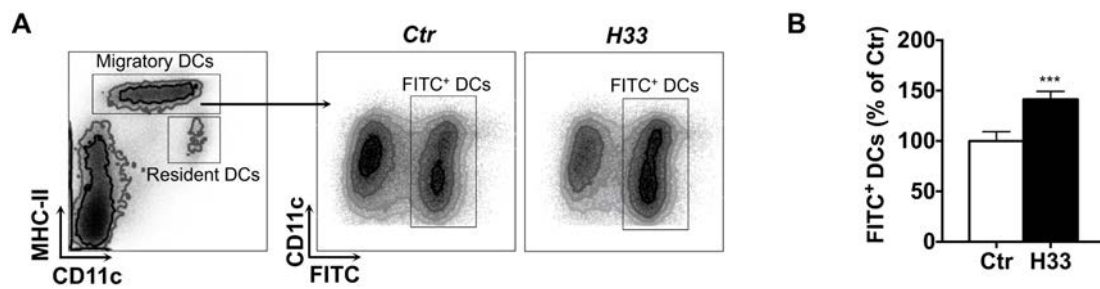
6.2. Figure 2



Blocking JAM-C increases the number of leukocytes recruited to the site of *L. major* infection.

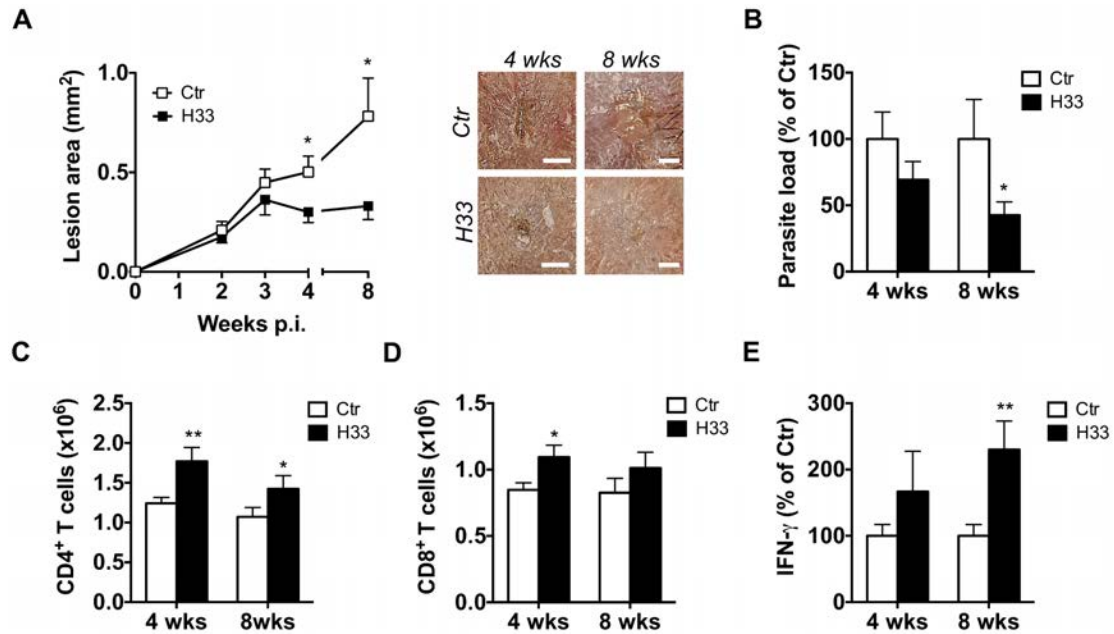
(A) Representative dot plots of neutrophils ($CD11b^+ Ly6C^+ Ly6G^+$); monocytes ($CD11b^+ Ly6C^+ Ly6G^- CD11c^- IA^-$); mo-DCs ($CD11b^+ Ly6C^+ Ly6G^- CD11c^+ IA^+$); dermal mφ ($CD11b^+ Ly6C^- Ly6G^- CD11c^{low} IA^+$); dermal DCs ($CD11b^+ Ly6C^- Ly6G^- CD11c^{high} IA^+$) in control versus H33-treated animals. (B-F) The number of neutrophils (B), monocytes (C), mo-DCs (D), dermal mφ (E) and dermal DCs (F) was measured in the H33-treated (H33, black bar) versus isotype control-treated mice (Ctr, white bars) 24 hours p.i. Data represent the mean \pm SEM of twenty mice per group pooled from 3 separate experiments, and were analyzed by the unpaired Student's t test with *: $p < 0.05$ and **: $p < 0.01$. (G) CCL3 protein levels normalized to the weight of ears were measured in H33-treated (H33, black bar) versus isotype control-treated mice (Ctr, white bars) 8 and 24 hours p.i.. Data represent the mean \pm SEM of ten mice per group pooled from 2 separate experiments, and were analyzed by the unpaired Student's t test with **: $p < 0.01$. (H-I) The parasite burden in infected ears (H) and draining lymph nodes (LN) (I) were measured 48 hours p.i. by limiting dilution assay (LDA). Data are expressed as a percentage of the mean of the control group \pm SEM of ten mice per group pooled from 2 separate experiments, and were analyzed by the unpaired Student's t test. For panel H and I, raw data of one representative experiment are provided in Figure S6.

6.3. Figure 3



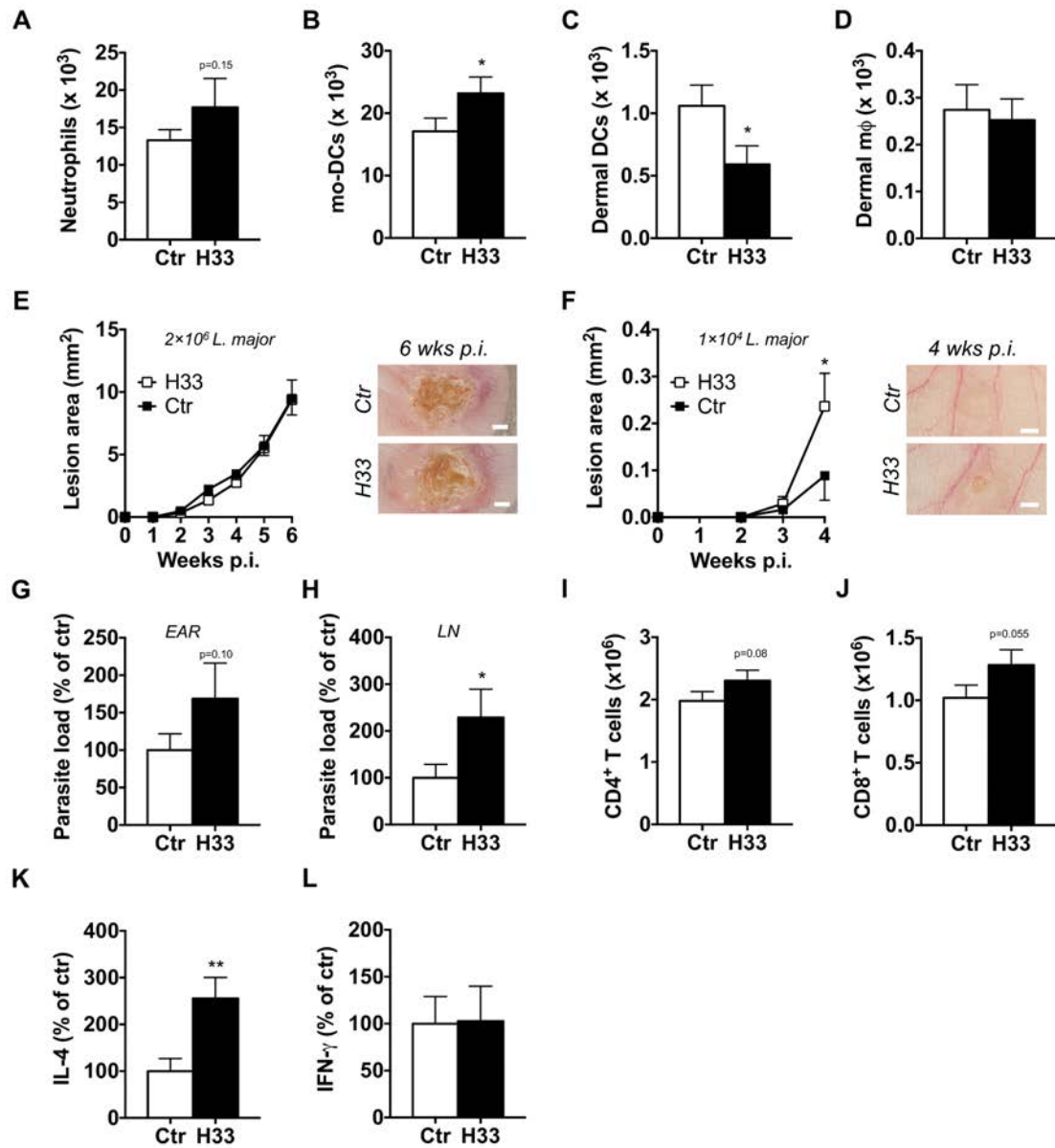
Blocking JAM-C increases the number of DCs migrating to the draining lymph node. (A) The ear draining lymph node cells were harvested and stained for FACS analysis 18 hours after FITC-painting. Representative FACS dot plots are shown. (B) The number of IA^{high} CD11c⁺ FITC⁺ migratory DCs was counted. Data are expressed as a percentage of the mean of the control group \pm SEM of eighteen mice per group pooled from 3 separate experiments, and were analyzed by the unpaired Student's t test with ***: $p < 0.001$. Raw data from one representative experiment are provided in Figure S7.

6.4. Figure 4



Blocking JAM-C improves the Th1 cell response and favours healing in C57BL/6 mice. (A-E) Mice were inoculated with *L. major* in the ear dermis and treated with H33 or isotype control antibody for 3 weeks, twice a week. (A) The area of the lesion was monitored weekly and representative pictures of ear lesions are shown at 4 and 8 weeks p.i. Scale bars, 0.5 mm. Data represent the mean \pm SEM of twenty mice per group pooled from two separate experiments for the time point 4 weeks; and fifteen mice per group pooled from two separate experiments for the time point 8 weeks. (B) The parasite burden in infected ears was measured by LDA 4 and 8 weeks p.i. Data are expressed as a percentage of the mean of the control group \pm SEM of mice from panel A. (C-D) The number of draining lymph node CD4⁺ (C) and CD8⁺ (D) T cells analyzed by flow cytometry 4 and 8 weeks p.i. Data represent the mean \pm SEM of mice from panel A. (E) Draining lymph node cells were restimulated for 72hrs with UV-irradiated *L. major* and the secreted IFN- γ was measured. Data are expressed as a percentage of the mean of the control group \pm SEM of mice from panel A. Data were analyzed by the unpaired Student's t test with *:p<0.05 and **:p<0.01. For panels B and E, raw data from one experiment are also provided in Figure S8.

6.5. Figure 5

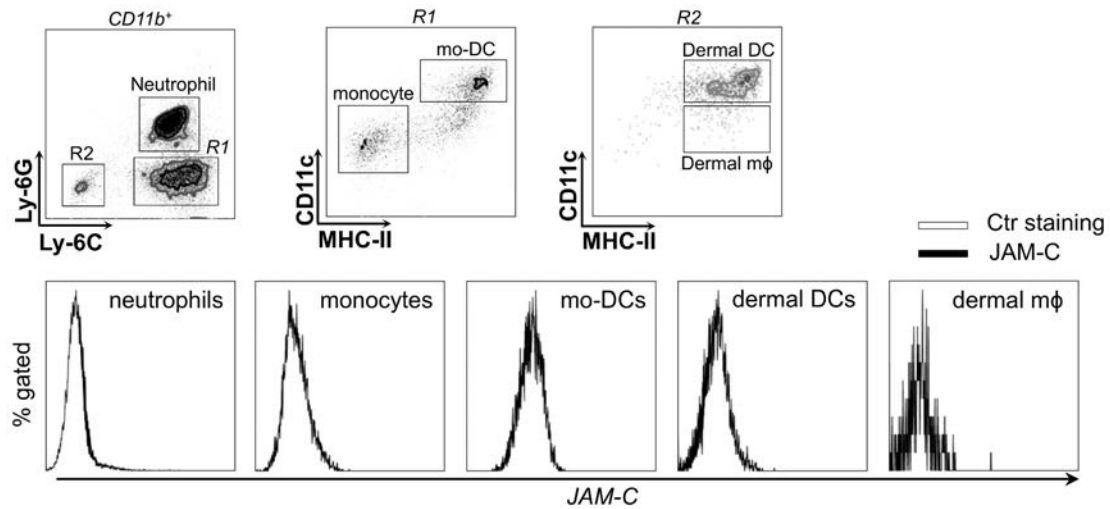


Blocking JAM-C boosts the Th2 cell response and worsens the disease in BALB/c mice.

The number of emigrating neutrophils (A), mo-DCs (B), dermal DCs (C) and dermal m ϕ (D) was measured in the ears of H33-treated (H33, black bar) versus isotype control-treated mice (Ctr, white bars) 24 hours post *L. major* infection. Data represent the mean \pm SEM of twelve mice per group pooled from 2 separate experiments, and were analyzed by the unpaired Student's t test with *: $p < 0.05$. (E) Mice were inoculated with 2×10^6 stationary phase *L. major* promastigotes in the ear dermis and treated with H33 or control antibody for 3 weeks. The area of the lesion was monitored weekly for 6 weeks. Representative ear pictures are shown. Scale bars, 1 mm. Data represent the mean \pm SEM of twenty mice per group

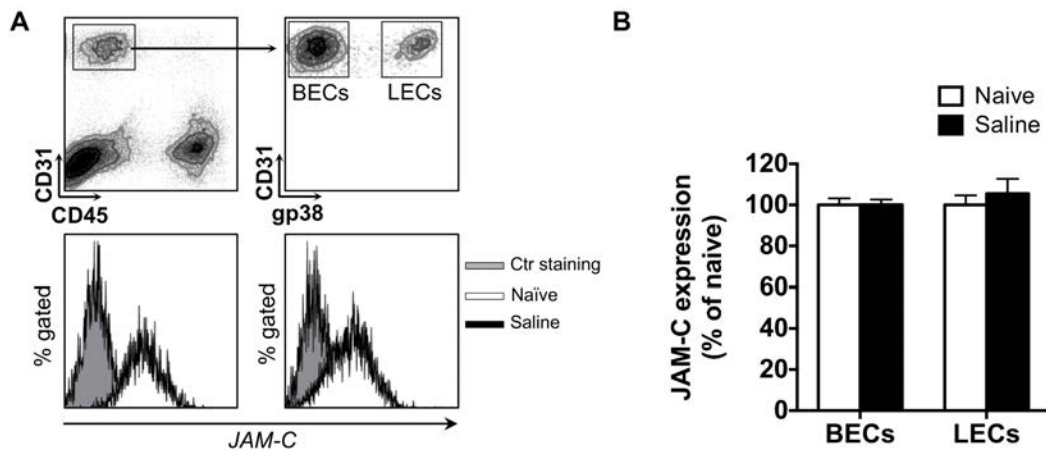
pooled from two separate experiments. (F-L) Mice were inoculated with 1×10^4 stationary phase *L. major* promastigotes in the ear dermis and treated with H33 or control antibody for 3 weeks. The area of the lesion was monitored weekly for 4 weeks. Representative ear pictures are shown. Scale bars, 0.5 mm. Data represent the mean \pm SEM of ten mice per group pooled from two separate experiments. (G-H) The parasite burden in infected ears (G) and draining lymph nodes (H) were measured by LDA. Data are expressed as a percentage of the mean of the control group \pm SEM of mice from panel F. (I-J) The number of CD4⁺ (I) and CD8⁺ (J) T cells were measured. Data represent the mean \pm SEM of mice from panel F. (K-L) Draining lymph nodes cells were restimulated with UV-irradiated *L. major* for 72 hours, and the IL-4 (K) and IFN- γ (L) produced were measured. Data are expressed as a percentage of the mean of the control group \pm SEM of mice from panel F. Data were analyzed by the unpaired Student's t test with *:p<0.05 and **: p<0.01. For panels expressing results as a percentage of the mean of the control, raw data of one experiment are provided in Figure S9.

6.6. Figure S1



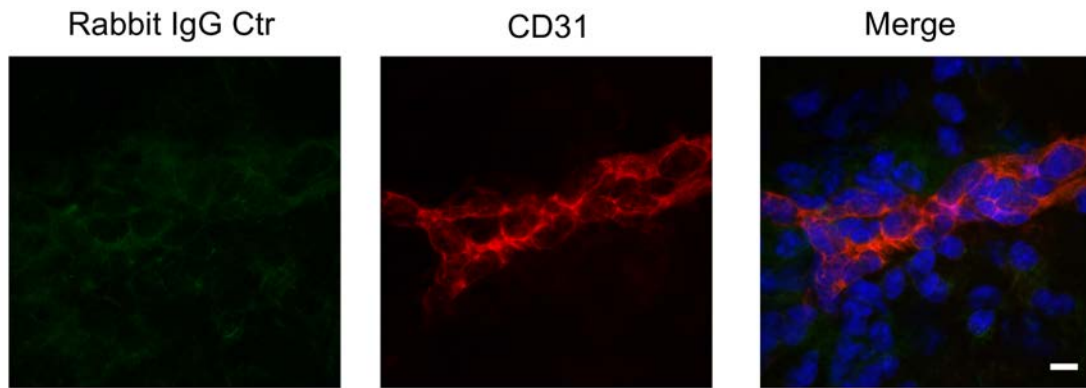
Leukocytes emigrating to the site of *L. major* infection do not express JAM-C. The expression of JAM-C by leukocytes emigrated from *L. major* infected ears was measured 24 hours post infection. CD11b⁺ Ly6C⁺ Ly6G⁺ represent neutrophils, CD11b⁺ Ly6C⁺ Ly6G⁻ CD11c⁻ IA⁻ are monocytes, CD11b⁺ Ly6C⁺ Ly6G⁻ CD11c⁺ IA⁺ are mo-DCs, CD11b⁺ Ly6C⁻ Ly6G⁻ CD11c^{low} IA⁺ are dermal mφ, and CD11b⁺ Ly6C⁻ Ly6G⁻ CD11c^{high} IA⁺ are dermal DCs. A representative histogram overlay of JAM-C expression is shown for each population, with JAM-C staining (black line), and isotype control staining (grey line). Data are representative of two separate experiments.

6.7. Figure S2



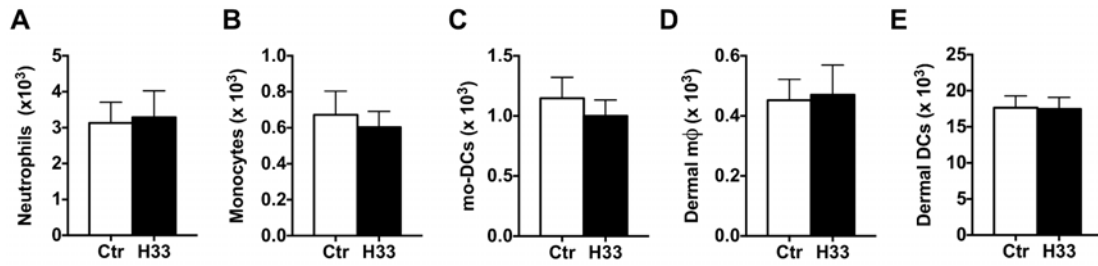
JAM-C expression in ear endothelial cells does not decrease 24 hours after saline injection. (A) JAM-C levels in endothelial cells populations of mouse ear. Ears were enzymatically digested and stained for FACS analysis. CD45⁻ CD31⁺ gp38⁻ cells represent blood endothelial cells (BECs), whereas CD45⁻ CD31⁺ gp38⁺ cells are lymphatic endothelial cells (LECs). For each population a representative histogram overlay is shown with JAM-C in endothelial cells from naïve ears (white filled), JAM-C in endothelial cells from saline injected ears (black filled), and the isotype control staining (grey filled). (B) The MFI of JAM-C in naïve mouse ears (white bars) versus saline injected mouse ears (black bars) was measured in BECs and LECs. The Y-axis scale represents MFI normalized to the mean MFI of naïve ears. Data represent the mean \pm SEM of five mice per group pooled from two separate experiments.

6.8. Figure S3



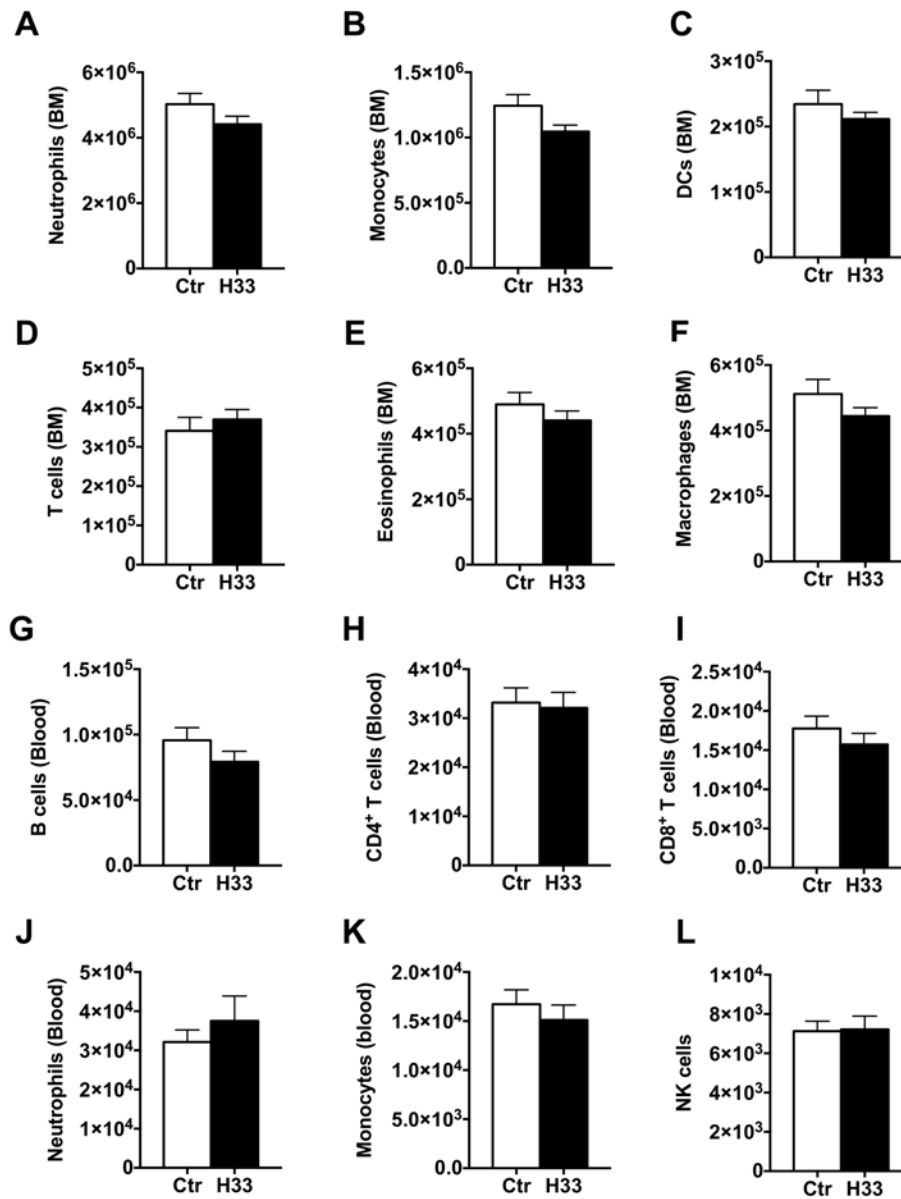
Control staining for JAM-C in ear endothelial cells. Ear sections were stained for Rabbit IgG control (green), CD31 (red). Nucleus was stained with DAPI (blue). Scale bars, 10 μ m. This supporting information is related to Figure 1D.

6.9. Figure S4



Blocking JAM-C does not result in leukocyte emigration to tissue in the steady state. The number of neutrophils (A), monocytes (B), mo-DCs (C), dermal m ϕ (D), and dermal DCs (E) emigrating from ears was measured in H33-treated (H33, black bar) versus isotype control-treated mice (Ctr, white bars) 24 hours after antibody administration. Data represent the mean \pm SEM of fifteen mice per group pooled from 3 separate experiments, and were analyzed by the unpaired Student's t test.

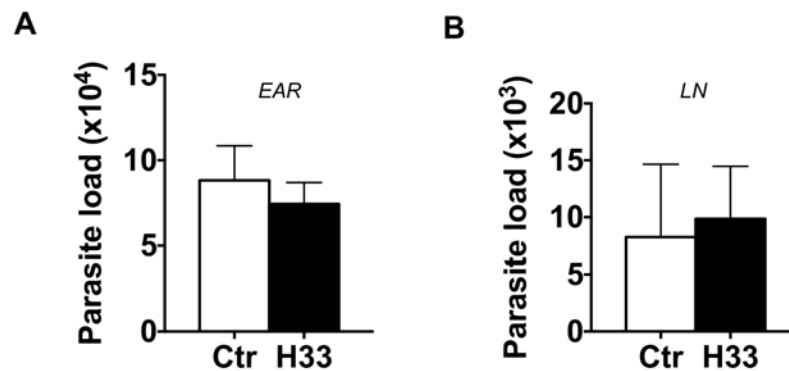
6.10. Figure S5



Blocking JAM-C in the steady state does neither increase hematopoiesis nor leukocyte migration from bone marrow to the blood.

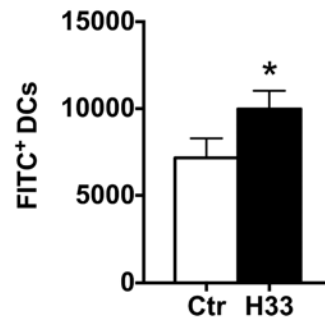
Naïve C57BL/6 mice were treated with H33 or isotype control antibody for 24 hours. The number of neutrophils (A), monocytes (B), DCs (C), T cells (D), eosinophils (E), and macrophages (F) from the bone marrow (BM); and B cells (G), CD4⁺ T cells (H), CD8⁺ T cells (I), neutrophils (J), monocytes (K), and NK cells (L) from blood in H33-treated (black bar) versus isotype control-treated mice (white bars) is shown. Data represent the mean \pm SEM of five mice per group, and were analyzed by the unpaired Student's t test. Data are representative of three separate experiments.

6.11. Figure S6



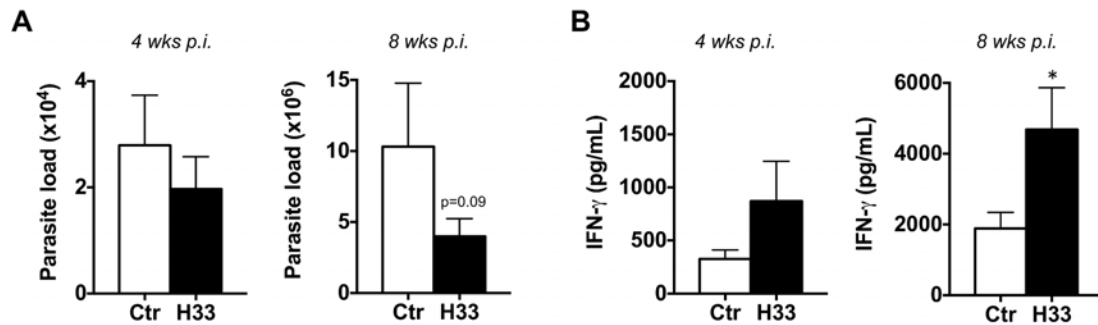
H33 antibody does neither decrease the parasite burden in infected ears, nor increase parasite dissemination to lymph nodes 48 hours p.i. (Raw data of Figure 2). The parasite burden in infected ears (A) and draining lymph nodes (B) were measured 48 hours p.i. by LDA. Data represent the mean \pm SEM of five mice per group from one representative experiment, and were analyzed by the unpaired Student's t test. These supporting informations are related to Figure 2H and I.

6.12. Figure S7



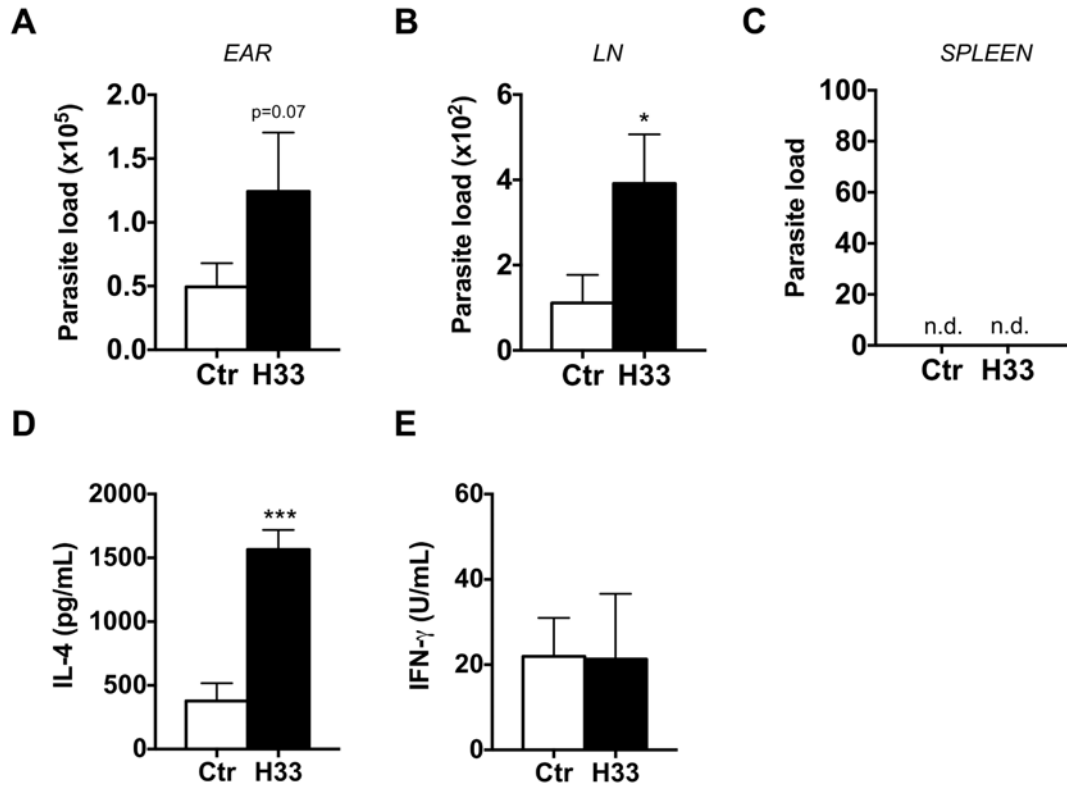
Blocking JAM-C increases the number of DCs migrating to the draining lymph node (Raw data of Figure 3). The ear draining lymph nodes were harvested and stained for FACS analysis 18 hours after FITC-painting. The number of IA^{high} CD11c⁺ FITC⁺ migratory DCs was counted. Data represent the mean ± SEM of six mice per group, and were analyzed by the unpaired Student's t test with *: p<0.05. This supporting information is related to Figure 3B.

6.13. Figure S8



Blocking JAM-C improves the Th1 cell response and favours healing in C57BL/6 mice (Raw data of Figure 4). Mice were inoculated with *L. major* in the ear dermis and treated with H33 or the isotype control antibody for 3 weeks, twice a week. (A) The parasite burden in infected ears was measured by LDA 4 and 8 weeks p.i. Data represent mean \pm SEM of ten mice per group for both time points. (B) Draining lymph node cells were restimulated for 72hrs with UV-irradiated *L. major* and the secreted IFN- γ was measured. Data represent the mean \pm SEM of mice from panel A. Data were analyzed by the unpaired Student's t test with *:p<0.05. These supporting informations are related to Figure 4B and E.

6.14. Figure S9



Blocking JAM-C boosts the Th2 cell response and worsens the disease in BALB/c mice (Raw data of Figure 5). (A-C) Mice were inoculated with 1×10^4 stationary phase *L. major* promastigotes in the ear dermis and treated with H33 or control antibody for 3 weeks. The parasite burden in infected ears (A), draining lymph nodes (B), and spleens (C) were measured by LDA. (D-E) Draining lymph nodes cells were restimulated with UV-irradiated *L. major* for 72 hours, and the IL-4 (D) and IFN- γ (E) produced were measured. Data represent the mean \pm SEM of 5 mice per group. Data were analyzed by the unpaired Student's t test with *: $p < 0.05$, ***: $p < 0.001$. n.d. not-detectable. These supporting informations are related to Figure 5G, H, K and L.

7. General discussion

7.1. Overview of the discussion

The project initially aimed to investigate the consequences of JAM-C blockade with the antibody H33 in the mouse model of cutaneous leishmaniasis. In addition to confirm the redistribution of JAM-C out of endothelial cell junction *ex vivo*, I observed significant effects on the vascular permeability and the innate leukocyte migration to the site of *L. major* infection, and to the draining lymph nodes.

This raises a broad spectrum of questions around the function of JAM-C, which I will discuss in the first sections of this discussion. I will debate of the function of JAM-C in vascular permeability regarding my results, and previous reports that used other JAM-C manipulations and different inflammatory models. I will propose a general mechanism of JAM-C function in vascular permeability (section 7.2). The precise role of JAM-C in the leukocyte cascade will then be challenged. Indeed, JAM-C is often associated with diapedesis, while I will argue for a role in adhesion after a detailed analysis of all the *in vivo* data currently available on JAM-C (section 7.3). From here, I will show that JAM-C shares more similarities with VE-cadherin and JAM-A than what one could think at a first glance (section 7.4). Finally, I will question the role of adhesion molecules in the migration of leukocytes through lymphatics, which likely involves different mechanisms than the classical migration through blood vessels (section 7.5).

The second part of the discussion will be dedicated to the impact of innate cell trafficking in the immune response to *L. major* infection. First, the particular case of neutrophils will be analyzed, especially since their immunomodulatory role varies from model to model (section 7.6). Then, I will discuss the consequences of JAM-C blockade in the immune response to *Leishmania*, and comment the potential translation of my findings into the clinics (section 7.7).

7.2. Role of JAM-C in vascular permeability: JAM-C as a gatekeeper?

To specifically address the function of JAM-C in vascular permeability *in vivo*, I used the multi-faceted H33 antibody that blocks JAM-C-JAM-B interactions and redistributes JAM-C out of tight junctions. The redistribution of JAM-C after H33 administration was initially observed with lymph node endothelial cells [275], which differ in their anatomical localization and function from the

venules of the skin. Therefore, I studied the distribution of JAM-C in venules of mouse ears 24 hours post injection with H33. In my setting, I was able to confirm that H33 removes JAM-C out from ear endothelial cell junctions. More importantly, this study showed for the first time that JAM-C blockade and redistribution mediated by H33 increases vascular permeability by 15% after *L. major* inoculation in the skin. Conversely, I did not observe increased vascular permeability after administration of H33 under steady state conditions. This increase is substantial, as vascular permeability in inflammation is an optimized process [393]. Moreover, the absence of the H33 effect on vascular permeability in normal homeostasis is not surprising as many other different junctional molecules can still ensure vascular integrity in absence of inflammatory signals, more particularly VE-cadherin [394]. As tight junctions are designed to ensure the junctional integrity, the finding that JAM-C redistribution out of tight junctions increases vascular permeability is physiologically relevant. It is worth noting that JAM-C naturally redistributes out of endothelial cell junctions after ischemia reperfusion injury [137]. Hence, the antibody H33 amplifies the natural redistribution of the molecule observed in acute inflammation.

Previously, Chavakis and coworkers had demonstrated that JAM-C is essential for cell contractility and vascular permeability *in vitro* using siRNA to knock-down the molecule [286]. Important to note that JAM-C blockade with antibodies and loss of JAM-C (with siRNA in that case) are two situations that have to be distinguished. Indeed, H33 does redistribute JAM-C out of junctions, but keeps the molecule at the cell surface. Therefore, our result does not contradict the finding that total loss of JAM-C stabilizes VE-cadherin mediated interactions, and therefore decreases vascular permeability [286]. Moreover, it is not excluded that H33 clusters JAM-C, therefore modulating RAP1 activity, and finally decreasing VE-cadherin mediated interactions, which would also contribute to increased vascular permeability. Overall, I propose that JAM-C acts as a gatekeeper that redistributes on the plasma membrane after inflammation [137], which renders the junctions more permeable, an effect that can be amplified by the application of the H33 anti-JAM-C antibody.

7.3. Role of JAM-C in leukocyte migration: a role in adhesion or transmigration?

Important to note that this major part of my discussion will be based on the detailed analysis of the key *in vivo* experiments related to specific JAM-C

manipulation (antibodies, or transgenic mice) to end up with a working model for JAM-C function in the adhesion cascade.

The first evidence of the specific role of JAM-C in leukocyte trafficking *in vivo* came from the use of the monoclonal rat anti-mouse JAM-C antibody **D33**, in a mouse model of LPS-induced lung inflammation [268]. In this case report appearing in 2005, D33 only partially impaired the recruitment of myeloid cells to the inflamed lungs [268] (**Figure 32**).

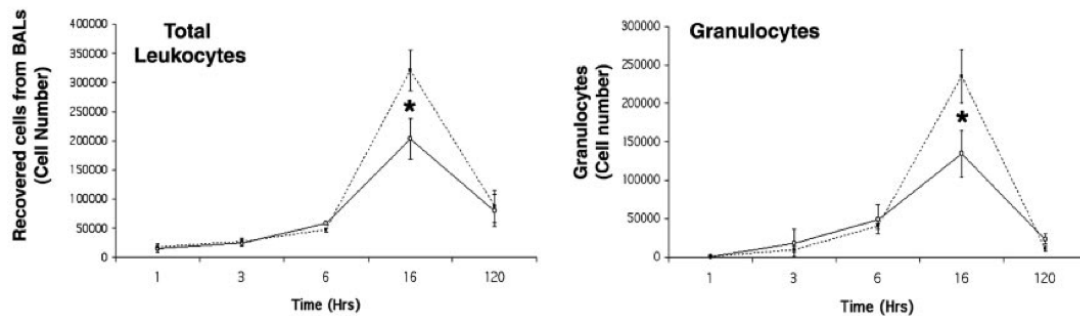


Figure 32. JAM-C is involved in the recruitment of granulocytes to site of inflammation. The D33 Ab against JAM-C (plain line) inhibits the recruitment of total leukocytes to the lungs of mice treated with LPS compared with the 9B5 isotype matched Ab (dashed line). The D33 mAb reduces by 40% the number of granulocytes migrating into the alveoli 16 h after challenge. Data represent means \pm SEM obtained 1 h (n=4), 3 h (n=4), 6 h (n=4), 16 h (n=15), and 120 h (n=12) after LPS challenge. *, $p < 0.05$, as calculated by Mann-Whitney method using StatView software. Text and figure adapted from [268].

In the same report, the authors described a transgenic mouse overexpressing JAM-C on endothelial cells (namely pHHNS-JAM-C). Strikingly, the **adhesion** and subsequent **extravasation** of neutrophils were increased in these animals after IL-1 β stimulation of cremasteric venules [268] (**Figure 33**). This clearly indicates that JAM-C controls the adhesion of neutrophils, adhesion being a prerequisite for the subsequent transmigration.

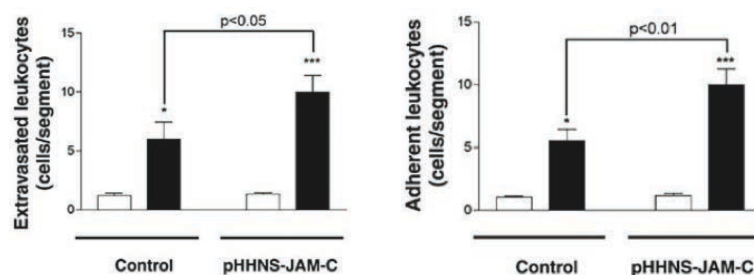


Figure 33. Enhanced neutrophil migration through IL-1 β -stimulated cremasteric venules of pHHNS-JAM-C transgenic mice. Wild-type or pHHNS-JAM-C transgenic were treated with intracrotal saline or IL-1 β (30 ng/animal), and 4 h later, the cremaster muscle was surgically exteriorized, and leukocyte firm adhesion, and transmigration were quantified by intravital microscopy. The data represent mean \pm SEM from n=4–8 mice/group. Text and figure adapted from [268].

In the same year, our laboratory published a second report that points out the properties of a fascinating anti-JAM-C antibody, the clone **H33**. This antibody was first shown to block JAM-B/JAM-C interactions at endothelial

cell-cell contacts [275]. More importantly, our laboratory reported that H33 could redistribute JAM-C from junctions to the apical side of lymph nodes endothelial cells *in vivo*, and postulated that this redistribution of JAM-C to the lumen would increase adhesion of leukocytes. Therefore, they treated mice *in vivo* with H33, or with other anti-JAM-C clones, and finally with a control antibody, and made frozen sections of lymph nodes in order to perform a Stamper-Woodruff adhesion assay with monocytes [275]. Strikingly, adhesion of monocytes was significantly increased in mice treated with H33. Moreover, treatment of monocytes with anti-Mac-1 antibodies abolished the increased adhesion observed with H33 [275] (**Figure 34**). This confirms the role of JAM-C in **adhesion**, and also clearly shows that H33 does not block the JAM-C/Mac-1 interactions required for adhesion.

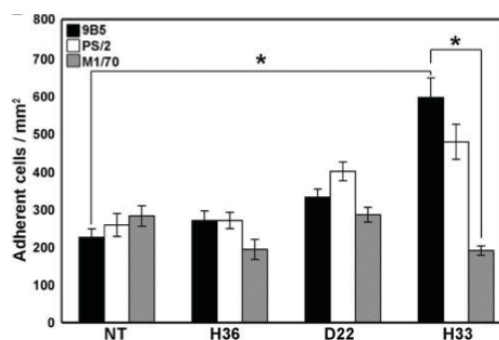


Figure 34. Treatment of mice with antibody H33 increases monocyte adhesion to lymph node sections in Stamper and Woodruff assays. Stamper and Woodruff adhesion assay was done on lymph node sections from mice treated with H36, D22, H33, or isotype-matched control antibodies. As shown, H33 antibody increases the adhesion of monocytoic cells when administrated to mice. Experiments were done in the presence of blocking antibodies against α_4 integrin (PS/2, white columns), against α_M integrin (M1/70, dashed columns) or isotype-matched control antibody (black columns). Data shown are the mean \pm SEM of the number of adhering cells/mm² found on eight sections per lymph nodes in three animals per condition. * $p < 0.05$. Text and figure adapted from [275].

In 2007, our laboratory found that H33 increases the frequency of reverse and repeated migration of human monocytes through HUVECs under physiological flow conditions [283] (**Figure 35**). This was confirmed *in vivo* using the mouse model of thioglycollate-induced peritonitis based on blood numbers of L-selectin negative inflammatory monocytes (i.e. supposed reverse transmigrated). At early time points, H33 increased the numbers of L-selectin⁻ monocytes, stating for increased reverse transmigration. However, at later time points, H33 decreased the number of L-selectin⁻ monocytes, this time arguing for increased repeated transmigration [283] (**Figure 35**).

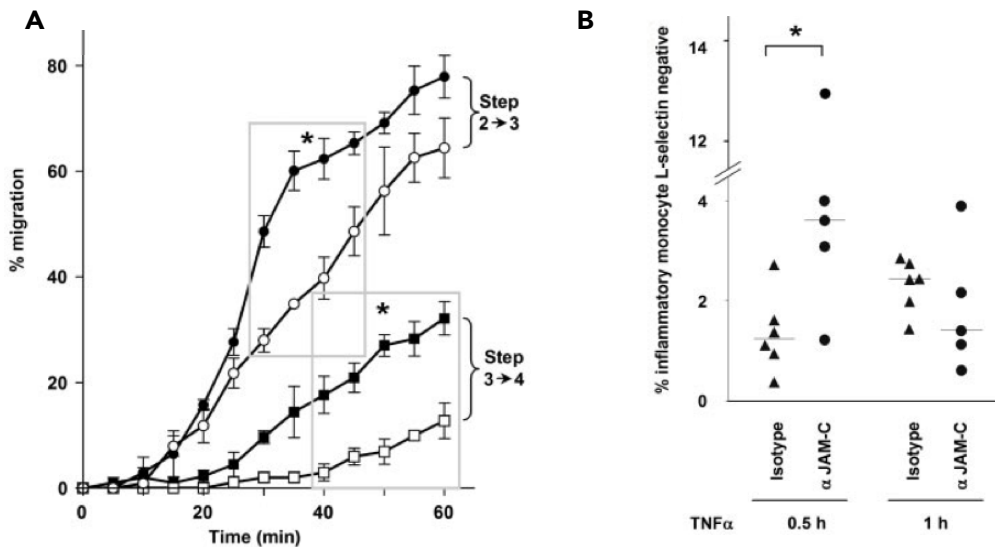


Figure 35. H33 increases reverse and repeated transmigration of monocytes in vitro and in vivo. A) Adherent monocytes in coculture with HUVECs were individually tracked and monitored for transmigration between different compartments over 60 minutes. Increased reverse transmigration was observed for cocultures treated with functional blocking mAbs to JAM-C (●) compared with nonfunctional blocking antibody D22 (○). Monocytes with a reverse-transmigratory phenotype treated with H33 repeat-transmigrate back into the ablumen at higher levels (□) compared with D22 (■). B) Mice treated with the JAM-C–blocking mAb H33 (n=5) showed a significant increase in L-selectin⁺ inflammatory monocytes in the blood (median, 3.61%) at 30 minutes compared with an isotype control antibody (median, 1.24%; n=6). The median value for each experimental group is marked with a horizontal bar. Statistical analysis was conducted using the Mann-Whitney U test (*P < 0.03). Text and figure adapted from [283].

In 2009, Scheiermann et al. confirmed that mice overexpressing JAM-C leads to increased adhesion and extravasation of leukocytes through inflamed cremasteric venules [284]. This time however, the inflammation was due to ischemia reperfusion injury, not IL-1 β stimulation. Interestingly, they also used knock-out animals in this model, and conversely observed decreased **adhesion**, and decreased **extravasation** of leukocytes (**Figure 36**). This definitively confirms that JAM-C controls the adhesion (likely through JAM-C/Mac-1 interactions), and therefore extravasation as a consequence.

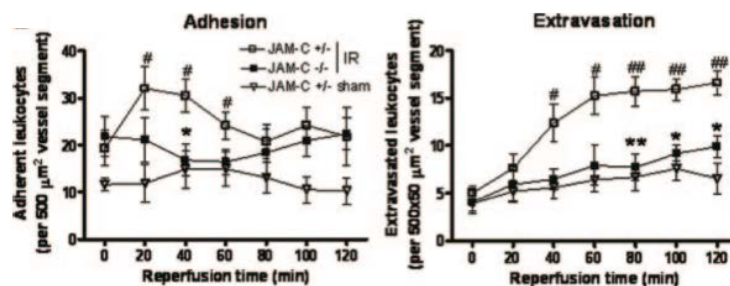


Figure 36. JAM-C^{-/-} mice exhibit reduced leukocyte adhesion and transmigration in cremasteric venules in response to I/R injury. The number of adherent and extravasated leukocytes was quantified in cremasteric venules by IVM. Text and figure adapted from [284].

Finally, with the antibody H33, but not with knock-out mice, higher frequency of neutrophils “hesitant” (i.e. movements back and forth) and reverse transmigration also occur [137] (**Figure 37**). Importantly, the frequency of

hesitant and reverse transmigration is higher in ischemia reperfusion injury than in any classical inflammatory models (**Figure 37**). This has to be linked to the observation that JAM-C naturally redistributes to non-junctional regions after ischemia reperfusion injury (**Figure 37**). In other words, H33 naturally mimics and amplifies the redistribution of JAM-C naturally occurring after some inflammatory stimuli.

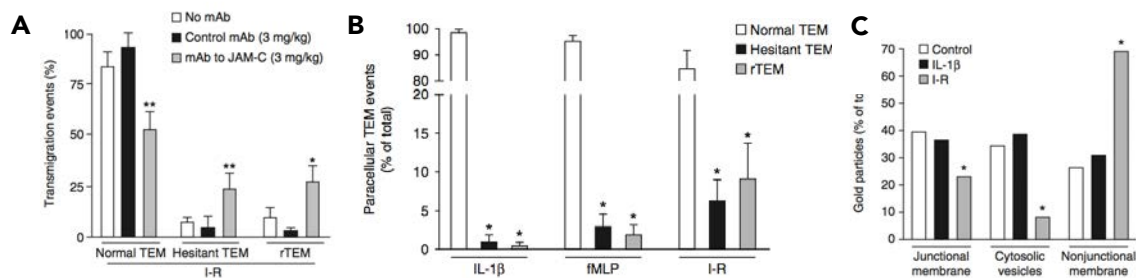


Figure 37. H33 increases reverse and repeated transmigration of neutrophils in vivo. A) Normal, hesitant and rTEM responses in *lys-EGFP*-ki mice pretreated with intravenous saline (no mAb), control nonblocking mAb H36 to JAM-C or blocking H33 mAb to JAM-C (each at a dose of 3 mg per kg body weight (3 mg/kg), then subjected to I-R injury; results are presented as frequency among total observed paracellular responses. *P < 0.05 and **P < 0.01 (multinomial logistic regression analysis). B) Frequency of normal, hesitant and reverse paracellular TEM events induced by IL-1β, fMLP or I-R, presented as frequency among total paracellular TEM events. C) Immunoelectron microscopy analysis of the distribution of JAM-C in ECs in control (saline-injected or sham-operated) tissues and cremaster muscles stimulated with IL-1β or subjected to I-R injury. Text and figured adapted from [137].

Regarding all the above key results, I propose that JAM-C redistributes under inflammatory conditions to support JAM-C/Mac-1 interactions with innate leukocytes, which is a prerequisite for the subsequent transmigration. As such, any JAM-C manipulation that abolishes JAM-C/Mac-1 interactions (e.g. knock-out, knock-down, or antibodies blocking JAM-C/Mac-1 interactions) reduce adhesion and transmigration, while manipulation that favours JAM-C/Mac-1 interactions (e.g. JAM-C overexpression, or JAM-C redistribution with antibody H33) facilitates transmigration events (**Figure 38**).

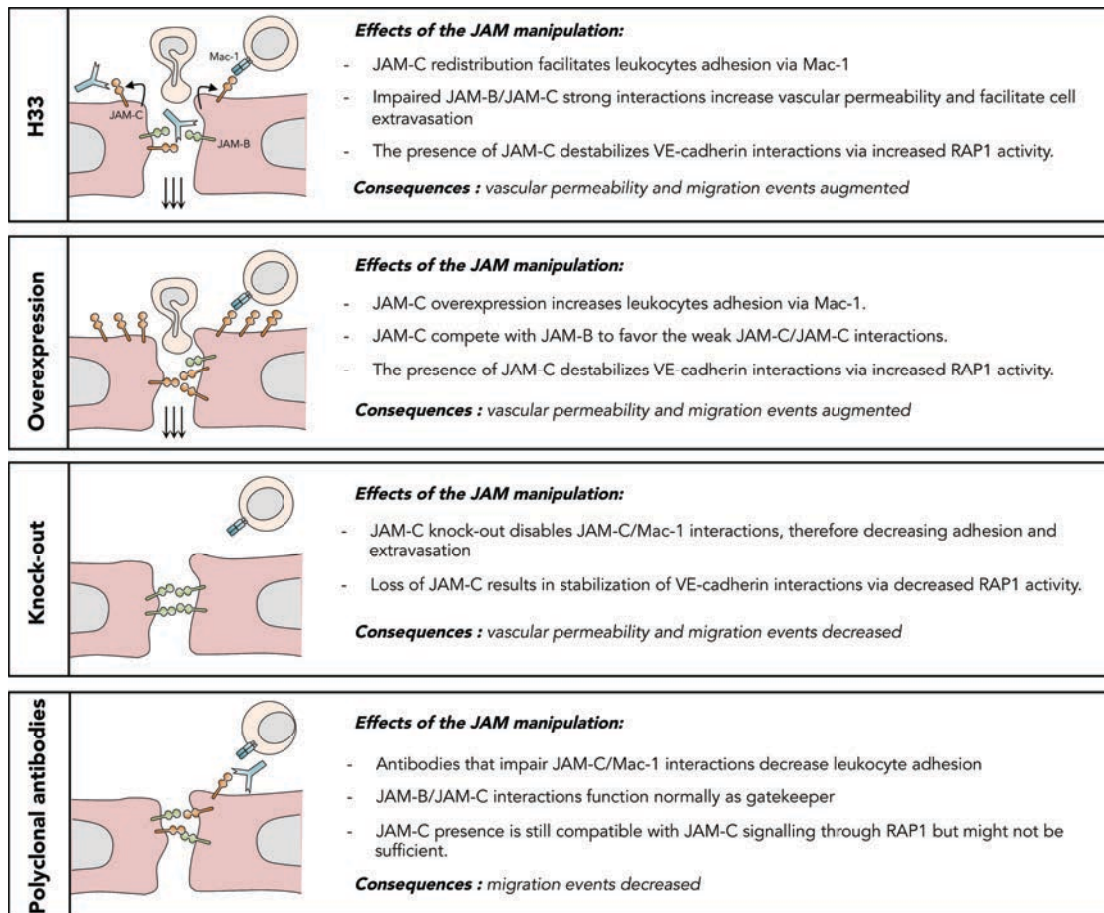


Figure 38. JAM-C manipulations and their consequences.

My results are in line with this model, as H33 treatment in *L. major* infection increases the migration of innate leukocytes to the site of infection, due to increased vascular permeability, and due to H33 redistribution that likely increases leukocyte adhesion. Regarding potential reverse transmigrating events, I believe that the high chemotactic gradients in tissue infected by *L. major* (**Figure 39**) associated with the strong chemotactic guidance of neutrophils towards *Leishmania* inoculum (**Figure 29**, p.57) does not indicate a potential relevance for reverse transmigration in this infectious disease, contrary to ischemia reperfusion injury [137]. Therefore, the use of H33 in the mouse model of cutaneous leishmaniasis amplifies the natural recruitment of innate leukocytes to the site of infection.

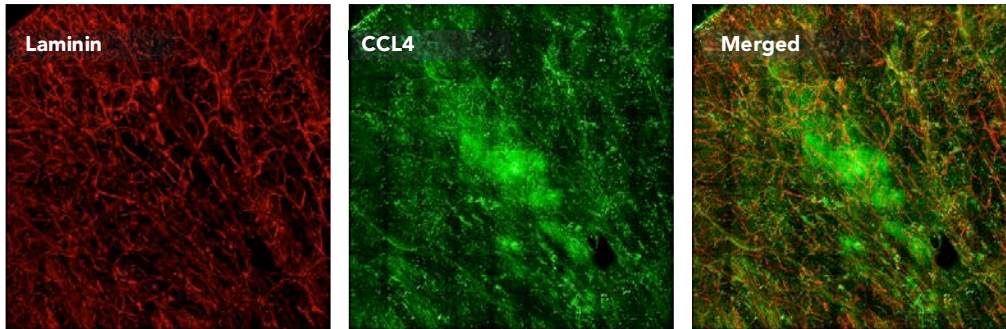


Figure 39. CCL4 chemokine gradients in *L. major* infected tissue. (Source : personal data)

7.4. Similarities between JAM-C and other adhesion molecules

One junctional adhesion molecule shares many features with JAM-C, namely JAM-A. First, the cell surface expression of JAM-A on HUVECs is slightly reduced after combined treatment with TNF- α and IFN- γ [395]. More importantly, the combined treatment of HUVECs with both cytokines redistributes JAM-A out of endothelial cell junctions similarly to JAM-C after ischemia reperfusion injury [293]. Unfortunately, no data currently confirm JAM-A redistribution *in vivo*. As a reminder, I have proposed in the previous section that JAM-C natural redistribution on the apical side of endothelial cells facilitates interactions with the β_2 integrin Mac1. In a similar manner, endothelial-expressed JAM-A interacts with the leukocyte β_2 integrin LFA-1 to promote T cell arrest *in vitro* on HUVECs [294]. Therefore, I suggest that both JAM-A and JAM-C redistribute after inflammation to participate to the adhesion of leukocytes using LFA-1 and Mac1, respectively.

Important to note are also the striking analogies between JAM-C and VE-cadherin. First of all, the migration of leukocytes between interendothelial junctions occurs through de novo formation of transient gaps in JAM-C or VE-cadherin [171,282]. In both cases, gaps reseal after the leukocyte passage (**Figure 40**). This indicates that neither JAM-C, nor VE-cadherin actively participate to the diapedesis process, but rather redistribute to facilitate the leukocyte diapedesis.

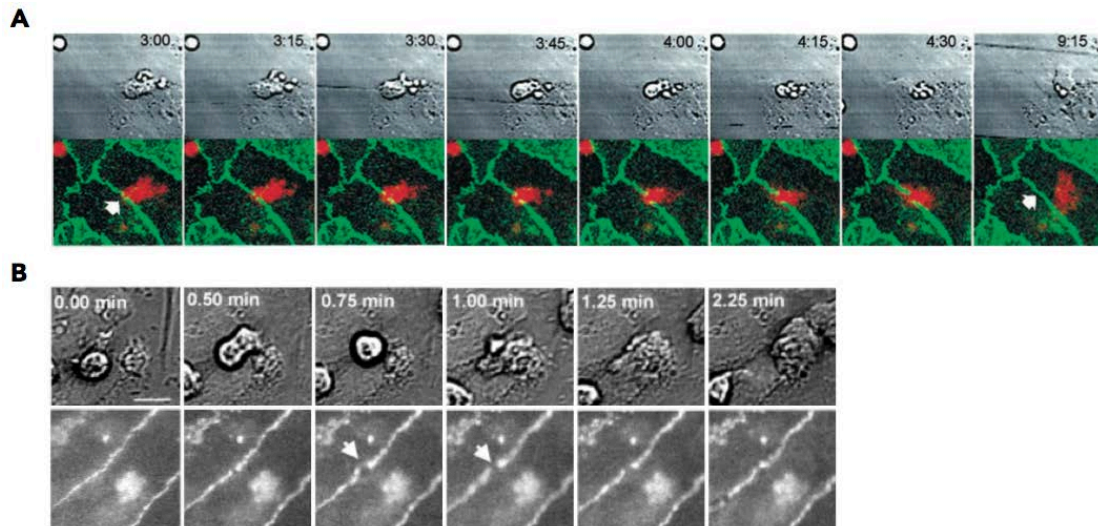


Figure 40. Dynamics of endothelial VE-Cadherin and endothelial JAM-C during leukocyte migration. (A) Time lapse video microscopy of a monocyte (red) transmigrating through HUVECs expressing GFP-VE-Cadherin (green). Figure taken from [171]. (B) Time lapse video microscopy of a neutrophil transmigrating through HUVECs expressing GFP-JAM-C. Figure taken from [282].

Moreover, similarly to H33 for JAM-C, the anti-mouse VE-Cadherin antibody BV13 redistributes VE-cadherin out of junctions, increases vascular permeability, and enhances leukocyte extravasation *in vivo* [173]. This phenotype was observed under steady state conditions, which shows the key role of VE-Cadherin in the maintenance of vascular integrity [173]. The fact that BV13 and H33 removes respectively VE-cadherin and JAM-C out of junctions with consequences on both vascular permeability and leukocyte migration raises important concerns: are vascular permeability and leukocyte transmigration regulated similarly? Two mechanisms of endothelial junction openings are described: either by destabilizing junctional adhesion, or by activating actomyosin-based pulling forces on junctions [396]. Both BV13 and H33 destabilize the junctions, with combined consequences on permeability and leukocyte migration. On the other hand, other regulatory mechanisms affect exclusively permeability and not leukocyte migration, or vice versa. This was elegantly shown for VE-cadherin, which displays two different tyrosine phosphorylation sites, Tyr685 and Tyr731, that independently control permeability and leukocyte extravasation, respectively [397].

7.5. Migration of DCs through lymphatics: passive or active process?

I also report that H33 increases the number of DCs leaving the ear dermis to the draining lymph node. This may be the direct consequence of JAM-C blockade at lymphatic endothelial cell junctions, which would facilitate DCs transendothelial migration (hypothesis 1). Alternatively, it could be the

indirect consequence of the higher number of DCs recruited to the site of inflammation that migrate to the lymph node as a consequence (hypothesis 2). The latter hypothesis is likely since DCs preferentially migrate in an integrin-independent manner through initial lymphatic capillaries by seeking pre-existing flaps between the oak leaf-shaped lymphatic endothelial cells [225,242]. Conversely, these results have been observed under steady state conditions, while other investigations under inflammatory conditions identified the key role of ICAM-1 and VCAM-1 in this process *in vivo* [244]. In a past report published by our laboratory, we have injected labeled bone marrow derived DCs subcutaneously together with LPS and observed similar numbers of DCs migrating to the lymph nodes in wild type and JAM-C deficient mice [280]. This result is in line with my second assumption, namely that the effect I observed is the result of the increased migration of DCs from the blood to the tissue inflamed by FITC painting, which migrate to the lymph node afterwards.

7.6. The role of neutrophils in *L. major* infection: a need for specific neutrophil depletion

In the *L. major* mouse model of cutaneous leishmaniasis, the kinetics of leukocyte recruitment, their specific function, and the crosstalk between the different subsets of cells have been and are still under investigation. It is now well accepted that neutrophils are the first cells recruited within hours to the infected tissue [223,350,351,361]. However, some discrepancies still exist concerning their immunoregulatory function, which may depend on the mode of parasite transmission and the number of pathogens inoculated. Indeed, in the *Leishmania* resistant C57BL/6 mice, Sacks and coworkers used the monocyte and neutrophil depleting RB8-6C5 antibody and a natural sand-fly transmission of *L. major* to show that depletion of these cells promotes rather than compromises host resistance [350]. More recently, they showed that efferocytosis of infected neutrophils by DCs decreases their activation and antigen presenting cell function, therefore dampening the protective pro-inflammatory response [361]. On the other hand, other reports using needle inoculation of high parasite doses like our study, have demonstrated a transient protective role for neutrophils in C57BL/6 mice [363-365]. These studies assessed the role of neutrophils mostly by depletion, mediated by the more neutrophil-specific antibody NIMP-R14 [351] or by the anti-Gr1 RB6-8C5 antibody recognizing inflammatory monocytes and neutrophils. All these neutrophil depletion studies resulted in transient increased lesion size and parasite loads. It is worth noting that RB6-8C5, the antibody used in most of the studies, not only depletes neutrophils

but also inflammatory monocytes, illustrating the importance of neutrophils and inflammatory monocytes in promoting resistance to infection. The contribution of monocytes and mo-DCs has been further investigated with the use of chemokine receptor CCR2 knock-out mice in the resistant C57BL/6 background. In these mice, monocytes do not leave the bone marrow, resulting in a deficiency of monocytes in the blood circulation [398]. The recruitment of inflammatory mo-DCs in the lymph node following *L. major* infection is therefore completely impaired, which dampens the Th1 cell response [385]. Subsequently, the CCR2 deficiency results in a non-healing phenotype similar to that observed in susceptible mice [386]. Our report is in line with these studies, as treatment with the antibody H33 increased the recruitment of neutrophils, inflammatory monocytes and mo-DCs, and thereby improved the Th1 immune response and the clinical outcome in C57BL/6 mice. In addition, Tacchini-Cottier and coworkers [91] emphasized the contribution of neutrophils in the recruitment of mo-DCs to the site of *L. major* infection through the secretion of the chemokine CCL3. In line with this finding, I observed a significant increase in the production of CCL3 within ears of H33 treated mice at time points when neutrophils are massively recruited to the site of infection. Therefore, I suggest that, by increasing the numbers of neutrophils recruited, H33 could indirectly increase the amount of CCL3 produced *in situ*. This additional mechanism may also contribute to further enhance the extravasation of mo-DCs in the ears of H33 treated C57BL/6 mice (**Figure 41**).

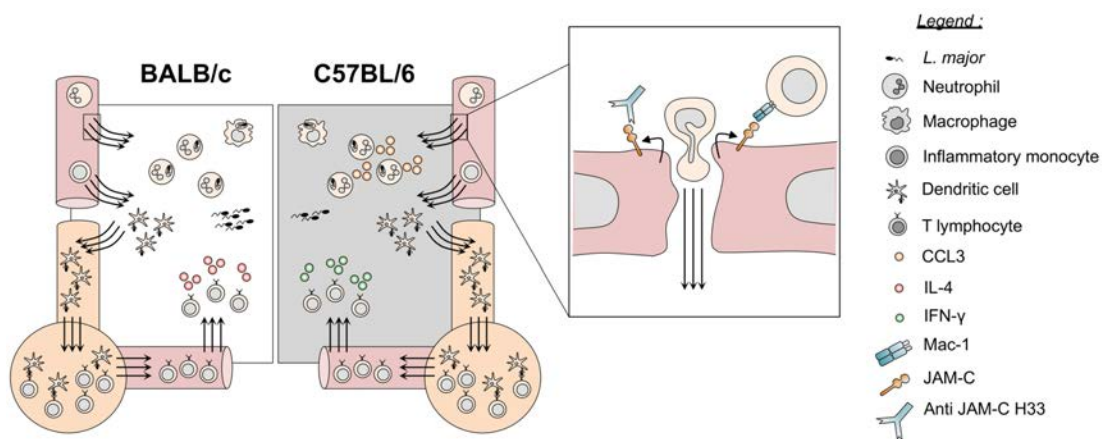


Figure 41. Blocking JAM-C enhances DC migration and boosts the immune responses to *L. major* infection. By removing JAM-C out of functions, H33 increases adhesion of leukocytes and potentiates vascular permeability and cell migration of leukocytes after *L. major* infection. Increased numbers of recruited neutrophils result in higher levels of the chemokine CCL3 attracting monocytes and mo-DCs in C57BL/6 mice. The number of migratory DCs to lymph nodes increases, and the subsequent T cell response is mounted more efficiently. Resistant C57BL/6 mice develop a higher IFN- γ -dominated Th1 response while susceptible BALB/c mice develop a stronger IL-4-dominated Th2 response. This has a significant healing effect in resistant animals whereas susceptible mice display an exacerbated disease.

7.7. Importance of innate cell trafficking in *L. major* infection: lessons from JAM-C manipulation

Finally, I used the properties of H33 treatment on vascular permeability and innate cell migration to assess the consequences on the clinical outcome. In C57BL/6 mice, the higher numbers of neutrophils or monocyte-derived cells recruited rapidly after infection may increase the early innate parasite killing. However, I observed no difference in the parasite load 48 hours after infection. This is likely due to the absence of the IFN- γ -dominated Th1 response that leads to activation of phagocytes and parasite killing at this early time point [325]. Moreover, the increased vascular permeability at the site of infection may have influenced the dissemination of the parasite to peripheral organs early after infection. But I did not find any change in the draining lymph nodes, while the parasite was undetectable in spleen. Strikingly, I found that H33 was able to boost the adaptive immune response in both susceptible and resistant mice by increasing DC migration, without changing the T cell polarization. It is worth noting that JAM-C is also well expressed by lymphatic sinuses from lymph nodes, which may influence T cell surveillance of DCs in the lymph nodes, and therefore T cell activation after H33 treatment. However, we had already demonstrated that the ability of DCs to prime T cells *in vivo* in JAM-C deficient animals is unchanged [280]. In lymph nodes, JAM-C is also expressed by high endothelial venules, and we cannot exclude an effect of H33 on T cell entry into lymph nodes.

In conclusion, this report is the first one to demonstrate that immune responses to pathogen infections can be finely-tuned by manipulating a single adhesion molecule, and in particular JAM-C. For instance, deletion of P- or E-selectin does not impact the immune response to *L. major* infection in a mixed 129/C57BL/6 background [388]. Finally, our findings in BALB/c mice confirm that susceptibility does not result from an overall lack of leukocyte migration to the site of infection, but rather from a genetic defect in redirecting the T cell response [325].

Whether these findings can be translated to human cases is an important question. Important to note that studies on human cutaneous leishmaniasis revealed mixed Th1/Th2 responses, which contrast with the clear Th1/Th2 dichotomy observed in the mouse model [399]. Moreover, JAM-C is expressed on leukocyte subsets in humans. This requires more specific antibodies that would recognize exclusively only endothelial JAM-C, such as bi-specific antibodies that would target JAM-C on one hand, and an endothelial specific marker on the other hand. Therefore, it is currently difficult to predict the therapeutic potential of anti-JAM-C treatment in the clinics.

8. Conclusion

This thesis provides valuable information regarding the role of JAM-C in the leukocyte adhesion cascade, the role of innate cells recruitment in the outcome of cutaneous leishmaniasis, and paves the way to new strategies boosting immune responses to infections.

Indeed, these findings, combined to previous data using various JAM-C manipulations in wide inflammatory models, definitively suggest that JAM-C is a gatekeeper in vascular junctions that redistributes to the apical plasma membrane to increase vascular permeability and cell migration in response to inflammatory stimuli.

Regarding the *L. major* model of cutaneous leishmaniasis, my data strongly suggest the idea that the Th2 response in susceptible animals does not result from an overall lack of innate leukocytes recruitment, in particular DCs, but rather from deeper genetical defects to redirect the immune response towards protective immunity.

Finally, our results highlight the underestimated importance of adhesion molecules in immune responses to pathogens, and raise the question of new pharmacological strategies targeting vascular adhesion molecules to finely tune immunity to infection.

9. Acknowledgements

9.1. Remerciements

Je tiens tout d'abord à exprimer ma gratitude au professeur **Beat Imhof**, pour m'avoir accueilli dans son laboratoire à bras ouverts, pour m'avoir fait confiance, et pour m'avoir confié tant de responsabilités tout au long de ces années.

Je remercie chaleureusement les professeurs **Fabienne Tacchini-Cottier**, **Britta Engelhardt**, et **Jean-Claude Martinou** pour avoir accepté de lire et d'évaluer ce travail.

Je remercie également les professeurs **Fabienne Tacchini-Cottier** et **Hans Acha-Orbea** qui ont œuvré, avec la collaboration de Beat, pour l'obtention d'un financement du **Fond National Suisse de la recherche** grâce auquel j'ai pu effectué ce travail de recherche. Merci également pour les précieuses suggestions apportées lors de nos rencontres.

J'exprime ma reconnaissance au Docteur **Marie Kosco-Vilbois** ainsi qu'au Professeur **Daniel Pinschewer** pour avoir accepté d'être mes parrains de thèse. En particulier je vous remercie Marie de m'avoir mis en contact avec Beat à la suite de mon stage de fin d'études, c'est là que l'aventure a démarré.

Je remercie également les différents membres de mon laboratoire, passés comme présents. Merci à vous tous pour la gentillesse et la disponibilité que vous m'avez témoignées toutes ces années. Deux personnes m'ont particulièrement épaulées tout au long de ce travail, il s'agit de **Yalin** et de **Stéphane**. Merci messieurs pour votre aide, sans oublier toutes nos discussions politico-philosophiques que nous menions avec beaucoup de passion et de panache!

Je remercie également les différentes plateformes et services de l'Université que j'ai régulièrement sollicité. Mention spéciale à la plateforme de cytométrie en flux tenue de main de maître par **Jean-Pierre** et **Cécile**.

Je tiens également à remercier du fond du cœur **Eric Hatterer** qui m'a brillamment transmis tout son savoir lors de mon stage de fin d'études à Novimmune. Sans toutes ces techniques que tu m'as apprises, je ne m'en serais tout simplement pas sorti. Un grand merci l'ami !

À titre plus personnel, j'ai une grande pensée envers toute ma famille, ma mère **Claudine**, mon père **Dominique**, et mon frère **Thomas**. Les valeurs que vous m'avez transmises, maman, papa, associées au modèle d'excellence que tu représentes Tom, sont sans aucun doute les clefs de ma réussite, étape après étape, marche après marche. Vous êtes et continuerez d'être une source de motivation et de dépassement de soi inépuisable.

Je remercie également **Alexia** pour son soutien tout au long de ma thèse.

J'ai aussi une pensée envers tous mes compagnons de course à pied, et vous êtes nombreux, pour toutes ces agréables ballades autour du CMU.

Je n'en oublie pas moins mes amis, ma famille, mes collègues passés ou présents, et toutes les personnes qui ont un jour, par des mots ou des actes, contribué à cet accomplissement. À vous tous, merci.

9.2. Acknowledgements

I would like to express my gratitude to Professor **Beat Imhof**. Thank you for your warm welcome into your lab, thank you for your trust, and for the high level of responsibilities you gave me all along this thesis.

Then, I would like to thank professors **Fabienne Tacchini-Cottier**, **Britta Engelhardt**, and **Jean-Claude Martinou** for the evaluation of this manuscript.

I am also very grateful to professors **Fabienne Tacchini-Cottier** and **Hans Acha-Orbea** who worked, together with Beat, to obtain the grant from the **Swiss National Science Foundation** that covered my experiments and salary.

I would like to thank Doctors **Marie Kosco-Vilbois** and **Daniel Pinschewer** for being my advocacy committee. More specifically, I am grateful to you Marie for getting me in touch with Beat, this is where this adventure started.

I thank all my lab members, past and present. You were always very friendly and helpful with me. I especially thank Yalin and Stephane for your assistance, and for all these intense discussions about science or just about life...

I thank the different core facilities of the University. I have a particular thought to **Jean-Pierre** and **Cécile** for regular assistance at the flow cytometry core facility.

I have a special thought to my friend and former supervisor at Novimmune, **Eric Hatterer**. I pulled through my doctorate mainly thanks to all what you taught me.

I thank my family, my mother **Claudine**, my father **Dominique**, my brother **Thomas**. Your love and support help me days after days. I also thank Alexia for her moral support during my PhD.

I have a thought for all my running partners with who I have shared nice and relaxing runs around the CMU.

Finally, I do not forget all the friends, relatives, and colleagues, who contributed this this work in one way or another. For all of you, thank you.

10. Appendix



Blocking Junctional Adhesion Molecule C Enhances Dendritic Cell Migration and Boosts the Immune Responses against *Leishmania major*

Romain Ballet^{1*}, Yalin Emre¹, Stéphane Jemelin¹, Mélanie Charmoy², Fabienne Tacchini-Cottier², Beat A. Imhof¹

¹Department of Pathology and Immunology, Centre Médical Universitaire, University of Geneva, Geneva, Switzerland, ²Department of Biochemistry, and WHO Immunology Research and Training Center, University of Lausanne, Epalinges, Switzerland

Abstract

The recruitment of dendritic cells to sites of infections and their migration to lymph nodes is fundamental for antigen processing and presentation to T cells. In the present study, we showed that antibody blockade of junctional adhesion molecule C (JAM-C) on endothelial cells removed JAM-C away from junctions and increased vascular permeability after *L. major* infection. This has multiple consequences on the output of the immune response. In resistant C57BL/6 and susceptible BALB/c mice, we found higher numbers of innate immune cells migrating from blood to the site of infection. The subsequent migration of dendritic cells (DCs) from the skin to the draining lymph node was also improved, thereby boosting the induction of the adaptive immune response. In C57BL/6 mice, JAM-C blockade after *L. major* injection led to an enhanced IFN- γ dominated T helper 1 (Th1) response with reduced skin lesions and parasite burden. Conversely, anti JAM-C treatment increased the IL-4-driven T helper 2 (Th2) response in BALB/c mice with disease exacerbation. Overall, our results show that JAM-C blockade can finely-tune the innate cell migration and accelerate the consequent immune response to *L. major* without changing the type of the T helper cell response.

Citation: Ballet R, Emre Y, Jemelin S, Charmoy M, Tacchini-Cottier F, et al. (2014) Blocking Junctional Adhesion Molecule C Enhances Dendritic Cell Migration and Boosts the Immune Responses against *Leishmania major*. PLoS Pathog 10(12): e1004550. doi:10.1371/journal.ppat.1004550

Editor: Ingrid Müller, Imperial College London, United Kingdom

Received: April 10, 2014; **Accepted:** November 3, 2014; **Published:** December 4, 2014

Copyright: © 2014 Ballet et al. This is an open-access article distributed under the terms of the Creative Commons Attribution License, which permits unrestricted use, distribution, and reproduction in any medium, provided the original author and source are credited.

Data Availability: The authors confirm that all data underlying the findings are fully available without restriction. All relevant data are within the paper and its Supporting Information files.

Funding: This work was supported by the Swiss National Science Foundation: PDFMP3-129700 to BAI and FTC; 310030-153456 to BAI; 31003AB-135701 to BAI. The funders had no role in study design, data collection and analysis, decision to publish, or preparation of the manuscript.

Competing Interests: The authors have declared that no competing interests exist.

* Email: ballet.r@gmail.com

Introduction

Leishmania is an obligate intracellular parasite responsible for a wide spectrum of clinical manifestations, such as cutaneous, mucocutaneous or visceral leishmaniasis [1]. After inoculation of *Leishmania major* in the skin of humans or rodents, promastigotes are taken up by phagocytic cells [2]. The infection leads to the development of cutaneous lesions, which eventually heal depending on the adaptive immune response of the host [3]. In the C57BL/6 mouse model, resistance to *L. major* infection is associated with the production of IFN- γ by CD4⁺ Th1 lymphocytes [4,5]. The secretion of IFN- γ by these Th1 cells then activates infected macrophages, and leads to efficient killing of the parasites [2,6]. Conversely, BALB/c mice mount a non-protecting T helper 2 response (Th2) characterized by production of anti-inflammatory cytokines such as IL-4, IL-10, and IL-13 [3,7].

Dendritic cells (DCs) are professional antigen-presenting cells that play a key role in the induction of the adaptive immune reaction against *L. major*. At early stages of infection in C57BL/6 mice, resident dermal DCs phagocytose the parasites [8] and promote the switch towards a Th1 response by producing IL-12 [9]. Monocytes, subsequently recruited to the site of infection can

also give rise to monocyte-derived DCs (mo-DCs). During the late phase of infection, such mo-DCs are essential mediators of the protective T cell response. They efficiently migrate from the site of infection to the draining lymph node, where they induce a specific immune reaction against the pathogen [10]. The fundamental role of monocytes and mo-DCs has been further highlighted with the use of the CCR2 knock-out in the C57BL/6 background. In these mice, the recruitment of mo-DC to the lymph nodes is severely reduced, diminishing the Th1 cells [11], and resulting in a non-healing phenotype similar to that observed in susceptible mice [12]. Therefore, migration of DCs to the infected skin and lymph node can be considered as fundamental steps towards immunity against *L. major*.

Transendothelial migration of leukocytes from blood to the site of inflammation is a complex process controlled by adhesion molecules, such as PECAM-1, ICAM-2, ICAM-1, CD99, ESAM, or junctional adhesion molecules (JAMs) [13]. The JAM family is composed of 6 molecules comprising the classical JAM-A, JAM-B, and JAM-C, mainly localized in the tight junctions of endothelial cells [14]. In humans, JAM-C is also found on subpopulations of T and B lymphocytes, and platelets [15,16], while murine JAM-C is restricted to endothelial and stromal cells [17–19]. In the steady

Author Summary

Leishmaniasis is a parasitic disease transmitted to humans through sand fly bites. Clinical symptoms vary from self-healing cutaneous lesions to death. Cutaneous leishmaniasis is particularly studied in mice inoculated with *Leishmania major*. In this model, some strains (e.g. C57BL/6) are resistant due to a Th1 immune response promoting parasite killing. Conversely, other strains (e.g. BALB/c) are susceptible due to a nonprotective Th2 response. DCs are professional antigen-presenting cells that educate antigen-specific T cells. Improving the migration of DCs from the site of infection to the lymph nodes, where T cells reside, may improve the T cell response. JAM-C is a vascular adhesion molecule implicated in leukocyte migration in different inflammatory models. We found that JAM-C blockade with antibodies increases vascular permeability and consequently improves the migration of DCs to sites of infection and draining lymph nodes. This increased leukocyte migration boosted the induction of the Th1 response in resistant mice, while in susceptible mice the Th2 response was augmented. This led to disease improvement or exacerbation, respectively. Our results illustrate the key role of a vascular adhesion molecule in controlling leukocyte migration and the subsequent immune events in response to pathogen infections.

state, JAM-C mainly interacts with JAM-B [20] at cell-cell contacts. Moreover, JAM-C and JAM-B can also bind the integrins $\alpha_M\beta_2$ (Mac-1) and $\alpha_4\beta_1$ (VLA-4), respectively [16,21].

We previously described a monoclonal antibody raised against mouse JAM-C, namely H33 [22]. H33 blocks JAM-C/JAM-B interaction and redistributes JAM-C away from tight junctions [20]. Interestingly, redistribution of JAM-C on the apical side of endothelial cells makes it available for interactions with its counter-receptor $\alpha_M\beta_2$, an integrin found on neutrophils and monocytes, therefore increasing their adhesion on endothelial cells [20]. More recently, it was shown that H33 increases reverse and repeated transmigration of monocytes and neutrophils, in mouse models of peritonitis, and ischemia reperfusion injury, respectively [23,24]. However, the role of endothelial JAM-C in leukocyte migration in the context of infectious disease was not addressed yet.

In this report, we studied the involvement of JAM-C in leukocyte trafficking and the subsequent immune response against *L. major* infection. We first observed that JAM-C expression by vascular endothelial cells is down regulated after infection with *L. major* at a time window when inflamed endothelium modulates and redistributes its network of junctional proteins for leukocyte transmigration [25]. To dissect the mechanism of JAM-C action in this infectious disease model, we used the antibody H33 to mimic the modulation of JAM-C observed after infection. Strikingly, blocking JAM-C after *L. major* infection *in vivo* increased vascular permeability and promoted leukocyte recruitment to the inflamed tissue, and DC migration to the draining lymph node. More importantly, sustained JAM-C blockade boosted the immune response in both resistant C57Bl/6 and susceptible BALB/c mice. On one hand, H33 treatment improved the IFN- γ -dominated Th1 response in resistant animals, together with decreased lesion size and parasite burden. On the other hand, JAM-C blockade boosted the IL-4-dominated Th2 response in susceptible mice, resulting in disease exacerbation. Collectively, our results show that JAM-C blockade potentiates the immune responses to pathogen infections by improving leukocyte migration.

Results

The antibody H33 mimics JAM-C downregulation after *L. major* inoculation, and locally increases vascular permeability after infection

Blood endothelial cells (BECs) and lymphatic endothelial cells (LECs) from the skin of mouse ears were analyzed by flow cytometry. In the steady state, BECs ($CD45^- CD31^+ gp38^-$) and LECs ($CD45^- CD31^+ gp38^+$) were JAM-C positive as previously described for other organs [14] (Fig. 1A). Conversely, leukocytes recruited to the infected ear following *L. major* inoculation were all JAM-C negative (S1 Figure). We observed a statistically significant decrease of JAM-C expression in BECs and LECs 24 hours after *L. major* infection (Fig. 1A and B). This was not the consequence of tissue injury caused by the needle, as saline injection did not downregulate JAM-C (S2 Figure). Interestingly, previous studies observed a peak of leukocytes migrating to the site of infection at the same time period [26,27]. Therefore, we postulated that JAM-C downregulation after infection could enhance vascular permeability and therefore promote inflammation and cell migration.

To study the effect of H33 on vascular permeability, we used a modified Miles assay in which mice were injected i.v. with Evan's blue [28]. Evan's blue is a small molecule that binds strongly to albumin. Consequently, this assay indirectly assesses the exudation of plasma into the tissue accounting for vascular permeability. Mice were treated with H33 or the isotype control antibody before injection of Evan's blue and *L. major* inoculation. Strikingly, treatment with H33 significantly increased the amount of Evan's blue that leaked into the inflamed tissue as compared to control. However, we did not observe any change in vascular permeability under steady state conditions (Fig. 1C).

To understand the mechanism leading to the increased vascular permeability, we investigated by immunofluorescence in our system whether H33 redistributes JAM-C out of ear endothelial cell junctions as previously proposed for other organs [20]. In control mice, JAM-C was strongly expressed at the cell border of CD31 positive endothelial cells (Fig. 1D, top panel), resulting in a U-shaped pattern of distribution of the molecule (Fig. 1E, top panel). In H33-treated animals however, JAM-C was removed from endothelial cell junctions (Fig. 1D, bottom panel), as confirmed by the smoothed pattern of distribution of JAM-C (Fig. 1E, bottom panel). Control staining for JAM-C is provided in S3 Figure.

Altogether, we concluded that the blockade of JAM-C with H33 redistributes JAM-C out of junctions, and increases vascular permeability after *L. major* infection.

Blocking JAM-C increases the number of circulating cells recruited in response to *L. major* infection

To study whether the effect of H33 on vascular permeability potentiates leukocyte recruitment after *L. major* infection, we used wild type C57BL/6 mice treated with H33, and analyzed by FACS the number of emigrating leukocytes 24 hours after infection (Fig. 2A). We observed a significant increase in the numbers of neutrophils, inflammatory monocytes, and mo-DCs in H33-treated animals as compared to control animals (Fig. 2B–D). Meanwhile, the number of non-migrating dermal macrophages (dermal m ϕ) was not modified (Fig. 2E). Finally, the number of emigrating dermal DCs, a cell type that efficiently migrates to the draining lymph node once activated, was decreased in H33-treated animals (Fig. 2F). In line with the absence of vascular permeability observed in the steady state (Fig. 1F), JAM-C blockade did not increase leukocyte emigration in naive mouse ears (S4 Figure). Moreover, we found no difference in the number

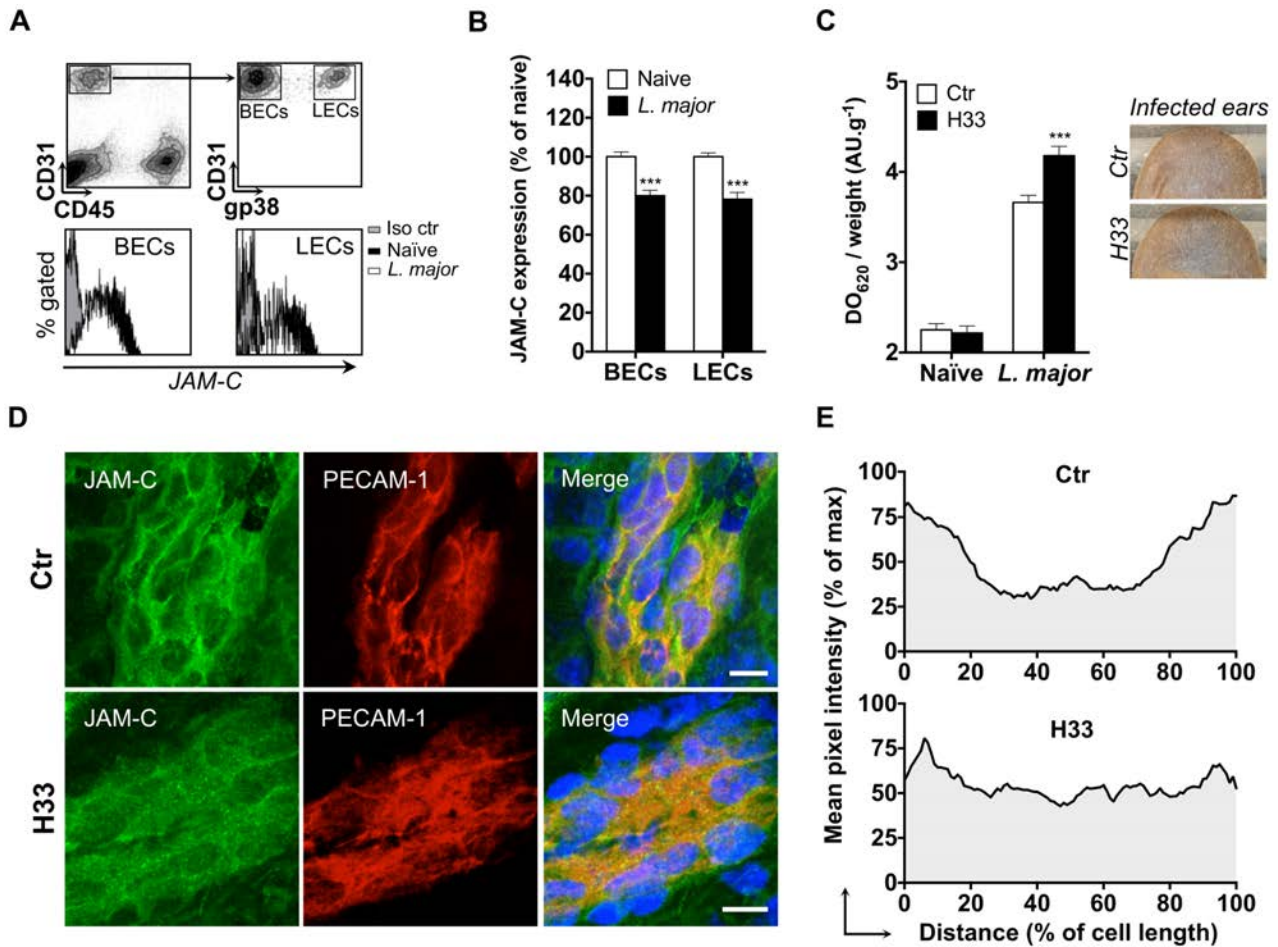


Fig. 1. The antibody H33 mimics JAM-C downregulation after *L. major* inoculation, and locally increases vascular permeability after infection. (A) JAM-C levels in endothelial cells populations of mouse ear. Ears were enzymatically digested and stained for FACS analysis. CD45⁻ CD31⁺ gp38⁻ cells represent blood endothelial cells (BECs), whereas CD45⁻ CD31⁺ gp38⁺ cells are lymphatic endothelial cells (LECs). For each population, a representative histogram overlay is shown with JAM-C in endothelial cells from naïve ears (black filled), JAM-C in endothelial cells from *L. major* infected ears (blank filled), and the isotype control staining (grey filled). (B) The median fluorescence intensity (MFI) of JAM-C in naïve mouse ears (white bars) versus *L. major* infected mouse ears (black bars) was measured in BECs and LECs. The Y-axis scale represents MFI normalized to the mean MFI of naïve ears. Data represent the mean \pm SEM of ten individual mice pooled from two separate experiments, and were analyzed by the unpaired Student's t test with ***: $p < 0.001$. (C) Mice were treated with H33 or control antibody 2 hours before Evans blue was injected i.v. and *L. major* inoculated i.d. in the ear dermis. Skin permeability was assessed by the absorbance of Evans blue extracted from the sample normalized to the weight of ear. Results are shown for naïve versus *L. major* infected animals treated with H33 (black bars) or control antibody (blank bars). Representative ear pictures are shown. Data represent the mean \pm SEM of seventeen mice per group pooled from two separate experiments, and were analyzed by the unpaired Student's t test with ***: $p < 0.001$. (D) Ear sections from control antibody-treated (top panel) or H33-treated mice (bottom panel) were stained for JAM-C (green) and CD31 (red). Nucleus was stained with DAPI (blue). Scale bars, 10 μ m. Control staining for JAM-C is shown in Figure S3. (E) The pixel intensity across 10 representative cells of similar size taken from three mice per group was measured and expressed as a percentage of the maximal pixel intensity. Data represent the average profile plot for the 10 cells per group analyzed. doi:10.1371/journal.ppat.1004550.g001

of leukocytes in the bone marrow and in the blood (S5 Figure). This suggests that H33 does neither increase haematopoiesis nor leukocyte emigration from the bone marrow to the blood in normal homeostasis.

We also measured higher levels of the monocytes and mo-DCs attracting chemokine CCL3 in H33 treated animals early after infection (Fig. 2G). This is in line with the increased number of neutrophils, a cell type known to produce CCL3 to attract mo-DCs in response to *L. major* [26]. Interestingly, the higher numbers of innate immune cells recruited with H33 did not impact on the parasite load early after infection (Fig. 2H and S6

Figure). Moreover, the dissemination of the parasites to the draining lymph node was unchanged (Fig. 2I and S6 Figure).

Overall, our data showed that JAM-C blockade with H33 increases leukocyte recruitment to the site of infection, and strongly suggest that H33 may influence DC migration to the draining lymph node.

Blocking JAM-C increases the number of DCs migrating to the draining lymph node

To investigate the effect of H33 on DC migration to the draining lymph node, we used the FITC painting assay. In this

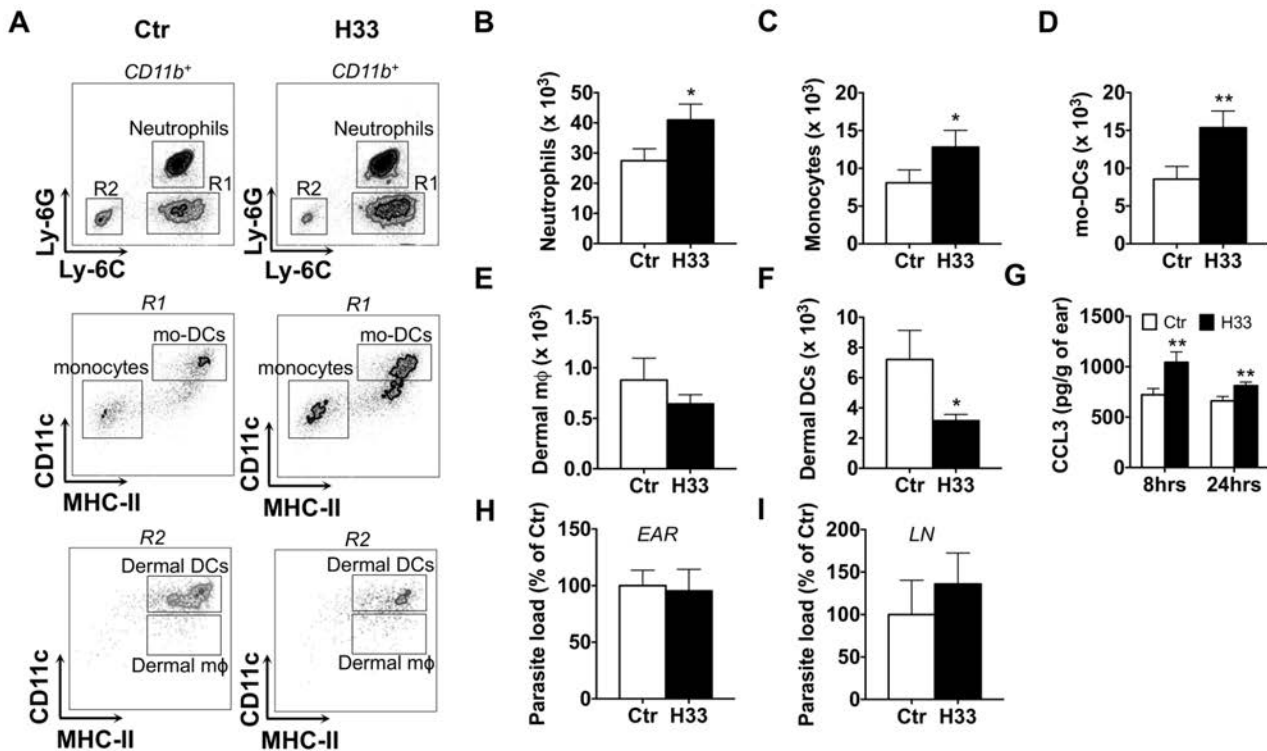


Fig. 2. Blocking JAM-C increases the number of leukocytes recruited to the site of *L. major* infection. (A) Representative dot plots of neutrophils ($CD11b^+ Ly6C^+ Ly6G^+$); monocytes ($CD11b^+ Ly6C^+ Ly6G^- CD11c^- IA^+$); mo-DCs ($CD11b^+ Ly6C^+ Ly6G^- CD11c^+ IA^+$); dermal mφ ($CD11b^+ Ly6C^- Ly6G^- CD11c^{low} IA^+$); dermal DCs ($CD11b^+ Ly6C^- Ly6G^- CD11c^{high} IA^+$) in control versus H33-treated animals. (B–F) The number of neutrophils (B), monocytes (C), mo-DCs (D), dermal mφ (E) and dermal DCs (F) was measured in the H33-treated (H33, black bar) versus isotype control-treated mice (Ctr, white bars) 24 hours p.i. Data represent the mean \pm SEM of twenty mice per group pooled from 3 separate experiments, and were analyzed by the unpaired Student’s t test with *: $p < 0.05$ and **: $p < 0.01$. (G) CCL3 protein levels normalized to the weight of ears were measured in H33-treated (H33, black bar) versus isotype control-treated mice (Ctr, white bars) 8 and 24 hours p.i. Data represent the mean \pm SEM of ten mice per group pooled from 2 separate experiments, and were analyzed by the unpaired Student’s t test with **: $p < 0.01$. (H–I) The parasite burden in infected ears (H) and draining lymph nodes (LN) (I) were measured 48 hours p.i. by limiting dilution assay (LDA). Data are expressed as a percentage of the mean of the control group \pm SEM of ten mice per group pooled from 2 separate experiments, and were analyzed by the unpaired Student’s t test. For panel H and I, raw data of one representative experiment are provided in S6 Figure. doi:10.1371/journal.ppat.1004550.g002

model, migration of dermal and epidermal DCs to lymph nodes is induced and peaks 18 hours after painting [29]. Based on MHC class II (IA) and CD11c, two populations of DCs can be distinguished by FACS in the lymph node: MHC-II^{high} CD11c⁺ migratory DCs, and MHC-II⁺ CD11c^{high} lymphoid resident DCs (Fig. 3A). Strikingly, we found higher numbers of FITC⁺ IA^{high} CD11c⁺ migratory DCs in lymph nodes of H33-treated mice as compared to control animals (Fig. 3A and B, and S7 Figure). Therefore, H33 treatment not only increases leukocyte recruitment to the site of infection, but also increases the migration of DCs to the draining lymph node.

Blocking JAM-C improves the Th1 cell response and favours healing in C57BL/6 mice

The increased DC migration to the draining lymph node in mice treated with H33 raised the question of an eventual effect on the subsequent T cell response and disease outcome. As previously reported, the induction of the T cell response starts between the second and third week after infection [10]. Therefore, mice were infected with *L. major* and treated with H33 for 3 weeks in order to boost DC migration and T cell activation. The disease was followed weekly by measuring the area of the lesions, and we assessed the *L. major* specific T cell response together with the

parasite burden 4 weeks and 8 weeks post infection (p.i.). In C57BL/6 mice, we found smaller lesions in H33-treated compared to control animals at both time points (Fig. 4A). Moreover, the reduction of the lesion area between the groups correlated with the decrease of the parasite load (Fig. 4B and S8 Figure). These results were in line with the increased numbers of CD4⁺ and CD8⁺ T cells observed (Fig. 4C and D). More importantly, draining lymph nodes T cells restimulated with UV-irradiated *L. major* produced significantly higher levels of IFN- γ at 8 weeks post infection, which accounts for the reduced lesion size and parasite load observed (Fig. 4E and S8 Figure). Taken together, these data suggest that H33 increases DC migration and therefore indirectly boosts the *L. major* specific IFN- γ -dominated Th1 cell response, resulting in a reduced severity of the disease.

Blocking JAM-C boosts the Th2 cell response and worsens the disease in BALB/c mice

Contrary to the C57BL/6 background, BALB/c mice develop a Th2 response promoting susceptibility rather than resistance to *L. major* infection [3]. Therefore, we investigated the effect of JAM-C blockade on leukocyte migration and disease outcome in susceptible BALB/c animals. After 24 hours of infection, we

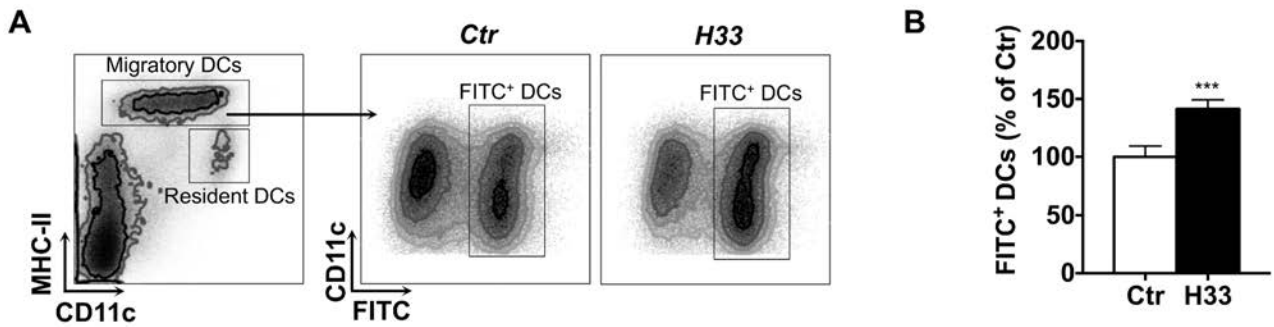


Fig. 3. Blocking JAM-C increases the number of DCs migrating to the draining lymph node. (A) The ear draining lymph node cells were harvested and stained for FACS analysis 18 hours after FITC-painting. Representative FACS dot plots are shown. (B) The number of IA^{high} CD11c⁺ FITC⁺ migratory DCs was counted. Data are expressed as a percentage of the mean of the control group \pm SEM of eighteen mice per group pooled from 3 separate experiments, and were analyzed by the unpaired Student's t test with ***: $p < 0.001$. Raw data from one representative experiment are provided in S7 Figure.
doi:10.1371/journal.ppat.1004550.g003

found increased numbers of neutrophils, and mo-DCs recruited to the site of infection in H33-treated BALB/c mice as compared to isotype control-treated mice (Fig. 5A and B). Moreover, we observed a decreased number of dermal DCs while unchanged numbers of dermal macrophages (Fig. 5C and D). These results showed that H33 influences leukocyte migration in a similar

manner in BALB/c than in C57BL/6 mice. We next wanted to assess whether this increased leukocyte migration could change the dominance of the Th2 response over the Th1 response along the course of the disease. To this end, BALB/c mice were injected with the same dose of *L. major* used with C57BL/6 mice. We did not find any change in the disease outcome with H33, most likely

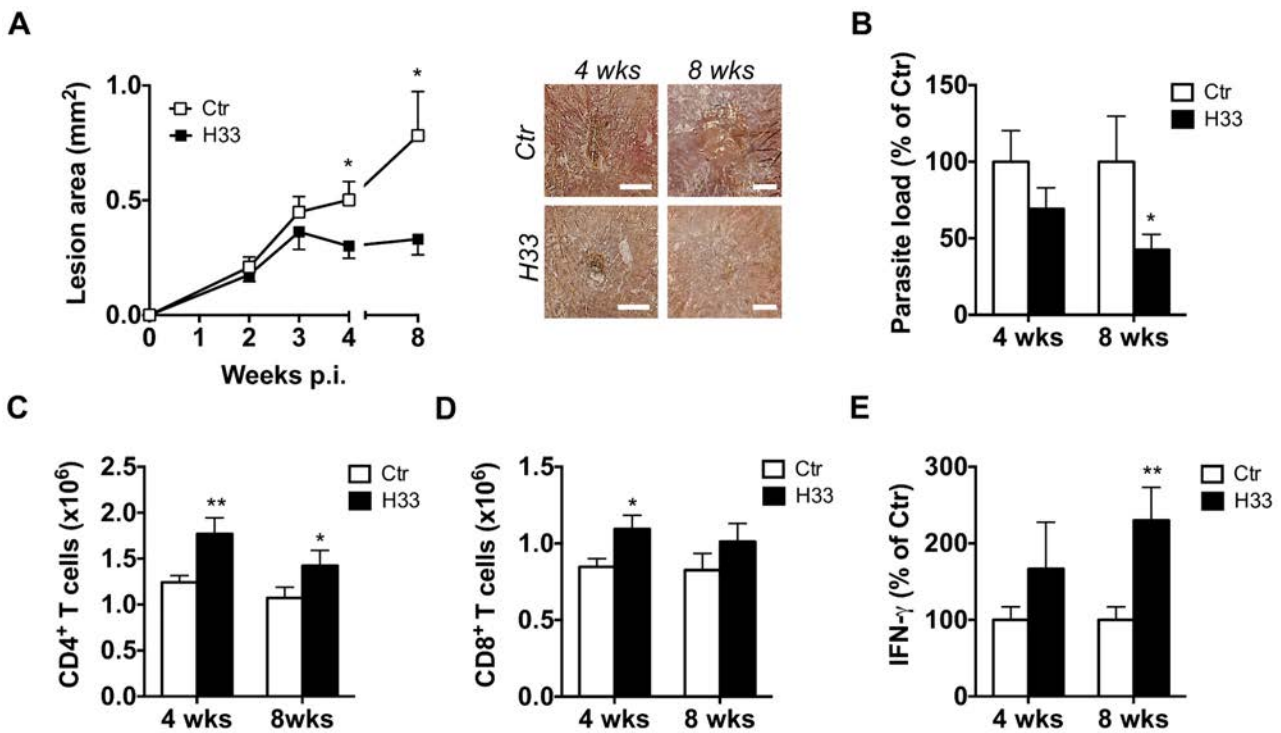


Fig. 4. Blocking JAM-C improves the Th1 cell response and favours healing in C57BL/6 mice. (A–E) Mice were inoculated with *L. major* in the ear dermis and treated with H33 or isotype control antibody for 3 weeks, twice a week. (A) The area of the lesion was monitored weekly and representative pictures of ear lesions are shown at 4 and 8 weeks p.i. Scale bars, 0.5 mm. Data represent the mean \pm SEM of twenty mice per group pooled from two separate experiments for the time point 4 weeks; and fifteen mice per group pooled from two separate experiments for the time point 8 weeks. (B) The parasite burden in infected ears was measured by LDA 4 and 8 weeks p.i. Data are expressed as a percentage of the mean of the control group \pm SEM of mice from panel A. (C–D) The number of draining lymph node CD4⁺ (C) and CD8⁺ (D) T cells analyzed by flow cytometry 4 and 8 weeks p.i. Data represent the mean \pm SEM of mice from panel A. (E) Draining lymph node cells were restimulated for 72 hrs with UV-irradiated *L. major* and the secreted IFN- γ was measured. Data are expressed as a percentage of the mean of the control group \pm SEM of mice from panel A. Data were analyzed by the unpaired Student's t test with *: $p < 0.05$ and **: $p < 0.01$. For panels B and E, raw data from one experiment are also provided in S8 Figure.
doi:10.1371/journal.ppat.1004550.g004

as a result of an exaggerated Th2 polarization with high parasite doses (Fig. 5E). Therefore, we designed a new experiment with 200 fold less parasites inoculated. Strikingly, we now observed higher lesions in H33-treated animals (Fig. 5F). This correlated with increased parasite loads in ears and draining lymph nodes (Fig. 5G and H), while parasites were undetectable in spleens (S9 Figure). The number of T cells was also augmented in draining lymph nodes (Fig. 5I and J) and they secreted higher levels of IL-4 upon restimulation with UV-irradiated *L. major* (Fig. 5K). The production of IFN- γ was however unchanged (Fig. 5L). Altogether, these results show that the increased DC migration boosts the polarized Th2 immune response without changing the type of the T helper cell response.

Discussion

In this study we investigated the involvement of JAM-C in the immune response against *L. major*. We first observed a decreased cell surface expression of endothelial JAM-C that corroborated with the strong accumulation of leukocytes at the site of *L. major* infection. We therefore postulated that JAM-C downregulation would render the endothelial junctions more permeable for inflammatory cells or fluids.

Previous findings reported that JAM-C mainly stabilizes cell junctions through trans-heterophilic, high affinity, low turnover interactions with its main partner JAM-B, while homophilic JAM-C-JAM-C interactions are weaker and occur with rapid dynamics [20]. The function of JAM-C in regulating endothelial permeability has been addressed by *in vivo* and *in vitro* studies using different approaches. *In vitro*, we have previously reported that CHO cells transfected with JAM-C exhibit an increased barrier function while MDCK cells transfected with JAM-C present increased paracellular permeability [22,30]. When HUVEC cells were stimulated with the permeability factors VEGF or thrombin, JAM-C redistributed rapidly into cell-cell contacts and permeability was augmented [31,32]. Overexpression of JAM-C *in vitro* also renders endothelial cells more permeable, probably due to the association in cis with the integrin $\alpha v \beta 3$ [32]. These findings strongly suggest that the integrity of the endothelium is the result of a finely regulated ratio of junctional molecules. Moreover, one should also consider that overexpression of JAM-C in such *in vitro* systems may interfere with the biogenesis of endogenous junctional proteins with unpredictable consequences for the barrier function [33]. More recently, Chavakis and coworkers addressed the permeability question by using wild type mice treated with soluble recombinant JAM-C in a histamine-mediated vascular permeability model [34]. They reported that soluble JAM-C reduces vascular permeability in this particular model. It is worth noting that soluble JAM-C binds to JAM-C but can also engage strong interactions with JAM-B, or with other unknown ligands. Therefore, the effect of soluble JAM-C may be the sum of several interactions, making interpretation of these results difficult.

To specifically address the function of JAM-C in vascular permeability *in vivo*, we used the multi-faceted H33 antibody that blocks JAM-C-JAM-B interactions and redistributes JAM-C out of tight junctions [20]. In our model, we were able to confirm that H33 removes JAM-C out from endothelial cell junctions. More importantly, this study showed for the first time that JAM-C blockade and redistribution with H33 increases vascular permeability by 15% after *L. major* inoculation in the skin. Conversely, we did not observe increased vascular permeability after administration of H33 in the steady state. This increase is substantial, as vascular permeability in inflammation is an optimized process [35]. Moreover, the absence of the H33 effect on vascular

permeability in normal homeostasis is not surprising as many other different junctional molecules can still ensure vascular integrity in absence of inflammatory signals [36]. In line with this observation, H33 treatment also does not increase leukocyte migration from the blood to the tissue in absence of pathogen-mediated, inflammatory signals. However, after *L. major* infection, the number of leukocytes that migrate to the inflamed tissue increased significantly in mice treated with H33. As recent findings showed that VE-cadherin controls permeability and transmigration independently [37], our data with H33 may be in part the result of increased vascular permeability or the redistribution of JAM-C away from junctions as well. Redistribution of JAM-C on the apical side of the lumen makes it available for interactions with Mac-1 found on neutrophils and monocytes [20]. Accumulation of more adherent leukocytes on the luminal side of vessels could then increase the number of transmigrating cells. Therefore, H33 may increase leukocyte adhesion to the inflamed endothelium in addition to promoting vascular permeability in the context of *L. major* infection (Fig. 6).

In the *L. major* mouse model of cutaneous leishmaniasis, the kinetics of leukocyte recruitment, their specific function, and the crosstalk between the different subsets of cells have been and are still under investigation. It is now well accepted that neutrophils are the first cells recruited within hours to the infected tissue [10,27,38,39]. However, some discrepancies still exist concerning their immunoregulatory function, which may depend on the mode of parasite transmission and the number of pathogens inoculated. Indeed, in the *Leishmania* resistant C57BL/6 mice, Sacks and coworkers used the monocyte and neutrophil depleting RB8-8C5 antibody and a natural sand-fly transmission of *L. major* to show that depletion of these cells promotes rather than compromises host resistance [38]. More recently, they showed that efferocytosis of infected neutrophils by DCs decreases their activation and antigen presenting cell function, therefore dampening the protective pro-inflammatory response [27]. On the other hand, other reports using needle inoculation of high parasite doses like our study, have demonstrated a transient protective role for neutrophils in C57BL/6 mice [40–42]. These studies assessed the role of neutrophils mostly by depletion, mediated by the more neutrophil-specific antibody NIMP-R14 [39] or by the anti-Gr1 RB6-8C5 antibody recognizing inflammatory monocytes and neutrophils. All these neutrophil depletion studies resulted in transient increased lesion size and parasite loads. It is worth noting that RB6-8C5, the antibody used in most of the studies, not only depletes neutrophils but also inflammatory monocytes, illustrating the importance of neutrophils and inflammatory monocytes in promoting resistance to infection. The contribution of monocytes and mo-DCs has been further investigated with the use of chemokine receptor CCR2 knock-out mice in the resistant C57BL/6 background. In these mice, monocytes do not leave the bone marrow, resulting in a deficiency of monocytes in the blood circulation [43]. The recruitment of inflammatory mo-DCs in the lymph node following *L. major* infection is therefore completely impaired, which dampens the Th1 cell response [11]. Subsequently, the CCR2 deficiency results in a non-healing phenotype similar to that observed in susceptible mice [12]. Our report is in line with these studies, as treatment with the antibody H33 increased the recruitment of neutrophils, inflammatory monocytes and mo-DCs, and thereby improving the Th1 immune response and the clinical outcome in C57BL/6 mice. In addition, Tacchini-Cottier and coworkers [26] emphasized the contribution of neutrophils in the recruitment of mo-DCs to the site of *L. major* infection through the secretion of the chemokine CCL3. In line with this finding, we observed a significant increase in the

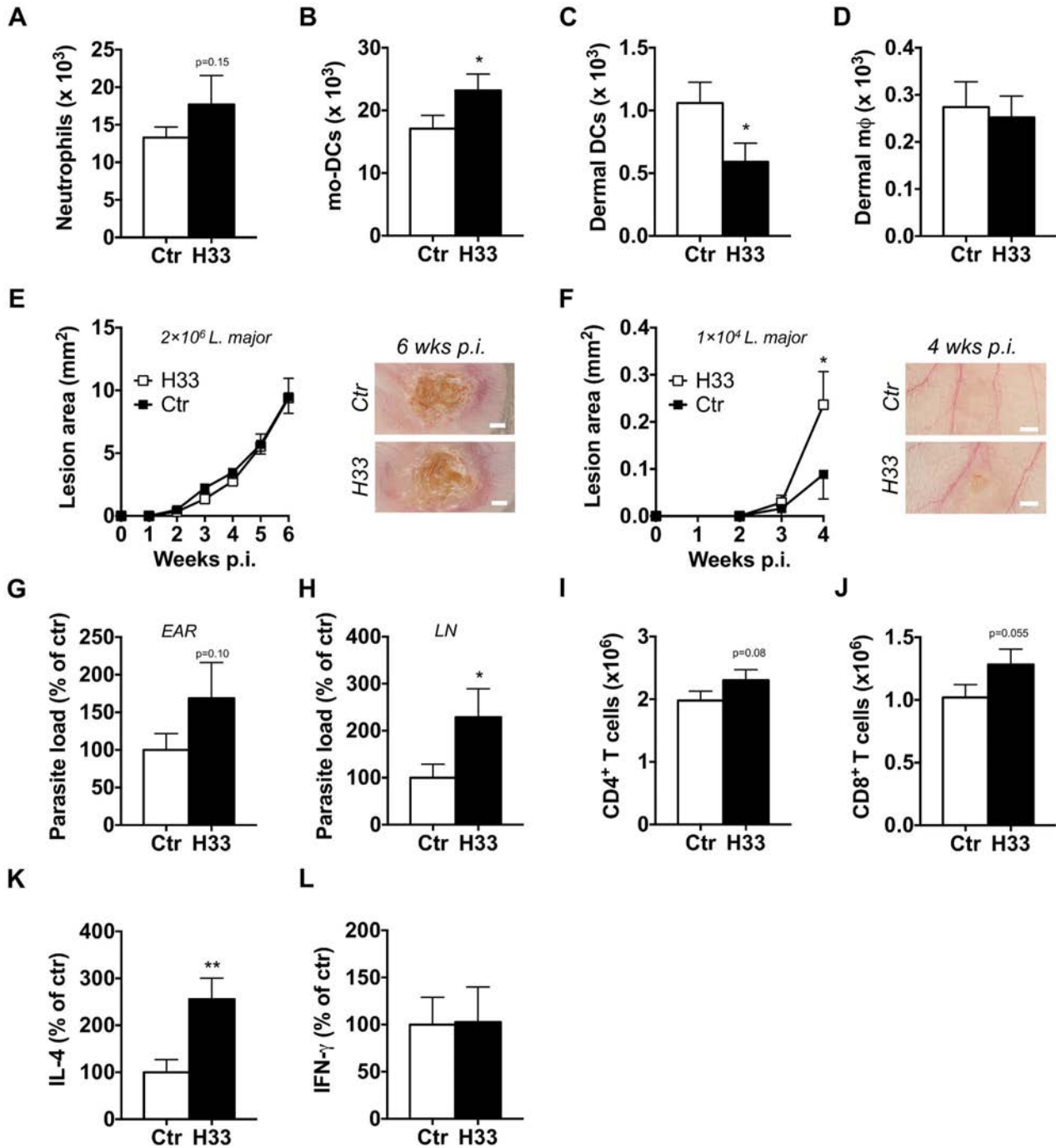


Fig. 5. Blocking JAM-C boosts the Th2 cell response and worsens the disease in BALB/c mice. The number of emigrating neutrophils (A), mo-DCs (B), dermal DCs (C) and dermal m ϕ (D) was measured in the ears of H33-treated (H33, black bar) versus isotype control-treated mice (Ctr, white bars) 24 hours post *L. major* infection. Data represent the mean \pm SEM of twelve mice per group pooled from 2 separate experiments, and were analyzed by the unpaired Student's t test with *: $p < 0.05$. (E) Mice were inoculated with 2×10^6 stationary phase *L. major* promastigotes in the ear dermis and treated with H33 or control antibody for 3 weeks. The area of the lesion was monitored weekly for 6 weeks. Representative ear pictures are shown. Scale bars, 1 mm. Data represent the mean \pm SEM of twenty mice per group pooled from two separate experiments. (F–L) Mice were inoculated with 1×10^4 stationary phase *L. major* promastigotes in the ear dermis and treated with H33 or control antibody for 3 weeks. The area of the lesion was monitored weekly for 4 weeks. Representative ear pictures are shown. Scale bars, 0.5 mm. Data represent the mean \pm SEM of ten mice per group pooled from two separate experiments. (G–H) The parasite burden in infected ears (G) and draining lymph nodes (H) were measured by LDA. Data are expressed as a percentage of the mean of the control group \pm SEM of mice from panel F. (I–J) The number of CD4⁺ (I) and CD8⁺ (J) T cells were measured. Data represent the mean \pm SEM of mice from panel F. (K–L) Draining lymph nodes cells were restimulated with UV-irradiated *L. major* for 72 hours, and the IL-4 (K) and IFN- γ (L) produced were measured. Data are expressed as a percentage of the mean of the control group \pm SEM of mice from panel F. Data were analyzed by the unpaired Student's t test with *: $p < 0.05$ and **: $p < 0.01$. For panels expressing results as percentage of the mean of the control, raw data of one experiment are provided in S9 Figure. doi:10.1371/journal.ppat.1004550.g005

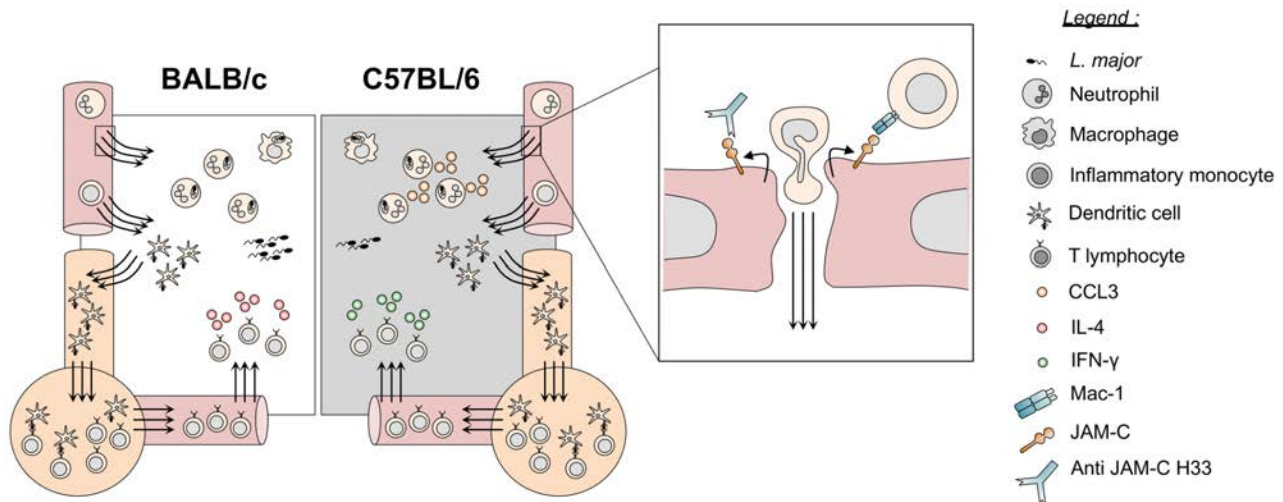


Fig. 6. Blocking JAM-C enhances DC migration and boosts the immune responses to *L. major* infection. By removing JAM-C out of functions, H33 increases adhesion of leukocytes and potentiates vascular permeability and cell migration of leukocytes after *L. major* infection. Increased numbers of recruited neutrophils result in higher levels of the chemokine CCL3 attracting monocytes and mo-DCs in C57BL/6 mice. The number of migratory DCs to lymph nodes increases, and the subsequent T cell response is mounted more efficiently. Resistant C57BL/6 mice develop a higher IFN- γ -dominated Th1 response while susceptible BALB/c mice develop a stronger IL-4-dominated Th2 response. This has a significant healing effect in resistant animals whereas susceptible mice display an exacerbated disease. doi:10.1371/journal.ppat.1004550.g006

production of CCL3 within ears of H33 treated mice at time points where neutrophils are massively recruited to the site of infection. Therefore, we suggest that, by increasing the numbers of neutrophils recruited, H33 could indirectly increase the amount of CCL3 produced *in situ*. This additional mechanism may also contribute to further enhance the extravasation of mo-DCs in the ears of H33 treated C57BL/6 mice (Fig. 6).

We also report that H33 increases the number of DCs leaving the ear dermis to the draining lymph node. This may be the direct consequence of JAM-C blocking at lymphatic endothelial cell junctions, which would facilitate DCs transendothelial migration. Alternatively, it could be the indirect consequence of the higher number of DCs recruited to the site of inflammation that migrate to the lymph node as a consequence. The later hypothesis is more likely since DCs preferentially migrate in an integrin-independent manner through initial lymphatic capillaries by seeking pre-existing flaps between the oak leaf-shaped lymphatic endothelial cells [44,45]. It is worth noting that JAM-C is also well expressed by lymphatic sinuses from lymph nodes, which may influence T cell surveillance of DCs in the lymph nodes, and therefore T cell activation after H33 treatment. However, we had already demonstrated that the ability of DCs to prime T cells *in vivo* in JAM-C deficient animals is unchanged [46]. In lymph nodes, JAM-C is also expressed by high endothelial venules, and we cannot exclude an effect of H33 on T cell entry into lymph nodes.

Finally, we used the properties of H33 treatment on vascular permeability and innate cell migration to assess the consequences on the clinical outcome. In C57BL/6 mice, the higher numbers of neutrophils or monocyte-derived cells recruited rapidly after infection may increase the early innate parasite killing. However, we observed no difference in the parasite load 48 hours after infection. This is likely due to the absence of the IFN- γ -dominated Th1 response that leads to activation of phagocytes and parasite killing at this early time point [3]. Moreover, the increased vascular permeability at the site of infection may have influenced the dissemination of the parasite to peripheral organs early after infection. But we did not find any change in the draining lymph

nodes, while the parasite was undetectable in spleen. Strikingly, we found that H33 was able to boost the adaptive immune response in both susceptible and resistant mice by increasing DC migration, without changing the T cell polarization. This report is the first one to demonstrate that immune responses to pathogen infections can be finely-tuned by manipulating a single adhesion molecule, and in particular JAM-C. For instance, deletion of P- or E-selectin does not impact the immune response to *L. major* infection in a mixed 129/C57BL/6 background [47]. Finally, our findings in BALB/c mice confirm that susceptibility does not result from an overall lack of leukocyte migration to the site of infection, but rather from a genetic defect in redirecting the T cell response [3].

Materials and Methods

Ethics statement

All animal procedures were performed in accordance with the Institutional Ethical Committee of Animal Care in Geneva, Switzerland. The protocol has been approved by the Ethics and Federal Veterinary office regulations of the state of Geneva. Our laboratory has the authorization number 1005-3753.1.

Mice and parasites

Female C57BL/6J and BALB/c mice were purchased from Charles River (Lyon, France). Mice were bred in the P2 animal facility at the CMU, and used between 6–8 weeks of age. *Leishmania major* LV39 (MRHO/Sv/59/P Strain) were used. In all experiments, C57BL/6 mice were infected in the ear dermis with 2×10^6 stationary phase *L. major* promastigotes in a volume of 10 μ L. The disease outcome in BALB/c was followed after infection with 2×10^6 and 1×10^4 stationary phase *L. major* promastigotes in a volume of 10 μ L.

Flow cytometry analysis of ear endothelial cells

The ventral and dorsal sheets of mouse ears were split with forceps, and digested with 3 mg/mL collagenase type IV (Invitrogen) and 1 mg/mL DNase type I (Sigma Aldrich) for

45 minutes at 37°C, filtered through a 70 µm gauge strainer (Becton Dickinson), and the cells labelled for FACS analysis. Fc receptors were blocked with the monoclonal antibody (mAb) 2.4G2 (Becton Dickinson). Cells were stained with the following reagents: Alexa Fluor 488-conjugated anti-mouse podoplanin (clone 8.1.1), PE-conjugated anti-mouse CD31 (clone 390), PE-Cy7-conjugated anti-mouse CD45 (clone 30-F11), all from affimetrix eBioscience. JAM-C was labelled with an affinity purified polyclonal anti-mouse JAM-C antibody raised in rabbit [31], while affinity purified rabbit IgG (Sigma) was used as a control. The secondary antibody used was an Alexa Fluor 647-conjugated anti-rabbit antibody (Jackson ImmunoResearch). Cells were analyzed with a Gallios FACS machine (Beckman Coulter) and the data were processed with Kaluza software (Beckman Coulters).

Leukocyte emigration for ear skin explants and FACS analysis

Mice were injected i.p. with the rat IgG2a anti-mouse JAM-C H33 or the rat IgG2a isotype control 2A3 (BioXCell), 200 µg/mice, 2 hours before inoculation of *L. major* in the ear dermis. Twenty-four hours post infection, mice were sacrificed and ears explanted. The ventral and dorsal sheets of the ears were separated with forceps, and transferred overnight in twelve well plates filled with RPMI-1640 medium supplemented with 10% fetal calf serum and antibiotics at 37°C. Over this period of time, the leukocytes that have been recruited to the infected ears spontaneously emigrated from the explants. Emigrated cells were then counted with a hemocytometer, and stained for FACS analysis. Fc receptors were blocked with the mAb 2.4G2. Cells were stained with the following reagents: Alexa Fluor 488-conjugated anti-mouse Ly6C (clone HK1.4, Biolegend), PercP-Cy5.5-conjugated anti-mouse Ly6G (clone 1A8, Biolegend), PE-Cy7-conjugated anti-mouse CD11b (clone M1/70, Biolegend), APC-Cy7-conjugated anti-mouse CD11c (clone N418, Biolegend), and efluor 450-conjugated anti-mouse IA/IE (clone M5/114.15.2, eBiosciences). Cells were analyzed with a Gallios FACS machine (Beckman Coulter) and data processed with Kaluza software (Beckman Coulters). The number of cells per population was calculated by multiplying the total number of emigrating cells with the percentage of cells of interest.

FACS analysis of leukocyte populations in steady state

Mice were injected i.p. with the mAb H33 or the control mAb 2A3 (200 µg/mice). Mice were then sacrificed 24 hours after treatment to collect ears, blood and femurs. Ears were processed as described above. Femurs were flushed to extract bone marrow cells. Red blood cells from blood and bone marrow samples were lysed with Ammonium-Chloride-Potassium (ACK) lysis buffer. A fraction of each sample was used for FACS staining using BD Trucount tubes according to the manufacturer's instructions. Fc receptors were blocked with the mAb 2.4G2. Bone marrow cells were stained with the following reagents: Alexa Fluor 488-conjugated anti-mouse Ly6C (clone HK1.4, Biolegend), PE-conjugated anti-mouse CD115 (clone AFS98, eBiosciences), PercP-Cy5.5-conjugated anti-mouse Ly6G (clone 1A8, Biolegend), PE-Cy7-conjugated anti-mouse F4/80 (clone BM8, Biolegend), APC-conjugated anti-mouse CD11c (clone HL3, BD), APC-Cy7-conjugated anti-mouse TCR β (clone H57-597, Biolegend), efluor 450-conjugated anti-mouse CD11b (clone M1/70, eBiosciences), Brilliant Violet 785-conjugated anti-mouse CD8 α (clone 53-6.7, Biolegend). Blood cells were stained with the following reagents: Alexa Fluor 488-conjugated anti-mouse Ly6C (clone HK1.4, Biolegend), PE-conjugated anti-mouse CD115 (clone AFS98),

PercP-Cy5.5-conjugated anti-mouse Ly6G (clone 1A8, Biolegend), PE-Cy7-conjugated anti-mouse CD4 (clone RM4-5, Biolegend), APC-conjugated anti-mouse NK1.1 (clone PK136, Biolegend), APC-Cy7-conjugated anti-mouse CD19 (clone 6D5, Biolegend), efluor 450-conjugated anti-mouse CD11b (clone M1/70, eBiosciences), Brilliant Violet 785-conjugated anti-mouse CD8 α (clone 53-6.7, Biolegend). Cells were analyzed with a Gallios FACS machine (Beckman Coulter) and the data were processed with Kaluza software (Beckman Coulter). The number of cells per population was calculated by multiplying the total number of cells with the percentage of cells of interest. The total number of cells was calculated using the number of Trucount beads analyzed by the flow cytometer.

FITC painting experiments

Mice were injected i.p. with the mAb H33 or the control mAb 2A3 (200 µg/mice) 2 hours before FITC painting of mice ears. FITC (Sigma) was used at 5 mg/mL and dissolved in acetone:dibutyl phthalate (1:1, v:v). Twenty microliters were applied to each side of the ear. Eighteen hours after painting, the ear draining lymph node was harvested and digested with 3 mg/mL collagenase type IV (Invitrogen) and 1 mg/mL DNase type I (Sigma) for 45' at 37°C, and filtered through a 70 µm gauge strainer (Becton Dickinson). The cells were counted with a hemocytometer, and labelled for FACS analysis. Fc receptors were blocked with the mAb 2.4G2. Cells were stained with the following reagents: APC-Cy7-conjugated anti-mouse CD11c, and efluor 450-conjugated anti-mouse IA/IE. Cells were analyzed with a Gallios FACS machine (Beckman Coulters) and data processed with Kaluza software (Beckman Coulters). The number of FITC⁺ migratory DCs was calculated by multiplying the total number of lymph node cells with the percentage of IA/IE^{high} CD11c⁺ FITC⁺ DCs.

Immunofluorescence microscopy

Mice were injected i.p. with the mAb H33 or the control mAb 2A3 (200 µg/mice). Twenty-four hours after injection, ears were embedded in Tissue-Tek OCK compound, frozen at -80°C, then cut (5 µm) with a cryostat. Fresh ear sections were fixed in cold acetone for 5 minutes, rehydrated in PBS for 10 minutes, and blocked with 10% normal donkey serum. CD31 was detected with an Alexa Fluor 647-conjugated rat anti mouse CD31 (clone GC51, home made), while JAM-C was detected with a polyclonal anti-mouse JAM-C antibody raised in rabbit [31] followed by an Alexa Fluor 488-conjugated donkey anti-rabbit antibody (Jackson ImmunoResearch). We used rabbit IgG as control for JAM-C staining. Cell nucleus was stained with DAPI and slides were mounted with mowiol mounting medium. Labelled ear sections were visualized with a Nikon A1R confocal microscope and the NIS Elements AR software. All images were acquired with a 100× objective. The maximal intensity projection image of the z-stack is shown. The images were analyzed with Image J. The distribution profile of JAM-C was plotted along the minor axis of the cells.

Vascular permeability assay

Mice were treated i.p. with the mAb H33 or the control mAb 2A3 (200 µg/mice) 2 hours before 100 µL of Evans blue (12 mg/mL) was injected i.v. and *L. major* inoculated i.d. in the ear. Five hours after infection, mice were killed, and the permeability of Evans blue in the ear documented by picturing each ear. Ears were then cut, weighted, split into dorsal and ventral sheets, and finally transferred into formamide for 2 days at room temperature to extract the Evans blue dye. The absorbance of the samples was measured at 620 nm (Ledetect 96, Labexim) and normalized to the weight of tissue.

CCL3 level in ear following *L. major* infection

Mice were injected i.p. with H33 or the control mAb 2A3 (200 µg/mice) 2 hours before *L. major* inoculation in the ear dermis. Eight or 24 hours after infection, ears were homogenized on ice in a protease inhibitor cocktail (Sigma Aldrich, P8340) using a polytron as tissue homogenizer. The expression of the chemokine CCL3 were measured in tissue homogenates with the BD CBA mouse Flex Set kit according to the manufacturer instructions. Beads were analyzed on a Cyan (Beckman Coulters) flow cytometer and data processed with the FCAP array software (Becton Dickinson).

T cell response in the draining lymph node and cytokine detection

The ear draining lymph nodes were digested with 3 mg/mL collagenase type IV (Invitrogen) and 1 mg/mL DNase type I (Sigma) for 45' at 37°C, and filtered through a 70 µm gauge strainer (Becton Dickinson). The cells were counted with a hemacytometer and labelled for FACS analysis. Fc receptors were blocked with the mAb 2.4G2. Cells were stained for cell surface antigens with the following reagents: FITC-conjugated anti-mouse TCRβ (clone H57-597, eBioscience), Brilliant Violet 421-conjugated anti-mouse CD8α (clone 53-6.7, Biolegend), Brilliant Violet 785-conjugated anti-mouse CD4 (clone RM4-5, Biolegend). Cells were analyzed with a Gallios FACS machine (Beckman Coulters) and the data were processed with Kaluza software (Beckman Coulters). The number of cells per population was calculated by multiplying the total number of lymph nodes cells with the percentage of cells of interest. For T cell restimulation, draining lymph nodes cells were incubated at 37°C under 5% CO₂ for 72 hours in the presence of UV-irradiated *L. major* (ratio 5:1, cell:parasite). Supernatant were collected and the levels of IL-4 and IFN-γ were measured by ELISA (eBioscience) or CBA (Becton Dickinson) according to the manufacturer instructions.

Lesion area measurement and parasite load

Mice were injected i.p. with the mAb H33 or the control mAb 2A3 (200 µg/mice) 2 hours before inoculation of *L. major* in the ear dermis. Injections of mAbs (100 µg/mice) were repeated twice a week for twenty-one days. The evolution of the lesion was documented weekly with a picture of each ear, as well as the picture of a 1 cm scale. The camera was fixed on a support for the scale to be unchanged from one picture to the other. The pictures were analyzed with ImageJ software. Briefly, the picture of the 1 cm scale provides the number of pixels per 1 cm unit. Each lesion was then defined manually with the software, and the precise lesion area calculated using the number of pixels in the selected area. For parasite burden, the infected ears were explanted, weighted, and separated into two halves. Ear leaflets were enzymatically digested before tissue dissociation with a gentleMACS Octo Dissociator (Miltenyi Biotech). Ears homogenates, lymph nodes or spleens cells were serially diluted, and the parasite load estimated by limiting dilution assay as described [48].

Statistical analysis

Data were analyzed with the GraphPad Prism statistics software. We used the Student's t-test for unpaired data for all experiments.

Supporting Information

Figure S1 Leukocytes emigrating to the site of *L. major* infection do not express JAM-C. The expression of JAM-C by leukocytes emigrated from *L. major* infected ears was measured

24 hours post infection. CD11b⁺ Ly6C⁺ Ly6G⁺ represent neutrophils, CD11b⁺ Ly6C⁺ Ly6G⁻ CD11c⁻ IA⁻ are monocytes, CD11b⁺ Ly6C⁺ Ly6G⁻ CD11c⁺ IA⁺ are mo-DCs, CD11b⁺ Ly6C⁻ Ly6G⁻ CD11c^{low} IA⁺ are dermal mφ, and CD11b⁺ Ly6C⁻ Ly6G⁻ CD11c^{high} IA⁺ are dermal DCs. A representative histogram overlay of JAM-C expression is shown for each population, with JAM-C staining (black line), and isotype control staining (grey line). Data are representative of two separate experiments.

(TIFF)

Figure S2 JAM-C expression in ear endothelial cells does not decrease 24 hours after saline injection (A) JAM-C levels in endothelial cells populations of mouse ear.

Ears were enzymatically digested and stained for FACS analysis. CD45⁻ CD31⁺ gp38⁻ cells represent blood endothelial cells (BECs), whereas CD45⁻ CD31⁺ gp38⁺ cells are lymphatic endothelial cells (LECs). For each population a representative histogram overlay is shown with JAM-C in endothelial cells from naïve ears (white filled), JAM-C in endothelial cells from saline injected ears (black filled), and the isotype control staining (grey filled). (B) The MFI of JAM-C in naïve mouse ears (white bars) versus saline injected mouse ears (black bars) was measured in BECs and LECs. The Y-axis scale represents MFI normalized to the mean MFI of naïve ears. Data represent the mean ± SEM of five mice per group pooled from two separate experiments.

(TIFF)

Figure S3 Control staining for JAM-C in ear endothelial cells.

Ear sections were stained for Rabbit IgG control (green), CD31 (red). Nucleus was stained with DAPI (blue). Scale bars, 10 µm. This supporting information is related to Fig. 1D.

(TIFF)

Figure S4 Blocking JAM-C does not result in leukocyte emigration to tissue in the steady state.

The number of neutrophils (A), monocytes (B), mo-DCs (C), dermal mφ (D), and dermal DCs (E) emigrating from ears was measured in H33-treated (H33, black bar) versus isotype control-treated mice (Ctr, white bars) 24 hours after antibody administration. Data represent the mean ± SEM of fifteen mice per group pooled from 3 separate experiments, and were analyzed by the unpaired Student's t test.

(TIFF)

Figure S5 Blocking JAM-C in the steady state does neither increase hematopoiesis nor leukocyte migration from bone marrow to the blood.

Naïve C57BL/6 mice were treated with H33 or isotype control antibody for 24 hours. The number of neutrophils (A), monocytes (B), DCs (C), T cells (D), eosinophils (E), and macrophages (F) from the bone marrow (BM); and B cells (G), CD4⁺ T cells (H), CD8⁺ T cells (I), neutrophils (J), monocytes (K), and NK cells (L) from blood in H33-treated (black bar) versus isotype control-treated mice (white bars) is shown. Data represent the mean ± SEM of five mice per group, and were analyzed by the unpaired Student's t test. Data are representative of three separate experiments.

(TIFF)

Figure S6 H33 antibody does neither decrease the parasite burden in infected ears, nor increase parasite dissemination to lymph nodes 48 hours p.i. (Raw data of Fig. 2).

The parasite burden in infected ears (A) and draining lymph nodes (B) were measured 48 hours p.i. by LDA. Data represent the mean ± SEM of five mice per group from one representative experiment, and were analyzed by the unpaired Student's t test. These supporting informations are related to Fig. 2H and I.

(TIFF)

Figure S7 Blocking JAM-C increases the number of DCs migrating to the draining lymph node (Raw data of Fig. 3). The ear draining lymph nodes were harvested and stained for FACS analysis 18 hours after FITC-painting. The number of IA^{high} CD11c⁺ FITC⁺ migratory DCs was counted. Data represent the mean \pm SEM of six mice per group, and were analyzed by the unpaired Student's t test with *: $p < 0.05$. This supporting information is related to Fig. 3B. (TIFF)

Figure S8 Blocking JAM-C improves the Th1 cell response and favours healing in C57BL/6 mice (Raw data of Fig. 4). Mice were inoculated with *L. major* in the ear dermis and treated with H33 or the isotype control antibody for 3 weeks, twice a week. (A) The parasite burden in infected ears was measured by LDA 4 and 8 weeks p.i. Data represent mean \pm SEM of ten mice per group for both time points. (B) Draining lymph node cells were restimulated for 72 hrs with UV-irradiated *L. major* and the secreted IFN- γ was measured. Data represent the mean \pm SEM of mice from panel A. Data were analyzed by the unpaired Student's t test with *: $p < 0.05$. These supporting informations are related to Fig. 4B and E. (TIFF)

Figure S9 Blocking JAM-C boosts the Th2 cell response and worsens the disease in BALB/c mice (Raw data of

Fig. 5). (A–C) Mice were inoculated with 1×10^4 stationary phase *L. major* promastigotes in the ear dermis and treated with H33 or control antibody for 3 weeks. The parasite burden in infected ears (A), draining lymph nodes (B), and spleens (C) were measured by LDA. (D–E) Draining lymph nodes cells were restimulated with UV-irradiated *L. major* for 72 hours, and the IL-4 (D) and IFN- γ (E) produced were measured. Data represent the mean \pm SEM of 5 mice per group. Data were analyzed by the unpaired Student's t test with *: $p < 0.05$, ***: $p < 0.001$. n.d. not-detectable. These supporting informations are related to Fig. 5G, H, K and L. (TIFF)

Acknowledgments

The authors would like to thank Yazmin Hauyon-La Torre and Dr. Floriane Auderset for help in parasite preparation; Cristina Riccadonna and Alexandra Gomez Alejandre for technical assistance; Dr. Marie Kosco-Vilbois for fruitful discussions and Nicholas Magon for critical reading of the manuscript.

Author Contributions

Conceived and designed the experiments: RB YE FTC BAI. Performed the experiments: RB YE SJ MC. Analyzed the data: RB YE. Contributed reagents/materials/analysis tools: FTC. Wrote the paper: RB YE FTC BAI.

References

- Murray HW, Berman JD, Davies CR, Saravia NG (2005) Advances in leishmaniasis. *The Lancet* 366: 1561–1577.
- Kaye P, Scott P (2011) Leishmaniasis: complexity at the host-pathogen interface. *Nat Rev Microbiol* 9: 604–615.
- Sacks D, Noben-Trauth N (2002) The immunology of susceptibility and resistance to *Leishmania major* in mice. *Nat Rev Immunol* 2: 845–858.
- Heinzel F, Sadick M, Mutha S, Locksley R (1991) Production of interferon-gamma, interleukin-2, interleukin-4, and interleukin-10 by CD4⁺ lymphocytes in vivo during healing and progressive murine leishmaniasis. *PNAS* 88: 7011–7015.
- Wang ZE, Reiner LR, Zheng S, Dalton DK, Lockley RM (1994) CD4⁺ Effector Cells Default to the Th2 Pathway in Interferon γ -deficient Mice Infected with *Leishmania major*. *J Exp Med* 179: 1367–1371.
- Liew F, Millott S, Parkinson C, Palmer R, Moncada S (1990) Macrophages killing of *Leishmania* parasite in vivo is mediated by nitric oxide from L-arginine. *J Immunol* 144: 4794–4797.
- Tacchini-Cottier F, Weinkopf T, Launois P (2012) Does T Helper Differentiation Correlate with Resistance or Susceptibility to Infection with *L. major*? Some Insights From the Murine Model. *Front Immunol* 3: 32.
- Ng LG, Hsu A, Mandell MA, Roediger B, Hoeller C, et al. (2008) Migratory dermal dendritic cells act as rapid sensors of protozoan parasites. *PLoS Pathog* 4: e1000222.
- Von Stebut E, Belkaid Y, Jakob T, Sacks D, Udey M (1998) Uptake of *Leishmania major* Amastigotes Results in Activation and Interleukin 12 Release from Murine Skin-derived Dendritic Cells: Implications for the Initiation of Anti-*Leishmania* Immunity. *J Exp Med* 188: 1547–1552.
- Leon B, Lopez-Bravo M, Ardavin C (2007) Monocyte-derived dendritic cells formed at the infection site control the induction of protective T helper 1 responses against *Leishmania*. *Immunity* 26: 519–531.
- De Trez C, Magez S, Akira S, Ryffel B, Carlier Y, et al. (2009) iNOS-producing inflammatory dendritic cells constitute the major infected cell type during the chronic *Leishmania major* infection phase of C57BL/6 resistant mice. *PLoS Pathog* 5: e1000494.
- Sato N, Ahuja SK, Quinones M, Kostecki V, Reddick RL, et al. (2000) CC Chemokine Receptor (CCR)2 Is Required for Langerhans Cell Migration and Localization of T Helper Cell Type 1 (Th1)-inducing Dendritic Cells: Absence of CCR2 Shifts the *Leishmania major*-resistant Phenotype to a Susceptible State Dominated by Th2 Cytokines, B Cell Outgrowth, and Sustained Neutrophilic Inflammation. *J Exp Med* 192: 205–218.
- Ley K, Laudanna C, Cybulsky MI, Nourshargh S (2007) Getting to the site of inflammation: the leukocyte adhesion cascade updated. *Nat Rev Immunol* 7: 678–689.
- Scheiermann C, Colom B, Meda P, Patel NS, Voisin MB, et al. (2009) Junctional adhesion molecule-C mediates leukocyte infiltration in response to ischemia reperfusion injury. *Arterioscler Thromb Vasc Biol* 29: 1509–1515.
- Liang T, Chiu H, Gurney A, Sidle A, Tumas D, et al. (2002) Vascular Endothelial-Junctional Adhesion Molecule (VE-JAM)/JAM 2 Interacts with T, NK, and Dendritic Cells Through JAM 3. *J Immunol* 168: 1618–1626.
- Santos S, Sachs UJH, Kroll H, Linder M, Ruf A, et al. (2002) The Junctional Adhesion Molecule 3 (JAM-3) on Human Platelets is a Counterreceptor for the Leukocyte Integrin Mac-1. *J Exp Med* 196: 679–691.
- Zen K, Babbitt BA, Liu Y, Whelan JB, Nusrat A, et al. (2004) JAM-C is a component of desmosomes and a ligand for CD11b/CD18-mediated neutrophil transepithelial migration. *Mol Biol Cell* 15: 3926–3937.
- Morris AP, Tawil A, Berkova Z, Wible L, Smith CW, et al. (2006) Junctional Adhesion Molecules (JAMs) are differentially expressed in fibroblasts and colocalize with ZO-1 to adherens-like junctions. *Cell Commun Adhes* 13: 233–247.
- Scheiermann C, Meda P, Aurrand-Lions M, Madani R, Yiangou Y, et al. (2007) Expression and function of junctional adhesion molecule-C in myelinated peripheral nerves. *Science* 318: 1472–1475.
- Lamagna C, Meda P, Mandicourt G, Brown J, Gilbert RJ, et al. (2005) Dual interaction of JAM-C with JAM-B and α (M) β 2 integrin: function in junctional complexes and leukocyte adhesion. *Mol Biol Cell* 16: 4992–5003.
- Cunningham SA, Rodriguez JM, Arrate MP, Tran TM, Brock TA (2002) JAM2 interacts with α 4 β 1. Facilitation by JAM3. *J Biol Chem* 277: 27589–27592.
- Aurrand-Lions M, Duncan L, Ballestrem C, Imhof BA (2001) JAM-2, a novel immunoglobulin superfamily molecule, expressed by endothelial and lymphatic cells. *J Biol Chem* 276: 2733–2741.
- Bradfield PF, Scheiermann C, Nourshargh S, Ody C, Lusinskas FW, et al. (2007) JAM-C regulates unidirectional monocyte transendothelial migration in inflammation. *Blood* 110: 2545–2555.
- Woodfin A, Voisin MB, Beyrau M, Colom B, Caille D, et al. (2011) The junctional adhesion molecule JAM-C regulates polarized transendothelial migration of neutrophils in vivo. *Nat Immunol* 12: 761–769.
- Vestweber D (2012) Relevance of endothelial junctions in leukocyte extravasation and vascular permeability. *Ann N Y Acad Sci* 1257: 184–192.
- Charmoy M, Brunner-Agten S, Aebischer D, Auderset F, Launois P, et al. (2010) Neutrophil-derived CCL3 is essential for the rapid recruitment of dendritic cells to the site of *Leishmania major* inoculation in resistant mice. *PLoS Pathog* 6: e1000755.
- Ribeiro-Gomes FL, Peters NC, Debrabant A, Sacks DL (2012) Efficient capture of infected neutrophils by dendritic cells in the skin inhibits the early anti-leishmania response. *PLoS Pathog* 8: e1002536.
- Miles AA, Miles EM (1952) Vascular reactions to histamine, histamine-liberator and leukotaxine in the skin of guinea-pigs. *J Physiol* 118: 228–257.
- Robbani DF, Finch RA, Jager D, Muller WA, Sartorelli AG, et al. (2000) The Leukotriene C4 Transporter MRP1 Regulates CCL19 (MIP-3b, ELC)-Dependent Mobilization of Dendritic Cells to Lymph Nodes. *Cell* 103: 757–768.
- Aurrand-Lions M, Johnson-Leger C, Wong C, Du Pasquier L, Imhof B (2001) Heterogeneity of endothelial junctions is reflected by differential expression and specific subcellular localization of the three JAM family members. *Blood* 98: 3699–3707.

31. Lamagna C, HodiVala-Dilke KM, Imhof BA, Aurrand-Lions M (2005) Antibody against Junctional Adhesion Molecule-C Inhibits Angiogenesis and Tumor Growth. *Cancer Res* 65: 5703–5710.
32. Li X, Stankovic M, Lee BP, Aurrand-Lions M, Hahn CN, et al. (2009) JAM-C induces endothelial cell permeability through its association and regulation of β_3 integrins. *Arterioscler Thromb Vasc Biol* 29: 1200–1206.
33. Tenan M, Aurrand-Lions M, Widmer V, Alimenti A, Burkhardt K, et al. (2010) Cooperative expression of junctional adhesion molecule-C and -B supports growth and invasion of glioma. *Glia* 58: 524–537.
34. Orlova VV, Economopoulou M, Lupu F, Santos S, Chavakis T (2006) Junctional adhesion molecule-C regulates vascular endothelial permeability by modulating VE-cadherin-mediated cell-cell contacts. *J Exp Med* 203: 2703–2714.
35. Spindler V, Schlegel N, Waschke J (2010) Role of GTPases in control of microvascular permeability. *Cardiovasc Res* 87: 243–253.
36. Goddard LM, Iruela-Arispe ML (2013) Cellular and molecular regulation of vascular permeability. *Thromb Haemost* 109: 407–415.
37. Wessel F, Winderlich M, Holm M, Frye M, Rivera-Galdos R, et al. (2014) Leukocyte extravasation and vascular permeability are each controlled in vivo by different tyrosine residues of VE-cadherin. *Nat Immunol*.
38. Peters NC, Egen JG, Secundino N, Debrabant A, Kimblin N, et al. (2008) In Vivo Imaging Reveals an Essential Role for Neutrophils in Leishmaniasis Transmitted by Sand Flies. *Science* 321: 970–974.
39. Tacchini-Cottier F, Zweifel C, Belkaid Y, Mukankundiye C, Vasei M, et al. (2000) An Immunomodulatory Function for Neutrophils During the Induction of a CD4 + Th2 Response in BALB/c Mice Infected with *Leishmania major*. *J Immunol* 165: 2628–2636.
40. Lima GM, Vallochi AL, Silva UR, Bevilacqua EM, Kiffer MM, et al. (1998) The role of polymorphonuclear leukocytes in the resistance to cutaneous Leishmaniasis. *Immunol Lett* 64: 145–151.
41. Ribeiro-Gomes FL, Otero AC, Gomes NA, Moniz-de-Souza MCA, Finkelstein LC, et al. (2004) Macrophage Interactions with Neutrophils Regulate *Leishmania major* Infection. *J Immunol* 172: 4454–4462.
42. Chen L, Zhang ZH, Watanabe T, Yamashita T, Kobayakawa T, et al. (2005) The involvement of neutrophils in the resistance to *Leishmania major* infection in susceptible but not in resistant mice. *Parasitol Int* 54: 109–118.
43. Serbina NV, Pamer EG (2006) Monocyte emigration from bone marrow during bacterial infection requires signals mediated by chemokine receptor CCR2. *Nat Immunol* 7: 311–317.
44. Baluk P, Fuxe J, Hashizume H, Romano T, Lashnits E, et al. (2007) Functionally specialized junctions between endothelial cells of lymphatic vessels. *J Exp Med* 204: 2349–2362.
45. Pflücke H, Sixt M (2009) Preformed portals facilitate dendritic cell entry into afferent lymphatic vessels. *J Exp Med* 206: 2925–2935.
46. Zimmerli C, Lee BP, Palmer G, Gabay C, Adams RH, et al. (2009) Adaptive Immune Response in JAM-C-Deficient Mice: Normal Initiation but Reduced IgG Memory. *J Immunol* 182: 4728–4736.
47. Zaph C, Scott P (2003) Th1 Cell-Mediated Resistance to Cutaneous Infection with *Leishmania major* Is Independent of P- and E-Selectins. *The Journal of Immunology* 171: 4726–4732.
48. Kropf P, Kadolsky UD, Rogers M, Cloke TE, Müller I (2010) The *Leishmaniasis* Model. *Methods in Microbiology* 37: 307–328.

11. References

1. Akira S, Uematsu S, Takeuchi O (2006) Pathogen recognition and innate immunity. *Cell* 124: 783-801.
2. Hwa C, Aird WC (2007) The history of the capillary wall: doctors, discoveries, and debates. *Am J Physiol Heart Circ Physiol* 293: H2667-2679.
3. Waller A (1846) Microscopic examination of some of the principal tissues of the animal frame, as observed in the tongue of the living frog, toad, etc. London, Edinburgh and Dublin Philosophical Magazine: 271-287.
4. Butcher EC (1991) Leukocyte-endothelial cell recognition: three (or more) steps to specificity and diversity. *Cell* 67: 1033-1036.
5. Springer TA (1994) Traffic signals for lymphocyte recirculation and leukocyte emigration: the multistep paradigm. *Cell* 76: 301-314.
6. Ley K, Laudanna C, Cybulsky MI, Nourshargh S (2007) Getting to the site of inflammation: the leukocyte adhesion cascade updated. *Nat Rev Immunol* 7: 678-689.
7. Gallatin WM, Weisman IL, Butcher EC (1983) A cell-surface molecule involved in organ-specific homing of lymphocytes. *Nature* 304: 30-34.
8. Hsu-Lin S, Berman CL, Furie BC, August D, Furie B (1984) A Platelet Membrane Protein Expressed during Platelet Activation and Secretion. *J Biol Chem* 259: 9121-9126.
9. McEver RP, Martin MN (1984) A monoclonal antibody to a membrane glycoprotein binds only to activated platelets. *J Biol Chem* 259: 9799-9804.
10. Johnston GI, Cook RG, McEver RP (1989) Cloning of GMP-140, a granule membrane protein of platelets and endothelium: sequence similarity to proteins involved in cell adhesion and inflammation. *Cell* 56: 1033-1044.
11. McEver RP, Beckstead JH, Moore KL, Marshall-Carlson L, Bainton DF (1989) GMP-140, a platelet alpha-granule membrane protein, is also synthesized by vascular endothelial cells and is localized in Weibel-Palade bodies. *J Clin Invest* 84: 92-99.
12. Bevilacqua MP, Pober JS, Mendrick DL, Cotran RS, Gimbrone MAJ (1987) Identification of an inducible endothelial-leukocyte adhesion molecule. *PNAS* 84: 9238-9242.
13. Pober JS, Lapierre LA, Stolpen AH, Brock TA, Springer TA, et al. (1987) Activation of cultured human endothelial cells by recombinant lymphotoxin: comparison with tumor necrosis factor and interleukin 1 species. *J Immunol* 138: 3319-3324.
14. Bevilacqua MP, Stengelin S, Gimbrone MA, Jr., Seed B (1989) Endothelial leukocyte adhesion molecule 1: an inducible receptor for neutrophils

- related to complement regulatory proteins and lectins. *Science* 243: 1160-1165.
15. Dwir O, Kansas GS, Alon R (2001) Cytoplasmic anchorage of L-selectin controls leukocyte capture and rolling by increasing the mechanical stability of the selectin tether. *J Cell Biol* 155: 145-156.
 16. Ivetic A, Deka J, Ridley A, Ager A (2002) The cytoplasmic tail of L-selectin interacts with members of the Ezrin-Radixin-Moesin (ERM) family of proteins: cell activation-dependent binding of Moesin but not Ezrin. *J Biol Chem* 277: 2321-2329.
 17. Kansas GS, Ley K, Munro JM, Tedder TF (1993) Regulation of leukocyte rolling and adhesion to high endothelial venules through the cytoplasmic domain of L-selectin. *J Exp Med* 177: 833-838.
 18. Setiadi H, Sedgewick G, Erlandsen SL, McEver RP (1998) Interactions of the cytoplasmic domain of P-selectin with clathrin-coated pits enhance leukocyte adhesion under flow. *J Cell Biol* 142: 859-871.
 19. McEver RP, Cummings RD (1997) Perspectives series: cell adhesion in vascular biology. Role of PSGL-1 binding to selectins in leukocyte recruitment. *J Clin Invest* 100: 485-491.
 20. Crocker PR, Feizi T (1996) Carbohydrate recognition systems: functional triads in cell-cell interactions. *Curr Opin Struct Biol* 6: 679-691.
 21. Asa D, Raycroft L, Ma L, Aeed P, Kaytes P, et al. (1995) The P-selectin glycoprotein ligand functions as a common human leukocyte ligand for P- and E-selectins. *Journal of Biological Chemistry* 270: 11662-11670.
 22. Goetz DJ, Greif DM, Ding H, Camphausen RT, Howes S, et al. (1997) Isolated P-selectin Glycoprotein Ligand-1 Dynamic Adhesion to P- and E-selectin. *J Cell Biol* 137: 509-519.
 23. Moore KL, Patel KD, Bruehl RE, Fugang L, Johnson DA, et al. (1995) P-Selectin Glycoprotein Ligand-1 Mediates Rolling of Human Neutrophils on P-Selectin. *J Cell Biol* 4: 661-671.
 24. Vachino G, Chang XJ, Veldman GM, Kumar R, Sako D, et al. (1995) P-selectin Glycoprotein Ligand-1 Is the Major Counter-receptor for P-selectin on Stimulated T Cells and Is Widely Distributed in Non-functional Form on Many Lymphocytic Cells. *Journal of Biological Chemistry* 270: 21966-21974.
 25. Ramos CL, Smith MJ, Snapp KR, Kansas GS, Stickney GW, et al. (1998) Functional characterization of L-selectin ligands on human neutrophils and leukemia cell lines: evidence for mucinlike ligand activity distinct from P-selectin glycoprotein ligand-1. *Blood* 91: 1067-1075.
 26. Sako D, Chang XJ, Barone KM, Vachino G, White HM, et al. (1993) Expression cloning of a functional glycoprotein ligand for P-selectin. *Cell* 75: 1179-1186.

27. Rivera-Nieves J, Burcin TL, Olson TS, Morris MA, McDuffie M, et al. (2006) Critical role of endothelial P-selectin glycoprotein ligand 1 in chronic murine ileitis. *J Exp Med* 203: 907-917.
28. da Costa Martins P, Garcia-Vallejo JJ, van Thienen JV, Fernandez-Borja M, van Gils JM, et al. (2007) P-selectin glycoprotein ligand-1 is expressed on endothelial cells and mediates monocyte adhesion to activated endothelium. *Arterioscler Thromb Vasc Biol* 27: 1023-1029.
29. Eriksson EE, Xie X, Werr J, Thoren P, Lindborn L (2001) Importance of Primary Capture and L-Selectin-dependent Secondary Capture in Leukocyte Accumulation in Inflammation and Atherosclerosis In Vivo. *J Exp Med* 194: 205-217.
30. Sperandio M, Smith ML, Forlow SB, Olson TS, Xia L, et al. (2003) P-selectin glycoprotein ligand-1 mediates L-selectin-dependent leukocyte rolling in venules. *J Exp Med* 197: 1355-1363.
31. Lasky LA, Singer MS, Dowbenko D, Imai Y, Henzel WJ, et al. (1992) An endothelial ligand for L-selectin is a novel mucin-like molecule. *Cell* 69: 927-938.
32. Imai Y, Singer MS, Fennie C, Lasky LA, Rosen SD (1991) Identification of a carbohydrate-based endothelial ligand for a lymphocyte homing receptor. *J Cell Biol* 113: 1213-1221.
33. Baumhater S, Singer MS, Henzel W, Hemmerich S, Renz M, et al. (1993) Binding of L-selectin to the vascular sialomucin CD34. *Science* 262: 436-438.
34. Puri KD, Finger EB, Gaudernack G, Springer TA (1995) Sialomucin CD34 is the major L-selectin ligand in human tonsil high endothelial venules. *J Cell Biol* 131: 261-270.
35. Sasseti C, Tangemann K, Singer MS, Kershaw DB, Rosen SD (1998) Identification of podocalyxin-like protein as a high endothelial venule ligand for L-selectin: parallels to CD34. *J Exp Med* 187: 1965-1975.
36. Nakache M, Berg EL, Streeter PR, Butcher EC (1989) The mucosal vascular addressin is a tissue-specific endothelial cell adhesion molecule for circulating lymphocytes. *Nature* 337: 179-181.
37. Streeter PR, Berg EL, Rouse BT, Bargatze RF, Butcher EC (1988) A tissue-specific endothelial cell molecule involved in lymphocyte homing. *Nature* 331: 41-46.
38. Berg EL, McEvoy LM, Berlin C, Bargatze RF, Butcher EC (1993) L-selectin-mediated lymphocyte rolling on MAdCAM-1. *Nature* 366: 695-698.
39. Norman KE, Moore KL, McEver RP, Ley K (1995) Leukocyte rolling in vivo is mediated by P-selectin glycoprotein ligand- 1. *Blood* 85: 4417-4421.
40. Borges E, Eytner R, Moll T, Steegmaier M, Campbell MA, et al. (1997) The P-Selectin Glycoprotein Ligand-1 Is Important for Recruitment of Neutrophils Into Inflamed Mouse Peritoneum. *Blood* 90: 1934-1942.

41. Borges E, Tietz W, Steegmaier M, Moll T, Hamann A, et al. (1997) P-Selectin Glycoprotein Ligand-1 (PSGL-1) on T Helper 1 but Not on T Helper 2 Cells Binds to P-Selectin and Supports Migration into Inflamed Skin. *J Exp Med* 185: 573-578.
42. Vestweber D, Blanks JE (1999) Mechanisms that regulate the function of the selectins and their ligands. *Physiol rev* 79: 181-213.
43. Picker LJ, Warnock RA, Burns AR, Doerschuk CM, Berg EL, et al. (1991) The Neutrophil Selectin LECAM-1 Presents Carbohydrate Ligands to the Vascular Selectins ELAM-1 and GMP-140. *Cell* 66: 921-933.
44. Lawrence MB, Bainton DF, Springer TA (1994) Neutrophil Tethering to and Rolling on E-selectin Are Separable by Requirement for L-selectin. *Immunity* 1: 137-145.
45. Levinovitz A, Mühlhoff J, Isenmann S, Vestweber D (1993) Identification of a glycoprotein ligand for E-selectin on mouse myeloid cells. *J Biol Chem* 268: 449-459.
46. Steegmaier M, Levinovitz A, Isenmann S, Borges E, Lenter M, et al. (1995) The E-selectin-ligand ESL-1 is a variant of a receptor for fibroblast growth factor. *Nature* 373: 615-620.
47. Dimitroff CJ, Lee JY, Rafii S, Fuhlbrigge RC, Sackstein R (2001) CD44 Is a Major E-Selectin Ligand on Human Hematopoietic Progenitor Cells. *J Cell Biol* 153: 1277-1286.
48. Katayama Y, Hidalgo A, Chang J, Peired A, Frenette PS (2005) CD44 is a physiological E-selectin ligand on neutrophils. *J Exp Med* 201: 1183-1189.
49. Hidalgo A, Peired AJ, Wild MK, Vestweber D, Frenette PS (2007) Complete identification of E-selectin ligands on neutrophils reveals distinct functions of PSGL-1, ESL-1, and CD44. *Immunity* 26: 477-489.
50. Erlandsen SL, Hasslen SR, Nelson RD (1993) Detection and spatial distribution of the beta 2 integrin (Mac-1) and L-selectin (LECAM-1) adherence receptors on human neutrophils by high-resolution field emission SEM. *Journal of Histochemistry & Cytochemistry* 41: 327-333.
51. Hasslen SR, von Andrian UH, Butcher EC, Nelson RD, Erlandsen SL (1995) Spatial distribution of L-selectin (CD62L) on human lymphocytes and transfected murine L1-2 cells. *Histochem J* 27: 547-554.
52. Geng JG, Bevilacqua MP, Moore KL, McIntyre TM, Prescott SM, et al. (1990) Rapid neutrophil adhesion to activated endothelium mediated by GMP-140. *Nature* 343: 757-760.
53. Yao L, Setiadi H, Xia L, Laszik Z, Taylor FB, et al. (1999) Divergent inducible expression of P-selectin and E-selectin in mice and primates. *Blood* 94: 3820-3828.

54. Alon R, Hammer DA, Springer TA (1995) Lifetime of the P-selectin-carbohydrate bond and its response to tensile force in hydrodynamic flow. *Nature* 374: 539-542.
55. Marshall BT, Long M, Piper JW, Yago T, McEver RP, et al. (2003) Direct observation of catch bonds involving cell-adhesion molecules. *Nature* 423: 190-193.
56. Bullard DC, Kunkel EJ, Kubo H, Hicks MJ, Lorenzo I, et al. (1996) Infectious Susceptibility and Severe Deficiency of Leukocyte Rolling and Recruitment in E-Selectin and P-Selectin Double Mutant Mice. *J Exp Med* 183: 2329-2336.
57. Frenette PS, Mayadas TN, Rayburn H, Hynes RO, Wagner DD (1996) Susceptibility to Infection and Altered Hematopoiesis in Mice Deficient in Both P- and E-Selectins. *Cell* 84: 563-574.
58. Kanwar S, Bullard DC, Hickey MJ, Smith CW, Beaudet AL, et al. (1997) The Association between alpha4-Integrin, P-Selectin, and E-Selectin in an Allergic Model of Inflammation. *J Exp Med* 186: 1077-1087.
59. Wang HB, Wang JT, Zhang L, Geng ZH, Xu WL, et al. (2007) P-selectin primes leukocyte integrin activation during inflammation. *Nat Immunol* 8: 882-892.
60. Ma YQ, Plow EF, Geng JG (2004) P-selectin binding to P-selectin glycoprotein ligand-1 induces an intermediate state of alphaMbeta2 activation and acts cooperatively with extracellular stimuli to support maximal adhesion of human neutrophils. *Blood* 104: 2549-2556.
61. Blanks JE, Moll T, Eytner R, Vestweber D (1998) Stimulation of P-selectin glycoprotein ligand-1 on mouse neutrophils activates beta 2-integrin mediated cell attachment to ICAM-1. *Eur J Immunol* 28: 433-443.
62. Atarashi K, Hirata T, Matsumoto M, Kanemitsu N, Miyasaka M (2005) Rolling of Th1 cells via P-selectin glycoprotein ligand-1 stimulates LFA-1-mediated cell binding to ICAM-1. *J Immunol* 174: 1424-1432.
63. Simon SI, Hu Y, Vestweber D, Smith CW (2000) Neutrophil tethering on E-selectin activates beta 2 integrin binding to ICAM-1 through a mitogen-activated protein kinase signal transduction pathway. *J Immunol* 164: 4348-4358.
64. Lo SK, Lee S, Ramos RA, Lobb R, Rosa M, et al. (1991) Endothelial-leukocyte adhesion molecule 1 stimulates the adhesive activity of leukocyte integrin CR3 (CD11b/CD18, Mac-1, alpha m beta 2) on human neutrophils. *J Exp Med* 173: 1493-1500.
65. Chesnutt BC, Smith DF, Raffler NA, Smith ML, White EJ, et al. (2006) Induction of LFA-1-dependent neutrophil rolling on ICAM-1 by engagement of E-selectin. *Microcirculation* 13: 99-109.

66. Berlin C, Bargatze RF, Campbell JJ, von Andrian UH, Szabo MC, et al. (1995) alpha 4 integrins mediate lymphocyte attachment and rolling under physiologic flow. *Cell* 80: 413-422.
67. Grabovsky V, Feigelson S, Chen C, Bleijs DA, Peled A, et al. (2000) Subsecond induction of alpha4 integrin clustering by immobilized chemokines stimulates leukocyte tethering and rolling on endothelial vascular cell adhesion molecule 1 under flow conditions. *J Exp Med* 192: 495-506.
68. Alon R, Kassner PD, Carr MW, Finger EB, Hemler ME, et al. (1995) The integrin VLA-4 supports tethering and rolling in flow on VCAM-1. *J Cell Biol* 128: 1243-1253.
69. Singbartl K, Thatte J, Smith ML, Wethmar K, Day K, et al. (2001) A CD2-green fluorescence protein-transgenic mouse reveals very late antigen-4-dependent CD8+ lymphocyte rolling in inflamed venules. *J Immunol* 166: 7520-7526.
70. Salas A, Shimaoka M, Kogan AN, Harwood C, von Andrian UH, et al. (2004) Rolling adhesion through an extended conformation of integrin alphaLbeta2 and relation to alpha I and beta I-like domain interaction. *Immunity* 20: 393-406.
71. Sigal A, Bleijs DA, Grabovsky V, van Vliet SJ, Dwir O, et al. (2000) The LFA-1 integrin supports rolling adhesions on ICAM-1 under physiological shear flow in a permissive cellular environment. *J Immunol* 165: 442-452.
72. Astrof NS, Salas A, Shimaoka M, Chen J, Springer TA (2006) Importance of force linkage in mechanochemistry of adhesion receptors. *Biochemistry* 45: 15020-15028.
73. Dunne JL, Ballantyne CM, Beaudet AL, Ley K (2002) Control of leukocyte rolling velocity in TNF-alpha-induced inflammation by LFA-1 and Mac-1. *Blood* 99: 336-341.
74. Kinashi T (2005) Intracellular signalling controlling integrin activation in lymphocytes. *Nat Rev Immunol* 5: 546-559.
75. Luo BH, Carman CV, Springer TA (2007) Structural basis of integrin regulation and signaling. *Annu Rev Immunol* 25: 619-647.
76. Harris ES, McIntyre TM, Prescott SM, Zimmerman GA (2000) The leukocyte integrins. *J Biol Chem* 275: 23409-23412.
77. Carman CV, Springer TA (2003) Integrin avidity regulation: are changes in affinity and conformation underemphasized? *Curr Opin Cell Biol* 15: 547-556.
78. Takagi J, Petre BM, Walz T, Springer TA (2002) Global conformational rearrangements in integrin extracellular domains in outside-in and inside-out signaling. *Cell* 110: 599-511.

79. Nishida N, Xie C, Shimaoka M, Cheng Y, Walz T, et al. (2006) Activation of leukocyte beta2 integrins by conversion from bent to extended conformations. *Immunity* 25: 583-594.
80. Bazzoni G, Hemler ME (1998) Are changes in integrin affinity and conformation overemphasized? *Trends Biochem Sci* 23: 30-34.
81. Stewart MP, McDowall A, Hogg N (1998) LFA-1-mediated adhesion is regulated by cytoskeletal restraint and by a Ca²⁺-dependent protease, calpain. *J Cell Biol* 140: 699-707.
82. Hogg N, Leitinger B (2001) Shape and shift changes related to the function of leukocyte integrins LFA-1 and Mac-1. *J Leukoc Biol* 69: 893-898.
83. Laudanna C, Kim JY, Constantin G, Butcher E (2002) Rapid leukocyte integrin activation by chemokines. *Immunol Rev* 186: 37-46.
84. Constantin G, Majeed M, Giagulli C, Piccio L, Kim JY, et al. (2000) Chemokines trigger immediate beta2 integrin affinity and mobility changes: differential regulation and roles in lymphocyte arrest under flow. *Immunity* 13: 759-769.
85. Middleton J, Neil S, Wintle J, Clark-Lewis I, Moore H, et al. (1997) Transcytosis and surface presentation of IL-8 by venular endothelial cells. *Cell* 91: 385-395.
86. Wolff B, Burns AR, Middleton J, Rot A (1998) Endothelial Cell "Memory" of Inflammatory Stimulation: Human Venular Endothelial Cells Store Interleukin 8 in Weibel-Palade Bodies. *J Exp Med* 188.
87. Colletti LM, Kunkel SL, Walz A, Burdick MD, Kunkel RG, et al. (1995) Chemokine expression during hepatic ischemia/reperfusion-induced lung injury in the rat. The role of epithelial neutrophil activating protein. *J Clin Invest* 95: 134-141.
88. Liu Y, Mei J, Gonzales L, Yang G, Dai N, et al. (2011) IL-17A and TNF- α exert synergistic effects on expression of CXCL5 by alveolar type II cells in vivo and in vitro. *J Immunol* 186: 3197-3205.
89. Huo Y, Schober A, Forlow SB, Smith DF, Hyman MC, et al. (2003) Circulating activated platelets exacerbate atherosclerosis in mice deficient in apolipoprotein E. *Nat Med* 9: 61-67.
90. von Hundelshausen P, Weber KS, Huo Y, Proudfoot AE, Nelson PJ, et al. (2001) RANTES deposition by platelets triggers monocyte arrest on inflamed and atherosclerotic endothelium. *Circulation* 103: 1772-1777.
91. Charmoy M, Brunner-Agten S, Aebischer D, Auderset F, Launois P, et al. (2010) Neutrophil-derived CCL3 is essential for the rapid recruitment of dendritic cells to the site of *Leishmania major* inoculation in resistant mice. *PLoS Pathog* 6: e1000755.

92. Tanaka Y, Adams DH, Hubscher S, Hirano H, Siebenlist U, et al. (1993) T-cell adhesion induced by proteoglycan-immobilized cytokine MIP-1 beta. *Nature* 361: 79-82.
93. Hoogewerf AJ, Kuschert GS, Proudfoot AE, Borlat F, Clark-Lewis I, et al. (1997) Glycosaminoglycans mediate cell surface oligomerization of chemokines. *Biochemistry* 36: 13570-13578.
94. Proudfoot AE, Handel TM, Johnson Z, Lau EK, LiWang P, et al. (2003) Glycosaminoglycan binding and oligomerization are essential for the in vivo activity of certain chemokines. *Proc Natl Acad Sci U S A* 100: 1885-1890.
95. Roscic-Mrkic B, Fischer M, Leemann C, Manrique A, Gordon CJ, et al. (2003) RANTES (CCL5) uses the proteoglycan CD44 as an auxiliary receptor to mediate cellular activation signals and HIV-1 enhancement. *Blood* 102: 1169-1177.
96. Halden Y, Rek A, Atzenhofer W, Szilak L, Wabnig A, et al. (2004) Interleukin-8 binds to syndecan-2 on human endothelial cells. *Biochem J* 377: 533-538.
97. Johnson Z, Proudfoot AE, Handel TM (2005) Interaction of chemokines and glycosaminoglycans: a new twist in the regulation of chemokine function with opportunities for therapeutic intervention. *Cytokine Growth Factor Rev* 16: 625-636.
98. Chan JR, Hyduk SJ, Cybulsky MI (2001) Chemoattractants induce a rapid and transient upregulation of monocyte alpha4 integrin affinity for vascular cell adhesion molecule 1 which mediates arrest: an early step in the process of emigration. *J Exp Med* 193: 1149-1158.
99. Shamri R, Grabovsky V, Gauguet JM, Feigelson S, Manevich E, et al. (2005) Lymphocyte arrest requires instantaneous induction of an extended LFA-1 conformation mediated by endothelium-bound chemokines. *Nat Immunol* 6: 497-506.
100. Crittenden JR, Bergmeier W, Zhang Y, Piffath CL, Liang Y, et al. (2004) CalDAG-GEFI integrates signaling for platelet aggregation and thrombus formation. *Nat Med* 10: 982-986.
101. Lim J, Dupuy AG, Critchley DR, Caron E (2010) Rap1 controls activation of the alpha(M)beta(2) integrin in a talin-dependent manner. *J Cell Biochem* 111: 999-1009.
102. Kim M, Carman CV, Springer TA (2003) Bidirectional transmembrane signaling by cytoplasmic domain separation in integrins. *Science* 301: 1720-1725.
103. Wegener KL, Partridge AW, Han J, Pickford AR, Liddington RC, et al. (2007) Structural basis of integrin activation by talin. *Cell* 128: 171-182.

104. Tadokoro S, Shattil SJ, Eto K, Tai V, Liddington RC, et al. (2003) Talin binding to integrin beta tails: a final common step in integrin activation. *Science* 302: 103-106.
105. Shattil SJ, Kim C, Ginsberg MH (2010) The final steps of integrin activation: the end game. *Nat Rev Mol Cell Biol* 11: 288-300.
106. Moser M, Legate KR, Zent R, Fassler R (2009) The tail of integrins, talin, and kindlins. *Science* 324: 895-899.
107. Abram CL, Lowell CA (2009) The ins and outs of leukocyte integrin signaling. *Annu Rev Immunol* 27: 339-362.
108. Kim M, Carman CV, Yang W, Salas A, Springer TA (2004) The primacy of affinity over clustering in regulation of adhesiveness of the integrin alpha L beta 2. *J Cell Biol* 167: 1241-1253.
109. Buensuceso C, de Virgilio M, Shattil SJ (2003) Detection of integrin alpha IIb beta 3 clustering in living cells. *J Biol Chem* 278: 15217-15224.
110. Hato T, Pampori N, Shattil SJ (1998) Complementary roles for receptor clustering and conformational change in the adhesive and signaling functions of integrin alpha IIb beta 3. *J Cell Biol* 141: 1685-1695.
111. Zhu J, Carman CV, Kim M, Shimaoka M, Springer TA, et al. (2007) Requirement of alpha and beta subunit transmembrane helix separation for integrin outside-in signaling. *Blood* 110: 2475-2483.
112. Giagulli C, Ottoboni L, Cavegion E, Rossi B, Lowell C, et al. (2006) The Src family kinases Hck and Fgr are dispensable for inside-out, chemoattractant-induced signaling regulating beta 2 integrin affinity and valency in neutrophils, but are required for beta 2 integrin-mediated outside-in signaling involved in sustained adhesion. *J Immunol* 177: 604-611.
113. Abram CL, Lowell CA (2007) The expanding role for ITAM-based signaling pathways in immune cells. *Sci STKE* 2007: re2.
114. Abram CL, Lowell CA (2007) Convergence of immunoreceptor and integrin signaling. *Immunol Rev* 218: 29-44.
115. Gakidis MA, Cullere X, Olson T, Wilsbacher JL, Zhang B, et al. (2004) Vav GEFs are required for beta2 integrin-dependent functions of neutrophils. *J Cell Biol* 166: 273-282.
116. Bargatze RF, Jutila MA, Butcher EC (1995) Distinct roles of L-selectin and integrins alpha 4 beta 7 and LFA-1 in lymphocyte homing to Peyer's patch-HEV in situ: the multistep model confirmed and refined. *Immunity* 3: 99-108.
117. Chuluyan HE, Issekutz AC (1993) VLA-4 integrin can mediate CD11/CD18-independent transendothelial migration of human monocytes. *J Clin Invest* 92: 2768-2777.

118. Luscinikas FW, Kansas GS, Ding H, Pizcueta P, Schleiffenbaum BE, et al. (1994) Monocyte rolling, arrest and spreading on IL-4-activated vascular endothelium under flow is mediated via sequential action of L-selectin, beta 1-integrins, and beta 2-integrins. *J Cell Biol* 125: 1417-1427.
119. Meerschaert J, Furie MB (1994) Monocytes use either CD11/CD18 or VLA-4 to migrate across human endothelium in vitro. *J Immunol* 152: 1915-1926.
120. Meerschaert J, Furie MB (1995) The adhesion molecules used by monocytes for migration across endothelium include CD11a/CD18, CD11b/CD18, and VLA-4 on monocytes and ICAM-1, VCAM-1, and other ligands on endothelium. *J Immunol* 154: 4099-4112.
121. Scharffetter-Kochanek K, Lu H, Norman K, van Nood N, Munoz F, et al. (1998) Spontaneous skin ulceration and defective T cell function in CD18 null mice. *J Exp Med* 188: 119-131.
122. Mizgerd JP, Kubo H, Kutkoski GJ, Bhagwan SD, Scharffetter-Kochanek K, et al. (1997) Neutrophil emigration in the skin, lungs, and peritoneum: different requirements for CD11/CD18 revealed by CD18-deficient mice. *J Exp Med* 186: 1357-1364.
123. Ding ZM, Babensee JE, Simon SI, Lu H, Perrard JL, et al. (1999) Relative contribution of LFA-1 and Mac-1 to neutrophil adhesion and migration. *J Immunol* 163: 5029-5038.
124. Schneeberger EE, Vu Q, LeBlanc BW, Doerschuk CM (2000) The accumulation of dendritic cells in the lung is impaired in CD18^{-/-} but not in ICAM-1^{-/-} mutant mice. *J Immunol* 164: 2472-2478.
125. Rose DM, Alon R, Ginsberg MH (2007) Integrin modulation and signaling in leukocyte adhesion and migration. *Immunol Rev* 218: 126-134.
126. Stossel TP (1994) The E. Donnall Thomas Lecture, 1993. The machinery of blood cell movements. *Blood* 84: 367-379.
127. Herter J, Zarbock A (2013) Integrin Regulation during Leukocyte Recruitment. *J Immunol* 190: 4451-4457.
128. Schenkel AR, Mamdouh Z, Muller WA (2004) Locomotion of monocytes on endothelium is a critical step during extravasation. *Nat Immunol* 5: 393-400.
129. Auffray C, Fogg D, Garfa M, Elain G, Join-Lambert O, et al. (2007) Monitoring of blood vessels and tissues by a population of monocytes with patrolling behavior. *Science* 317: 666-670.
130. Phillipson M, Heit B, Colarusso P, Liu L, Ballantyne CM, et al. (2006) Intraluminal crawling of neutrophils to emigration sites: a molecularly distinct process from adhesion in the recruitment cascade. *J Exp Med* 203: 2569-2575.

131. Sanchez-Martin L, Sanchez-Sanchez N, Gutierrez-Lopez MD, Rojo AI, Vicente-Manzanares M, et al. (2004) Signaling through the leukocyte integrin LFA-1 in T cells induces a transient activation of Rac-1 that is regulated by Vav and PI3K/Akt-1. *J Biol Chem* 279: 16194-16205.
132. Green CE, Schaff UY, Sarantos MR, Lum AF, Staunton DE, et al. (2006) Dynamic shifts in LFA-1 affinity regulate neutrophil rolling, arrest, and transmigration on inflamed endothelium. *Blood* 107: 2101-2111.
133. Phillipson M, Heit B, Parsons SA, Petri B, Mullaly SC, et al. (2009) Vav1 is essential for mechanotactic crawling and migration of neutrophils out of the inflamed microvasculature. *J Immunol* 182: 6870-6878.
134. Shulman Z, Shinder V, Klein E, Grabovsky V, Yeger O, et al. (2009) Lymphocyte crawling and transendothelial migration require chemokine triggering of high-affinity LFA-1 integrin. *Immunity* 30: 384-396.
135. Burns AR, Walker DC, Brown ES, Thurmon LT, Bowden RA, et al. (1997) Neutrophil transendothelial migration is independent of tight junctions and occurs preferentially at tricellular corners. *J Immunol* 159: 2893-2903.
136. Vestweber D (2007) Adhesion and signaling molecules controlling the transmigration of leukocytes through endothelium. *Immunol Rev* 218: 178-196.
137. Woodfin A, Voisin MB, Beyrau M, Colom B, Caille D, et al. (2011) The junctional adhesion molecule JAM-C regulates polarized transendothelial migration of neutrophils in vivo. *Nat Immunol* 12: 761-769.
138. Millan J, Ridley AJ (2005) Rho GTPases and leucocyte-induced endothelial remodelling. *Biochem J* 385: 329-337.
139. Greenwood J, Amos CL, Walters CE, Couraud PO, Lyck R, et al. (2003) Intracellular domain of brain endothelial intercellular adhesion molecule-1 is essential for T lymphocyte-mediated signaling and migration. *J Immunol* 171: 2099-2108.
140. Muller WA (2003) Leukocyte-endothelial-cell interactions in leukocyte transmigration and the inflammatory response. *Trends in Immunology* 24: 326-333.
141. Barreiro O, Yanez-Mo M, Serrador JM, Montoya MC, Vicente-Manzanares M, et al. (2002) Dynamic interaction of VCAM-1 and ICAM-1 with moesin and ezrin in a novel endothelial docking structure for adherent leukocytes. *J Cell Biol* 157: 1233-1245.
142. Carman CV, Springer TA (2004) A transmigratory cup in leukocyte diapedesis both through individual vascular endothelial cells and between them. *J Cell Biol* 167: 377-388.

143. Phillipson M, Kaur J, Colarusso P, Ballantyne CM, Kubes P (2008) Endothelial domes encapsulate adherent neutrophils and minimize increases in vascular permeability in paracellular and transcellular emigration. *PLoS One* 3: e1649.
144. Dejana E (2004) Endothelial cell-cell junctions: happy together. *Nat Rev Mol Cell Biol* 5: 261-270.
145. Muller WA, Ratti CM, McDonnell SL, Cohn ZA (1989) A human endothelial cell-restricted, externally disposed plasmalemmal protein enriched in intercellular junctions. *J Exp Med* 170: 399-414.
146. Newman PJ, Berndt MC, Gorski J, White GC, 2nd, Lyman S, et al. (1990) PECAM-1 (CD31) cloning and relation to adhesion molecules of the immunoglobulin gene superfamily. *Science* 247: 1219-1222.
147. Buckley CD, Doyonnas R, Newton JP, Blystone SD, Brown EJ, et al. (1996) Identification of alpha v beta 3 as a heterotypic ligand for CD31/PECAM-1. *J Cell Sci* 109 (Pt 2): 437-445.
148. Newman PJ (1997) The biology of PECAM-1. *J Clin Invest* 100: S25-29.
149. Ilan N, Madri JA (2003) PECAM-1: old friend, new partners. *Curr Opin Cell Biol* 15: 515-524.
150. Newman PJ, Newman DK (2003) Signal transduction pathways mediated by PECAM-1: new roles for an old molecule in platelet and vascular cell biology. *Arterioscler Thromb Vasc Biol* 23: 953-964.
151. Woodfin A, Voisin MB, Nourshargh S (2007) PECAM-1: a multi-functional molecule in inflammation and vascular biology. *Arterioscler Thromb Vasc Biol* 27: 2514-2523.
152. Privratsky JR, Newman PJ (2014) PECAM-1: regulator of endothelial junctional integrity. *Cell Tissue Res* 355: 607-619.
153. Muller WA, Weigl SA, Deng X, Phillips DM (1993) PECAM-1 is required for transendothelial migration of leukocytes. *J Exp Med* 178: 449-460.
154. Liao F, Huynh HK, Eiroa A, Greene T, Polizzi E, et al. (1995) Migration of monocytes across endothelium and passage through extracellular matrix involve separate molecular domains of PECAM-1. *J Exp Med* 182: 1337-1343.
155. Bogen S, Pak J, Garifallou M, Deng X, Muller WA (1994) Monoclonal antibody to murine PECAM-1 (CD31) blocks acute inflammation in vivo. *J Exp Med* 179: 1059-1064.
156. Liao F, Ali J, Greene T, Muller WA (1997) Soluble domain 1 of platelet-endothelial cell adhesion molecule (PECAM) is sufficient to block transendothelial migration in vitro and in vivo. *J Exp Med* 185: 1349-1357.
157. Vaporciyan AA, DeLisser HM, Yan HC, Mendiguren, II, Thom SR, et al. (1993) Involvement of platelet-endothelial cell adhesion molecule-1 in neutrophil recruitment in vivo. *Science* 262: 1580-1582.

158. Schenkel AR, Mamdouh Z, Chen X, Liebman RM, Muller WA (2002) CD99 plays a major role in the migration of monocytes through endothelial junctions. *Nat Immunol* 3: 143-150.
159. Dangerfield J, Larbi KY, Huang MT, Dewar A, Nourshargh S (2002) PECAM-1 (CD31) homophilic interaction up-regulates alpha6beta1 on transmigrated neutrophils in vivo and plays a functional role in the ability of alpha6 integrins to mediate leukocyte migration through the perivascular basement membrane. *J Exp Med* 196: 1201-1211.
160. Duncan GS, Andrew DP, Takimoto H, Kaufman SA, Yoshida H, et al. (1999) Genetic evidence for functional redundancy of Platelet/Endothelial cell adhesion molecule-1 (PECAM-1): CD31-deficient mice reveal PECAM-1-dependent and PECAM-1-independent functions. *J Immunol* 162: 3022-3030.
161. Thompson RD, Noble KE, Larbi KY, Dewar A, Duncan GS, et al. (2001) Platelet-endothelial cell adhesion molecule-1 (PECAM-1)-deficient mice demonstrate a transient and cytokine-specific role for PECAM-1 in leukocyte migration through the perivascular basement membrane. *Blood* 97: 1854-1860.
162. Gelin C, Aubrit F, Phalipon A, Raynal B, Cole S, et al. (1989) The E2 antigen, a 32 kd glycoprotein involved in T-cell adhesion processes, is the MIC2 gene product. *EMBO J* 8: 3253-3259.
163. Bixel G, Kloep S, Butz S, Petri B, Engelhardt B, et al. (2004) Mouse CD99 participates in T-cell recruitment into inflamed skin. *Blood* 104: 3205-3213.
164. Lou O, Alcaide P, Luscinskas FW, Muller WA (2007) CD99 is a key mediator of the transendothelial migration of neutrophils. *J Immunol* 178: 1136-1143.
165. Suh YH, Shin YK, Kook MC, Oh KI, Park WS, et al. (2003) Cloning, genomic organization, alternative transcripts and expression analysis of CD99L2, a novel paralog of human CD99, and identification of evolutionary conserved motifs. *Gene* 307: 63-76.
166. Bixel MG, Petri B, Khandoga AG, Khandoga A, Wolburg-Buchholz K, et al. (2007) A CD99-related antigen on endothelial cells mediates neutrophil but not lymphocyte extravasation in vivo. *Blood* 109: 5327-5336.
167. Bixel MG, Li H, Petri B, Khandoga AG, Khandoga A, et al. (2010) CD99 and CD99L2 act at the same site as, but independently of, PECAM-1 during leukocyte diapedesis. *Blood* 116: 1172-1184.
168. Seelige R, Natsch C, Marz S, Jing D, Frye M, et al. (2013) Cutting edge: Endothelial-specific gene ablation of CD99L2 impairs leukocyte extravasation in vivo. *J Immunol* 190: 892-896.

169. Mehta D, Malik AB (2006) Signaling mechanisms regulating endothelial permeability. *Physiol Rev* 86: 279-367.
170. Lampugnani MG, Resnati M, Raiteri M, Pigott R, Pisacane A, et al. (1992) A novel endothelial-specific membrane protein is a marker of cell-cell contacts. *J Cell Biol* 118: 1511-1522.
171. Shaw SK, Bamba PS, Perkins BN, Luscinskas FW (2001) Real-time imaging of vascular endothelial-cadherin during leukocyte transmigration across endothelium. *J Immunol* 167: 2323-2330.
172. Allport JR, Muller WA, Luscinskas FW (2000) Monocytes induce reversible focal changes in vascular endothelial cadherin complex during transendothelial migration under flow. *J Cell Biol* 148: 203-216.
173. Corada M, Mariotti M, Thurston G, Smith K, Kunkel R, et al. (1999) Vascular endothelial-cadherin is an important determinant of microvascular integrity in vivo. *Proc Natl Acad Sci U S A* 96: 9815-9820.
174. Gotsch U, Borges E, Bosse R, Boggemeyer E, Simon M, et al. (1997) VE-cadherin antibody accelerates neutrophil recruitment in vivo. *J Cell Sci* 110 (Pt 5): 583-588.
175. Broermann A, Winderlich M, Block H, Frye M, Rossaint J, et al. (2011) Dissociation of VE-PTP from VE-cadherin is required for leukocyte extravasation and for VEGF-induced vascular permeability in vivo. *J Exp Med* 208: 2393-2401.
176. Schulte D, Kuppers V, Dartsch N, Broermann A, Li H, et al. (2011) Stabilizing the VE-cadherin-catenin complex blocks leukocyte extravasation and vascular permeability. *EMBO J* 30: 4157-4170.
177. Staunton DE, Dustin ML, Springer TA (1989) Functional cloning of ICAM-2, a cell adhesion ligand for LFA-1 homologous to ICAM-1. *Nature* 339: 61-64.
178. Rothlein R, Dustin ML, Marlin SD, Springer TA (1986) A human intercellular adhesion molecule (ICAM-1) distinct from LFA-1. *J Immunol* 137: 1270-1274.
179. Reiss Y, Hoch G, Deutsch U, Engelhardt B (1998) T cell interaction with ICAM-1-deficient endothelium in vitro: essential role for ICAM-1 and ICAM-2 in transendothelial migration of T cells. *Eur J Immunol* 28: 3086-3099.
180. Issekutz AC, Rowter D, Springer TA (1999) Role of ICAM-1 and ICAM-2 and alternate CD11/CD18 ligands in neutrophil transendothelial migration. *J Leukoc Biol* 65: 117-126.
181. Lehmann JC, Jablonski-Westrich D, Haubold U, Gutierrez-Ramos JC, Springer T, et al. (2003) Overlapping and selective roles of endothelial intercellular adhesion molecule-1 (ICAM-1) and ICAM-2 in lymphocyte trafficking. *J Immunol* 171: 2588-2593.

182. Springer TA (1990) Adhesion receptors of the immune system. *Nature* 346: 425-434.
183. Sumagin R, Sarelius IH (2006) TNF-alpha activation of arterioles and venules alters distribution and levels of ICAM-1 and affects leukocyte-endothelial cell interactions. *Am J Physiol Heart Circ Physiol* 291: H2116-2125.
184. Huang MT, Larbi KY, Scheiermann C, Woodfin A, Gerwin N, et al. (2006) ICAM-2 mediates neutrophil transmigration in vivo: evidence for stimulus specificity and a role in PECAM-1-independent transmigration. *Blood* 107: 4721-4727.
185. Gorina R, Lyck R, Vestweber D, Engelhardt B (2014) beta2 integrin-mediated crawling on endothelial ICAM-1 and ICAM-2 is a prerequisite for transcellular neutrophil diapedesis across the inflamed blood-brain barrier. *J Immunol* 192: 324-337.
186. Halai K, Whiteford J, Ma B, Nourshargh S, Woodfin A (2014) ICAM-2 facilitates luminal interactions between neutrophils and endothelial cells in vivo. *J Cell Sci* 127: 620-629.
187. Reymond N, Imbert AM, Devilard E, Fabre S, Chabannon C, et al. (2004) DNAM-1 and PVR regulate monocyte migration through endothelial junctions. *J Exp Med* 199: 1331-1341.
188. Liu L, Cara DC, Kaur J, Raharjo E, Mullaly SC, et al. (2005) LSP1 is an endothelial gatekeeper of leukocyte transendothelial migration. *J Exp Med* 201: 409-418.
189. Petri B, Kaur J, Long EM, Li H, Parsons SA, et al. (2011) Endothelial LSP1 is involved in endothelial dome formation, minimizing vascular permeability changes during neutrophil transmigration in vivo. *Blood* 117: 942-952.
190. Azcutia V, Routledge M, Williams MR, Newton G, Frazier WA, et al. (2013) CD47 plays a critical role in T-cell recruitment by regulation of LFA-1 and VLA-4 integrin adhesive functions. *Mol Biol Cell* 24: 3358-3368.
191. Azcutia V, Stefanidakis M, Tsuboi N, Mayadas T, Croce KJ, et al. (2012) Endothelial CD47 promotes vascular endothelial-cadherin tyrosine phosphorylation and participates in T cell recruitment at sites of inflammation in vivo. *J Immunol* 189: 2553-2562.
192. Feng D, Nagy JA, Pyne K, Dvorak HF, Dvorak AM (1998) Neutrophils emigrate from venules by a transendothelial cell pathway in response to FMLP. *J Exp Med* 187: 903-915.
193. Muller WA (2011) Mechanisms of leukocyte transendothelial migration. *Annu Rev Pathol* 6: 323-344.

194. Carman CV, Sage PT, Sciuto TE, de la Fuente MA, Geha RS, et al. (2007) Transcellular diapedesis is initiated by invasive podosomes. *Immunity* 26: 784-797.
195. Millan J, Hewlett L, Glyn M, Toomre D, Clark P, et al. (2006) Lymphocyte transcellular migration occurs through recruitment of endothelial ICAM-1 to caveola- and F-actin-rich domains. *Nat Cell Biol* 8: 113-123.
196. Mamdouh Z, Mikhailov A, Muller WA (2009) Transcellular migration of leukocytes is mediated by the endothelial lateral border recycling compartment. *J Exp Med* 206: 2795-2808.
197. Mamdouh Z, Chen X, Pierini LM, Maxfield FR, Muller WA (2003) Targeted recycling of PECAM from endothelial surface-connected compartments during diapedesis. *Nature* 421: 748-753.
198. Mamdouh Z, Kreitzer GE, Muller WA (2008) Leukocyte transmigration requires kinesin-mediated microtubule-dependent membrane trafficking from the lateral border recycling compartment. *J Exp Med* 205: 951-966.
199. Hallmann R, Horn N, Selg M, Wendler O, Pausch F, et al. (2005) Expression and function of laminins in the embryonic and mature vasculature. *Physiol Rev* 85: 979-1000.
200. Nourshargh S, Hordijk PL, Sixt M (2010) Breaching multiple barriers: leukocyte motility through venular walls and the interstitium. *Nat Rev Mol Cell Biol* 11: 366-378.
201. Wang S, Dangerfield JP, Young RE, Nourshargh S (2005) PECAM-1, alpha6 integrins and neutrophil elastase cooperate in mediating neutrophil transmigration. *J Cell Sci* 118: 2067-2076.
202. Werr J, Eriksson EE, Hedqvist P, Lindbom L (2000) Engagement of beta2 integrins induces surface expression of beta1 integrin receptors in human neutrophils. *J Leukoc Biol* 68: 553-560.
203. Wang S, Voisin MB, Larbi KY, Dangerfield J, Scheiermann C, et al. (2006) Venular basement membranes contain specific matrix protein low expression regions that act as exit points for emigrating neutrophils. *J Exp Med* 203: 1519-1532.
204. Voisin MB, Probstl D, Nourshargh S (2010) Venular basement membranes ubiquitously express matrix protein low-expression regions: characterization in multiple tissues and remodeling during inflammation. *Am J Pathol* 176: 482-495.
205. Stratman AN, Malotte KM, Mahan RD, Davis MJ, Davis GE (2009) Pericyte recruitment during vasculogenic tube assembly stimulates endothelial basement membrane matrix formation. *Blood* 114: 5091-5101.

206. Wang S, Cao C, Chen Z, Bankaitis V, Tzima E, et al. (2012) Pericytes regulate vascular basement membrane remodeling and govern neutrophil extravasation during inflammation. *PLoS One* 7: e45499.
207. Voisin MB, Woodfin A, Nourshargh S (2009) Monocytes and neutrophils exhibit both distinct and common mechanisms in penetrating the vascular basement membrane in vivo. *Arterioscler Thromb Vasc Biol* 29: 1193-1199.
208. Steadman R, Irwin MH, St John PL, Blackburn WD, Heck LW, et al. (1993) Laminin cleavage by activated human neutrophils yields proteolytic fragments with selective migratory properties. *J Leukoc Biol* 53: 354-365.
209. Mydel P, Shipley JM, Adair-Kirk TL, Kelley DG, Broekelmann TJ, et al. (2008) Neutrophil elastase cleaves laminin-332 (laminin-5) generating peptides that are chemotactic for neutrophils. *J Biol Chem* 283: 9513-9522.
210. Lammermann T, Germain RN (2014) The multiple faces of leukocyte interstitial migration. *Semin Immunopathol* 36: 227-251.
211. Friedl P, Weigelin B (2008) Interstitial leukocyte migration and immune function. *Nat Immunol* 9: 960-969.
212. Sixt M (2011) Interstitial locomotion of leukocytes. *Immunol Lett* 138: 32-34.
213. McDonald B, Pittman K, Menezes GB, Hirota SA, Slaba I, et al. (2010) Intravascular danger signals guide neutrophils to sites of sterile inflammation. *Science* 330: 362-366.
214. Campbell JJ, Foxman EF, Butcher EC (1997) Chemoattractant receptor cross talk as a regulatory mechanism in leukocyte adhesion and migration. *Eur J Immunol* 27: 2571-2578.
215. Foxman EF, Campbell JJ, Butcher EC (1997) Multistep Navigation and the Combinatorial Control of Leukocyte Chemotaxis. *J cell Biol* 139: 1349-1360.
216. Heit B, Tavener S, Raharjo E, Kubes P (2002) An intracellular signaling hierarchy determines direction of migration in opposing chemotactic gradients. *J Cell Biol* 159: 91-102.
217. Lammermann T, Afonso PV, Angermann BR, Wang JM, Kastenmuller W, et al. (2013) Neutrophil swarms require LTB4 and integrins at sites of cell death in vivo. *Nature* 498: 371-375.
218. Graham DB, Zinselmeyer BH, Mascarenhas F, Delgado R, Miller MJ, et al. (2009) ITAM signaling by Vav family Rho guanine nucleotide exchange factors regulates interstitial transit rates of neutrophils in vivo. *PLoS One* 4: e4652.

219. Lammermann T, Bader BL, Monkley SJ, Worbs T, Wedlich-Soldner R, et al. (2008) Rapid leukocyte migration by integrin-independent flowing and squeezing. *Nature* 453: 51-55.
220. Werr J, Xie X, Hedqvist P, Ruoslahti E, Lindbom L (1998) beta1 integrins are critically involved in neutrophil locomotion in extravascular tissue *In vivo*. *J Exp Med* 187: 2091-2096.
221. Werr J, Johansson J, Eriksson EE, Hedqvist P, Ruoslahti E, et al. (2000) Integrin alpha(2)beta(1) (VLA-2) is a principal receptor used by neutrophils for locomotion in extravascular tissue. *Blood* 95: 1804-1809.
222. Overstreet MG, Gaylo A, Angermann BR, Hughson A, Hyun YM, et al. (2013) Inflammation-induced interstitial migration of effector CD4(+) T cells is dependent on integrin alphaV. *Nat Immunol* 14: 949-958.
223. Leon B, Lopez-Bravo M, Ardavin C (2007) Monocyte-derived dendritic cells formed at the infection site control the induction of protective T helper 1 responses against *Leishmania*. *Immunity* 26: 519-531.
224. Ng LG, Hsu A, Mandell MA, Roediger B, Hoeller C, et al. (2008) Migratory dermal dendritic cells act as rapid sensors of protozoan parasites. *PLoS Pathog* 4: e1000222.
225. Baluk P, Fuxe J, Hashizume H, Romano T, Lashnits E, et al. (2007) Functionally specialized junctions between endothelial cells of lymphatic vessels. *J Exp Med* 204: 2349-2362.
226. Dieu MC, Vanbervliet B, Vicari A, Bridon JM, Oldham E, et al. (1998) Selective recruitment of immature and mature dendritic cells by distinct chemokines expressed in different anatomic sites. *J Exp Med* 188: 373-386.
227. Sallusto F, Schaerli P, Loetscher P, Scharniel C, Lenig D, et al. (1998) Rapid and coordinated switch in chemokine receptor expression during dendritic cell maturation. *Eur J Immunol* 28: 2760-2769.
228. Sozzani S, Allavena P, D'Amico G, Luini W, Bianchi G, et al. (1998) Differential regulation of chemokine receptors during dendritic cell maturation: a model for their trafficking properties. *J Immunol* 161: 1083-1086.
229. Yanagihara S, Komura E, Nagafune J, Watarai H, Yamaguchi Y (1998) EBI1/CCR7 is a new member of dendritic cell chemokine receptor that is up-regulated upon maturation. *J Immunol* 161: 3096-3102.
230. Forster R, Schubel A, Breitfeld D, Kremmer E, Renner-Muller I, et al. (1999) CCR7 coordinates the primary immune response by establishing functional microenvironments in secondary lymphoid organs. *Cell* 99: 23-33.
231. MartIn-Fontecha A, Sebastiani S, Hopken UE, Ugucioni M, Lipp M, et al. (2003) Regulation of dendritic cell migration to the draining lymph

- node: impact on T lymphocyte traffic and priming. *J Exp Med* 198: 615-621.
232. Saeki H, Moore AM, Brown MJ, Hwang ST (1999) Cutting edge: secondary lymphoid-tissue chemokine (SLC) and CC chemokine receptor 7 (CCR7) participate in the emigration pathway of mature dendritic cells from the skin to regional lymph nodes. *J Immunol* 162: 2472-2475.
233. Robbiani DF, Finch RA, Jager D, Muller WA, Sartorelli AC, et al. (2000) The leukotriene C(4) transporter MRP1 regulates CCL19 (MIP-3beta, ELC)-dependent mobilization of dendritic cells to lymph nodes. *Cell* 103: 757-768.
234. Britschgi MR, Favre S, Luther SA (2010) CCL21 is sufficient to mediate DC migration, maturation and function in the absence of CCL19. *Eur J Immunol* 40: 1266-1271.
235. Luther SA, Tang HL, Hyman PL, Farr AG, Cyster JG (2000) Coexpression of the chemokines ELC and SLC by T zone stromal cells and deletion of the ELC gene in the plt/plt mouse. *Proc Natl Acad Sci U S A* 97: 12694-12699.
236. Weber M, Hauschild R, Schwarz J, Moussion C, de Vries I, et al. (2013) Interstitial dendritic cell guidance by haptotactic chemokine gradients. *Science* 339: 328-332.
237. Schumann K, Lammermann T, Bruckner M, Legler DF, Polleux J, et al. (2010) Immobilized chemokine fields and soluble chemokine gradients cooperatively shape migration patterns of dendritic cells. *Immunity* 32: 703-713.
238. Tal O, Lim HY, Gurevich I, Milo I, Shipony Z, et al. (2011) DC mobilization from the skin requires docking to immobilized CCL21 on lymphatic endothelium and intralymphatic crawling. *J Exp Med* 208: 2141-2153.
239. de Noronha S, Hardy S, Sinclair J, Blundell MP, Strid J, et al. (2005) Impaired dendritic-cell homing in vivo in the absence of Wiskott-Aldrich syndrome protein. *Blood* 105: 1590-1597.
240. Frittoli E, Matteoli G, Palamidessi A, Mazzini E, Maddaluno L, et al. (2011) The signaling adaptor Eps8 is an essential actin capping protein for dendritic cell migration. *Immunity* 35: 388-399.
241. Platt AM, Randolph GJ (2013) Dendritic cell migration through the lymphatic vasculature to lymph nodes. *Adv Immunol* 120: 51-68.
242. Pflücke H, Sixt M (2009) Preformed portals facilitate dendritic cell entry into afferent lymphatic vessels. *J Exp Med* 206: 2925-2935.
243. Alitalo K, Tammela T, Petrova TV (2005) Lymphangiogenesis in development and human disease. *Nature* 438: 946-953.

244. Johnson LA, Clasper S, Holt AP, Lalor PF, Baban D, et al. (2006) An inflammation-induced mechanism for leukocyte transmigration across lymphatic vessel endothelium. *J Exp Med* 203: 2763-2777.
245. Ma J, Wang JH, Guo YJ, Sy MS, Bigby M (1994) In vivo treatment with anti-ICAM-1 and anti-LFA-1 antibodies inhibits contact sensitization-induced migration of epidermal Langerhans cells to regional lymph nodes. *Cell Immunol* 158: 389-399.
246. Xu H, Guan H, Zu G, Bullard D, Hanson J, et al. (2001) The role of ICAM-1 molecule in the migration of Langerhans cells in the skin and regional lymph node. *Eur J Immunol* 31: 3085-3093.
247. Braun A, Worbs T, Moschovakis GL, Halle S, Hoffmann K, et al. (2011) Afferent lymph-derived T cells and DCs use different chemokine receptor CCR7-dependent routes for entry into the lymph node and intranodal migration. *Nat Immunol* 12: 879-887.
248. Bradfield PF, Nourshargh S, Aurrand-Lions M, Imhof BA (2007) JAM family and related proteins in leukocyte migration (Vestweber series). *Arterioscler Thromb Vasc Biol* 27: 2104-2112.
249. Weber C, Fraemohs L, Dejana E (2007) The role of junctional adhesion molecules in vascular inflammation. *Nat Rev Immunol* 7: 467-477.
250. Arcangeli ML, Frontera V, Aurrand-Lions M (2013) Function of junctional adhesion molecules (JAMs) in leukocyte migration and homeostasis. *Arch Immunol Ther Exp (Warsz)* 61: 15-23.
251. Du Pasquier L, Zucchetti I, De Santis R (2004) Immunoglobulin superfamily receptors in protochordates: before RAG time. *Immunol Rev* 198: 233-248.
252. Ebnet K, Suzuki A, Ohno S, Vestweber D (2004) Junctional adhesion molecules (JAMs): more molecules with dual functions? *J Cell Sci* 117: 19-29.
253. Aurrand-Lions M, Duncan L, Ballestrem C, Imhof BA (2001) JAM-2, a novel immunoglobulin superfamily molecule, expressed by endothelial and lymphatic cells. *J Biol Chem* 276: 2733-2741.
254. Aurrand-Lions M, Johnson-Leger C, Wong C, Du Pasquier L, Imhof B (2001) Heterogeneity of endothelial junctions is reflected by differential expression and specific subcellular localization of the three JAM family members. *Blood* 98: 3699-3707.
255. Santoso S, Sachs UJH, Kroll H, Linder M, Ruf A, et al. (2002) The Junctional Adhesion Molecule 3 (JAM-3) on Human Platelets is a Counterreceptor for the Leukocyte Integrin Mac-1. *J Exp Med* 196: 679-691.
256. Kostrewa D, Brockhaus M, D'Arcy A, Dale GE, Nelboeck P, et al. (2001) X-ray structure of junctional adhesion molecule: structural basis for

- homophilic adhesion via a novel dimerization motif. *EMBO J* 20: 4391-4398.
257. Prota AE, Campbell JA, Schelling P, Forrest JC, Watson MJ, et al. (2003) Crystal structure of human junctional adhesion molecule 1: implications for reovirus binding. *Proc Natl Acad Sci U S A* 100: 5366-5371.
258. Ebnet K, Schulz CU, Meyer Zu Brickwedde MK, Pendl GG, Vestweber D (2000) Junctional adhesion molecule interacts with the PDZ domain-containing proteins AF-6 and ZO-1. *J Biol Chem* 275: 27979-27988.
259. Morris AP, Tawil A, Berkova Z, Wible L, Smith CW, et al. (2006) Junctional Adhesion Molecules (JAMs) are differentially expressed in fibroblasts and co-localize with ZO-1 to adherens-like junctions. *Cell Commun Adhes* 13: 233-247.
260. Ebnet K, Aurrand-Lions M, Kuhn A, Kiefer F, Butz S, et al. (2003) The junctional adhesion molecule (JAM) family members JAM-2 and JAM-3 associate with the cell polarity protein PAR-3: a possible role for JAMs in endothelial cell polarity. *J Cell Sci* 116: 3879-3891.
261. Aurrand-Lions MA, Duncan L, Du Pasquier L, Imhof BA (2000) Cloning of JAM-2 and JAM-3: an emerging junctional adhesion molecular family? *Curr Top Microbiol Immunol* 251: 91-98.
262. Arrate MP, Rodriguez JM, Tran TM, Brock TA, Cunningham SA (2001) Cloning of human junctional adhesion molecule 3 (JAM3) and its identification as the JAM2 counter-receptor. *J Biol Chem* 276: 45826-45832.
263. Zen K, Babbin BA, Liu Y, Whelan JB, Nusrat A, et al. (2004) JAM-C is a component of desmosomes and a ligand for CD11b/CD18-mediated neutrophil transepithelial migration. *Mol Biol Cell* 15: 3926-3937.
264. Keiper T, Al-Fakhri N, Chavakis E, Athanasopoulos AN, Isermann B, et al. (2005) The role of junctional adhesion molecule-C (JAM-C) in oxidized LDL-mediated leukocyte recruitment. *FASEB J* 19: 2078-2080.
265. Imhof BA, Zimmerli C, Glikli G, Ducrest-Gay D, Juillard P, et al. (2007) Pulmonary dysfunction and impaired granulocyte homeostasis result in poor survival of Jam-C-deficient mice. *J Pathol* 212: 198-208.
266. Scheiermann C, Meda P, Aurrand-Lions M, Madani R, Yiangou Y, et al. (2007) Expression and function of junctional adhesion molecule-C in myelinated peripheral nerves. *Science* 318: 1472-1475.
267. Glikli G, Ebnet K, Aurrand-Lions M, Imhof BA, Adams RH (2004) Spermatid differentiation requires the assembly of a cell polarity complex downstream of junctional adhesion molecule-C. *Nature* 431: 320-324.

268. Aurrand-Lions M, Lamagna C, Imhof BA (2005) Junctional Adhesion Molecule-C Regulates the Early Influx of Leukocytes into Tissues during Inflammation. *J Immunol*.
269. Liang T, Chiu H, Gurney A, Sidle A, Tumas D, et al. (2002) Vascular Endothelial-Junctional Adhesion Molecule (VE-JAM)/JAM 2 Interacts with T, NK, and Dendritic Cells Through JAM 3. *J Immunol* 168: 1618-1626.
270. Ody C, Jungblut-Ruault S, Cossali D, Barnet M, Aurrand-Lions M, et al. (2007) Junctional adhesion molecule C (JAM-C) distinguishes CD27+ germinal center B lymphocytes from non-germinal center cells and constitutes a new diagnostic tool for B-cell malignancies. *Leukemia* 21: 1285-1293.
271. Johnson-Leger CA, Aurrand-Lions M, Beltraminelli N, Fasel N, Imhof BA (2002) Junctional adhesion molecule-2 (JAM-2) promotes lymphocyte transendothelial migration. *Blood* 100: 2479-2486.
272. Ludwig RJ, Zollner TM, Santoso S, Hardt K, Gille J, et al. (2005) Junctional adhesion molecules (JAM)-B and -C contribute to leukocyte extravasation to the skin and mediate cutaneous inflammation. *J Invest Dermatol* 125: 969-976.
273. Vonlaufen A, Aurrand-Lions M, Pastor CM, Lamagna C, Hadengue A, et al. (2006) The role of junctional adhesion molecule C (JAM-C) in acute pancreatitis. *J Pathol* 209: 540-548.
274. Lamagna C, Hodivala-Dilke KM, Imhof BA, Aurrand-Lions M (2005) Antibody against Junctional Adhesion Molecule-C Inhibits Angiogenesis and Tumor Growth. *Cancer Res* 65: 5703-5710.
275. Lamagna C, Meda P, Mandicourt G, Brown J, Gilbert RJ, et al. (2005) Dual interaction of JAM-C with JAM-B and alpha(M)beta2 integrin: function in junctional complexes and leukocyte adhesion. *Mol Biol Cell* 16: 4992-5003.
276. Santoso S, Orlova VV, Song K, Sachs UJ, Andrei-Selmer CL, et al. (2005) The homophilic binding of junctional adhesion molecule-C mediates tumor cell-endothelial cell interactions. *J Biol Chem* 280: 36326-36333.
277. Hogg N, Takacs L, Palmer DG, Selvendran Y, Allen C (1986) The p150,95 molecule is a marker of human mononuclear phagocytes: comparison with expression of class II molecules. *Eur J Immunol* 16: 240-248.
278. Keizer GD, Borst J, Visser W, Schwarting R, de Vries JE, et al. (1987) Membrane glycoprotein p150,95 of human cytotoxic T cell clone is involved in conjugate formation with target cells. *J Immunol* 138: 3130-3136.

279. Akiyama H, McGeer PL (1990) Brain microglia constitutively express beta-2 integrins. *J Neuroimmunol* 30: 81-93.
280. Zimmerli C, Lee BP, Palmer G, Gabay C, Adams RH, et al. (2009) Adaptive Immune Response in JAM-C-Deficient Mice: Normal Initiation but Reduced IgG Memory. *J Immunol* 182: 4728-4736.
281. Chavakis T, Keiper T, Matz-Westphal R, Hersemeyer K, Sachs UJ, et al. (2004) The junctional adhesion molecule-C promotes neutrophil transendothelial migration in vitro and in vivo. *J Biol Chem* 279: 55602-55608.
282. Sircar M, Bradfield PF, Aurrand-Lions M, Fish RJ, Alcaide P, et al. (2007) Neutrophil transmigration under shear flow conditions in vitro is junctional adhesion molecule-C independent. *J Immunol* 178: 5879-5887.
283. Bradfield PF, Scheiermann C, Nourshargh S, Ody C, Luscinskas FW, et al. (2007) JAM-C regulates unidirectional monocyte transendothelial migration in inflammation. *Blood* 110: 2545-2555.
284. Scheiermann C, Colom B, Meda P, Patel NS, Voisin MB, et al. (2009) Junctional adhesion molecule-C mediates leukocyte infiltration in response to ischemia reperfusion injury. *Arterioscler Thromb Vasc Biol* 29: 1509-1515.
285. Li X, Stankovic M, Lee BP, Aurrand-Lions M, Hahn CN, et al. (2009) JAM-C induces endothelial cell permeability through its association and regulation of β_3 integrins. *Arterioscler Thromb Vasc Biol* 29: 1200-1206.
286. Orlova VV, Economopoulou M, Lupu F, Santoso S, Chavakis T (2006) Junctional adhesion molecule-C regulates vascular endothelial permeability by modulating VE-cadherin-mediated cell-cell contacts. *J Exp Med* 203: 2703-2714.
287. Mandicourt G, Iden S, Ebnet K, Aurrand-Lions M, Imhof BA (2007) JAM-C regulates tight junctions and integrin-mediated cell adhesion and migration. *J Biol Chem* 282: 1830-1837.
288. Martin-Padura I, Lostaglio S, Schneemann M, Williams L, Romano M, et al. (1998) Junctional adhesion molecule, a novel member of the immunoglobulin superfamily that distributes at intercellular junctions and modulates monocyte transmigration. *J Cell Biol* 142: 117-127.
289. Williams LA, Martin-Padura I, Dejana E, Hogg N, Simmons DL (1999) Identification and characterisation of human Junctional Adhesion Molecule (JAM). *Mol Immunol* 36: 1175-1188.
290. Liu Y, Nusrat A, Schnell FJ, Reaves TA, Walsh S, et al. (2000) Human junction adhesion molecule regulates tight junction resealing in epithelia. *J Cell Sci* 113 (Pt 13): 2363-2374.

291. Bazzoni G, Martinez-Estrada OM, Orsenigo F, Cordenonsi M, Citi S, et al. (2000) Interaction of junctional adhesion molecule with the tight junction components ZO-1, cingulin, and occludin. *J Biol Chem* 275: 20520-20526.
292. Ebnet K, Suzuki A, Horikoshi Y, Hirose T, Meyer Zu Brickwedde MK, et al. (2001) The cell polarity protein ASIP/PAR-3 directly associates with junctional adhesion molecule (JAM). *EMBO J* 20: 3738-3748.
293. Ozaki H, Ishii K, Horiuchi H, Arai H, Kawamoto T, et al. (1999) Cutting edge: combined treatment of TNF-alpha and IFN-gamma causes redistribution of junctional adhesion molecule in human endothelial cells. *J Immunol* 163: 553-557.
294. Ostermann G, Weber KS, Zerneck A, Schroder A, Weber C (2002) JAM-1 is a ligand of the beta(2) integrin LFA-1 involved in transendothelial migration of leukocytes. *Nat Immunol* 3: 151-158.
295. Mandell KJ, McCall IC, Parkos CA (2004) Involvement of the junctional adhesion molecule-1 (JAM1) homodimer interface in regulation of epithelial barrier function. *J Biol Chem* 279: 16254-16262.
296. Bazzoni G, Martinez-Estrada OM, Mueller F, Nelboeck P, Schmid G, et al. (2000) Homophilic interaction of junctional adhesion molecule. *J Biol Chem* 275: 30970-30976.
297. Shaw SK, Ma S, Kim MB, Rao RM, Hartman CU, et al. (2004) Coordinated redistribution of leukocyte LFA-1 and endothelial cell ICAM-1 accompany neutrophil transmigration. *J Exp Med* 200: 1571-1580.
298. Del Maschio A, De Luigi A, Martin-Padura I, Brockhaus M, Bartfai T, et al. (1999) Leukocyte recruitment in the cerebrospinal fluid of mice with experimental meningitis is inhibited by an antibody to junctional adhesion molecule (JAM). *J Exp Med* 190: 1351-1356.
299. Lechner F, Sahrbacher U, Suter T, Frei K, Brockhaus M, et al. (2000) Antibodies to the junctional adhesion molecule cause disruption of endothelial cells and do not prevent leukocyte influx into the meninges after viral or bacterial infection. *J Infect Dis* 182: 978-982.
300. Woodfin A, Reichel CA, Khandoga A, Corada M, Voisin MB, et al. (2007) JAM-A mediates neutrophil transmigration in a stimulus-specific manner in vivo: evidence for sequential roles for JAM-A and PECAM-1 in neutrophil transmigration. *Blood* 110: 1848-1856.
301. Corada M, Chimenti S, Cera MR, Vinci M, Salio M, et al. (2005) Junctional adhesion molecule-A-deficient polymorphonuclear cells show reduced diapedesis in peritonitis and heart ischemia-reperfusion injury. *Proc Natl Acad Sci U S A* 102: 10634-10639.
302. Khandoga A, Kessler JS, Meissner H, Hanschen M, Corada M, et al. (2005) Junctional adhesion molecule-A deficiency increases hepatic

- ischemia-reperfusion injury despite reduction of neutrophil transendothelial migration. *Blood* 106: 725-733.
303. Cera MR, Del Prete A, Vecchi A, Corada M, Martin-Padura I, et al. (2004) Increased DC trafficking to lymph nodes and contact hypersensitivity in junctional adhesion molecule-A-deficient mice. *J Clin Invest* 114: 729-738.
304. Cunningham SA, Arrate MP, Rodriguez JM, Bjercke RJ, Vanderslice P, et al. (2000) A novel protein with homology to the junctional adhesion molecule. Characterization of leukocyte interactions. *J Biol Chem* 275: 34750-34756.
305. Palmeri D, van Zante A, Huang CC, Hemmerich S, Rosen SD (2000) Vascular endothelial junction-associated molecule, a novel member of the immunoglobulin superfamily, is localized to intercellular boundaries of endothelial cells. *J Biol Chem* 275: 19139-19145.
306. Aurrand-Lions M, Johnson-Leger C, Wong C, Du Pasquier L, Imhof BA (2001) Heterogeneity of endothelial junctions is reflected by differential expression and specific subcellular localization of the three JAM family members. *Blood* 98: 3699-3707.
307. Liang TW, Chiu HH, Gurney A, Sidle A, Tumas DB, et al. (2002) Vascular endothelial-junctional adhesion molecule (VE-JAM)/JAM 2 interacts with T, NK, and dendritic cells through JAM 3. *J Immunol* 168: 1618-1626.
308. Cunningham SA, Rodriguez JM, Arrate MP, Tran TM, Brock TA (2002) JAM2 interacts with alpha4beta1. Facilitation by JAM3. *J Biol Chem* 277: 27589-27592.
309. Arcangeli ML, Frontera V, Bardin F, Thomassin J, Chetaille B, et al. (2012) The Junctional Adhesion Molecule-B regulates JAM-C-dependent melanoma cell metastasis. *FEBS Lett* 586: 4046-4051.
310. Hirata K, Ishida T, Penta K, Rezaee M, Yang E, et al. (2001) Cloning of an immunoglobulin family adhesion molecule selectively expressed by endothelial cells. *J Biol Chem* 276: 16223-16231.
311. Nasdala I, Wolburg-Buchholz K, Wolburg H, Kuhn A, Ebnet K, et al. (2002) A transmembrane tight junction protein selectively expressed on endothelial cells and platelets. *J Biol Chem* 277: 16294-16303.
312. Wegmann F, Ebnet K, Du Pasquier L, Vestweber D, Butz S (2004) Endothelial adhesion molecule ESAM binds directly to the multidomain adaptor MAGI-1 and recruits it to cell contacts. *Exp Cell Res* 300: 121-133.
313. Wegmann F, Petri B, Khandoga AG, Moser C, Khandoga A, et al. (2006) ESAM supports neutrophil extravasation, activation of Rho, and VEGF-induced vascular permeability. *J Exp Med* 203: 1671-1677.

314. Stalker TJ, Wu J, Morgans A, Traxler EA, Wang L, et al. (2009) Endothelial cell specific adhesion molecule (ESAM) localizes to platelet-platelet contacts and regulates thrombus formation in vivo. *J Thromb Haemost* 7: 1886-1896.
315. Mapoles JE, Krah DL, Crowell RL (1985) Purification of a HeLa cell receptor protein for group B coxsackieviruses. *J Virol* 55: 560-566.
316. Bergelson JM, Cunningham JA, Droguett G, Kurt-Jones EA, Krithivas A, et al. (1997) Isolation of a common receptor for Coxsackie B viruses and adenoviruses 2 and 5. *Science* 275: 1320-1323.
317. Bewley MC, Springer K, Zhang YB, Freimuth P, Flanagan JM (1999) Structural analysis of the mechanism of adenovirus binding to its human cellular receptor, CAR. *Science* 286: 1579-1583.
318. van Raaij MJ, Chouin E, van der Zandt H, Bergelson JM, Cusack S (2000) Dimeric structure of the coxsackievirus and adenovirus receptor D1 domain at 1.7 Å resolution. *Structure* 8: 1147-1155.
319. Cohen CJ, Shieh JT, Pickles RJ, Okegawa T, Hsieh JT, et al. (2001) The coxsackievirus and adenovirus receptor is a transmembrane component of the tight junction. *Proc Natl Acad Sci U S A* 98: 15191-15196.
320. Walters RW, Freimuth P, Moninger TO, Ganske I, Zabner J, et al. (2002) Adenovirus fiber disrupts CAR-mediated intercellular adhesion allowing virus escape. *Cell* 110: 789-799.
321. Moog-Lutz C, Cave-Riant F, Guibal FC, Breau MA, Di Gioia Y, et al. (2003) JAML, a novel protein with characteristics of a junctional adhesion molecule, is induced during differentiation of myeloid leukemia cells. *Blood* 102: 3371-3378.
322. Zen K, Liu Y, McCall IC, Wu T, Lee W, et al. (2005) Neutrophil migration across tight junctions is mediated by adhesive interactions between epithelial coxsackie and adenovirus receptor and a junctional adhesion molecule-like protein on neutrophils. *Mol Biol Cell* 16: 2694-2703.
323. Hirabayashi S, Tajima M, Yao I, Nishimura W, Mori H, et al. (2003) JAM4, a junctional cell adhesion molecule interacting with a tight junction protein, MAGI-1. *Mol Cell Biol* 23: 4267-4282.
324. Cox FE (2002) History of human parasitology. *Clin Microbiol Rev* 15: 595-612.
325. Sacks D, Noben-Trauth N (2002) The immunology of susceptibility and resistance to *Leishmania major* in mice. *Nat Rev Immunol* 2: 845-858.
326. Kaye P, Scott P (2011) Leishmaniasis: complexity at the host-pathogen interface. *Nat Rev Microbiol* 9: 604-615.
327. Strazzulla A, Cocuzza S, Pinzone MR, Postorino MC, Cosentino S, et al. (2013) Mucosal leishmaniasis: an underestimated presentation of a neglected disease. *Biomed Res Int* 2013: 805108.

328. McGwire BS, Satoskar AR (2014) Leishmaniasis: clinical syndromes and treatment. *QJM* 107: 7-14.
329. Stockdale L, Newton R (2013) A review of preventative methods against human leishmaniasis infection. *PLoS Negl Trop Dis* 7: e2278.
330. Singh B, Sundar S (2012) Leishmaniasis: vaccine candidates and perspectives. *Vaccine* 30: 3834-3842.
331. Kumar R, Engwerda C (2014) Vaccines to prevent leishmaniasis. *Clin Transl Immunology* 3: e13.
332. Nasser M, Modabber FZ (1979) Generalized infection and lack of delayed hypersensitivity in BALB/c mice infected with *Leishmania tropica major*. *Infect Immun* 26: 611-614.
333. Kellina OI (1973) [Differences in the sensitivity of inbred mice of different lines to *Leishmania tropica major*]. *Med Parazitol (Mosk)* 42: 279-285.
334. Howard JG, Hale C, Chan-Liew WL (1980) Immunological regulation of experimental cutaneous leishmaniasis. 1. Immunogenetic aspects of susceptibility to *Leishmania tropica* in mice. *Parasite Immunol* 2: 303-314.
335. Howard JG, Hale C, Liew FY (1980) Immunological regulation of experimental cutaneous leishmaniasis. III. Nature and significance of specific suppression of cell-mediated immunity in mice highly susceptible to *Leishmania tropica*. *J Exp Med* 152: 594-607.
336. Heinzl FP, Sadick MD, Holaday BJ, Coffman RL, Locksley RM (1989) Reciprocal expression of interferon gamma or interleukin 4 during the resolution or progression of murine leishmaniasis. Evidence for expansion of distinct helper T cell subsets. *J Exp Med* 169: 59-72.
337. Liew F, Millott S, Parkinson C, Palmer R, Moncada S (1990) Macrophages killing of *Leishmania* parasite in vivo is mediated by nitric oxide from L-arginine. *J Immunol* 144: 4794-4797.
338. Wang ZE, Reiner LR, Zheng S, Dalton DK, Lockley RM (1994) CD4 + Effector Cells Default to the Th2 Pathway in Interferon γ -deficient Mice Infected with *Leishmania major*. *J Exp Med* 179: 1367-1371.
339. Magram J, Connaughton SE, Warriar RR, Carvajal DM, Wu CY, et al. (1996) IL-12-deficient mice are defective in IFN γ production and type 1 cytokine responses. *Immunity* 4: 471-481.
340. Mattner F, Magram J, Ferrante J, Launois P, Di Padova K, et al. (1996) Genetically resistant mice lacking interleukin-12 are susceptible to infection with *Leishmania major* and mount a polarized Th2 cell response. *Eur J Immunol* 26: 1553-1559.
341. Tacchini-Cottier F, Weinkopff T, Launois P (2012) Does T Helper Differentiation Correlate with Resistance or Susceptibility to Infection with *L. major*? Some Insights From the Murine Model. *Front Immunol* 3: 32.

342. Beebe AM, Mauze S, Schork NJ, Coffman RL (1997) Serial backcross mapping of multiple loci associated with resistance to *Leishmania major* in mice. *Immunity* 6: 551-557.
343. Nabors GS, Nolan T, Croop W, Li J, Farrell JP (1995) The influence of the site of parasite inoculation on the development of Th1 and Th2 type immune responses in (BALB/c x C57BL/6) F1 mice infected with *Leishmania major*. *Parasite Immunol* 17: 569-579.
344. Suffia I, Reckling SK, Salay G, Belkaid Y (2005) A role for CD103 in the retention of CD4+CD25+ Treg and control of *Leishmania major* infection. *J Immunol* 174: 5444-5455.
345. Gonzalez-Lombana C, Gimblet C, Bacellar O, Oliveira WW, Passos S, et al. (2013) IL-17 mediates immunopathology in the absence of IL-10 following *Leishmania major* infection. *PLoS Pathog* 9: e1003243.
346. Segal AW (2005) How neutrophils kill microbes. *Annu Rev Immunol* 23: 197-223.
347. Nauseef WM (2007) How human neutrophils kill and degrade microbes: an integrated view. *Immunol Rev* 219: 88-102.
348. Papayannopoulos V, Zychlinsky A (2009) NETs: a new strategy for using old weapons. *Trends Immunol* 30: 513-521.
349. Tecchio C, Micheletti A, Cassatella MA (2014) Neutrophil-derived cytokines: facts beyond expression. *Front Immunol* 5: 508.
350. Peters NC, Egen JG, Secundino N, Debrabant A, Kimblin N, et al. (2008) In Vivo Imaging Reveals an Essential Role for Neutrophils in Leishmaniasis Transmitted by Sand Flies. *Science* 321: 970-974.
351. Tacchini-Cottier F, Zweifel C, Belkaid Y, Mukankundiye C, Vasei M, et al. (2000) An Immunomodulatory Function for Neutrophils During the Induction of a CD4 + Th2 Response in BALB/c Mice Infected with *Leishmania major*. *J Immunol* 165: 2628-2636.
352. Beil WJ, Meinardus-Hager G, Neugebauer DC, Sorg C (1992) Differences in the onset of the inflammatory response to cutaneous leishmaniasis in resistant and susceptible mice. *J Leukoc Biol* 52: 135-142.
353. Oghumu S, Lezama-Davila CM, Isaac-Marquez AP, Satoskar AR (2010) Role of chemokines in regulation of immunity against leishmaniasis. *Exp Parasitol* 126: 389-396.
354. Müller K, Zandbergen G, Hansen B, Laufs H, Jahnke N, et al. (2001) Chemokines, natural killer cells and granulocytes in the early course of *Leishmania major* infection in mice. *Medical Microbiology and Immunology* 190: 73-76.
355. Filardy AA, Costa-da-Silva AC, Koeller CM, Guimaraes-Pinto K, Ribeiro-Gomes FL, et al. (2014) Infection with *Leishmania major* induces a cellular stress response in macrophages. *PLoS One* 9: e85715.

356. Racoosin EL, Beverley SM (1997) *Leishmania major*: Promastigotes Induce Expression of a Subset of Chemokine Genes in Murine Macrophages. *Exp Parasitol* 85: 283-295.
357. Jacobs T, Andra J, Gaworski I, Graefe S, Mellenthin K, et al. (2005) Complement C3 is required for the progression of cutaneous lesions and neutrophil attraction in *Leishmania major* infection. *Med Microbiol Immunol* 194: 143-149.
358. van Zandbergen G, Hermann N, Laufs H, Solbach W, Laskay T (2002) *Leishmania* Promastigotes Release a Granulocyte Chemotactic Factor and Induce Interleukin-8 Release but Inhibit Gamma Interferon-Inducible Protein 10 Production by Neutrophil Granulocytes. *Infection and Immunity* 70: 4177-4184.
359. Laufs H, Muller K, Fleischer J, Reiling N, Jahnke N, et al. (2002) Intracellular survival of *Leishmania major* in neutrophil granulocytes after uptake in the absence of heat-labile serum factors. *Infect Immun* 70: 826-835.
360. Moradin N, Descoteaux A (2012) *Leishmania* promastigotes: building a safe niche within macrophages. *Front Cell Infect Microbiol* 2: 121.
361. Ribeiro-Gomes FL, Peters NC, Debrabant A, Sacks DL (2012) Efficient capture of infected neutrophils by dendritic cells in the skin inhibits the early anti-leishmania response. *PLoS Pathog* 8: e1002536.
362. Ribeiro-Gomes FL, Otero AC, Gomes NA, Moniz-De-Souza MC, Cysne-Finkelstein L, et al. (2004) Macrophage interactions with neutrophils regulate *Leishmania major* infection. *J Immunol* 172: 4454-4462.
363. Lima GM, Vallochi AL, Silva UR, Bevilacqua EM, Kiffer MM, et al. (1998) The role of polymorphonuclear leukocytes in the resistance to cutaneous Leishmaniasis. *Immunol Lett* 64: 145-151.
364. Ribeiro-Gomes FL, Otero AC, Gomes NA, Moniz-de-Souza MCA, Finkelstein LC, et al. (2004) Macrophage Interactions with Neutrophils Regulate *Leishmania major* Infection. *J Immunol* 172: 4454-4462.
365. Chen L, Zhang ZH, Watanabe T, Yamashita T, Kobayakawa T, et al. (2005) The involvement of neutrophils in the resistance to *Leishmania major* infection in susceptible but not in resistant mice. *Parasitol Int* 54: 109-118.
366. Reis e Sousa C (2006) Dendritic cells in a mature age. *Nat Rev Immunol* 6: 476-483.
367. Hochrein H, O'Keeffe M (2008) Dendritic cell subsets and toll-like receptors. *Handb Exp Pharmacol*: 153-179.
368. Liu YJ (2001) Dendritic cell subsets and lineages, and their functions in innate and adaptive immunity. *Cell* 106: 259-262.

369. Steinman RM, Cohn ZA (1973) Identification of a novel cell type in peripheral lymphoid organs of mice. I. Morphology, quantitation, tissue distribution. *J Exp Med* 137: 1142-1162.
370. Ashok D, Acha-Orbea H (2014) Timing is everything: dendritic cell subsets in murine *Leishmania* infection. *Trends Parasitol* 30: 499-507.
371. Karrich JJ, Jachimowski LC, Uittenbogaart CH, Blom B (2014) The Plasmacytoid Dendritic Cell as the Swiss Army Knife of the Immune System: Molecular Regulation of Its Multifaceted Functions. *J Immunol* 193: 5772-5778.
372. Merad M, Ginhoux F, Collin M (2008) Origin, homeostasis and function of Langerhans cells and other langerin-expressing dendritic cells. *Nat Rev Immunol* 8: 935-947.
373. Leon B, Ardavin C (2008) Monocyte-derived dendritic cells in innate and adaptive immunity. *Immunol Cell Biol* 86: 320-324.
374. Malissen B, Tamoutounour S, Henri S (2014) The origins and functions of dendritic cells and macrophages in the skin. *Nat Rev Immunol* 14: 417-428.
375. Sathe P, Metcalf D, Vremec D, Naik SH, Langdon WY, et al. (2014) Lymphoid tissue and plasmacytoid dendritic cells and macrophages do not share a common macrophage-dendritic cell-restricted progenitor. *Immunity* 41: 104-115.
376. Moll H, Fuchs H, Blank C, Rollinghoff M (1993) Langerhans cells transport *Leishmania major* from the infected skin to the draining lymph node for presentation to antigen-specific T cells. *Eur J Immunol* 23: 1595-1601.
377. Moll H, Scharner A, Kampgen E (2002) Increased interleukin 4 (IL-4) receptor expression and IL-4-induced decrease in IL-12 production by Langerhans cells infected with *Leishmania major*. *Infect Immun* 70: 1627-1630.
378. Ritter U, Meissner A, Scheidig C, Korner H (2004) CD8 alpha- and Langerin-negative dendritic cells, but not Langerhans cells, act as principal antigen-presenting cells in leishmaniasis. *Eur J Immunol* 34: 1542-1550.
379. Kautz-Neu K, Noordegraaf M, Dinges S, Bennett CL, John D, et al. (2011) Langerhans cells are negative regulators of the anti-*Leishmania* response. *J Exp Med* 208: 885-891.
380. Misslitz AC, Bonhagen K, Harbecke D, Lippuner C, Kamradt T, et al. (2004) Two waves of antigen-containing dendritic cells in vivo in experimental *Leishmania major* infection. *Eur J Immunol* 34: 715-725.
381. Brewig N, Kissenpfennig A, Malissen B, Veit A, Bickert T, et al. (2009) Priming of CD8+ and CD4+ T cells in experimental leishmaniasis is initiated by different dendritic cell subtypes. *J Immunol* 182: 774-783.

382. Iezzi G, Frohlich A, Ernst B, Ampenberger F, Saeland S, et al. (2006) Lymph Node Resident Rather Than Skin-Derived Dendritic Cells Initiate Specific T Cell Responses after *Leishmania major* Infection. *J Immunol* 177: 1250-1256.
383. Hochrein H, Shortman K, Vremec D, Scott B, Hertzog P, et al. (2001) Differential production of IL-12, IFN- α , and IFN- γ by mouse dendritic cell subsets. *J Immunol* 166: 5448-5455.
384. Henri S, Curtis J, Hochrein H, Vremec D, Shortman K, et al. (2002) Hierarchy of susceptibility of dendritic cell subsets to infection by *Leishmania major*: inverse relationship to interleukin-12 production. *Infect Immun* 70: 3874-3880.
385. De Trez C, Magez S, Akira S, Ryffel B, Carlier Y, et al. (2009) iNOS-producing inflammatory dendritic cells constitute the major infected cell type during the chronic *Leishmania major* infection phase of C57BL/6 resistant mice. *PLoS Pathog* 5: e1000494.
386. Sato N, Ahuja SK, Quinones M, KostECKI V, Reddick RL, et al. (2000) CC Chemokine Receptor (CCR)2 Is Required for Langerhans Cell Migration and Localization of T Helper Cell Type 1 (Th1)-inducing Dendritic Cells: Absence of CCR2 Shifts the *Leishmania major*-resistant Phenotype to a Susceptible State Dominated by Th2 Cytokines, B Cell Outgrowth, and Sustained Neutrophilic Inflammation. *J Exp Med* 192: 205-218.
387. Ashok D, Schuster S, Ronet C, Rosa M, Mack V, et al. (2014) Cross-presenting dendritic cells are required for control of *Leishmania major* infection. *Eur J Immunol* 44: 1422-1432.
388. Zaph C, Scott P (2003) Th1 Cell-Mediated Resistance to Cutaneous Infection with *Leishmania major* Is Independent of P- and E-Selectins. *The Journal of Immunology* 171: 4726-4732.
389. Leon B, Ardavin C (2008) Monocyte migration to inflamed skin and lymph nodes is differentially controlled by L-selectin and PSGL-1. *Blood* 111: 3126-3130.
390. Kropf P, Kadolsky UD, Rogers M, Cloke TE, Müller I (2010) The Leishmaniasis Model. *Methods in Microbiology* 37: 307-328.
391. Miles AA, Miles EM (1952) Vascular reactions to histamine, histamine-liberator and leukotaxine in the skin of guinea-pigs. *J Physiol* 118: 228-257.
392. Robbiani DF, Finch RA, Jager D, Muller WA, Sartorelli AC, et al. (2000) The Leukotriene C4 Transporter MRP1 Regulates CCL19 (MIP-3b, ELC)-Dependent Mobilization of Dendritic Cells to Lymph Nodes. *Cell* 103: 757-768.
393. Spindler V, Schlegel N, Waschke J (2010) Role of GTPases in control of microvascular permeability. *Cardiovasc Res* 87: 243-253.

394. Goddard LM, Iruela-Arispe ML (2013) Cellular and molecular regulation of vascular permeability. *Thromb Haemost* 109: 407-415.
395. Shaw SK, Perkins BN, Lim YC, Liu Y, Nusrat A, et al. (2001) Reduced expression of junctional adhesion molecule and platelet/endothelial cell adhesion molecule-1 (CD31) at human vascular endothelial junctions by cytokines tumor necrosis factor-alpha plus interferon-gamma Does not reduce leukocyte transmigration under flow. *Am J Pathol* 159: 2281-2291.
396. Vestweber D, Wessel F, Nottebaum AF (2014) Similarities and differences in the regulation of leukocyte extravasation and vascular permeability. *Semin Immunopathol* 36: 177-192.
397. Wessel F, Winderlich M, Holm M, Frye M, Rivera-Galdos R, et al. (2014) Leukocyte extravasation and vascular permeability are each controlled in vivo by different tyrosine residues of VE-cadherin. *Nat Immunol*.
398. Serbina NV, Pamer EG (2006) Monocyte emigration from bone marrow during bacterial infection requires signals mediated by chemokine receptor CCR2. *Nat Immunol* 7: 311-317.
399. Tripathi P, Singh V, Naik S (2007) Immune response to leishmania: paradox rather than paradigm. *FEMS Immunol Med Microbiol* 51: 229-242.